APRIL 28, 2021
VOLUME 121
NUMBER 8

pubs.acs.org/CR

CHEMICAL REVIEWS

ACS Publications
Most Trusted. Most Cited. Most Read.

www.acs.org

CHEMICAL REVIEWS

pubs.acs.org/CR Review

Soft Materials by Design: Unconventional Polymer Networks Give Extreme Properties

Xuanhe Zhao,* Xiaoyu Chen,# Hyunwoo Yuk,# Shaoting Lin,# Xinyue Liu, and German Parada

Cite This: https://doi.org/10.1021/acs.chemrev.0c01088 Read Online

ACCESS | Metrics & More | Article Recommendations

ABSTRACT: Hydrogels are polymer networks infiltrated with water. Many biological hydrogels in animal bodies such as muscles, heart valves, cartilages, and tendons possess extreme mechanical properties including being extremely tough, strong, resilient, adhesive, and fatigue-resistant. These mechanical properties are also critical for hydrogels' diverse applications ranging from drug delivery, tissue engineering, medical implants, wound dressings, and contact lenses to sensors, actuators, electronic devices, optical devices, batteries, water harvesters, and soft robots. Whereas numerous hydrogels have been developed over the last few decades, a set of general principles that can rationally guide the design of hydrogels using different materials and fabrication methods for various applications remain a central need in the field of soft materials. This review is aimed at synergistically reporting: (i) general design principles for hydrogels to achieve extreme mechanical and physical properties, (ii) implementation strategies for the design principles using *unconventional polymer networks*, and (iii) future directions for the orthogonal design of hydrogels to achieve multiple combined mechanical, physical, chemical, and biological properties. Because these design principles and implementation strategies are based on generic polymer networks, they are also applicable to other soft materials including elastomers and organogels. Overall, the review will not only provide comprehensive and systematic guidelines on the rational design of soft materials, but also provoke interdisciplinary discussions on a fundamental question: why does nature select soft materials with unconventional polymer networks to constitute the major parts of animal bodies?

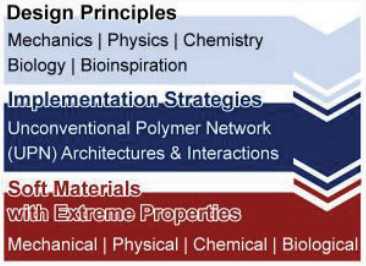

CONTENTS

Received: October 6, 2020

https://doi.org/10.1021/acs.chemrev.0c01088
Chem. Rev. XXXX, XXX, XXX−XXX

1. INTRODUCTION

As hydrophilic polymer networks infiltrated with water,[1] hydrogels are the major components of animal bodies, constituting most of their cells, extracellular matrices, tissues, and organs (Figure 1 and Figure 2). Not surprisingly, hydrogels have been widely used in biological and biomedical applications such as vehicles for drug delivery,[2−5] scaffolds for tissue engineering,[6−8] models for biological studies,[9−13] medical implants,[14,15] wound dressings,[16−18] and contact lenses.[15,19] More recently, intensive efforts have been devoted to exploring hydrogels' emerging applications in devices and machines[20] such as hydrogel sensors,[21−24] actuators,[25−28] soft robots,[26,29,30] electronic devices,[31−33] batteries,[34,35] supercapacitors,[36] iontronic devices,[27,37] magnetic devices,[28,38−40] optical devices,[41−43] acoustic devices,[44,45] living devices,[24,46] underwater adhesives,[47−49] bioadhesive devices,[47,50] and coatings[51,52] (Figure 3).

Mechanical properties of hydrogels are crucial to the survival and wellbeing of animals, and greatly affect the above-mentioned applications of hydrogels. The pioneering works in the field of polymers and soft materials have laid the foundation for understanding the elasticity, swelling, poroelasticity, viscoelasticity, fracture, and fatigue of hydrogels (e.g., refs 53−66 and the references therein). However, the inverse question—how to design hydrogels that possess certain mechanical properties or certain properties in general—still poses a grand challenge in the field of polymers and soft materials.[66−69] This challenge becomes even more daunting, when one targets hydrogels'

https://doi.org/10.1021/acs.chemrev.0c01088
Chem. Rev. XXXX, XXX, XXX−XXX

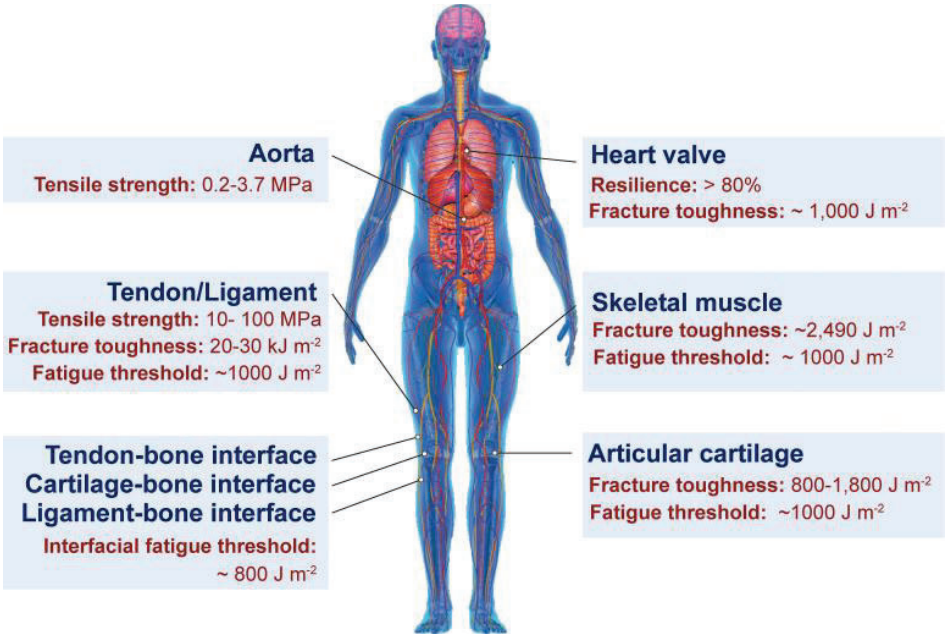

Figure 1. Biological hydrogels in the human body can possess extreme mechanical properties. Aorta with tensile strength of 0.2−3.7 MPa;[80] heart valve with resilience above 80% and fracture toughness around 1000 J m^{-2};[87,88] tendon with tensile strength of 10−100 MPa,[105] fracture toughness of 20−30 kJ m^{-2} and fatigue threshold around 1000 J m^{-2};[106] skeletal muscle with fracture toughness around 2490 J m^{-2} and fatigue threshold around 1000 J m^{-2};[80] articular cartilage with fracture toughness of 800−1800 J m^{-2};[107] and tendon/cartilage/ligament-bone interfaces with interfacial fatigue threshold around 800 J m^{-2}.[78,91] These biological hydrogels can provide inspirations for the design of synthetic hydrogels that possess extreme mechanical properties.

extreme mechanical properties, such as extremely high values of fracture toughness,[70] strength,[71,72] resilience,[73,74] interfacial toughness,[49] fatigue threshold,[75−77] and interfacial fatigue threshold.[78]

Despite the above-mentioned grand challenge, the design of hydrogels with extreme mechanical properties is of both fundamental and practical importance. From the fundamental aspect, many biological hydrogels have achieved extreme mechanical properties necessary for their survival and well-being through evolution (Figure 1). For example, cartilage is a tough connective tissue that covers the surfaces of joints to provide reduced friction.[79] The human knee joint cartilage (i.e., articular cartilage) typically needs to sustain compressive stresses of 4−9 MPa for 1 million cycles per year, while maintaining high fracture toughness around 1000 J m^{-2} (Figure 2a).[80] The high fracture toughness of articular cartilage is mainly attributed to its abundant strong collagen fibers interpenetrated with proteoglycan macromolecules. This structure of articular cartilage provides both viscoelasticity and poroelasticity for mechanical dissipation.[81,82] The viscoelasticity of articular cartilage is mainly associated with local rearrangement of aggrecan, adhesive interactions of aggrecan, and reconfiguration of collagen;[82] the poroelasticity of articular cartilage is governed by the interstitial fluid movement through the porous extracellular matrix.[81] Tendon is a strong connective tissue that connects muscle to bone and muscle to muscle. The human patellar tendon can sustain a high tensile strength over 50 MPa,[83,84] owing to its unique hierarchical fibrous structure that enables the simultaneous stiffening of bundles of collagen fibers before their tensile failure (Figure 2b).[85,86] Heart valves generally possess both high resilience above 80% and high fracture toughness around 1200 J m^{-2},[87,88] which are two seemingly contradictory properties (Figure 2c). The elastin and crimped collagen fibers in the heart valve are elastic and nondissipative under moderate deformation, leading to the high resilience of the heart valve.[89] However, under large deformation, the stiffening and fracture of the collagen fibers dissipate substantial mechanical energy, endowing the heart valve with the high toughness as well.[90] The adhesion of soft connective tissues on bones can be extremely fatigue-resistant. For example, the cartilage−bone interface in the human knee joint can sustain compressive stresses of 1 MPa along with an interfacial toughness around 800 J m^{-2} over 1 million cycles of loads per year (Figure 2d).[80,91,92] The fatigue-resistant adhesion of soft tissues (e.g., tendons, ligaments, and cartilages) to rigid bones is commonly achieved through nanostructured interfaces composed of aligned collagen nanofibrils and ordered hydroxyapatite nanocrystals.[93−95] What are nature's design principles for various biological hydrogels besides the above-mentioned ones (Figure 2) to achieve extreme mechanical properties? This is still a largely unanswered question, even in light of the pioneering works in the field of polymers and soft materials (e.g., refs 53−65 and the references therein).

From the practical aspect, applications of hydrogels generally require the hydrogels to possess a set of specific properties. For example, hydrogels designed with different moduli and viscoelastic properties have been used to regulate stem cell fate and activity (Figure 3).[10,12,93,96] The applications of hydrogels as artificial cartilages and spinal discs require the hydrogels to be fatigue-resistant under cyclic mechanical loading.[75,76,97,98] The mesh size of hydrogels' polymer networks is critical to their applications in controlled drug delivery (Figure 3).[42,99,100] More recent applications of hydrogels as various devices and machines require the hydrogels to possess specific properties, for instance, stimuli-sensitivity for hydrogel sensors and actuators,[30,101−103] strong adhesion for hydrogel coatings,[49]

https://doi.org/10.1021/acs.chemrev.0c01088
Chem. Rev. XXXX, XXX, XXX−XXX

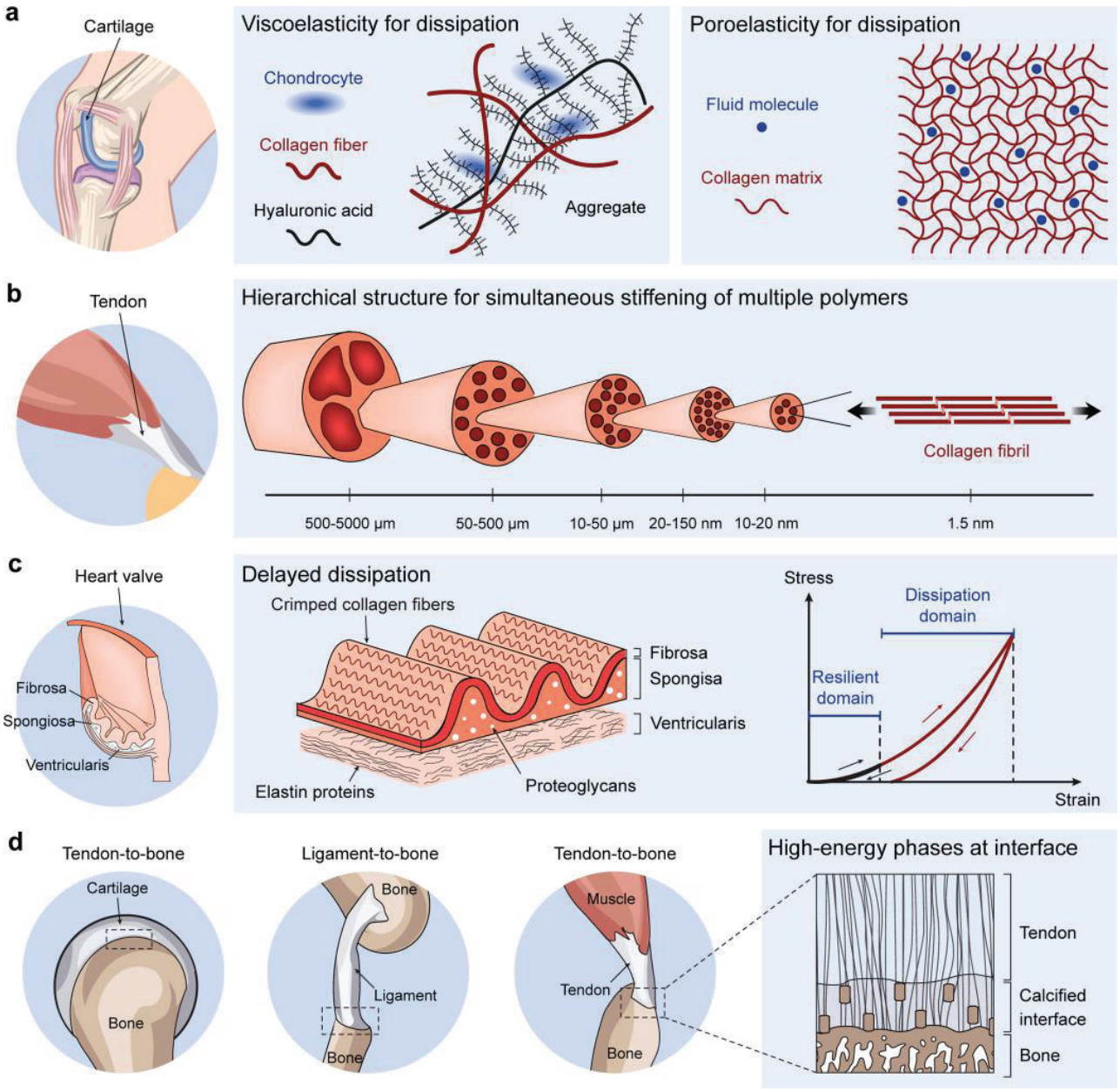

Figure 2. Design principles and implementation strategies for various biological hydrogels to achieve extreme mechanical properties: (a) high toughness of cartilage due to viscoelastic and poroelastic dissipation of the polymer networks,[82,108,109] (b) high tensile strength of tendon due to simultaneous stiffening of multiple polymers in the fibrous hierarchical structure,[85,105] (c) high resilience and facture toughness of heart valve due to delayed mechanical dissipation,[110,111] (d) high interfacial fatigue threshold of cartilage−/ligament−/tendon−bone interfaces due to intrinsically high-energy phases including nanocrystals and nanofibers strongly bonded on the interfaces.[78] Panel (a) is reproduced with permission from ref 108. Copyright 2006 American Chemical Society. Panel (b) is reproduced with permission from ref 85. Copyright 2013 Elsevier. Panel (c) is reproduced with permission from refs 110 and 111. Copyright 2014 PLoS and 2018 IntechOpen. Panel (d) is reproduced with permission from ref 78. Copyright 2020 Springer Nature.

optical transparency for hydrogel optics,[42] electrical conductivity for hydrogel electronics,[32] and water absorption/release for hydrogel water harvesters[104] (Figure 3).

Over the last few decades, intensive efforts have led to the development of a plethora of hydrogels that possess extreme mechanical properties using diverse material candidates, including various natural and synthetic polymers, nano-/micro-/macrofillers, and nano-/micro-/macrofibers. Whereas the properties of these hydrogels are remarkable, their design often follows the Edisonian approach—trial and error with specific material candidates. As the field rapidly evolves, emerging applications of hydrogels in biomedicine and machines (Figure 3) pose escalating demands on the rationally guided design of hydrogels beyond the Edisonian approach, so that one can select from diverse material candidates and fabrication methods to design the hydrogels achieving multiple combined extreme properties. However, a set of general principles capable of rationally guiding the design of hydrogels

https://doi.org/10.1021/acs.chemrev.0c01088
Chem. Rev. XXXX, XXX, XXX−XXX

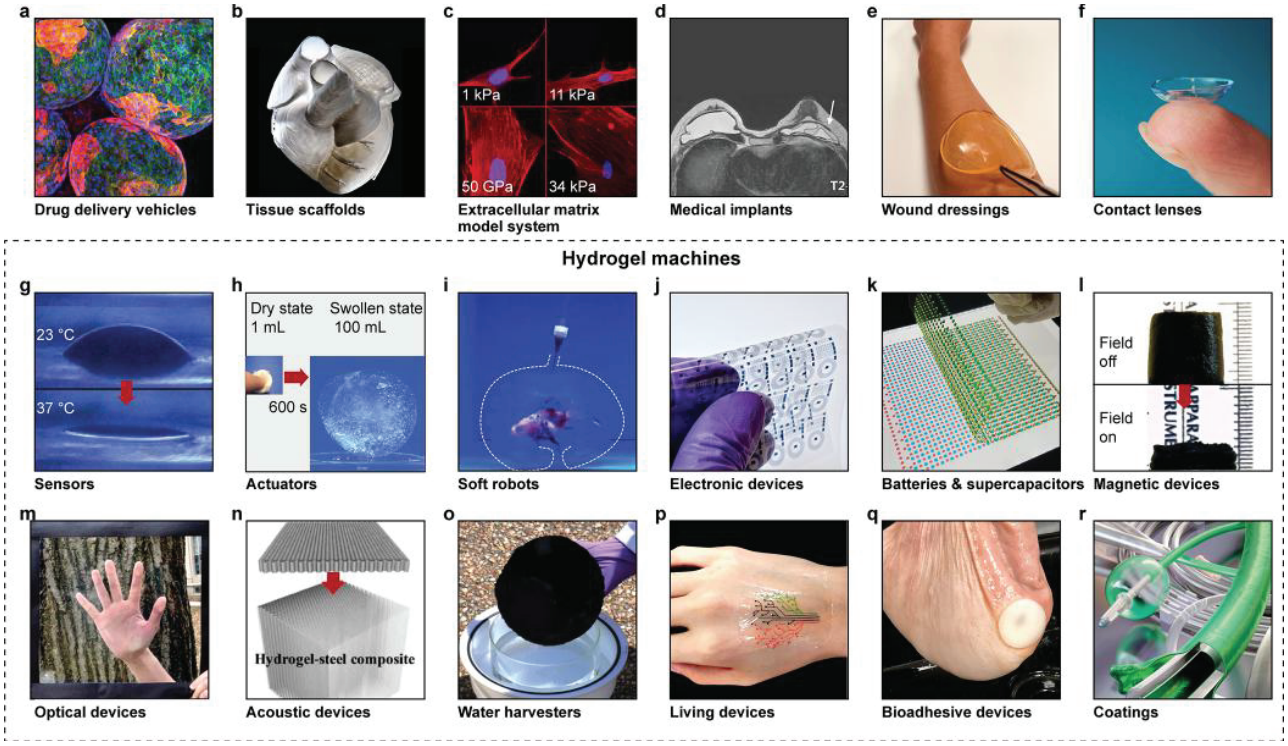

Figure 3. Hydrogels have been widely used in applications including (a) vehicles for drug delivery, (b) scaffolds for tissue engineering, (c) models for biological studies, (d) medical implants, (e) wound dressings, (f) contact lenses, (g) sensors, (h) actuators, (i) soft robots, (j) electronic devices, (k) batteries and supercapacitors, (l) magnetic devices, (m) optical devices, (n) acoustic devices, (o) water harvesters, (p) living devices, (q) bioadhesive devices, and (r) coatings. Panel (a) is reproduced with permission from ref 112. Copyright 2015 Springer Nature. Panel (b) is reproduced with permission from ref 113. Copyright 2019 American Association for the Advancement of Science. Panel (c) is reproduced with permission from ref 10. Copyright 2006 Elsevier. Panel (d) is reproduced with permission from ref 114. Copyright 2015 The Korean Society of Magnetic Resonance in Medicine. Panel (g) is reproduced with permission from ref 21. Copyright 2006 Springer Nature. Panel (h) is reproduced with permission from ref 115. Copyright 2019 Springer Nature. Panel (i) is reproduced with permission from ref 26. Copyright 2017 Springer Nature. Panel (j) is reproduced with permission from ref 116. Copyright 2020 Springer Nature. Panel (k) is reproduced with permission from ref 34. Copyright 2017 Springer Nature. Panel (l) is reproduced with permission from ref 28. Copyright 2011 National Academy of Sciences. Panel (m) is reproduced with permission from ref 43. Copyright 2019 Wiley. Panel (n) is reproduced with permission from ref 45. Copyright 2020 American Association for the Advancement of Science. Panel (o) is reproduced with permission from ref 104. Copyright 2018 Springer Nature. Panel (p) is reproduced with permission from ref 46. Copyright 2018 Wiley. Panel (q) is reproduced with permission from ref 47. Copyright 2020 Springer Nature. Panel (r) is reproduced with permission from ref 51. Copyright 2019 Wiley.

using different materials and fabrication methods for various applications remains a central need in the field of soft materials. In this review, we aim to provide

(i). A set of general principles for the rational design of hydrogels to achieve extreme mechanical properties, including extremely high fracture toughness, tensile strength, resilience, interfacial toughness, fatigue threshold, and interfacial fatigue threshold; and extreme physical properties, including high electrical conductivity, patterned magnetization, high refractive index and transparency, tunable acoustic impedance, and self-healing. The design principles are generally based on fundamental mechanics and physics (beyond polymers) and/or inspired by biological hydrogels (e.g., muscles, cartilages, tendons, and heart valves) (Figure 4).

(ii). A set of general strategies to implement the design principles discussed in (i) with various materials and fabrication methods using *unconventional polymer networks* (UPNs). The UPNs can be broadly categorized into UPN architectures including ideal polymer networks, polymer networks with slidable cross-links, interpenetrating and semi-interpenetrating polymer networks, polymer networks with high-functionality cross-links, and nano-/microfibrous polymer networks; and UPN interactions including strong physical cross-links, weak physical cross-links, and dynamic covalent cross-links (Figure 4).

(iii). A set of orthogonal design principles and synergistic implementation strategies for the design and fabrication of future hydrogels to achieve multiple combined mechanical, physical, chemical, and biological properties (Figure 4).

Notably, because the aforementioned design principles and implementation strategies for hydrogels are based on generic polymer networks, they are also applicable to other soft materials comprised of polymer networks, including elastomers and organogels (i.e., polymer networks infiltrated with organic solvents).[117−119] In fact, many extreme mechanical and physical properties were first achieved in other soft materials than hydrogels. For example, high values of fracture toughness, tensile strength, resilience, and interfacial toughness were realized in elastomers long before in hydrogels; ferromagnetic domains in soft materials were first programmed and 3D printed with elastomeric inks as well.[38,39]

https://doi.org/10.1021/acs.chemrev.0c01088
Chem. Rev. XXXX, XXX, XXX−XXX

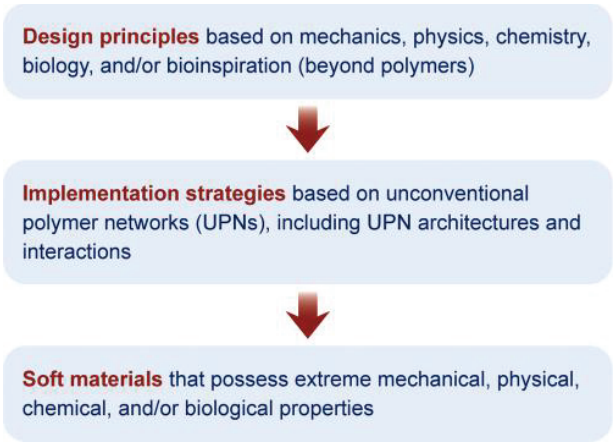

Figure 4. This review systematically discusses the design principles and implementation strategies for soft materials including hydrogels, elastomers, and organogels to achieve extreme properties.

The review is organized as follows. Section 2 will discuss a variety of natural polymers, synthetic polymers, and permanent covalent cross-links commonly used for the design and fabrication of hydrogels. Section 3 will introduce conventional polymer networks and then show that a number of mechanical properties of conventional polymer networks are coupled. Section 4 will define a set of unconventional polymer networks (UPNs), including both UPN architectures and UPN interactions, and then discuss that UPNs can provide decoupled mechanical properties. Thereafter, section 5 will systematically discuss the design principles for various extreme mechanical properties of hydrogels and the implemention strategies for the design principles using UPNs. Section 6 will briefly discuss the design principles and implementation strategies for hydrogels to achieve a set of extreme physical properties. In section 7, we will conclude the review by proposing the orthogonal design principles and synergistic implementation strategies to design future hydrogels that can achieve multiple combined mechanical, physical, chemical and biological properties.

2. COMMON POLYMERS AND CROSS-LINKS FOR HYDROGELS

A rich library of polymers and cross-links have been used for the design and fabrication of various hydrogels. These polymers can be broadly categorized into natural polymers and synthetic polymers. In this section, we will briefly discuss the commonly used natural polymers, synthetic polymers, and permanent covalent cross-links for hydrogels. We will discuss other types of cross-links for hydrogels in section 4.

2.1. Natural Polymers for Hydrogels

Naturally derived polymers have been widely used to compose the polymer networks of hydrogels (Figure 5a). Hydrogels based on natural polymers usually possess properties compatible with biological tissues due to the similarity in their compositions. In addition, the natural polymer networks can often degrade in and be absorbed by the body through metabolism and tissue remodeling processes. Furthermore, the majority of natural polymers have reactive sites amenable to cross-linking and modification, which can endow the corresponding hydrogels with tailored biological and/or mechanical properties. In this subsection, we will briefly discuss a few natural polymers commonly used for hydrogels. For more detailed discussions, a few classical reviews are recommended.[4−6,68,120]

2.1.1. Alginate. Alginate is a polysaccharide usually obtained from brown-algae cell walls and two kinds of bacteria, *Azotobacter* and *Pseudomonas*.[121] Alginate is known to be a family of linear copolymers containing blocks of β-(1 → 4)-linked D-mannuronic (M) and α-(1 → 4)-linked L-guluronic acid (G) residues. The blocks are composed of consecutive G residues (GGGGGG), consecutive M residues (MMMMMM), and alternating M and G residues (GMGMGM).[122] Alginate hydrogels can be formed with various covalent and physical cross-links. In particular, the ionic cross-links have been widely used for alginate hydrogels because the G blocks[123] (and GM blocks[124]) in alginate can be readily bound with one another by divalent cations such as Ca^{2+}, Mg^{2+}, Ba^{2+}, and Sr^{2+}.[125−127] The mechanical properties of alginate hydrogels can be tuned to match those of various biological tissues by changing different parameters, such as the molecular weight, polymer concentration, chemical modification, G/M ratio, and type or density of cross-links.[123,128] Alginate hydrogels have been widely used as scaffolds in tissue engineering, such as in intervertebral disk regeneration,[129] adipose tissue regeneration,[130] cardiac regeneration,[131] and liver regeneration[132] since alginate allows the formation of hydrogels under physiological conditions and thus enables easy cell and drug encapsulation.

2.1.2. Hyaluronic Acid. Hyaluronic acid (also known as hyaluronan or hyaluronate) is a linear polymer of disaccharides, which is composed of D-glucuronic acid and *N*-acetyl-D-glucosamine, linked together via alternating β-(1 → 4)-linked and β-(1 → 3)-linked glycosidic bonds.[133,134] Hyaluronic acid is present in all mammals, especially in various soft connective tissues, acting as a space filler, lubricant, and/or osmotic buffer.[135] Hyaluronic acid can be covalently cross-linked into hydrogels by various hydrazide derivatives.[136,137] The abundant carboxyl and hydroxyl groups on the polysaccharide structure of hyaluronic acid also offer many active sites for chemical modifications.[138] For example, hyaluronic acid can be modified with thiol,[139,140] haloacetate,[141] dihydrazide,[136,142] aldehyde,[143,144] and tyramine[145] groups, which can react with corresponding covalent cross-linkers through addition or condensation reactions.[146] As another example, hyaluronic acid can also be modified by methacrylic anhydride or glycidyl methacrylate to possess reactive methacrylic groups, which can be polymerized by radical polymerization.[147−149] Owing to the naturally derived, nonimmunogenic, biodegradable, and non-adhesive properties,[150−152] hyaluronic acid hydrogels have been widely used as scaffolds in cell therapy and tissue engineering, such as in cell delivery,[153] molecule delivery,[154,155] stem cell therapy,[156,157] cartilage engineering,[154,158] cardiac repair,[159] and valvular engineering.[160]

2.1.3. Collagen. Collagen is one of the major proteins in animal bodies. There are approximately 29 types of collagens discovered so far.[161] The structures of collagens can be defined at different levels, including primary structure (amino acid triplet), secondary structure (α-helix), tertiary structure (triple helix), and quaternary structure (fibril).[162,163] The primary structure of collagen is the tripeptide sequence of −(Gly−X−Y−)$_n$−, where Gly is glycine, X and Y are other amino acids than Gly. The sequence of the amino acids governs how the peptide folds into a secondary structure, mainly left-handed α-helix, which is stabilized by the hydrogen bonds between amino acid residues.[164] Three left-handed α-helix polypeptide chains then form a tertiary structure via the aldol condensation cross-linking,

https://doi.org/10.1021/acs.chemrev.0c01088
Chem. Rev. XXXX, XXX, XXX−XXX

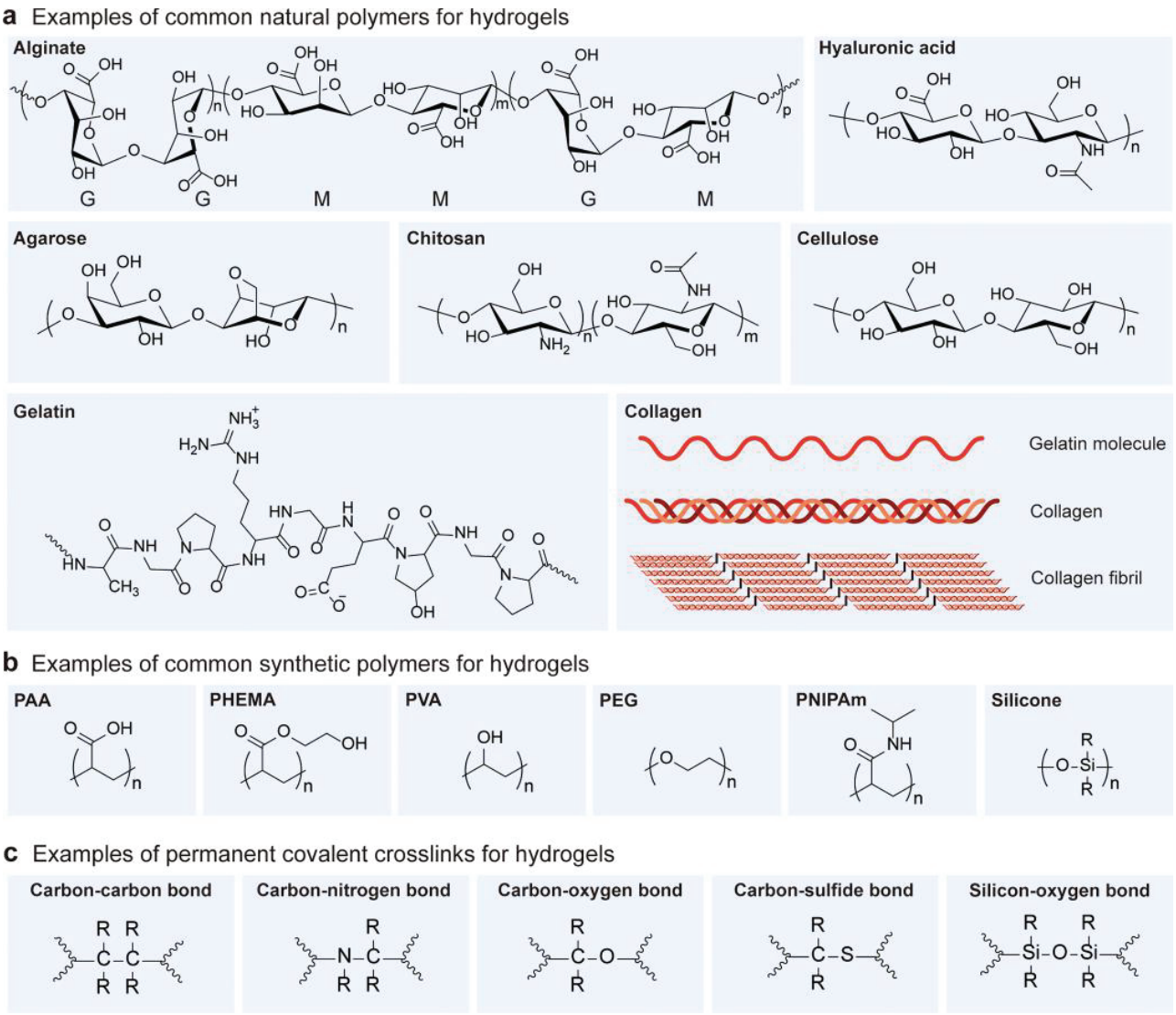

Figure 5. Chemical structures and schematics of typical examples of (a) common natural polymers, (b) common synthetic polymers, and (c) permanent covalent cross-links for hydrogels. R represents an organyl substituent or hydrogen.

aldehyde amine condensation cross-linking, and aldol histidine cross-linking.[165] The triple strands can further self-assemble into a collagen fiber as the quaternary structure.[166]

Acid-solubilized collagens can self-assemble to form physically cross-linked hydrogels when the collagen solutions are neutralized and heated. Since the physically cross-linked collagen hydrogels are usually mechanically weak and thermally unstable,[167,168] they have been strengthened and stabilized with chemical cross-links such as glutaraldehyde, genipin, carbodiimides, and diphenylphosphoryl azide.[169−171] Collagens can be biodegraded by collagenases and metalloproteases; the cross-linked collagens usually have slower degradation rates than the un-cross-linked collagens.[172] Because collagens usually have low antigenicity, low inflammatory response, good biocompatibility, and natural cell-adhesive motifs,[173−175] collagen hydrogels have been widely used as scaffolds for drug and protein delivery[176,177] and for reconstructions of liver,[178] skin,[179] blood vessel,[180] small intestine,[181] cartilage,[182] vocal cord,[183] and spinal cord.[184]

2.1.4. Gelatin. Gelatins are naturally derived polymers obtained through breaking the triple-helix structures of collagens into single-strand molecules. There are two types of gelatins, type A and type B, which are obtained with acid and alkaline treatments of collagens, respectively.[185] Gelatins can be physically cross-linked by simply reducing the temperature of aqueous solutions of gelatins below a certain temperature.[186,187] The physically cross-linked gelatins are usually unstable for long-term biomedical applications under physiological conditions. To further stabilize the physically cross-linked gelatin hydrogels, covalent cross-linkers[188] such as aldehydes (e.g., formaldehyde, glutaraldehyde, and glyceraldehyde),[189,190] polyepoxides,[191] and isocyanates[192] have been widely used to react with and bridge the free amine groups (from lysine and hydroxylysine) and free carboxylic acids (from glutamic and aspartic acid) on the gelatin molecules. Besides the introduction of covalent cross-linkers, the gelatin backbones can also be modified by methacrylates to form covalently cross-linked gelatin methacryloyl hydrogels.[193] In addition, synthetic polymers can also be coupled on gelatin chains through the grafting-from,[194] grafting-to,[195] and grafting-through[196] methods to enhance the mechanical properties of gelatin hydrogels. Furthermore, the

https://doi.org/10.1021/acs.chemrev.0c01088
Chem. Rev. XXXX, XXX, XXX−XXX

gelatin molecules tend to form physical interactions with various dopants, such as carbon nanotubes,[197] graphene oxide,[198] inorganic nanoparticles, and minerals.[199,200] The aforementioned covalent cross-links, modifications, and interactions can significantly improve the mechanical properties of gelatin hydrogels.[189,201] The easy gelation process and the excellent biocompatibility of gelatin hydrogels make them attractive for biomedical applications, such as drug delivery[202] and tissue engineering.[203,204]

2.1.5. Fibrin. Fibrin is a naturally derived polymer obtained from thrombin-treated fibrinogen.[205] Fibrin is involved in the natural wound healing process by forming extensive fibrous networks. Fibrin can form clots or hydrogels when mixing fibrinogen and thrombin solutions at the room temperature.[206] The resultant fibrin hydrogels usually have weak mechanical properties due to the nature of physical cross-links. To improve the mechanical properties of fibrin hydrogels, chemical cross-linkers such as genipin can be introduced to cross-link the amine residues on fibrin proteins, which subsequently form stable covalently cross-linked networks.[207] In addition, fibrin hydrogels can also be combined with synthetic polymers such as polyurethane,[208] polycaprolactone,[209] β-tricalciumphosphate,[210] and polyethylene glycol[211] to enhance the mechanical strength of the hydrogels. Fibrin hydrogels have been widely used as tissue sealants and adhesives to control bleeding in surgery,[212] and as scaffolds for cardiac tissue engineering,[213] neurological regeneration,[214] ocular therapy,[215] cartilage and bone reparation,[216,217] muscle tissue engineering,[218] and exogenous delivery in wound healing.[219] In particular, fibrin hydrogels can be produced autologously from a patient's own blood, thereby reducing the risk of foreign-body reactions.[220]

2.1.6. Agarose. Agarose is a neutral polysaccharide composed of β-D-galactopyranosyl and 3,6-anhydro-α-L-galactopyranosyl, mainly extracted from red algae (Rhodophyceae).[221] As a thermoresponsive polymer, agarose can be heated to dissolve in water and then cooled down to form a hydrogel. During this gelation process, the agarose structure changes from a random-coil configuration to bundles of associated double helices with multiple-chain aggregation in the junction zone.[222,223] The gelling temperature and mechanical properties of agarose hydrogels can be tuned by changing the concentration, molecular weight, and structure of the agarose in the hydrogels.[224,225] Agarose hydrogels have been used as scaffolds for cell encapsulation,[226] cartilage reparation,[227] and nerve regeneration,[228] due to its low immunoreaction in human bodies.[229] Notably, since the native agarose does not possess cell adhesion motifs, cell adhesion peptides have been covalently conjugated to the agarose backbone to enhance the interactions between cells and agarose hydrogels.[230]

2.1.7. Chitosan. Chitosan is a linear polysaccharide composed of β-(1 → 4)-linked D-glucosamine and *N*-acetyl-D-glucosamine. Chitosan is mainly prepared by partial deacetylation of chitin (obtained from crab and shrimp shells) to less than 40% of *N*-acetyl-D-glucosamine residues.[231,232] The physical, chemical, and biological properties of chitosan materials are highly related to the molecular weight and the degree of deacetylation of chitosan.[233,234] Chitosan can form physically cross-linked hydrogels by hydrophobic interaction, hydrogen bonding,[235,236] metal coordination (with metal ions such as Pt(II), Pd(II), Mo(VI)[237,238]), and electrostatic interaction (with multivalent anions such as sulfate, citrate, and phosphate ions;[239,240] with anionic polyelectrolytes[231] such as polysaccharides,[241,242] proteins,[243,244] and synthetic polymers[245]). These physically cross-linked chitosan hydrogels usually have weak mechanical properties and short lifetime, which are also highly influenced by pH, temperature, and ionic strength.[232,246] To enhance the mechanical properties and stability of chitosan hydrogels, covalent cross-linkers have been introduced into the hydrogels. The commonly used covalent cross-linkers include dialdehydes,[247,248] formaldehyde,[249] diglycidyl ether,[250] and genipin,[251,252] which can react with the residual functional groups (such as OH, COOH, and NH_2) on chitosan backbones to form the amide bonds, ester bonds, and Schiff base linkages.[235,253,254] In addition, chitosan can also be modified with methacrylate or aryl azide groups to form photo-cross-linkable macromers.[255] The gelation degree and mechanical properties of these photo-cross-linkable chitosan hydrogels can be controlled by UV irradiation time and intensity.[256−258] Furthermore, chitosan hydrogels can be modified with biofunctional ligands such as Arg-Gly-Asp (RGD) peptides to facilitate cell adhesion and proliferation.[259,260] Chitosan hydrogels have been widely used in biomedical applications such as drug delivery,[261] cell encapsulation,[262] neural tissue engineering,[263] and bone regeneration,[262] owing to their excellent biocompatibility and biodegradability.[264]

2.1.8. Cellulose. Cellulose is the most abundant natural polysaccharide and the main constituent of plants and natural fibers such as cotton and linen.[265−267] Some bacteria such as acetobacter xylinum are also able to produce cellulose.[268] Cellulose consists of β-(1 → 4)-linked D-glucose units, which result in cellulose's high crystallinity (over 40%) and difficulty in dissolving in water and other common solvents.[269] Solvents such as *N*-methylmorpholine-*N*-oxide,[270,271] ionic liquids,[272,273] and alkali/urea (or thiourea) aqueous systems[274,275] have been developed to dissolve native cellulose. Cellulose can also be modified through partial esterification or etherification of the hydroxyl groups on the backbone.[265] These cellulose derivatives, including methyl cellulose,[276] hydroxypropyl cellulose,[277] hydroxypropylmethyl cellulose,[278,279] and carboxymethyl cellulose[280] are easier to dissolve and process compared to the native cellulose.

Cellulose and its derivatives can be chemically cross-linked to form stable three-dimensional networks. Bifunctional and multifunctional molecules, such as 1,2,3,4-butanetetracarboxylic dianhydride,[281] succinic anhydride,[282] citric acid,[283] epichlorohydrin,[284] ethylene glycol diglycidyl ether,[285] and divinyl sulfone[286] can form covalent ester or ether bonds between cellulose chains. Cellulose chains can also be covalently cross-linked by the irradiation of electron beams and γ rays,[287,288] which avoids the usage of toxic cross-linkers and allows the simultaneous sterilization of the resultant hydrogels. Cellulose and its derivatives can also be blended with natural polymers, such as chitosan,[289] starch,[290] alginates[291] and hyaluronic acid,[292] or synthetic polymers such as polyethylene glycol,[293] poly(vinyl alcohol,)[294] and poly(*N*,*N*-dimethylacrylamide)[295] to form interpenetrating polymer networks with excellent mechanical properties. Notably, bacterial cellulose produced from certain bacterial species such as acetobacter xylinum can directly form cellulose hydrogels with high purity and tensile strength.[296,297] Since cellulose-based hydrogels are proven to have superior hydrophilicity, biodegradability, biocompatibility, and transparency, they have been widely used in drug delivery,[298] tissue engineering,[299] blood purification,[300] strain sensors,[301] as well as water purification.[302]

https://doi.org/10.1021/acs.chemrev.0c01088
Chem. Rev. XXXX, XXX, XXX−XXX

2.2. Synthetic Polymers for Hydrogels

In addition to natural polymers, synthetic polymers have been widely used for the design and fabrication of hydrogels (Figure 5b). The synthetic polymer networks of hydrogels are commonly formed by copolymerization of monomers for the polymer backbones and cross-linkers, or by reactions of synthetic polymers, macromers, and/or cross-linkers.

2.2.1. Poly(acrylic acid). Poly(acrylic acid) (PAA) is a linear polymer prepared by radical polymerization of acrylic acid monomers. The backbone of PAA contains a large number of carboxyl groups. PAA can form hydrogels through covalent and physical cross-linking. Covalently cross-linked PAA hydrogels are usually formed by copolymerization of di/multivinyl cross-linkers together with acrylic acid monomers.[303] In addition, the carboxyl groups of PAA can form physical interactions with various doping agents such as clay,[304] graphene oxide,[305] and cations,[306] which can act as physical cross-links for PAA hydrogels; the carboxyl groups can also form hydrogen bonds between PAA chains and introduce self-healing or self-adhesive properties to PAA hydrogels.[307] Furthermore, the abundant carboxyl groups on PAA can associate with water molecules to facilitate the absorption of water by PAA hydrogels.[115] Since the carboxyl groups are sensitive to pH and ionic strength, the equilibrium swelling ratio of PAA hydrogels is affected by the pH and ionic strength of the solutions for the hydrogels.[308,309] PAA hydrogels can also incorporate other linear polymers, such as biological polymers, to form various adhesives and hydrogels for biomedical applications.[47,310]

2.2.2. Poly(2-hydroxyethyl methacrylate). Poly(2-hydroxyethyl methacrylate) (PHEMA) hydrogels can be prepared by free-radical polymerization of 2-hydroxyethyl methacrylate (HEMA) monomers with covalent cross-linkers such as trimethylene glycol dimethacrylate (TEGDMA), initiators such as sodium pyrosulfite (SMBS), and ammonium persulfate (APS). The HEMA monomers can also be copolymerized with acrylic or acrylamide monomers to control the swelling and mechanical properties of the resultant hydrogels.[311] PHEMA hydrogels are optically transparent and mechanically stable in the physiological environments. Pure PHEMA hydrogels are also resistant to cell adhesion and difficult to degrade in the physiological environments; however, various biofunctional and bioactive motifs can be coupled onto the hydrogels to improve their cell interactions and degradability.[312,313] PHEMA hydrogels are famous for their ophthalmic applications such as contact lens[314] and artificial cornea.[315]

2.2.3. Poly(vinyl alcohol). Poly(vinyl alcohol) (PVA) is mainly obtained from the partial hydrolysis of poly(vinyl acetate).[316] PVA can form stable and elastic hydrogels through either physical or covalent cross-linking.[317,318] The physically cross-linked PVA hydrogels are commonly obtained by repeated freezing and thawing of PVA solutions,[319] which give elastic, tough, strong, and fatigue-resistant PVA hydrogels.[76,78,320] PVA can also be covalently cross-linked through the use of difunctional cross-linkers such as glutaraldehyde, epichlorohydrin, boric acid, and dialdehyde.[321,322] Electron-beam and gamma irradiation can also cross-link PVA to avoid residual covalent cross-linkers in the hydrogels.[323] Pure PVA hydrogels are nonadhesive to cells, but several oligopeptide sequences can be conjugated onto the backbones of PVA hydrogels to enhance their cellular interactions.[324] PVA hydrogels have been extensively studied and used in biomedical applications,[325,326] such as articular cartilage replacement and regeneration.[327,328]

2.2.4. Poly(ethylene glycol) or Poly(ethylene oxide). Poly(ethylene glycol)(PEG) is usually obtained from the anionic or cationic polymerization of ethylene oxide. When the PEG has a molecular weight more than 10 kDa, it is also named poly(ethylene oxide) (PEO) since the end groups are negligible.[329] There are various methods to cross-link PEG polymers into hydrogels. The ends of PEG chains can be modified with unsaturated groups, such as acrylate or methacrylate ends, and then be used as macro-cross-linkers to form hydrogels with other unsaturated monomers by the photo-/UV-induced radical polymerization.[330,331] PEG can also form hydrogels by electron beam irradiation via radiation-induced free radical processes.[332] Furthermore, the end groups of the PEG chain can be modified with various reactive pairs, such as *N*-hydroxysuccinimide/NH_2,[333] maleimide/thiol,[334] and acetylene/azide.[335] Since these functional chain-end motifs usually have high reaction efficiency and fast reaction kinetics, the obtained hydrogels by the coupling reactions of these groups can give relatively well-defined network architectures.[74]

PEG polymers can also form physically cross-linked networks. Similar to the chemical cross-linking method, the ends of PEG chains can be modified with various motifs for physical cross-linking. For example, nucleobase pairs of adenines and thymines,[336] ureido-pyrimidinone (UPy) units,[337] or host−guest molecules[338] can be introduced onto the chain-ends of PEG molecules to prepare physically cross-linked PEG hydrogels. These physically cross-linked PEG hydrogels can exhibit switchable, self-healable, or stimuli-responsive properties and high mechanical strength.[339] Besides the modification and utilization of chain-end groups, physically cross-linked PEG hydrogel can also be prepared by using PEG block copolymers.[340] PEG-*b*-PPG (poly(propylene glycol)) is one of the most widely used PEG-derived block copolymers to prepare thermoresponsive physical hydrogels.[341] These physical hydrogels are formed by the hydrophobic interaction of the PPG blocks. The phase transition behavior of these hydrogels can be optimized by balancing the hydrophobic PPG blocks and the hydrophilic PEG blocks. On the basis of the same gelation mechanism, PEG block copolymers with poly(DL-lactic acid) (PDLLA),[342] poly(dl-lactic acid-*co*-glycolic acid) (PLGA),[343,344] polylactide (PLA),[345] poly(caprolactone) (PCL),[346] and poly(propylene sulfide) (PPS)[347] can also form physically cross-linked hydrogels with injectable or stimuli-responsive properties. PEG, as well as its derivatives, are widely used in biomedical applications due to their nontoxic and nonimmunogenic properties.[348] While the inert biological property of PEG hydrogels can prevent undesired interactions between native PEG hydrogels and cells,[349,350] PEG hydrogels can also be modified with various bioactive conjugations such as growth factors[351] and cell-adhesive peptides[352] through Michael-type addition[353,354] or click chemistry.[350] PEG hydrogels with these bioactive molecules can facilitate their biomedical applications[355] such as drug or cell delivery[356,357] and tissue engineering.[358]

2.2.5. Poly(*N*-isopropylacrylamide). Acrylamide and its derivatives have been widely used to prepare hydrogels by radical copolymerization with cross-linkers. One interesting hydrogel based on acrylamide and its derivatives is the poly(*N*-isopropylacrylamide) (PNIPAm) hydrogel. Un-cross-linked linear PNIPAm exhibits a coil-to-globule phase transition in aqueous solutions when the temperature is raised above a critical temperature.[359,360] The PNIPAm can be covalently cross-linked by cross-linkers such as bis-acrylamide derivatives through the

https://doi.org/10.1021/acs.chemrev.0c01088
Chem. Rev. XXXX, XXX, XXX−XXX

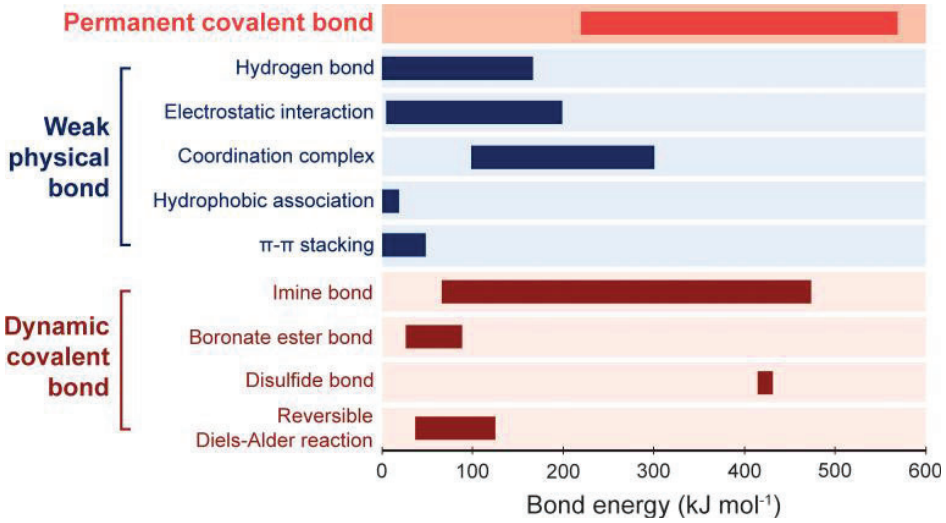

Figure 6. Bond energies of various types of permanent covalent cross-links,[385−387] weak physical cross-links,[388−391] and dynamic covalent cross-links.[387,392−396]

radical polymerization process. The cross-linked PNIPAm hydrogels also possess reversible thermoresponsive behavior with a critical temperature of around 34 °C,[361] above which the hydrogel structure will collapse and exude water.[362,363] While the thermoresponsive behavior of PNIPAm hydrogels is usually slow, many studies have improved the phase-transition speed of PNIPAm hydrogels by incorporating porous structures during the hydrogel formation.[364,365] The thermoresponsive PNIPAm hydrogels can be used as actuators for soft robotics,[366] injectable scaffolds for tissue engineering,[367] and thermoresponsive substrates for on-demand detachment of cell sheets.[368,369]

2.2.6. Silicone. Silicone hydrogels are hydrogels that contain silicone polymers as one of its polymer components.[370] Silicone polymers are commonly hydrophobic.[371] In order to form silicone hydrogels, hydrophilic monomers and/or polymers have been introduced into the silicone matrix by blending or copolymerization to improve the hydrophilicity of silicone hydrogels.[14,372,373] For example, hydrophilic polymers such as PHEMA can be blended directly into the silicone polymer matrix, forming a hydrophilic interpenetrating polymer network.[374] Hydrophilic monomers such as *N*-vinylpyrrolidone (NVP) can be copolymerized with silicon macromers to form hydrophilic silicone hydrogels.[375] Hydrophilic polymer segments such as PEG[376] can also be copolymerized onto silicone segments to form block-modified[377,378] or graft-modified[379] hydrophilic silicone hydrogels. Since these hydrophilic silicone hydrogels usually have excellent gas permeability as well good biocompatibility, they have been used in biomedical applications such as contact lenses,[14,380] histological engineering materials,[381,382] and drug-delivery carriers.[383,384]

2.3. Permanent Covalent Cross-Links for Hydrogels

In this subsection, we will discuss permanent covalent cross-links that are commonly used in hydrogels (Figure 5c). We will discuss other types of cross-links in section 4. The energy of permanent covalent cross-links ranges from 220 kJ mol^{-1} to 570 kJ mol^{-1} (Figure 6).[385−387]

2.3.1. Carbon−Carbon Bonds. The energy of the carbon−carbon bond is around 300 kJ mol^{-1} to 450 kJ mol^{-1}.[385−387] Hydrogels covalently cross-linked by carbon−carbon bonds are usually formed by radical copolymerization of monomers and di-/multivinyl cross-linkers. The cross-linkers can be small molecules with two double bonds such as *N,N′*-methylenebis-(acrylamide) (MBA) or macromolecules with several acrylate groups.[6,397] These cross-linkers are compatible with various initiation and polymerization systems.[4,254,398] For example, photoradical initiators can be added into the prepolymerization solution together with monomers and di-/multivinyl cross-linkers.[318,399,400] Once the initiator is irradiated by UV light, radicals will be generated to initiate the polymerization of the double bonds on monomers as well as cross-linkers.[401,402] As a result, hydrogels can be formed in situ and with patterned structures or biological functions.[399,403] The polymerization of vinyl monomers and cross-linkers can also be carried out with a system composed of peroxydisulfate and *N,N,N′N′*-tetramethylene-diamine (TEMED), where TEMED can accelerate the decomposition of peroxydisulfate to generate a large number of radicals.[404] This initiation and polymerization system can effectively and rapidly form various hydrogels under room temperature.

The carbon−carbon cross-links of hydrogels can also be formed by high-energy irradiation (e.g., gamma and electron beams). Similar to UV light, high-energy radiation can be used to polymerize unsaturated compounds such as monomers and cross-linkers with vinyl groups or acrylate groups.[405,406] High-energy radiation can also cross-link polymers without unsaturated bonds,[407] because radicals can be generated from the homolytic scission of the polymer chains under high-energy radiation. The radiolysis of water molecules in the solvent can also generate hydroxyl radicals that attack polymer chains to form macroradicals.[408] These radicals can then undergo recombination and termination to form covalent polymer networks cross-linked by carbon−carbon bonds.

2.3.2. Carbon−Nitrogen Bonds. The energy of the carbon−nitrogen bond is around 300 kJ mol^{-1} to 430 kJ mol^{-1}.[385−387] Hydrogels covalently cross-linked by carbon−nitrogen bonds are usually formed by highly effective chemical reactions of complementary groups. For example, the amide bonds have been widely used as the covalent cross-links for hydrogels by the condensation reactions between amines with carboxylic acids and derivatives.[409] *N*-Hydroxysuccinimide (NHS) and *N,N*-(3-(dimethylamino)propyl)-*N*-ethyl carbodii-

https://doi.org/10.1021/acs.chemrev.0c01088
Chem. Rev. XXXX, XXX, XXX−XXX

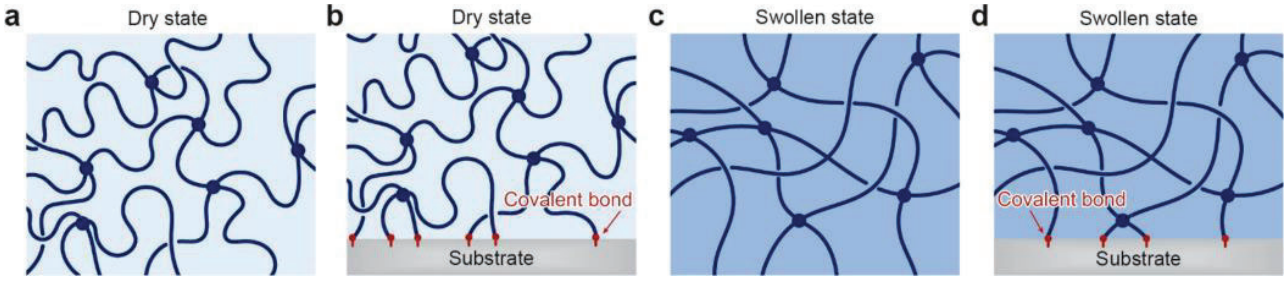

Figure 7. Schematics of a conventional polymer network (a) in the dry state and (b) covalently bonded on a substrate, and (c) in the swollen state and (d) covalently bonded on a substrate.

mide (EDC) are widely used to facilitate the condensation reaction of amines with carboxylic acids.[74] The addition of NHS and EDC will also suppress possible side reactions and give better control of the cross-link density in the hydrogels.[410] The carbon−nitrogen bonds can also be formed through the addition reactions of amines with electrophiles such as adipic acid dihydrazide and diisocyanate cross-linkers.[6,120,411] These difunctional cross-linkers have been widely used to cross-link natural macromolecules due to the high reaction efficiency. The mechanical properties of the resultant hydrogels can be controlled by tuning the concentration and ratio of the polymers and the cross-linking agents. Another category of reactions that can form carbon−nitrogen cross-links for hydrogels is the azide−alkyne cycloaddition reaction, which is one typical click reaction to connect alkyne and azide into triazole. The click reaction has a high efficiency without side reactions.[412] Furthermore, the azide−alkyne cycloaddition can be conducted in the absence of metal catalysis,[413] expanding the applicability of the azide−alkyne cycloaddition for preparing biocompatible hydrogels.

2.3.3. Carbon−Oxygen Bonds. The energy of the carbon−oxygen bond is around 280 kJ mol^{-1} to 370 kJ mol^{-1}.[385−387] The most common carbon−oxygen bond is the ester bond formed by the reactions between hydroxyl groups and carboxylic acids or derivatives.[414] Such ester cross-links can be hydrolyzed easily and make the hydrogels degradable under ambient temperature and physiological conditions. Besides the ester cross-links, the carbon−oxygen bonds are also present in ether groups and urethane groups, which can become cross-links due to the reaction between side groups on polymers (such as hydroxyl groups on polysaccharides and PVA) and reactive cross-linkers (such as glutaraldehyde,[415,416] divinyl sulfone,[417] dibromide,[418] and diisocyanate[419]).

2.3.4. Carbon−Sulfide Bonds. The energy of the carbon−sulfide bond is around 220 kJ mol^{-1} to 310 kJ mol^{-1}.[387] The covalent cross-linking of hydrogels through carbon−sulfide bonds is mainly formed by the thiol-click reactions.[420,421] The inherent electron density of the sulfide atom makes thiols prone to react with many functional groups through a radical or catalyzed process.[422,423] Thiol groups can be easily converted into nucleophilic thiolates or electrophilic thiyl radicals, which then proceed with nucleophilic reactions or radical chain processes to achieve the thiol-click reactions.[424] Specifically, for the radical thiol-click reactions, the thiol group can be activated by heat and/or UV light to generate radicals that initiate the radical-mediated thiol−ene or thiol−yne reactions.[425] For the nucleophilic thiol-click reactions initiated by strong bases, the thiol groups can readily react with electron-poor ene-functional compounds through the Michael addition, with isocyanates derivatives through carbonyl addition, with halide through S_N2 nucleophilic substitution, and with epoxy motifs through S_N2 ring-opening reactions.[426−429] The thiol-click reactions commonly have a high efficiency and high conversion rate without any side products, even in the presence of water, ions, and oxygen. The thiol-click reactions have been extensively used to prepare hydrogels for various biomedical applications.[430,431]

2.3.5. Silicon−Oxygen Bonds. The energy of the silicon−oxygen bond is around 420 kJ mol^{-1} to 570 kJ mol^{-1}.[385−387] The silicon−oxygen bonds are mainly used in the formation of silicone-based hydrogels[376,432,433] and can usually enhance the mechanical properties of the silicone-based hydrogels.[434] In addition, silicon−oxygen bonds have been widely used to form strong bonding between hydrogels and diverse engineering materials with modified surfaces such as salinized surfaces.[49]

3. CONVENTIONAL POLYMER NETWORKS

As illustrated in Figure 7, a conventional polymer network is defined as polymer chains cross-linked via permanent covalent bonds into a network, in which entanglements, physical cross-links, and reversible cross-links of the polymer chains are negligible.[54,57,62] Conventional polymer networks have provided the basic models for the development of unentangled rubber elasticity, including the affine network model and the phantom network model.[54,57,62] Conventional polymer networks have also been widely adopted in synthetic hydrogels, although biological hydrogels (Figures 1 and 2) generally rely on unconventional polymer networks which will be discussed in section 4.

3.1. Conventional Polymer Networks in the Dry State

In the dry state (Figure 7a), a conventional polymer network contains n polymer chains per unit volume, where a polymer chain is defined as the segment of polymer between two successive covalent cross-links. Each polymer chain contains N Kuhn monomers, and the length of each Kuhn monomer is b. The end-to-end distances of a polymer chain at the relaxed and fully stretched states are $\sqrt{N}b$ and Nb, respectively. Therefore, the stretch limit of the polymer chains λ_{lim} in the dry polymer network can be calculated as[54,57,62]

$$\lambda_{lim} = \frac{Nb}{\sqrt{N}b} = N^{1/2} \quad (1)$$

The stretch limit of the bulk polymer network scales with the chain stretch limit λ_{lim}, and the prefactor of the scaling relation depends on the polymer network architecture.[61]

Assuming that the dry polymer network follows the affine network model, the shear modulus of the network under initial deformation can be expressed as[54,57,62]

https://doi.org/10.1021/acs.chemrev.0c01088
Chem. Rev. XXXX, XXX, XXX−XXX

$$G = nkT \tag{2}$$

where k is the Boltzmann constant and T is the absolute temperature.

Following the Lake−Thomas model,[56] the fracture toughness of the dry polymer network is its intrinsic fracture energy Γ_0, which is the energy required to fracture a single layer of polymer chains per unit area,

$$\Gamma_0 = n\sqrt{N}b \cdot NU_f = nbN^{3/2}U_f \tag{3}$$

where $n\sqrt{N}b$ is the number of polymer chains per unit area, NU_f is the energy required to fracture a polymer chain, and U_f is the energy required to fracture a single Kuhn monomer.

Also on the basis of the Lake−Thomas model,[55,56] the fatigue threshold of the dry polymer network is the intrinsic fracture energy Γ_0. If the dry polymer network is covalently bonded on a substrate (Figure 7b), both the interfacial toughness and the interfacial fatigue threshold of the adhesion are on the level of Γ_0 as well.[49,78,435]

By substituting the typical values of b, N, n, kT, and U_f into eqs 1−3, we can estimate that the shear modulus G can be on the order of kilopascals to megapascals, the chain stretch limit λ_{lim} can reach up to a few tens (without entanglement), and the intrinsic fracture energy Γ_0 can reach up to a few hundreds of joules per meter squared.[62]

The mechanical properties of the dry polymer network are coupled with one another. It is commonly assumed that the polymer chains occupy the major volume of the polymer network in the dry state, and therefore the volume conservation of the polymer network gives

$$Nnv = 1 \tag{4}$$

where v is the volume of a Kuhn monomer.

By substituting eq 4 into eqs 1−3, we can express the chain stretch limit λ_{lim}, shear modulus G, and intrinsic fracture energy Γ_0 of a conventional polymer network in the dry state as functions of its chain length N,

$$\lambda_{lim} = N^{1/2}, \quad G = N^{-1}v^{-1}kT, \quad \Gamma_0 = N^{1/2}v^{-1}bU_f \tag{5}$$

From eq 5, it is evident that enhancing the chain length N increases the chain stretch limit λ_{lim} and the intrinsic fracture energy Γ_0 but decreases the shear modulus G of the conventional polymer network in the dry state. These mechanical properties of the conventional polymer network in the dry state are coupled through the following relation,

$$\lambda_{lim} \sim \Gamma_0 \sim G^{-1/2} \tag{6}$$

3.2. Conventional Polymer Networks in the Swollen State

A dry conventional polymer network with the parameters discussed in section 3.1 can imbibe water and swell into a hydrogel composed of the conventional polymer network and water (Figure 7c). The swelling of the dry polymer network stretches polymer chains in the network by a ratio of λ_s, named the chain stretch of swelling.

Since the swelling of the dry polymer network stretches its polymer chains by a ratio of λ_s, the end-to-end distance of a polymer chain in the hydrogel at the relaxed and fully stretched states are $\lambda_s\sqrt{N}b$ and Nb, respectively. Therefore, the stretch limit of polymer chains λ_{lim} in the hydrogel can be calculated as,

$$\lambda_{lim} = \frac{Nb}{\lambda_s\sqrt{N}b} = N^{1/2}\lambda_s^{-1} \tag{7}$$

The stretch limit of the bulk hydrogel scales with the chain stretch limit λ_{lim}, and the prefactor of the scaling relation depends on the polymer network architecture.[61]

The swelling of the dry polymer network reduces its shear modulus by a ratio of λ_s.[54] Therefore, the shear modulus of the hydrogel under initial deformation can be expressed as

$$G = nkT\lambda_s^{-1} \tag{8}$$

Note that n in eq 8 is the number of polymer chains per unit volume of the dry polymer network.

The swelling of the dry polymer network reduces the number of polymer chains per unit area by a ratio of λ_s^2 but does not significantly change the energy required for fracturing a polymer chain in the network. Therefore, the intrinsic fracture energy Γ_0 of the hydrogel can be calculated as

$$\Gamma_0 = \frac{n\sqrt{N}b}{\lambda_s^2} \cdot NU_f = nbN^{3/2}U_f\lambda_s^{-2} \tag{9}$$

The fracture toughness and fatigue threshold of a hydrogel with the conventional polymer network are the hydrogel's intrinsic fracture energy Γ_0.[55,56] If the hydrogel's polymer network is covalently bonded on a substrate (Figure 7d), both the interfacial toughness and the interfacial fatigue threshold of the adhesion are on the order of the hydrogel's intrinsic fracture energy Γ_0 as well.[49,78,435]

By comparing eqs 1−3 and eqs 7−9, we can see that swelling the dry polymer network into the hydrogel reduces the chain stretch limit λ_{lim}, shear modulus G and intrinsic fracture energy Γ_0 of the dry network by factors of λ_s, λ_s and λ_s^2, respectively.[54,57,62] By substituting the typical values of λ_s, b, N, n, kT, and U_f into eqs 7−9, we estimate that the shear modulus G of the hydrogel with the conventional polymer network can be on the order of pascals to megapascals, the chain stretch limit λ_{lim} can reach up to a few times (without entanglement), and the intrinsic fracture energy Γ_0 can reach a few tens of joules per meter squared.

By substituting eq 4 into eqs 7−9, we can express the chain stretch limit λ_{lim}, shear modulus G and intrinsic fracture energy Γ_0 of the hydrogel with the conventional polymer network as functions of its chain length N,

$$\lambda_{lim} = N^{1/2}\lambda_s^{-1}, \quad G = N^{-1}v^{-1}kT\lambda_s^{-1}, \quad \Gamma_0 = N^{1/2}v^{-1}bU_f\lambda_s^{-2} \tag{10}$$

From eq 10, it is evident that enhancing the chain length N increases the chain stretch limit λ_{lim} and the intrinsic fracture energy Γ_0 but decreases the shear modulus G of the hydrogel with the conventional polymer network. These mechanical properties of the hydrogel are coupled through the following relation,

$$\lambda_{lim} \sim \Gamma_0 \sim G^{-1/2} \tag{11}$$

Notably, the chain stretches due to equilibrium swelling of a conventional polymer network can be calculated. Without loss of generality, let us consider a dry conventional polymer network with a cubic shape. When the polymer network reaches the equilibrium state in water, one side of the cube increases its length from the dry state by a ratio of λ_{eq}. At the equilibrium state, the Helmholtz free energy for stretching polymer chains $W_{stretch}$ and for mixing polymers and water W_{mix} per unit volume of the dry polymer network can be expressed as[54,436]

https://doi.org/10.1021/acs.chemrev.0c01088
Chem. Rev. XXXX, XXX, XXX−XXX

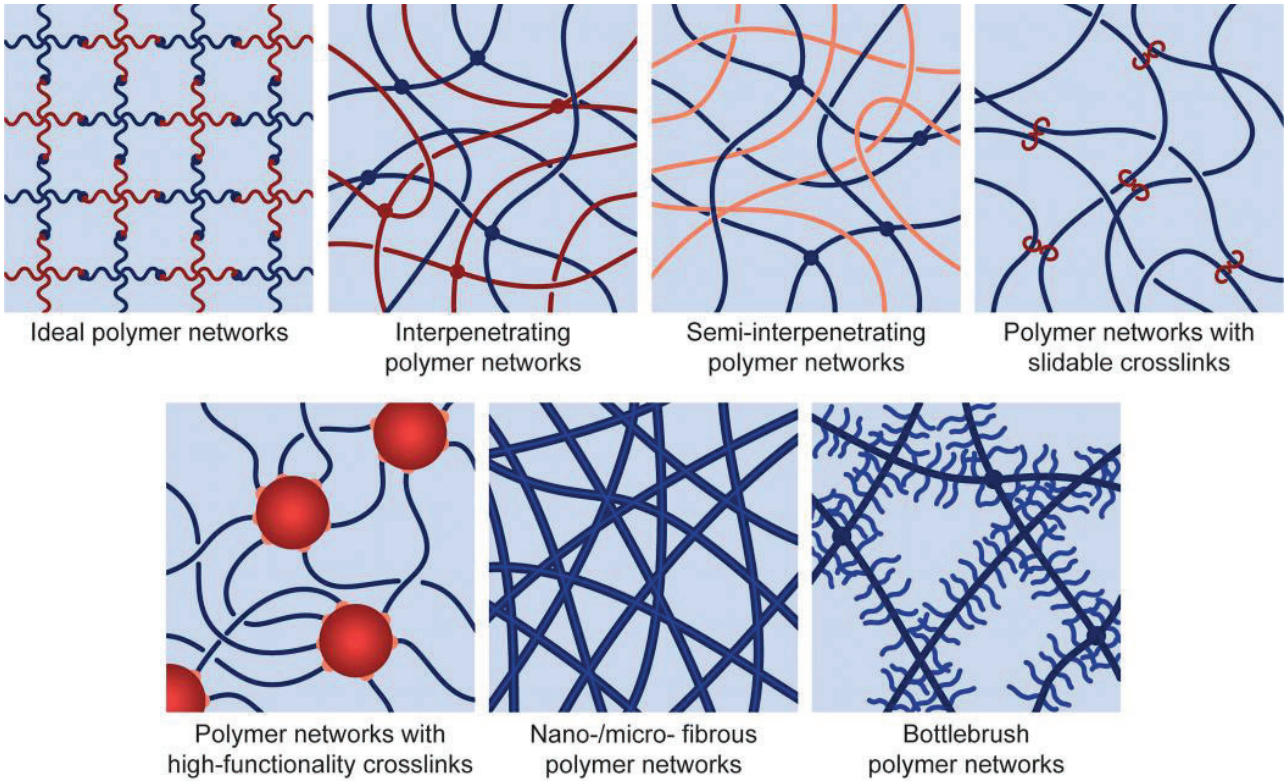

Figure 8. Schematics of unconventional polymer network architectures, including ideal polymer networks, polymer networks with slidable cross-links, interpenetrating polymer networks, semi-interpenetrating polymer networks, polymer networks with high-functionality cross-links, nano-/microfibrous polymer networks, and bottlebrush polymer networks.

$$W_{\text{stretch}} = \frac{1}{2}nkT(3\lambda_{\text{eq}}^2 - 3 - 6\log\lambda_{\text{eq}}) \tag{12a}$$

$$W_{\text{mix}} = -\frac{kT}{v_s}[(1-\lambda_{\text{eq}}^3)\log(1-\lambda_{\text{eq}}^{-3}) + \chi\lambda_{\text{eq}}^{-3}] \tag{12b}$$

where χ is the Flory polymer−solvent interaction parameter and v_s is the volume of a solvent molecule. Subsequently, the Helmholtz free energy per unit volume of the dry polymer network can be expressed as[54,436]

$$W = W_{\text{stretch}} + W_{\text{mix}} \tag{13}$$

When the polymer network reaches the equilibrium state in water, λ_{eq} minimizes the Helmholtz free energy,[54,436] giving

$$\frac{\partial W}{\partial \lambda_{\text{eq}}} = 0 \tag{14}$$

By solving eq 14, one can obtain λ_{eq} of the hydrogel at the equilibrium swollen state. The stretch of polymer chains λ_s in the hydrogel scales with λ_{eq}, and the prefactor of the scaling relation depends on the polymer network architecture.[61] While eqs 12−14 assume that the polymer network of the hydrogel is uncharged, the effect of charges on the equilibrium swelling of hydrogels can be accounted for by introducing additional terms to the Helmholtz free energy function, eq 12.[54,437] It should be noted that hydrogels are not necessary to reach the equilibrium swollen state in many situations, for example, when the hydrogels are insulated from water or do not have sufficient time to equilibrate with water.

4. UNCONVENTIONAL POLYMER NETWORKS

Section 3 has established that elastomers and hydrogels with conventional polymer networks have intrinsically coupled mechanical properties, including shear modulus, stretch limit, fracture toughness, fatigue threshold, interfacial toughness of adhesion, and interfacial fatigue threshold of adhesion (eqs 6 and 11). This section will discuss *unconventional polymer networks* (UPNs), which constitute most biological hydrogels (Figures 1 and 2) and have been widely used in synthetic hydrogels to achieve extreme mechanical properties.

The UPNs are defined as polymer networks that are different from the conventional polymer networks in terms of the architectures of the networks and/or the interactions among polymer chains in the networks.[70,438−446] Therefore, the UPNs can be broadly classified into two categories: the UPN architectures and the UPN interactions.

4.1. Unconventional Polymer Network Architectures

As illustrated in Figure 8, the UPN architectures are distinctly different from the architecture of the conventional polymer networks composed of randomly cross-linked polymer chains with covalent bonds (Figure 5). Almost all biological tissues (Figures 1 and 2) possess certain types of UPN architectures. Over the last few decades, multiple UPN architectures have been designed and synthesized for soft materials including elastomers, hydrogels, and organogels to achieve extreme properties. On the basis of their topologies, the typical UPN architectures can be classified into a number of categories, including ideal polymer networks, polymer networks with slidable cross-links, interpenetrating polymer networks, semi-interpenetrating polymer networks, polymer networks with high-functionality cross-links,

https://doi.org/10.1021/acs.chemrev.0c01088
Chem. Rev. XXXX, XXX, XXX−XXX

Table 1. Examples of Unconventional Polymer Network Architectures

UPN architectures	examples	refs
ideal polymer networks	covalently cross-linked 4-arm end-functionalized PEG	74, 333, 372, 450−465
	reversibly cross-linked 4-arm end-functionalized PEG	
polymer networks with slidable cross-links	PEG with polyrotaxanes as slidable cross-links	67, 372, 466, 469−473, 475−480
	PCL with polyrotaxanes as slidable cross-links	
	PPO with polyrotaxanes as slidable cross-links	
interpenetrating polymer networks	covalently cross-linked PAMPS interpenetrated with covalently cross-linked PAAm	67, 70, 372, 398, 482−485, 491
	covalently cross-linked polysaccharide interpenetrated with covalently cross-linked PHEMA, PEG, PAAm, PNIPAm, and PDMA	
semi-interpenetrating polymer networks	covalently cross-linked PAAm interpenetrated with reversibly cross-linked or un-cross-linked PVA, alginate, chitosan, and hyaluronan	67, 70, 372, 398, 481, 483, 484, 490, 492
	covalently cross-linked gelatin interpenetrated with reversibly cross-linked or un-cross-linked alginate	
	covalently cross-linked PEG-DA, gelatin interpenetrated with reversibly cross-linked or un-cross-linked alginate, chitosan, and hyaluronan	
	covalently cross-linked PAAm interpenetrated with reversibly cross-linked or un-cross-linked PVA	
polymer networks with high-functionality cross-links	PVA with crystalline domains as high-functionality cross-links	67, 232, 316, 318, 372, 398, 451, 492, 493, 497, 500, 503−511
	poly(methyl methacrylate) with glassy spheres as high-functionality cross-links	
	polyacrylamide with exfoliated particles as high-functionality cross-links	
	mixtures of polystyrene, poly(butyl acrylate), and poly(acrylic acid) with microsphere composites as high-functionality cross-links	
nano-/microfibrous polymer networks	cellulose, cellulose-derivative, collagen, gelatin, fibrin and elastin nano-/microfibrous networks	6, 120, 397, 522−536
other UPN architectures	poly(dimethylsiloxane) bottlebrush; poly(*n*-butyl acrylate) bottlebrush; poly polylactic acid-*b*-polyethylene glycol-*b*-poly(*N*-isopropylacrylamide) triblock bottlebrush	537−539

nano-/microfibrous polymer networks, and bottlebrush polymer networks (Figure 8 and Table 1).

4.1.1. Ideal Polymer Networks. Ideal polymer networks are polymer networks that have uniform chain length, uniform functionality, and no defect (Figure 8).[333] Following the pioneer work by Sakai et al.,[333,447−449] the ideal polymer networks have been commonly fabricated using multiarm macromers, where the arms of adjacent macromers are cross-linked into polymer chains. Because the lengths of the macromer arms are uniform and the reaction efficiency of the cross-linking process is high, various ideal polymer networks with uniform chain length, uniform functionality, and almost no defects have been achieved.[74,333,450−460] The tetra-arm PEG[333,461,462] is among the most frequently used macromers for the fabrication of hydrogels with ideal polymer networks. The ends of the PEG macromers are commonly modified with pairs of reaction groups such as *N*-hydroxysuccinimide and amine,[74,333,463] tetrabenzaldehyde and tetrabenzaacylhydrazide,[464] maleimide and thiol,[465] or boronic acid and diol.[450,454,461] Because of the almost defect-free nature, the ideal polymer networks have been made highly stretchable and resilient.[74] It should be noted that, although the conventional polymer networks usually have nonuniform chain lengths and topological defects, their mechanical properties are commonly calculated based on the models of ideal polymer networks, such as the affine network model and the phantom network model (section 3). Therefore, the ideal polymer networks by themselves still have coupled mechanical properties.

4.1.2. Polymer Networks with Slidable Cross-Links. A slidable cross-link, commonly in the form of two covalently cross-linked polymer rings, can interconnect two polymer chains that thread through and slide inside the rings (Figure 8).[466] Polymer networks with slidable cross-links are both mechanically stable and reconfigurable due to the permanent and slidable nature of the cross-links, respectively. Under mechanical loads, the slidable cross-links tend to reconfigure the polymer network in a way that the polymer chains in the network sustain the same level of forces, so that the reconfigured polymer network approximates an ideal polymer network.

The polymer networks with slidable cross-links are mainly synthesized from cyclodextrin-based polyrotaxanes.[467−469] Cyclodextrins are a series of cyclic oligosaccharides with six, seven, or eight glucose units (named α-, β-, or γ- cyclodextrin, respectively). Cyclodextrin-based polyrotaxanes are inclusion complexes composed of linear polymer chains that are threaded through the cyclodextrin molecules and then capped by bulky groups at the chain ends.[469−471] The formation of cyclodextrin-based polyrotaxanes mainly depends on the size matching between the interior cavities of the cyclodextrins and the cross-section of the polymer chains.[472] Many polymer chains have been investigated to form cyclodextrin-based polyrotaxanes including linear homopolymers, linear block copolymers, as well as branched polymers.[472] The α-cyclodextrin has the smallest cavity size and can form inclusion complexes with PEG or PCL, but not with poly(*p*-phenylene oxide) (PPO) chains.[473,474] The β-cyclodextrin can form complexes with PCL or PPO, but not with PEG.[473,475,476] The γ-cyclodextrin, which has the largest cavity size, can thread through a PPO chain or two chains of PEG or PCL.[477] The cyclodextrins can be cross-linked with each other to interconnect the threaded polymer chains and form the polymer networks with slidable cross-links.[67,372] Because a polymer network with slidable cross-links under mechanical loads approximates an ideal polymer network, the mechanical properties of the polymer network with slidable cross-links are usually coupled with one another as discussed in section 3.[466,478−480]

4.1.3. Interpenetrating and Semi-Interpenetrating Polymer Networks. An interpenetrating polymer network is

https://doi.org/10.1021/acs.chemrev.0c01088
Chem. Rev. XXXX, XXX, XXX−XXX

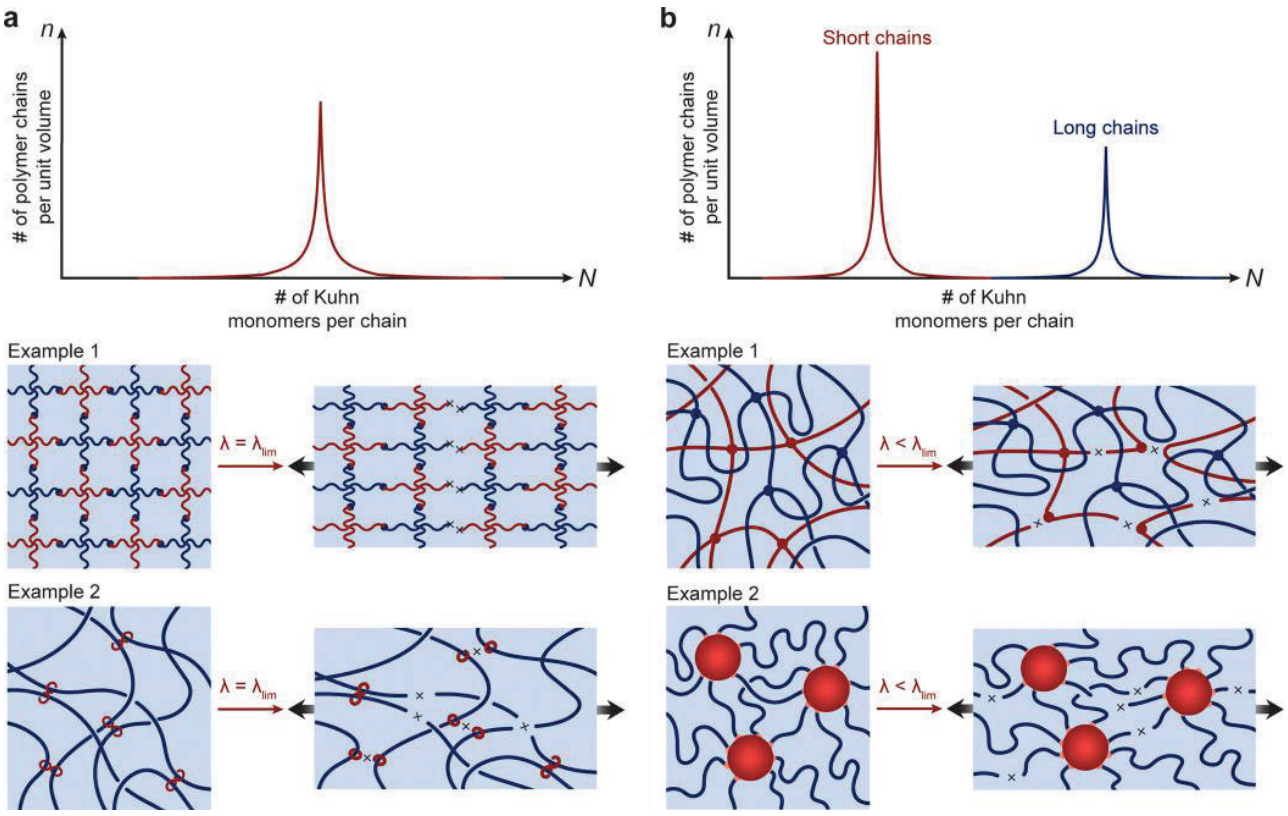

Figure 9. Decoupled mechanical properties of hydrogels due to UPN architectures: (a) unimodal polymer networks such as ideal polymer networks and polymer networks with slidable cross-links give coupled mechanical properties; (b) multimodal polymer networks such as interpenetrating polymer networks, semi-interpenetrating polymer networks and polymer networks with high-functionality cross-links can decouple the mechanical properties.

comprised of two or more interpenetrated polymer networks, which are individually cross-linked but not joined together (Figure 8); a semi-interpenetrating polymer network is comprised of two or more interpenetrated polymer networks, in which at least one network is un-cross-linked and others are individually cross-linked but not joined together (Figure 8).[372,398,481−488] The interpenetrating and semi-interpenetrating polymer networks are entangled or interlocked in a way that they cannot be pulled apart unless the networks are broken.[485−488] Hydrogels based on the interpenetrating and semi-interpenetrating polymer networks are commonly prepared following the sequential or simultaneous method. In the sequential method, one polymer network is first prepared and then immersed into a solution of monomers, initiators, and/or cross-linkers for another polymer network. Thereafter, the interpenetrating or semi-interpenetrating polymer network is formed by polymerizing the second polymer network within the first network. As a remarkable example, Gong et al. have adopted the sequential method to fabricate the double-network hydrogels with high fracture toughness.[70] In the simultaneous method, a mixture of the polymers, monomers, initiators, and cross-linkers for all polymer networks form the interpenetrating or semi-interpenetrating polymer networks in one step or one pot.[489] This one-step or one-pot fabrication process is a desirable feature of the simultaneous method compared to the sequential method. One remarkable example of the simultaneous method is the simple fabrication of the polyacrylamide-alginate hydrogel with high stretchability and fracture toughness.[490] A wide range of material candidates including both natural and synthetic polymers as discussed in section 2[67,372,398,482−484,490−492] have been used to synthesize hydrogels with interpenetrating and semi-interpenetrating polymer networks via various cross-linking strategies.[254,398,484,493] As will be discussed in section 4.1.7 and section 5, the interpenetrating and semi-interpenetrating polymer networks can provide decoupled and extreme mechanical properties for hydrogels, such as extremely high stretchability and fracture toughness.[70,490,494−496]

4.1.4. Polymer Networks with High-Functionality Cross-Links. The functionality of a cross-link refers to the number of polymer chains interconnected at the cross-link. Common covalent cross-links as discussed in section 2.3 usually have relatively low functionality (e.g., less than 10), and there is usually a single polymer chain bridging between two adjacent covalent cross-links. To dramatically enhance the functionality of a polymer network, various types of high-functionality cross-links can be introduced into the polymer networks, including crystalline domains,[232,316,318,497] glassy nodules,[498,499] nano-/microparticles,[372,398,492,497,500−502] and microphase separations[503−505] (Figure 8). For example, poly(vinyl alcohol) can form nanocrystalline domains to cross-link the polymer networks through the freeze−thaw method;[318,506] poly(methyl methacrylate) can form glassy spheres to cross-link poly(methyl methacrylate)-based block copolymers into networks;[507] exfoliated particles, such as nanoclays,[508] graphene oxide,[509] and stratified lamellar bilayers,[510] can cross-link polyacrylamide

https://doi.org/10.1021/acs.chemrev.0c01088
Chem. Rev. XXXX, XXX, XXX−XXX

into moldable and self-healable hydrogels; mixtures of styrene, butyl acrylate, and acrylic acid can form microspheres to cross-link the residual polymer chains into microsphere-composite hydrogels.[511]

Multiple polymer chains (e.g., over 10) can be interconnected at each high-functionality cross-link (Figure 8). In addition, there can be multiple polymer chains bridging between two neighboring high-functionality cross-links, where the lengths of the polymer chains can be highly nonuniform (Figure 8).[67,451] As will be discussed in section 4.1.7 and section 5, the polymer networks with high-functionality cross-links can provide decoupled and extreme mechanical properties for hydrogels, such as extremely high fracture toughness, resilience, tensile strength, and fatigue resistance.

4.1.5. Nano-/Microfibrous Polymer Networks. Both synthetic and natural polymers can assemble into fibers (or fibrils referring to short fibers) with diameters ranging from nanometers to micrometers via covalent or physical bonds. The nano-/microfibers can further entangle, aggregate, and cross-link into percolated polymer networks[6,71,512−517] (Figure 8). In biological organisms, cells can secrete proteins (e.g., collagens) and polysaccharides (e.g., celluloses), which then assemble into nano-/microfibrous polymer networks.[120,267,518−521] These naturally derived fibers and fibrous networks have been widely harnessed for the fabrication of hydrogels with nano-/microfibrous polymer networks.[397,522−525] In addition, a wide range of natural and synthetic polymers have been fabricated into nano-/microfibrous polymer networks with the spinning techniques,[526−528] among which the electrospinning is most popular due to its simplicity, low cost, and wide applicability.[529] In particular, the diameter, alignment, and density of the fibers can be readily controlled by tuning the parameters of the electrospinning process.[530−534] As will be discussed in section 4.1.7 and section 5, the nano-/microfibrous polymer networks can provide decoupled and extreme mechanical properties for hydrogels, such as extremely high fracture toughness, tensile strength, resilience, and fatigue resistance.[535,536]

4.1.6. Other Unconventional Polymer Network Architectures. Many other types of UPN architectures can provide extraordinary mechanical properties as well. For example, the bottlebrush polymer networks (Figure 8) have shown extremely low shear moduli and tissue-like stress−strain relations in the solvent-free state.[537,538] Although these UPN architectures have not been widely used in hydrogels, they can be exploited for the design of hydrogels in the future.[539] Furthermore, it is also expected that new UPN architectures will be invented together with the development of polymers and soft materials.

4.1.7. Decoupled Mechanical Properties Due to Unconventional Polymer Network Architectures. Polymer chains in the ideal polymer networks have uniform chain lengths (i.e., the same N), and the polymer networks with slidable cross-links also tend to give relatively uniform chain lengths under mechanical loads. These polymer networks with relatively uniform chain lengths are named unimodal polymer networks (Figure 9a).[60,63,443] Because the shear moduli, stretch limits, and intrinsic fracture energy of conventional polymer networks have been derived based on the unimodal polymer networks, these mechanical properties are still coupled in hydrogels with the ideal polymer networks and the polymer networks with slidable cross-links (section 3).

The interpenetrating polymer networks, semi-interpenetrating polymer networks, and polymer networks with high-functionality cross-links can integrate polymer chains with varying chain lengths (i.e., different N) into the same polymer networks, which are often named multimodal polymer networks (Figure 9b).[60,63,443] Let us classify the polymer chains in a multimodal polymer network into different types based on their chain lengths (Figure 9b). For the ith type of polymer chains, the number of the polymer chains per unit volume of the polymer network in the dry state, the number of Kuhn monomers per polymer chain, and the volume of the Kuhn monomer are denoted as n_i, N_i, and v_i, respectively.

The multimodal polymer network (Figure 9b) can be designed such that the corresponding hydrogel can sustain its integrity up to the stretch limit of the longest polymer chains λ_{lim}, which can be expressed as[70,490]

$$\lambda_{lim} = \sqrt{N_{max}}\lambda_s^{-1} \tag{15}$$

where N_{max} is the number of Kuhn monomers on the longest polymer chain, and λ_s^{-1} accounts for the effect of swelling on the chain stretch limit λ_{lim}. The stretch limit of the bulk hydrogel scales with λ_{lim} and the prefactor of the scaling relation depends on the polymer network architecture.[61]

On the basis of the affine network model, the shear modulus of the hydrogel with the multimodal polymer network (Figure 9b) can be expressed as

$$G = \sum n_i kT\lambda_s^{-1} \tag{16}$$

where n_i and λ_s^{-1} account for the effects of the ith type of polymer chains and swelling on the initial shear modulus of the hydrogel.

Following the Lake−Thomas model, the intrinsic fracture energy of the hydrogel with the multimodal polymer network (Figure 9b) can be calculated as

$$\Gamma_0 = \sum n_i b_i N_i^{3/2} U_i \lambda_s^{-2} \tag{17}$$

where b_i and U_i are the length and the fracture energy of a Kuhn monomer on the ith type of polymer chain, respectively, and λ_s^{-2} accounts for the effect of swelling on the intrinsic fracture energy. It should be noted that the fracture toughness and interfacial fracture toughness of the multimodal polymer network (Figure 9b) can be much higher than the intrinsic fracture energy, which will be discussed in section 5.

It is commonly assumed that the polymer chains occupy the major volume of the polymer network in the dry state, and therefore the volume conservation of the multimodal polymer network (Figure 9b) gives

$$\sum N_i n_i v_i = 1 \tag{18}$$

Despite the relation of eq 18, the stretch limit, shear modulus, and intrinsic fracture energy of a hydrogel with the multimodal polymer network (Figure 9b) can still be decoupled and independently designed. Without loss of generality, let us consider a hydrogel with bimodal distribution of chain lengths as an example (Figure 9b). A high density of the short polymer chains can give a high initial shear modulus of the hydrogel. While these short chains will be fractured when the hydrogel is highly stretched, the long polymer chains can still maintain the integrity and high stretch limit of the hydrogel.[70,490] Similarly, the long polymer chains can give a relatively high intrinsic fracture energy of the hydrogel.[540]

The mechanical properties of the nano-/microfibrous polymer networks are determined by their fibers, interactions of the fibers (e.g., cross-links between fibers), and topologies of

https://doi.org/10.1021/acs.chemrev.0c01088
Chem. Rev. XXXX, XXX, XXX−XXX

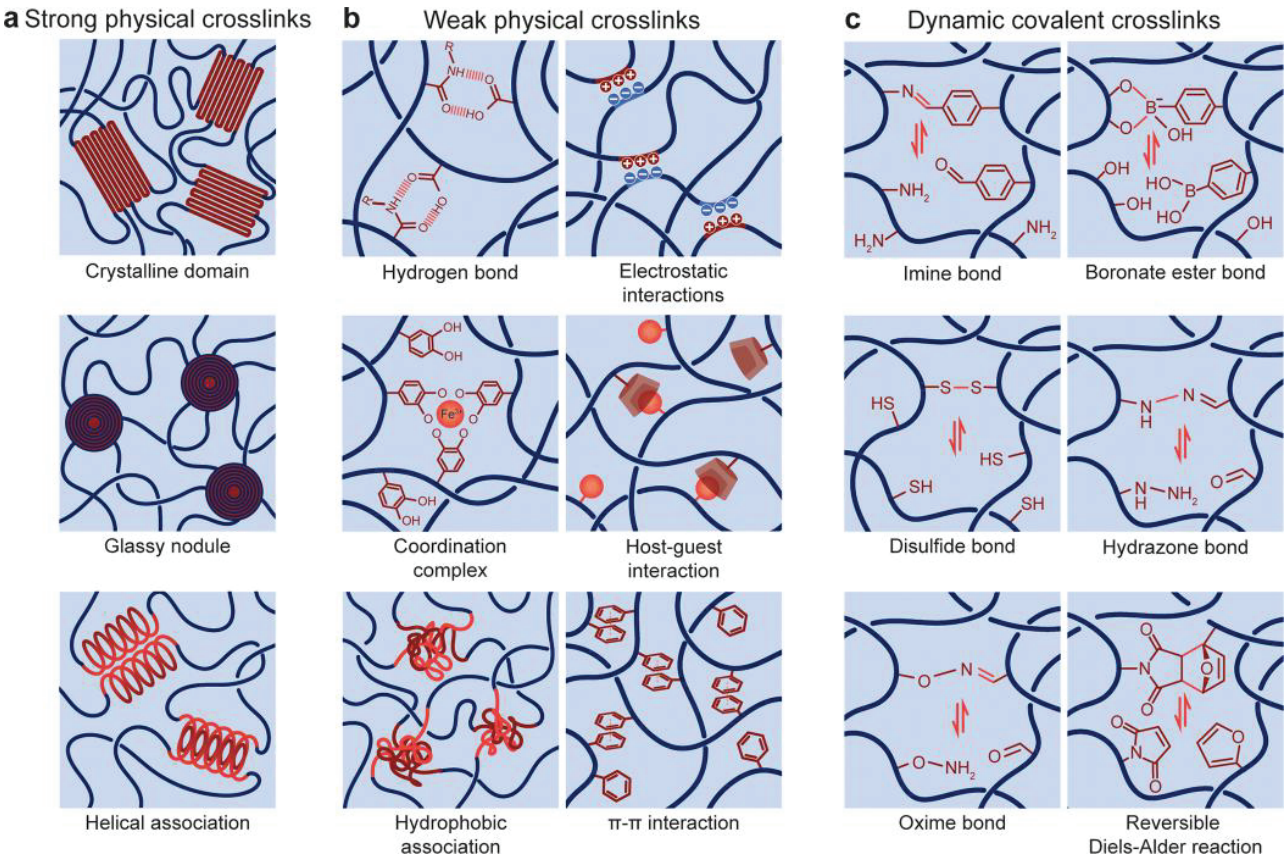

Figure 10. Schematics of unconventional polymer network interactions including (a) strong physical cross-links, (b) weak physical cross-links, and (c) dynamic covalent cross-links.

the fibrous polymer networks. Therefore, the stretch limit, shear modulus, and intrinsic fracture energy of nano-/microfibrous hydrogels do not follow the coupling relations for the conventional polymer networks (eqs 13 and 14), and therefore they can be independently designed.

4.2. Unconventional Polymer Network Interactions

As illustrated in Figure 10, the UPN interactions are defined as interpolymer and intrapolymer interactions that are different from those in the conventional polymer networks (i.e., permanent covalent cross-links, excluded volumes, and osmotic interactions) (Figure 10). The UPN interactions are vastly abundant in biological organisms,[541] and the UPN interactions have been intensively studied for the design of soft materials such as elastomers, hydrogels and organogels to achieve extreme mechanical properties among many other purposes.[254] On the basis of the nature of the UPN interactions, they can be broadly classified into three categories:[62] strong physical cross-links, weak physical cross-links, and dynamic covalent cross-links (Figure 10 and Table 2).

4.2.1. Strong Physical Cross-Links. In addition to the permanent covalent cross-links discussed in section 2.3, various types of strong physical bonds can act as effectively permanent cross-links in polymer networks. Typical examples of strong physical cross-links include crystalline domains, glassy nodules, and helical structures. The energy of strong physical cross-links is similar to those of permanent covalent cross-links (Figure 6).

4.2.1.1. Crystalline Domain. A specific subset of synthetic and natural polymers can form crystalline domains under appropriate conditions. A crystalline domain, with the size from nanometers to micrometers, can serve as a strong physical cross-link for multiple amorphous polymer chains connected to the crystalline domain (Figure 10). As an example in synthetic polymers, PVA can form crystalline domains by repeated freeze−thaw cycles or by annealing at temperatures above its glass transition temperature.[316,318,497] The formation of PVA crystalline domains is mainly due to the hydrogen-bonding interactions of the hydroxyl groups on PVA chains.[4] As an example in natural polymers, chitin and chitosan can form semicrystalline polymer networks with crystalline domains cross-linking amorphous chains by treating the chitin and chitosan with strongly acidic or basic solutions to overcome the interchain electrostatic repulsions.[232,235] As another example in natural polymers, cellulose can also form highly crystallized nanofibers due to the strong interaction between glucose units.[542] These cellulose nanofibers can further aggregate and form a stable network by alkaline treatments.[512,543] It should be noted that heating the above-mentioned semicrystalline polymer networks above their melting temperatures can destroy the crystalline domains in the networks, although most crystalline domains are stable at room and body temperatures.

Because a crystalline domain usually interconnects multiple polymer chains, they often act as high-functionality cross-links in the polymer networks as discussed in section 4.1.4. In addition, the energy required to pull a polymer chain out of a crystalline domain is much higher than that required to fracture the same polymer chain;[78] therefore, crystalline domains can also act as intrinsically high-energy phases in the polymer networks. These

https://doi.org/10.1021/acs.chemrev.0c01088
Chem. Rev. XXXX, XXX, XXX−XXX

Table 2. Examples of Unconventional Polymer Network Interactions

UPN interactions		examples	refs
strong physical cross-links	crystalline domain	PVA treated by freeze−thawing or annealing	4, 316, 318, 497
		chitin and chitosan treated by acidic or basic solutions	232, 235
		cellulose treated by alkalines	512, 542, 543
	glassy nodule	polystyrene-*b*-poly(*N*-isopropylacrylamide)-*b*-polystyrene	546
		poly(methyl methacrylate)-*b*-poly(n-butyl acrylate)	507
	helical association	self-assemble of agarose or gelatin	6, 120, 550, 551
		self-assemble of collagen or fibrinogen	6, 120, 548, 549
		self-assemble of elastin-like polypeptides	522, 525
weak physical cross-links	hydrogen bond	PAA or polymethacrylic acid (PMA) with PEG	493, 554−556
		PEG, PHEMA, PNIPAM with self-complementary hydrogen-bond groups (triazine moieties or ureido pyrinimidone moieties)	493, 505, 556−558
	electrostatic interaction	alginate with Ca^{2+}, Ba^{2+}, Mg^{2+}, Zn^{2+}	6, 120, 122, 562
		chitosan with tripolyphosphate, citrate ions	563−565
		cationic polyelectrolytes with anionic polyelectrolytes	560, 566
	coordination complex	bisphosphonate-containing polymers with metal ions (Ca^{2+}, Mg^{2+}, or Ag^{+})	573, 588, 589
		catechol-containing polymers with metal ions (Cu^{2+}, Zn^{2+}, and Fe^{3+})	493, 576, 577, 590−594, 596
		histidine-containing polymers with metal ions (Cu^{2+}, Co^{2+}, and Ni^{2+})	493, 595, 596
	host−guest interaction	polymers containing β-CD moieties with azobenzene group, adamantyl group, ferrocene group, *t*-butyl group, cyclohexyl(ester) group, cyclododecyl(amide) group, benzyl group, 2-naphthylmethyl group, 1-pyrenylmethyl group	398, 472, 493, 556, 602, 604−610
		polymers containing α-CD moieties with *n*-butyl group, adamantyl group, benzyl group, trans-azobenzene group	398, 493, 556, 602, 603
		polymers containing curcubit[*n*]uril moieties with spermine, diaminohexane, viologens, naphtalenes	398, 556, 621, 622
	hydrophobic association	PEG, PAAm, PNIPAM, PDMAA, PVA containing hydrophobic moieties (octylphenol-PEG acrylate, stearyl acrylate, lauryl acrylate)	493, 503, 505, 628, 629
		triblock amphiphilic copolymers with PEG, PAAm, PVA, PHEMA middle blocks, and *n*-alkyl acrylate end blocks	630−632
	$\pi-\pi$ stacking	polymers modified with aromatic moieties or conjugated structures	514, 636, 637
		hydrogels containing carbon nanotubes, polythiophene, and graphene-based nanomaterials	32, 116, 638−641
dynamic covalent cross-links	imine bond	polymers containing amine and aldehyde (or ketone) functional groups	398, 440, 646−650, 652−655
	boronate ester bond	polymers containing boronic acid and diol functional groups	398, 658, 664, 669, 670, 676
	disulfide bond	polymers containing disulfide functional groups	398, 631, 682, 688, 689, 693
	hydrazone bond	polymers containing hydrazide and aldehyde (or ketone) functional groups	693, 694, 696−700, 702−704
	oxime bond	polymers containing hydroxylamine and aldehyde (or ketone) functional groups	709−712
	reversible Diels−Alder reaction	polymers containing diene and dienophile functional groups	715, 720, 725, 726

attributes of crystalline domains have endowed the hydrogels containing crystalline domains with extreme mechanical properties, such as being tough, strong, resilient, and fatigue-resistant, which will be discussed in section 5.

4.2.1.2. Glassy Nodule. Glassy nodules are formed by the reversible liquid-glass transition of amorphous polymers when the temperature is decreased below their glass-transition temperatures.[544] In order to harness glassy nodules as strong physical cross-links, block copolymers that contain at least one segment with a high glass-transition temperature have been commonly used. As the temperature reduces to room or body temperature, the segments with the high glass-transition temperature form glassy nodules that effectively cross-link the adjacent amorphous polymer chains (Figure 10).[545] For example, the polystyrene segments in the polystyrene-*b*-poly(*N*-isopropylacrylamide)-*b*-polystyrene copolymers can form glassy nodules at room temperature to cross-link the block copolymer chains into a polymer network.[546] As another example, poly(methyl methacrylate) has a glass transition temperature around 115 °C;[547] therefore, the poly(methyl methacrylate) segments in the poly(methyl methacrylate)-*b*-poly(*n*-butyl acrylate) copolymers can form glassy spheres at room temperature to cross-link the polymer network.[507] Similar to crystalline domains, glassy nodules can also act as high-functionality cross-links and intrinsically high-energy phases in polymer networks to give the corresponding hydrogels extreme mechanical properties, which will be discussed in section 5.

4.2.1.3. Helical Association. Many natural polymers, due to their precisely controlled structures, can assemble into nanometer-scale helical fibers (or fibrils), which then can aggregate or entangle to form a cross-linked network (Figure 10).[120,522,524,525] For example, the well-known triple-helix structure of type I collagen is formed by the self-assembly of three peptide strands. These collagen triple helices can pack

https://doi.org/10.1021/acs.chemrev.0c01088
Chem. Rev. XXXX, XXX, XXX−XXX

together to form collagen nanofibers, which further self-assemble into an interconnected hydrogel network.[548,549] As another example, the linear agarose chains are disordered coils in aqueous solutions at high temperatures and can form double-helix strings[550] or simple helical chains[551] when the temperature is decreased to the room or body temperature. These stings or chains can associate to form agarose fibers through hydrogen bonding and further be entangled to form the interconnected hydrogel network.[552]

4.2.2. Weak Physical Cross-Links. Compared to the strong physical cross-links, many other physical cross-links in polymer networks are relatively weak, transient, and reversible. Typical examples of weak physical cross-links include hydrogen bond, electrostatic interaction, metal coordination, guest−host interaction, hydrophobic association, and $\pi-\pi$ stacking (Figure 10). The energy of weak physical cross-links is usually lower than those of strong physical cross-links and permeant covalent cross-links (Figure 6).

4.2.2.1. Hydrogen Bond. The energy of a single hydrogen bond ranges from 0.8 kJ mol^{-1} to 167 kJ mol^{-1} (Figure 6).[388,389] Many natural polymers can form hydrogels by the intermolecular hydrogen bonds. For example, gelatin can form polymer networks of helical structures cross-linked by hydrogen bonds;[187] certain types of polysaccharides, such as agarose, amylose, amylopectin, and carrageenan, can also form helical structures in solutions and be cross-linked into hydrogels by hydrogen bonds.[553] A number of synthetic polymers are also capable of forming physical hydrogels via hydrogen bonds. For example, PVA hydrogels can be obtained by forming hydrogen bonds between polymer chains through repeated freezing and thawing of PVA solutions.[319] Polymethacrylic acid (PMA) or PAA can form complexes with PEG by hydrogen bonds between the oxygen groups of PEG and the carboxyl groups of PMA[554] or PAA.[555]

Despite the abundance of hydrogen-bond groups (-OH, -NH, -C═O, -C-O) in natural and synthetic polymers, the hydrogen-bond interactions in hydrogels are usually screened due to the water molecules in hydrogels. To enable effective hydrogen-bond cross-links, hydrophobic moieties with multiple self-complementary hydrogen-bond groups have been introduced onto the polymers.[493,556,557] For instance, functionalizing PEG, PHMEA, and PNIPAM with amine triazine or diamino triazine groups enables the formation of triple hydrogen bonds per cross-link.[493,505,556,558] Similarly, the introduction of ureidopyrinimidone (UPy) groups onto PEG, PHMEA, PNIPAM, PAA, and PDMAA chains gives quadruple hydrogen bonds per cross-link.[493,556,557] Complementary DNA base pairs (A-T, C-G) can also serve as hydrogen-bond motifs when the DNA pairs are attached to polymer chains.[559]

4.2.2.2. Electrostatic Interaction. The energy of electrostatic interactions ranges from 5 kJ mol^{-1} to 200 kJ mol^{-1} (Figure 6).[390] Natural and synthetic polymers with fixed charges, named polyelectrolytes, can be physically cross-linked by electrostatic interactions.[122,490,560,561] As a typical example of the anionic polyelectrolytes, alginate has been physically cross-linked with a wide range of divalent cations such as Ca^{2+}, Ba^{2+}, and Mg^{2+}. Although the energy of a single ionic bond in alginate is relatively low, multiple (e.g., over 20) adjacent ionic cross-links on the alginate chains can form a densely cross-linked region following the "eggbox" model,[6,120,122,562] giving relatively stable alginate hydrogels. As a typical example of the cationic polyelectrolytes, chitosan has been cross-linked by multivalent anions such as citrate and tripolyphosphate.[563−565] Electrostatic interactions of oppositely charged polyelectrolytes can also give physically cross-linked hydrogels. For example, anionic poly(L-glutamic acid) and cationic poly(L-lysine) can form an injectable hydrogel by simply mixing them in phosphate buffered saline solutions.[560] As another example, poly(3-(methacryloylamino) propyltrimethylammonium chloride) and poly(sodium *p*-styrenesulfonate) can form polyion complexes and give a series of tough and self-healing hydrogels by the stepwise polymerization of the oppositely charged monomers.[566] It should be noted that the formation of ionic cross-links usually requires low ionic strength of the solvents for the hydrogels to avoid charge shielding.

4.2.2.3. Coordination Complex. A coordination complex consists of a central metal ion, especially transition metal ion, and a surrounding array of organic ligands.[567,568] The energy of coordination complexes ranges from 100 kJ mol^{-1} to 300 kJ mol^{-1} (Figure 6).[390] Coordination bonds provide structural support in many living tissues, such as human bone,[569] insect mandible,[570] as well as mussel byssal thread.[571] Hydrogels cross-linked by coordination complexes are primarily achieved by functionalizing polymer backbones with chelating ligands, which then form coordination complexes with metal ions. Bisphosphonate,[572−574] catechol,[575−577] histidine,[578−580] thiolate,[581,582] carboxylate,[583,584] pyridine,[585] bipyridine,[586] and iminodiacetate[580,587] have been widely used as the chelating ligands; Cu^{2+}, Zn^{2+}, Fe^{3+}, Co^{2+}, and Ni^{2+} are the commonly used metal ions. Bisphosphonate ligands can be modified onto hyaluronan,[588] gelatin,[589] and PEG[573] to form coordination complex with Ca^{2+}, Mg^{2+}, and Ag^{+}. Besides bisphosphonate, catechol ligands are also widely used to functionalize various polymers such as PEG,[590,591] gelatin,[592] hyaluronic acid,[593] chitosan,[594] polyacrylamide,[576] and PAA.[577] As a typical example, PEG-modified with 3,4-dihydroxyphenyl-L-alanine (DOPA) residues can form coordination complexes with metal ions (Cu^{2+}, Zn^{2+}, and Fe^{3+} ions) when the pH is above 8.[493,591] In natural proteins, the histidine amino acid can give an imidazole ligand residue,[59] which is one of the most important chelators in the human body.[595] PEG-modified with histidine can form coordination complexes with metal ions (Cu^{2+}, Co^{2+} and Ni^{2+} ions) to achieve physical cross-linking of the PEG hydrogels.[493,596] The mechanical properties of the hydrogels cross-linked by coordination complexes can be tuned by varying the metal ions and/or the chelating ligands.[578,597]

4.2.2.4. Host−Guest Interactions. Host−guest interactions refer to two or more molecules or ions that are held together in unique structural relationships by forces other than those of covalent bonds.[476,598,599] The two most common host moieties are cyclodextrins and curcubit[*n*]urils. Cyclodextrins (CDs) are cyclic oligosaccharides composed of 6−8 D-glucose repeating units linked by α-(1 → 4)-linked glycosidic bonds.[600,601] Commonly used CDs include α-, β-, and γ-CDs which are composed of six, seven, and eight D-glucose repeating units, respectively. These CDs have a truncated cone shape with the secondary and primary hydroxyl groups on the smaller cone rim exposed to the solvent,[599] which makes the CDs show a relatively hydrophobic inner cavity and a relatively hydrophilic outer surface. Therefore, these CDs can act as the host molecules for various hydrophobic guest molecules with appropriate molecular sizes through hydrophobic and van der Waals interactions.[398,472,476] For example, common guests for α-CD include azobenzene[602] and ferrocene;[603] common guests for β-CD include adamantane,[604] benzimidazole,[605] 3-(trimethylsilyl)propionic acid,[606] azobenzene,[602] ferrocene,[607] bipyridine,[608] phenolphthalein[609] and cholesterol;[610] and

https://doi.org/10.1021/acs.chemrev.0c01088
Chem. Rev. XXXX, XXX, XXX−XXX

common guests for γ-CD include ferrocene.[603] Among various guest molecules, adamantane has one of the greatest affinities due to its complementary size for β-CD and its high hydrophobicity.[611] In addition, the complexation of azobenzene or ferrocene to CDs is responsive to light[612] or redox conditions,[613,614] respectively.

The cucurbit[n]urils (CB[n, n = 5−8]) are pumpkin-shaped macrocyclic oligomers made from the condensation reactions of formaldehyde and glycoluril.[599,615] The CB[n]'s usually have a structure of a rigid hydrophobic cavity with two identical hydrophilic polar carbonyl groups surrounding the portals. The cavity size ranges from 4.4 to 8.8 Å (for CB[n], n = 5−8) and the portal diameter ranges from 2.4 to 6.9 Å.[616] The binding affinities of CBs are often greater than that of other cavitands,[617] mainly due to the formation of the strong charge−dipole, hydrogen bonding, and hydrophobic/hydrophilic interactions by the rigid inner cavities and the negative portals of CB[n]'s.[618−620] CB[8] also displays remarkable binding affinities toward positively charged and relatively large guests such as amantadine derivatives. Furthermore, the cavity of CB[8] is large enough to accommodate two organic guests simultaneously, thus forming highly stable ternary complexes. For example, CB[8] can form stable complexes with two 2,6-bis(4,5-dihydro-1*H*-imidazol-2-yl)naphthalene molecules,[621] or one viologen (paraquat) and one 2,6-dihydroxynaphthalene together.[622]

Hydrogels crossslinked by the host−guest interactions are usually constructed with polymer networks modified by the guest molecules and/or host molecules. For example, monomers, host molecules, and guest molecules can be copolymerized into polymer networks crossslinked by the host−guest interactions.[623] The host/guest molecules can also be attached to the backbones or ends of polymers such as PEG, PDMAA, hyaluronic acid, and PAA, and then the addition of the corresponding difunctional guest/host cross-linkers will cross-link the polymer network.[599] Alternatively, guest-functionalized and host-functionalized polymers can also be synthesized separately, and a mixture of the two types of polymers gives hydrogels cross-linked by the host−guest interactions.[624,625] Supramolecular hydrogels with these host−guest interactions have been extensively utilized to fabricate responsive materials[626] and other dynamically assembling systems.[472,627]

4.2.2.5. Hydrophobic Association. The physical cross-link of hydrophobic association relies on the microphase separation and aggregation of hydrophobic domains of the polymer chains.[493,505] The energy of hydrophobic association ranges from 0.1 kJ mol^{-1} to 20 kJ mol^{-1} (Figure 6).[390] The hydrophobic domains can be introduced by postpolymerization modification (e.g., via the grafting-to approach) or by copolymerizing hydrophobic monomers within the polymer chains, either randomly or as blocks.[628] These modifications usually require the usage of nonaqueous solvents, mixed solvents, or micellar systems.[503,629] As a typical example of introducing the hydrophobic domains, hydrophobic stearyl acrylate monomers have been copolymerized within polyacrylamide (PAAm) chains.[503] Another example of introducing the hydrophobic domains is the synthesis of multiblock copolymers with hydrophobic *n*-alkyl acrylate end blocks and a large middle block of PEG, PAAm, PAA, or PHEMA polymers.[630−632] Notably, because one hydrophobic association can interconnect multiple polymer chains, the hydrophobic association has also been used as high-functionality cross-links in hydrogels,[307,633] although the energy of hydrophobic association is usually lower than those of crystalline domains and glassy nodules.

4.2.2.6. π−π Stacking. The π−π stacking interaction is a type of noncovalent interaction that refers specifically to the attractive interactions between π electrons in the aromatic groups.[634] The π−π interactions can be divided into the edge-to-face (T-shaped), offset, and face-to-surface stacking structures based on the geometry of the aromatic interactions.[635] The energy of π−π stacking ranges from 1 kJ mol^{-1} to 50 kJ mol^{-1} (Figure 6).[391] Natural amino acids with aromatic rings, such as phenylalanine, tyrosine, and tryptophan, and other compounds with conjugated structures such as fluorenylmethyloxycarbonyl (Fmoc), 1-pyrenebutyric acid, 2-naphthalene acetic acid, and nitrophenyl methacrylate can be used to design and prepare polymers with aromatic moieties for gelation by the π−π stacking interactions.[514,636,637] For example, the aromatic moiety containing short peptides and *N*-terminal Fmoc-amino acids can self-assemble into robust supramolecular architectures.[514] In addition, carbon nanotubes,[638,639] polythiophene,[32,116] and graphene-based nanomaterials[640,641] (including single-layer graphene, multilayer graphene, graphene oxide, and reduced graphene oxide) are also capable to form π−π interactions, which are useful for preparing electrically conductive hydrogels.[642,643]

4.2.3. Dynamic Covalent Cross-Links. In addition to the weak physical bonds, dynamic covalent bonds can also act as reversible cross-links that are cleavable by external stimuli. The energy of dynamic covalent bonds is usually similar to or lower than those of permanent covalent bonds[644] and higher than those of weak physical bonds (Figure 6). Typical examples of dynamic covalent cross-links in hydrogels include imine bond, boronate ester bond, disulfide bond, cyclohexenes hydrazone bond, oxime bond, and reversible Diels−Alder reaction (Figure 10).

4.2.3.1. Imine Bond. An imine is a carbon−nitrogen double bond commonly formed by reactions between amines and aldehydes or ketones.[645] In particular, the imine cross-links in hydrogels are usually formed through the Schiff base reactions, which give aliphatic Schiff bases or aromatic Schiff bases.[646−649] The reversible nature of the imine cross-links endows the resultant hydrogels with properties such as mechanical dissipation, self-healing, and stimuli responses.[650] The energy of the Schiff bases ranges from 67 kJ mol^{-1} to 477 kJ mol^{-1} (Figure 6).[387,392] The aromatic Schiff bases usually have higher energy and stability than the aliphatic Schiff bases.[651,652]

The imide bonds are particularly useful for preparing biopolymer-based hydrogels, because most biopolymers such as proteins contain amine groups. These amines can form imide bonds with various aldehydic cross-linkers at mild conditions.[650,653] The obtained hydrogels with imine bonds are usually sensitive to various chemical and biological stimuli, including pH, free amine, and free aldehydes.[652] These hydrogels can be used as self-healing materials and injectable scaffolds in biomedical applications.[440,654,655]

4.2.3.2. Boronate Ester Bond. The dynamic boronate ester bonds are formed by the reaction of diols and boronic acid.[656−658] The energy of boronate ester bonds ranges from 27.2 kJ mol^{-1} to 93.3 kJ mol^{-1} (Figure 6),[393] highly dependent on pH and temperature.[659−661] The boronic acid can be introduced into hydrogels by polymerizing boronic acid-containing monomers together with other monomers, such as acrylamide (AAm)[662] and *N*-isopropylacrylamide (NIPAM).[663] Alternatively, boronic acid functional groups can also be grafted

https://doi.org/10.1021/acs.chemrev.0c01088
Chem. Rev. XXXX, XXX, XXX−XXX

onto preformed polymer chains through the carbodiimide chemistry.[664,665]

The boronic acid-containing polymers can react with polymers containing diol functional groups. For example, polymers modified with boronic acid can form the dynamic boronate ester cross-links with salicyl hydroxamic acid groups in an acidic environment or catechol groups in an alkaline environment.[590,660,666−668] As another example, polyhydroxy polymers such as PVA,[669,670] alginate,[671,672] and cellulose[673] can also be cross-linked into dynamic hydrogels by mixing the polyhydroxy polymers with boronic acid-containing polymers in aqueous solutions. The transient boronate ester networks usually can dynamically restructure after fracture, making the resultant hydrogels injectable and self-healable.[674,675] In addition, the boronate ester cross-linked hydrogels are also glucose-sensitive, because glucose can compete with diol groups to form boronate−glucose complexes and therefore de-cross-link the hydrogels.[669] These glucose-sensitivity hydrogels, based on the boronate ester bonds, have been used for self-regulated insulin release and glucose sensing.[398,664,669,676]

4.2.3.3. Disulfide Bond. Disulfide bonds are dynamic covalent bonds based on thiol−thiol interactions at slightly alkaline environments or at mild oxidative conditions.[677,678] The energy of disulfide bonds is around 425 kJ mol^{-1} (Figure 6).[387,394] Many natural polymers have disulfide bonds to stabilize their structures such as fibrinogen[679] and collagen.[680] The disulfide bond can also be introduced into polymers by using disulfide bond-containing cross-linkers such as 3,3′-dithiobis(propanoic dihydrazide)[681,682] and *N*,*N*′-cystamine-bis-acrylamide.[683−685] The thiol−thiol reaction has relatively fast kinetics and can be used to prepare dynamic hydrogels.[686,687] Hydrogels cross-linked by disulfide bonds can be used to encapsulate various types of cells, due to the mild reaction conditions.[688,689] In addition, the disulfide bonds can be cleaved by reducing agents such as tris(2-carboxyethyl)-phosphine,[690] 1,4-dithiothreitol,[691] and glutathione.[686,692]

4.2.3.4. Hydrazone Bond. Hydrazone bonds are formed by the reaction of aldehyde and hydrazide groups.[693] Polymers with hydroxyl groups, such as PEG,[694] cellulose,[695] and polysaccharide,[647] can be easily modified with aldehydes and hydrazide (or acylhydrazine) motifs. The reversible hydrazone bonds can be formed by simply mixing the aldehyde- and hydrazide-containing polymers under physiological conditions.[696−698]

Hydrogels cross-linked by the hydrazone bonds can exhibit reversible sol−gel transition properties by changing the pH.[694,699−701] Hydrogels cross-linked by hydrazone bonds can be used for in situ cell encapsulation due to the cytocompatibility and fast gelation kinetics of the aldehyde and hydrazide coupling.[702,703] The mechanical properties of these hydrogels can be easily tuned, which facilitates the study of the relationships between cell behaviors and mechanics (such as stress-relaxation kinetics) of the hydrogels.[704] Hydrazone bonds can also be used to prepare self-healing and injectable hydrogels based on the reversibility of hydrazone bonds at the mildly acid environment (pH 4.0−6.0).[696,698,700]

4.2.3.5. Oxime Bond. Oxime bonds are formed by the reaction between hydroxylamine and aldehyde or ketone with high efficiency under mild conditions.[705] The reactive aldehyde or ketone groups can be modified onto polymers through radical polymerization[706] or oxidation,[707,708] while the hydroxylamine motifs are mainly modified onto hydroxyl-containing polymers through a sequential *N*-hydroxyphthalimide induced Mitsunobu reaction and hydrazine reduction.[709] Then, the oxime bonds can be formed by mixing the aldehyde- or ketone-containing polymers with the hydroxylamine-containing polymers in a neutral or slightly acid aqueous solution.[710] This reaction is biocompatible without cytotoxic side products and can be used to cross-link biopolymers into hydrogels.[709,711] Because of the dynamic nature, oxime bonds have been used for building self-healing and injectable hydrogels which show higher hydrolytic stability than the hydrogels cross-linked by imines and hydrazones.[710,712]

4.2.3.6. Reversible Diels−Alder Reaction. Diels−Alder reaction is a click reaction between diene and dienophile groups.[713,714] The energy of Diels−Alder bonds ranges from 37.6 kJ mol^{-1} to 130 kJ mol^{-1} (Figure 6).[395,396] To harness the dynamic Diels−Alder reaction as reversible cross-links for hydrogels, natural polymers (such as hyaluronic acid,[715] cellulose,[716] and other polysaccharides[717]) and synthetic polymers (such as PNIPAM[718] and PEG[719]) can be modified with diene (such as furan) functional groups and dienophile (such as maleimide) functional groups on their backbones or chain ends. The equilibrium of the Diels−Alder linkage is thermally responsive. For example, the adducted Diels−Alder linkage can reform maleimide and furan moieties when increasing the temperature.[720,721] The Diels−Alder reaction can be performed in aqueous media at physiologically compatible conditions without any side reactions or by-products.[722−725] Therefore, the Diels−Alder reaction has been used for preparing self-healing or adaptable hydrogels for biological applications in drug delivery and tissue engineering.[715,725,726]

4.2.4. Decoupled Mechanical Properties Due to Unconventional Polymer Network Interactions. The crystalline domains and glassy nodules have been widely used as the high-functionality cross-links in UPNs, whose stretch limit, shear moduli, and intrinsic fracture energy are decoupled as discussed in section 4.1.7 (Figure 9b).

The weak physical cross-links and dynamic covalent cross-links can act as reversible cross-links in polymer networks, leading to decoupled mechanical properties of the resultant hydrogels (Figure 11). Without loss of generality, let us consider a conventional polymer network with long polymer chains (i.e., polymer network sparsely cross-linked by permanent covalent bonds that gives a high N value), whose stretch limit, shear modulus, and intrinsic fracture energy are given by eqs 7−9, respectively. We next introduce reversible cross-links such as weak physical cross-links and dynamic covalent cross-links into the polymer network. When the polymer network undergoes initial small deformation, the reversible cross-links act as additional cross-links,[450] increasing the effective chain density of the polymer network to n_{eff}. Therefore, the shear modulus of the hydrogel with the reversible cross-links under initial deformation increases to

$$G = n_{\text{eff}} kT \lambda_s^{-1} \tag{19}$$

As the hydrogel is highly stretched, the reversible cross-links can be de-cross-linked. However, the covalently cross-linked long polymer chains (i.e., polymers with high N) still endow the hydrogel with a high stretch limit and high intrinsic fracture energy according to eq 13. Notably, hydrogels with only reversible cross-links will display permanent plastic deformation when the reversible cross-links are de-cross-linked under mechanical loads, because there is no permanent covalent cross-link to maintain the shape or elasticity of the hydrogels. Therefore, hybrid reversible and permanent cross-links, instead

https://doi.org/10.1021/acs.chemrev.0c01088
Chem. Rev. XXXX, XXX, XXX−XXX

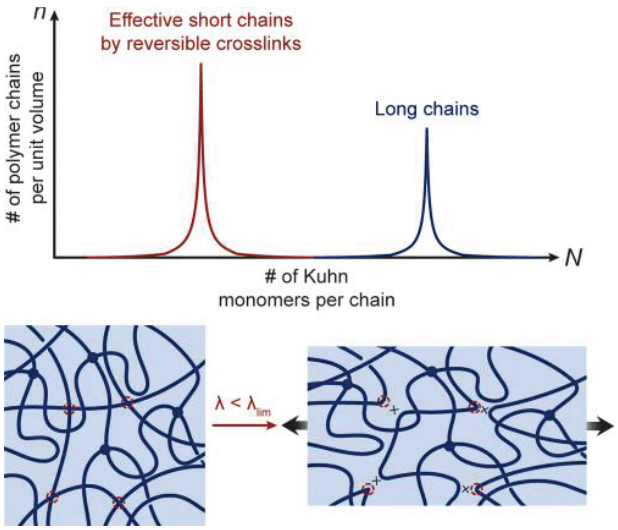

Figure 11. Decoupled mechanical properties of hydrogels due to UPN interactions. The reversible cross-links give an effectively high density of short chains for high modulus, and the sparse covalent cross-links give long chains for high stretchability and high intrinsic fracture energy.

of solely reversible cross-links, are critical to achieving decoupled and extreme mechanical properties of hydrogels.

4.3. Synergy of Unconventional Polymer Network Architectures and Interactions

It is not uncommon for an unconventional polymer network to simultaneously possess both UPN architectures and UPN interactions. In some cases, the UPN architectures and interactions are interdependent. The formation of certain UPN architectures requires certain UPN interactions, or certain UPN interactions naturally lead to the self-assembly of polymers into certain UPN architectures. For example, the UPN interactions of strong physical cross-links such as crystalline domains and glassy nodules mostly have high functionalities, giving rise to UPN architectures with high-functionality cross-links. As another example, the self-assembly of polymer chains into nano-/microfibers usually requires the UPN interactions such as weak physical cross-links.

In other cases, specific types of UPN architectures and UPN interactions can be separately designed and then integrated into the same UPN. For example, weak physical cross-links and dynamic covalent cross-links have been introduced into various UPN architectures in order to design tough hydrogel,[490] because the dissociation and reformation of these reversible cross-links can dissipate mechanical energy to toughen the hydrogels.

5. DESIGN OF HYDROGELS WITH EXTREME MECHANICAL PROPERTIES

While numerous UPN architectures and UPN interactions have been developed over the last few decades, the design of hydrogels that possess extreme mechanical properties has largely followed an Edisonian approach—trial and error with specific polymers. The rational design of hydrogels using different material candidates and fabrication methods for various applications remains a central need in the field of soft materials. In this section, we will summarize a set of general design principles for hydrogels to achieve the corresponding extreme mechanical properties, including extremely high fracture toughness, tensile strength, resilience, interfacial toughness,

Table 3. Typical Examples of Hydrogels That Possess Extreme Mechanical Properties[a]

hydrogel	Young's modulus (kPa)	water content (vol %)	nominal tensile strength (kPa)	fracture toughness (J m^{-2})	fatigue threshold (J m^{-2})	resilience (%)	refs
freeze−thawed PVA	100	85	1,200	100−500	310	30	76, 481, 831
directional freeze−thawed PVA	30−100	88−90	300−1,200	160−420	-	40−50	832
PAMPS−PAAm	100−1,000	90	1,500	1,000−3,000	200−400	30−50	70, 733, 833, 834
PAAm-alginate	10−100	90	170	8700	53	30−40	490
Agar/PAAm	100	80	1,000	-	-	40−50	835
prestretched PAAm-alginate	2	90	-	1,900	-	95	73
polyampholyte	100−2,200	50−70	100−2,000	1,000−4,000	67−71	10−20	825, 836
PNaSS/PMPTC	10−1,000	50	3,300	7,700	-	10−20	566
tetra-PEG	18	95	10	10−30	-	∼100	74, 333, 837
dry annealed PVA	300−9,000	58−75	1,000−9,000	1,000−9,000	300−1,000	40−50	75
mechanically trained PVA	200	84	5,000	1,200	1,200	∼100	76
elastomer-hydrogel composites	200	60−70	180−250	4,500	1,290	90	77
dual-cross-linked p(AAm-*co*-AAc)	500−3,500	60−70	3,000−6,500	-	-	20−40	838
nanoclay reinforced PNIPAM	0.8−26	90	27−300	-	-	-	839
wood hydrogel	200,000	65	500−35,000	-	-	-	781
fiber reinforced PAAm-Alginate	660−6,370	100−700	200−1,000	6,000−32,000	-	70−80	777
PA-GF	606,000	38	-	100,000−400,000	-	-	840
wool reinforced PAAm-alginate	50−7,000	86	200−700	-	-	-	778
PNAGA	50−200	70	100−1,100	200−1,100	-	60	750

[a]-, Indicates not reported.

https://doi.org/10.1021/acs.chemrev.0c01088
Chem. Rev. XXXX, XXX, XXX−XXX

Table 4. Typical Examples of Hydrogel Adhesions That Possess Extreme Mechanical Properties[a]

hydrogel adhesion	water content (vol %)	Young's modulus (kPa)	interfacial toughness ($J\ m^{-2}$)	interfacial fatigue threshold ($J\ m^{-2}$)	refs
PAAm-alginate to nonporous surfaces	90	10−100	1,000−1,700	68	78, 831
bioadhesive double-sided tapes to tissues	90	7.5−15	710	-	47
PAAm-alginate to tissues	90	12	580	24.4	50, 829
PAAm-alginate to elastomers	90	10−100	1,000	-	788
PAMPS−PAAm to porous surfaces	90	-	200−900	-	793
dry annealed PVA to glass	38−68	-	8,000	800	78
PDA-clay-PAAm to glass	80	100−200	-	-	841
Dopa-modified PEG to porcine skin	90	2	-	-	842
PAAm to polyester cloth	90	-	1,400	300	828

[a]-, Indicates not reported.

fatigue threshold, interfacial toughness, and interfacial fatigue threshold (Table 3 and Table 4). Then, we will discuss the implementations strategies for these design principles using the UPN architectures and/or the UPN interactions.

5.1. Tough: Build Dissipation into Stretchy Polymer Networks

5.1.1. Fracture Toughness. Fracture toughness has been widely used to characterize a material's capability to resist fracture under mechanical loads. One common definition for the fracture toughness of a material is the energy required to propagate a crack in the material over a unit area measured in the undeformed state (Figure 12a) which can be quantitatively expressed as

$$\Gamma = G_c = -\frac{dU}{dA} \tag{20}$$

where Γ is the fracture toughness, U is the total potential energy of the system, A is the crack area measured in the undeformed state, and G_c is the critical energy release rate that drives crack propagation. According to eq 20, the unit for the fracture toughness is joule per meter squared (i.e., $J\ m^{-2}$).

The fracture toughness of soft materials such as elastomers and hydrogels has been measured with many experimental methods such as the pure-shear test and the single-notch test, which have been summarized in a few recent review papers.[67,727,728] For example, in the pure-shear test, two identical pieces of a hydrogel are fabricated with the same thickness T, width W, and height H, where $W \gg H \gg T$ (Figure 12a). Both pieces of the samples are clamped along their long edges (i.e., along the width direction) with rigid plates. A notch with a length of $\sim 0.5W$ is introduced into the first sample, which is then gradually pulled to a stretch of λ_c times of its undeformed height until a crack begins to propagate from the notch (Figure 12a). The second sample without notch is uniformly stretched above the critical stretch λ_c to measure the nominal stress s vs stretch λ relation (Figure 12a). Thereafter, the fracture toughness of the hydrogel can be calculated as $\Gamma = H\int_1^{\lambda_c} s\, d\lambda$, based on the measured λ_c and s-λ relation in the pure-shear tests.

As discussed in section 3, the fracture toughness of a conventional polymer network is its intrinsic fracture energy Γ_0, which is the energy required to fracture a layer of polymer chains over a unit area (Figure 12b). Evaluated with typical parameters of conventional polymer networks, the fracture toughness of the corresponding hydrogels is commonly limited to a few tens of joules per meter squared. In addition, the fracture toughness of hydrogels with conventional polymer networks is also coupled with their stretch limits and shear moduli (eqs 11). For example, in order to increase the fracture toughness of a conventional polymer network, the chain length (i.e., N) and thus the stretch limit of the polymer network need to be increased. Consequently, the chain density (i.e., n) and thus the shear modulus of the polymer network will be decreased.

5.1.2. Design Principle for Tough Hydrogels. The design principle for tough hydrogels is the same as the principle for toughening various engineering materials (such as metals,[729] ceramics,[730] composites,[731] and polymers[64]) and various biological tissues (such as tendons, cartilages, muscles, and blood vessels[732]). That is to integrate both ductility and mechanical dissipation in the same material, so that a process zone with substantial mechanical dissipation develops around the crack tip prior to crack propagation (Figure 12c−e). The mechanical dissipation of a material manifests as the hysteresis loop on its stress−stretch curve under a loading−unloading cycle (Figure 12c−e). The ductility of hydrogels generally relies on the high stretchability (or the high stretch limit) of their polymer networks (Figure 12c−e). Overall, the design principle for tough hydrogels is *to build dissipation into stretchy polymer networks*.[67,733] Quantitatively, the total fracture toughness of a hydrogel with the capability of mechanical dissipation can be expressed as[67,734]

$$\Gamma = \Gamma_0 + \Gamma_D \tag{21}$$

where Γ, Γ_0, and Γ_D are the total fracture toughness, the intrinsic fracture energy, and the contribution of mechanical dissipation in the process zone to the total fracture toughness, respectively. While the intrinsic fracture energy for hydrogels is usually limited to a few tens of joules per meter squared, the contribution of the process-zone dissipation can be extremely high because both the dissipated energy per volume of the process zone and the size of the process zone can be large values (Figure 12c−e). Indeed, the fracture toughness of tough hydrogels has exceeded 10,000 $J\ m^{-2}$, orders of magnitude higher than that of hydrogels with conventional polymer networks.[67]

5.1.3. Implementation Strategies for Tough Hydrogels. The design principle for tough hydrogels requires the following: (i) at least one polymer network in the hydrogel maintains a high stretch limit, and therefore the polymer chains in that polymer network need to have a high N value according to eq 7; and (ii) at least one component in the hydrogel dissipates substantial mechanical energy under the deformation typically experienced in the process zone. The design principle for tough hydrogels has been implemented using various types of

https://doi.org/10.1021/acs.chemrev.0c01088
Chem. Rev. XXXX, XXX, XXX−XXX

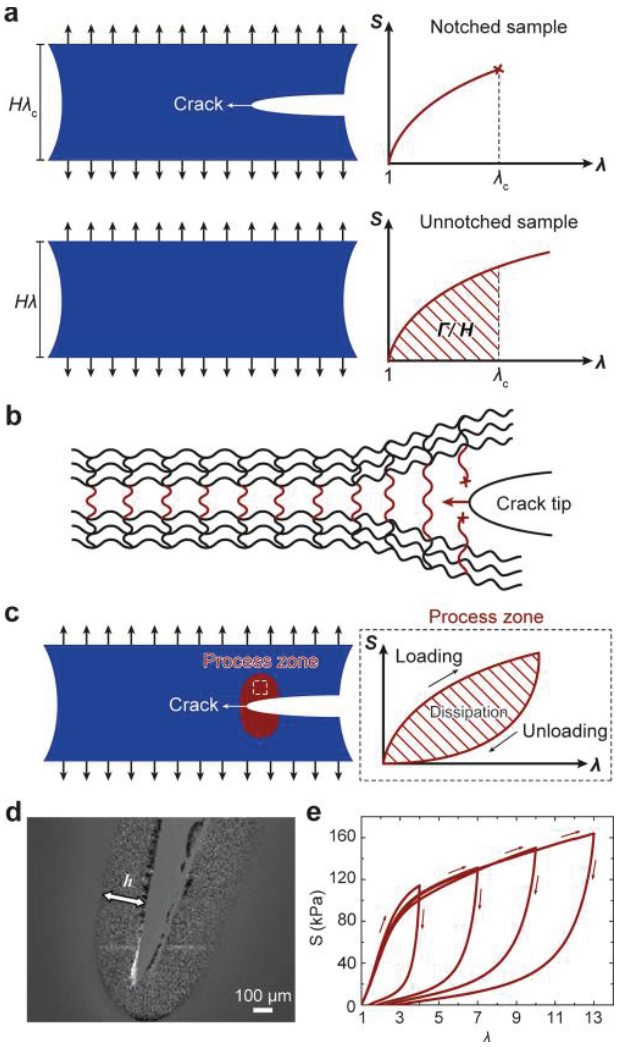

Figure 12. Design principle for tough hydrogels: build dissipation into stretchy polymer networks. (a) definition of fracture toughness, and the pure-shear test to measure the fracture toughness. When a notched sample with height H at the undeformed state is stretched by a critical ratio of λ_c under the pure-shear deformation, the crack begins to propagate (top). The relation of the nominal stress s and the stretch λ is measured for an un-notched sample (otherwise the same as the notched sample) under the pure-shear deformation (bottom). The fracture toughness can be calculated as $\Gamma = H\int_1^{\lambda_c} s\, d\lambda$ based on the measured λ_c and s-λ relation in the pure-shear tests. (b) The intrinsic fracture energy Γ_0 from fracturing a layer of polymer chains. (c) The mechanical dissipation in the process zone around the crack tip contributes to the total fracture toughness by Γ_D. The mechanical dissipation manifests as a hysteresis loop on the stress−stretch curve. The total fracture toughness of the tough hydrogel is $\Gamma = \Gamma_0 + \Gamma_D$. (d) Microscope image of the process zone around the crack in a PAMPS−PAAm hydrogel.[735] (e) Nominal stress s vs stretch λ relations for a PAAm-alginate hydrogel under loading and unloading cycles.[490] Panel (d) is reproduced with permission from ref 735. Copyright 2009 American Chemical Society. Panel (e) is reproduced with permission from ref 490. Copyright 2012 Springer Nature.

UPN architectures and UPN interactions. We will discuss a few examples in the following paragraphs.

The interpenetrating polymer networks and semi-interpenetrating polymer networks have been widely used for the design of tough hydrogels since the pioneer work of double-network hydrogels by Gong et al. in 2003 (Figure 13a).[70] A typical double-network hydrogel interpenetrates a long-chain

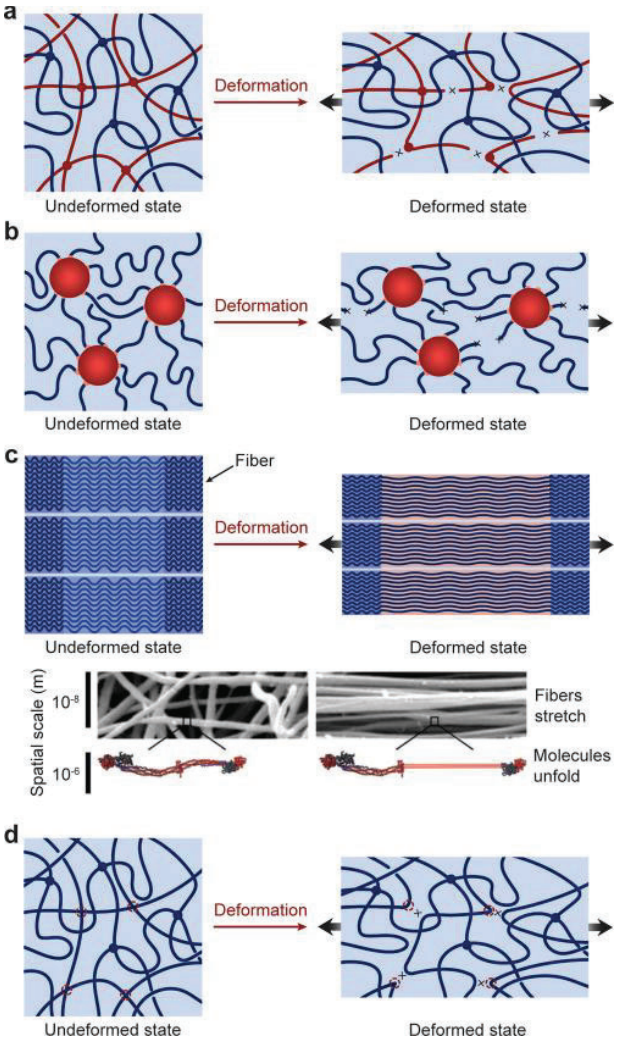

Figure 13. Implementation strategies for tough hydrogels with UPNs. Schematics of the implementation strategies with (a) interpenetrating or semi-interpenetrating polymer networks, (b) polymer networks with high-functionality cross-links, (c) nano-/microfibrous polymer networks, and (d) polymer networks with reversible cross-links. The bottom panel of c is a microscope image of a fibrous fibrin hydrogel.[748] The bottom panel of (c) is reproduced with permission from ref 748. Copyright 2009 American Association for the Advancement of Science.

network (with high N) and a short-chain network (with low N).[70] As the double-network hydrogel deforms, the short-chain network fractures and dissipates substantial mechanical energy, while the long-chain network maintains the integrity of the hydrogel even under high stretches, implementing the design principle for tough hydrogels (Figure 12c).[70,733,735] Gong et al. first demonstrated that the fracture toughness of double-network hydrogels can exceed 1000 Jm.[2,70] Other interpenetrating and semi-interpenetrating polymer networks such as the triple-network architecture have also been developed for tough hydrogels[736] and elastomers,[737] implementing the design principle. Notably, since the fracture of the short-chain network is usually irreversible, these hydrogels' capability of mechanical

https://doi.org/10.1021/acs.chemrev.0c01088
Chem. Rev. XXXX, XXX, XXX−XXX

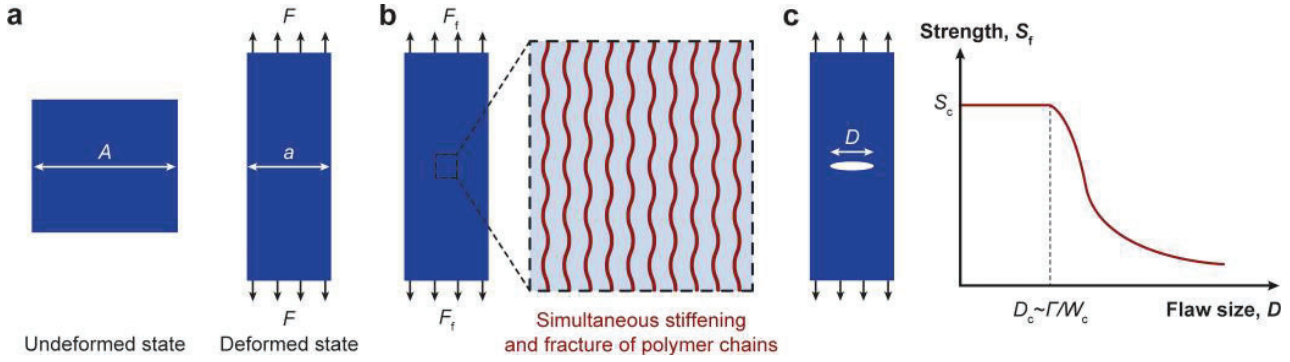

Figure 14. Design principle for strong hydrogels: synchronize stiffening and fracture of multiple polymer chains. (a) Definition and measurement of the tensile strength. *A* and *a* are the cross-section areas of the sample in the undeformed and deformed states, respectively, and *F* is the applied tensile force. (b) The simultaneous stiffening and fracture of multiple polymer chains give a high tensile strength.[771] F_f is the tensile force at the failure of the sample. (c) The nominal tensile strength s_c increases with the decrease of the defect size *D* up to a critical value D_c, below which the tensile strength is defect-insensitive.[773,774]

dissipation may be substantially reduced after a few cycles of large deformation.[734]

The polymer networks with high-functionality cross-links have given tough hydrogels based on various types of polymers and high-functionality cross-links. There are multiple polymer chains (e.g., over 10) bridging between two adjacent high-functionality cross-links, and the lengths of these polymer chains are usually nonuniform (Figure 13b). As the hydrogel deforms, the relatively short polymer chains fracture or detach from the high-functionality cross-links, while the relatively long polymer chains maintain the integrity and high stretchability of the hydrogel, implementing the design principle for tough hydrogels. The bonds between the polymer chains and the high-functionality cross-links can be permanent covalent cross-links,[738] strong physical cross-links,[739,740] weak physical cross-links,[741,742] and dynamic covalent cross-links,[743,744] or a combination of them.[501] Depending on the number and lengths of polymer chains between adjacent cross-links and the types of bonds between polymer chains and cross-links, the corresponding hydrogel can have different capabilities of mechanical dissipation and stretchability and therefore different fracture toughness.

The nano-/microfibrous hydrogels have also been used to implement the design principle for tough hydrogels. The nano-/microfibers can be made intrinsically stretchable (Figure 13c), and their reorientation and realignment in hydrogels under deformation further enhance the stretchability of the hydrogels (Figure 13c).[740,743,745−748] The fracture of the nano-/microfibers and pull-out of the nano-/microfibers from the hydrogel matrices can dissipate substantial mechanical energy. A combination of the high stretchability and the mechanical dissipation enabled by the nano-/microfibrous polymer networks implements the design principle for tough hydrogels.

In addition to the above-mentioned UNP architectures, the UPN interactions have also been widely used to implement the design principle for tough hydrogels.[749] The strong physical cross-links such as crystalline domains and glassy nodules naturally act as high-functionality cross-links for the corresponding UPN architectures (Figure 13b), which lead to tough hydrogels as discussed above.

The weak physical cross-links[566,584,623,750−757] and dynamic covalent cross-links[743] have been added into polymer networks with long polymer chains (i.e., sparsely cross-linked polymer networks via permanent covalent bonds) to design tough hydrogels. The weak physical cross-links and dynamic covalent cross-links act as reversible cross-links in these hydrogels (Figure 13d). As the hydrogel deforms, many of these reversible cross-links dissociate or de-cross-link to dissipate substantial mechanical energy, and the sparsely cross-linked long-chain polymer network still sustains the high stretchability of the polymer network (Figure 13d). A synergy of the mechanical dissipation and the high stretchability enabled by the hybrid reversible and covalent cross-links implements the design principle for tough hydrogels.

The weak physical cross-links and dynamic covalent cross-links have also been added into UPN architectures such as the interpenetrating polymer networks (Figure 13a),[490,563,758−765] polymer networks with high-functionality cross-links (Figure 13b),[739,741,742,766−769] and nano-/microfibrous polymer networks (Figure 13c)[745,746,767,770] to further toughen the resultant hydrogels, leveraging these reversible bonds' capability of dissipating additional mechanical energy. Furthermore, unlike irreversibly fractured polymer chains, the dissociated weak physical cross-links and dynamic covalent cross-links may reassociate due to their reversible nature, potentially endowing the tough hydrogels with recoverable dissipation over cyclic loads.[490] For further detailed discussion on the design principle and implementation strategies for tough hydrogels, a recent review paper is recommended.[67]

5.2. Strong: Synchronize Stiffening and Fracture of Multiple Polymer Chains

5.2.1. Tensile Strength. Multiple types of strengths such as tensile strength, compressive strength, and shear strength have been used to characterize the strength of a material. We will focus on tensile strengths of hydrogels in this paper due to two reasons: (1) The tensile, compressive, and shear deformations of a sample are related to one another. For example, the uniaxial compression of a sample is equivalent to the biaxial tension of the sample; the pure shear of a sample is equivalent to the sample being elongated in one direction and shortened perpendicularly. (2) The tensile strength is easier to measure than the shear strength, and the tensile strength is less affected by boundary conditions in the measurement (such as friction) than the compressive strength.

Since soft materials such as elastomers and hydrogels usually do not yield plastically, their tensile strengths are commonly defined as the stresses at which the ultimate tensile failure occurs

https://doi.org/10.1021/acs.chemrev.0c01088
Chem. Rev. XXXX, XXX, XXX−XXX

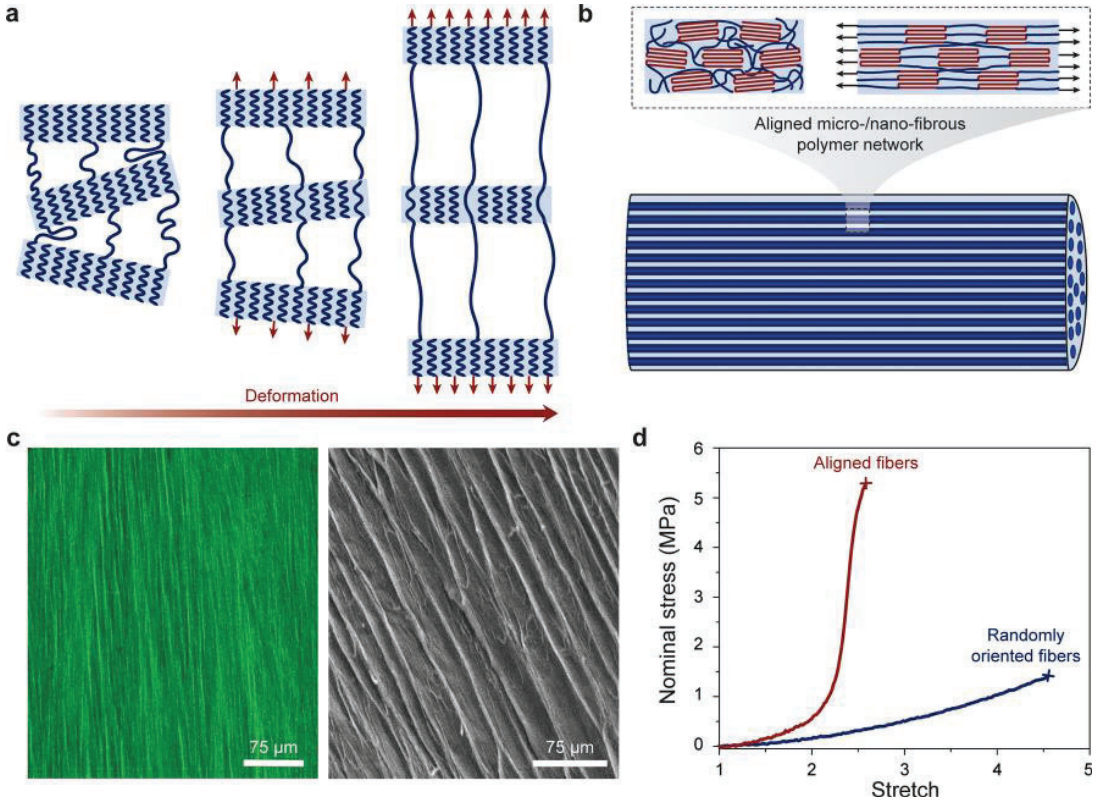

Figure 15. Implementation strategies for strong hydrogels with UPNs. Schematics on the implementation with (a) polymer networks with high-functionality cross-links, (b) nano-/microfibrous polymer networks. (c) Confocal (left) and SEM (right) images of a fibrous PVA hydrogel with aligned fibers.[76] (d) Nominal stress–stretch curves of the fibrous PVA hydrogels with aligned and randomly oriented fibers.[76] Panels c and d are reproduced with permission from ref 76. Copyright 2019 National Academy of Sciences.

in the uniaxial tensile test. In addition, since the hydrogel samples usually undergo large deformation before failure, the tensile strength can be defined based on either the nominal stress or the true stress (Figure 14a),

$$s_f = \frac{F_f}{A}, \quad \sigma_f = \frac{F_f}{a} \tag{22}$$

where F_f is the tensile force at the failure of the sample, A and a are the cross-section areas of the sample in the reference (undeformed) and current (deformed) states, respectively, and s_f and σ_f are the nominal and true tensile strengths, respectively. The nominal tensile strengths of hydrogels with conventional polymer networks and even tough hydrogels are commonly lower than 1 MPa,[70,490] much lower than the tensile strengths of engineering materials such as metals and biological tissues such as tendons.

5.2.2. Design Principle for Strong Hydrogels. A generic principle for the design of strong hydrogels is to make a substantial number of polymer chains in the polymer network to stiffen and then fracture simultaneously (Figure 14b). Following this principle, the nominal and true tensile strengths of the polymer network can be evaluated as

$$s_f = M_f f_f, \quad \sigma_f = m_f f_f \tag{23}$$

where f_f is the force required to fracture a single polymer chain, which is on the order of a few nanonewtons,[385] and M_f and m_f are the numbers of simultaneously fractured polymer chains per unit area of the polymer network at the undeformed and deformed states, respectively. It has been evaluated that s_f and σ_f can reach up to 1 and 10 GPa, respectively, in an ideal scenario where all polymer chains in the polymer network fracture simultaneously.[771]

In realistic situations, almost all materials contain defects in the forms such as notches, microcracks, cavities, impurities, and missing polymer chains or cross-links. The presence of defects usually significantly reduces the tensile strengths of the materials.[772−774] Without loss of generality, let us assume the largest defect in the tensile sample is a notch with length D in the undeformed state perpendicular to the tensile direction (Figure 14c). The tensile strength of the sample generally increases with the decrease of the defect size D up to a critical value D_c, below which the tensile strength is defect-insensitive (Figure 14c). A scaling relation for the critical defect size D_c can be expressed as[773,774]

$$D_c \approx \frac{\Gamma}{W_c} \tag{24}$$

where W_c is the work for tensile failure of a unit volume of the defect-insensitive sample, and Γ is the fracture toughness of the sample.

In order to achieve strong hydrogels, it is highly desirable for the hydrogel samples to have defect-insensitive tensile strengths.[771] According to eq 24, a tougher material (i.e., with higher Γ) can be insensitive to larger defects due to a larger critical defect size (i.e., larger D_c). For example, the critical defect size is on the order of a few nanometers for glass and ceramics, a few micrometers for brittle hydrogels, and a few millimeters for tough elastomers and hydrogels.[773,774] Furthermore, it is a

https://doi.org/10.1021/acs.chemrev.0c01088
Chem. Rev. XXXX, XXX, XXX−XXX

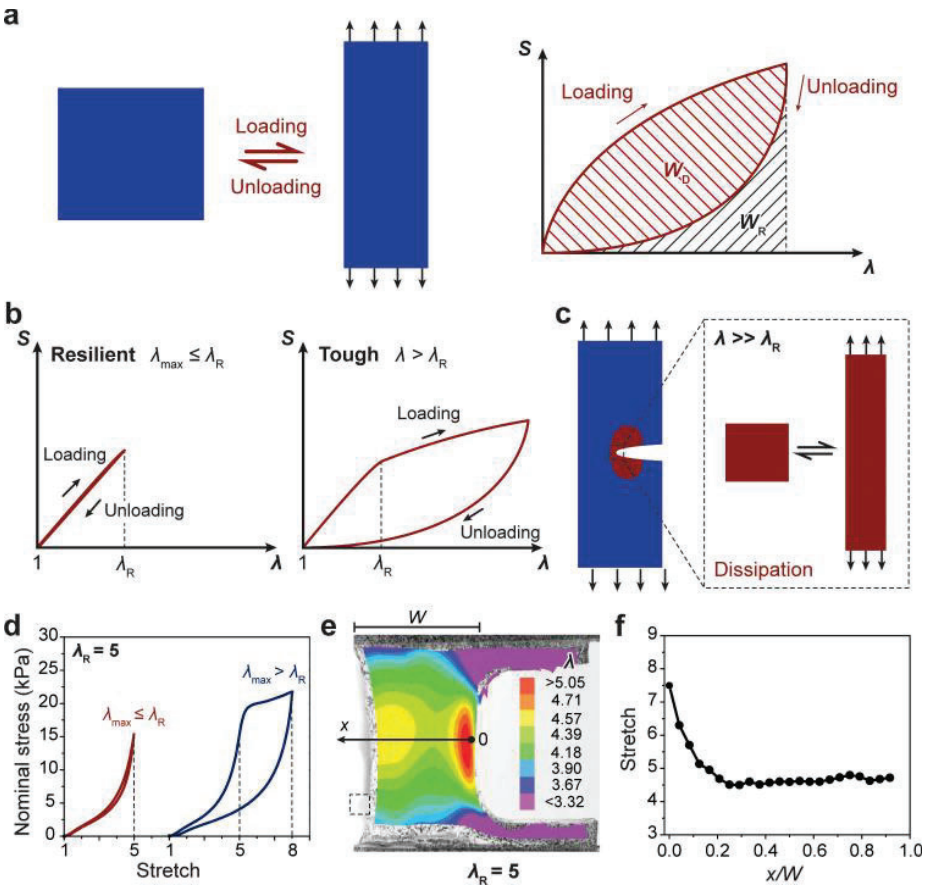

Figure 16. Design principle for resilient and tough hydrogels: delay dissipation. (a) Definition and measurement of resilience. The relation of nominal stress s and stretch λ of a sample is measured under uniaxial tension in a loading−unloading cycle. W_R and W_D are the energy released in the unloading and the dissipated energy per unit volume of the sample, respectively. The resilience can be calculated as $R = W_R/(W_R + W_D)$. (b) When the stretch is below a critical stretch λ_R, the hydrogel releases most of the stored elastic energy during deformation recovery, giving high resilience; when the stretch is above λ_R, the hydrogel dissipates substantial mechanical energy, giving high fracture toughness.[73] (c) The stretch in the process zone around the crack is usually much higher than λ_R, dissipating substantial mechanical energy and giving high fracture toughness.[73] (d) The nominal stress vs stretch curves of a PAAm-alginate hydrogel with $\lambda_R = 5$.[73] (e) The measured deformation around a crack in the PAAm-alginate hydrogel with $\lambda_R = 5$. (f) The stretch in the process zone can be much higher than $\lambda_R = 5$.[73] Panels (b) and (c) are reproduced with permission from ref 73. Copyright 2014 Elsevier. Panels d, e, and f are reproduced with permission from ref 73. Copyright 2014 Elsevier.

common strategy to set the characteristic size of the sample (e.g., the diameter of the sample in Figure 14c) to be similar to or smaller than the critical defect size D_c, so that the tensile strength of the sample is guaranteed to be insensitive to any possible defects in the sample.[771]

5.2.3. Implementation Strategies for Strong Hydrogels. The UPNs with high-functionality cross-links such as nanocrystalline domains have been widely used for the design of strong hydrogels.[75] As the hydrogels undergo large deformation, relatively short polymer chains are gradually pulled out of the nanocrystalline domains, so that the polymer chains bridging adjacent nanocrystalline domains tend to have similar lengths and therefore stiffen and then fracture simultaneously—implementing the design principle for strong hydrogels (Figure 15a).

The nano-/microfibrous polymer networks are another type of UPN architecture that implements the design principle for strong hydrogels (Figure 15b). The diameters of the nano-/microfibers can be readily controlled below the critical defect size D_c. Bundles of polymer chains in the nano-/microfibers can be designed to stiffen and then fracture simultaneously to endow the fibers with high tensile strengths up to the ideal strengths (Figure 15b).[76,740,743,747,775] Consequently, the resultant nano-/microfibrous hydrogels can reach extremely high tensile strengths (Figure 15c,d). Notably, biological hydrogels such as tendons, ligaments, and muscles commonly adopt nanofibers and microfibers, often in hierarchical architectures, to achieve high tensile strengths (Figure 2).

In addition to the aforementioned UPN architectures, the UPN interactions can facilitate the implementation of the design principle for strong hydrogels. The strong physical cross-links such as crystalline domains allow the pull-out of polymer chains from them to achieve simultaneous stiffening and then fracture of multiple polymer chains (Figure 15a).[75] The weak physical cross-links such as the hydrogen bonds can facilitate the alignment and self-assembly of polymer chains into bundles (Figure 15b), which tend to stiffen and then fracture simultaneously to give high tensile strengths of the hydrogels.

On a structural level, high-strength macrofibers made of polymers,[776,777] steel,[778] glass,[779,780] and wood[781] have been utilized to strengthen hydrogels, and the tensile strengths of the

https://doi.org/10.1021/acs.chemrev.0c01088
Chem. Rev. XXXX, XXX, XXX−XXX

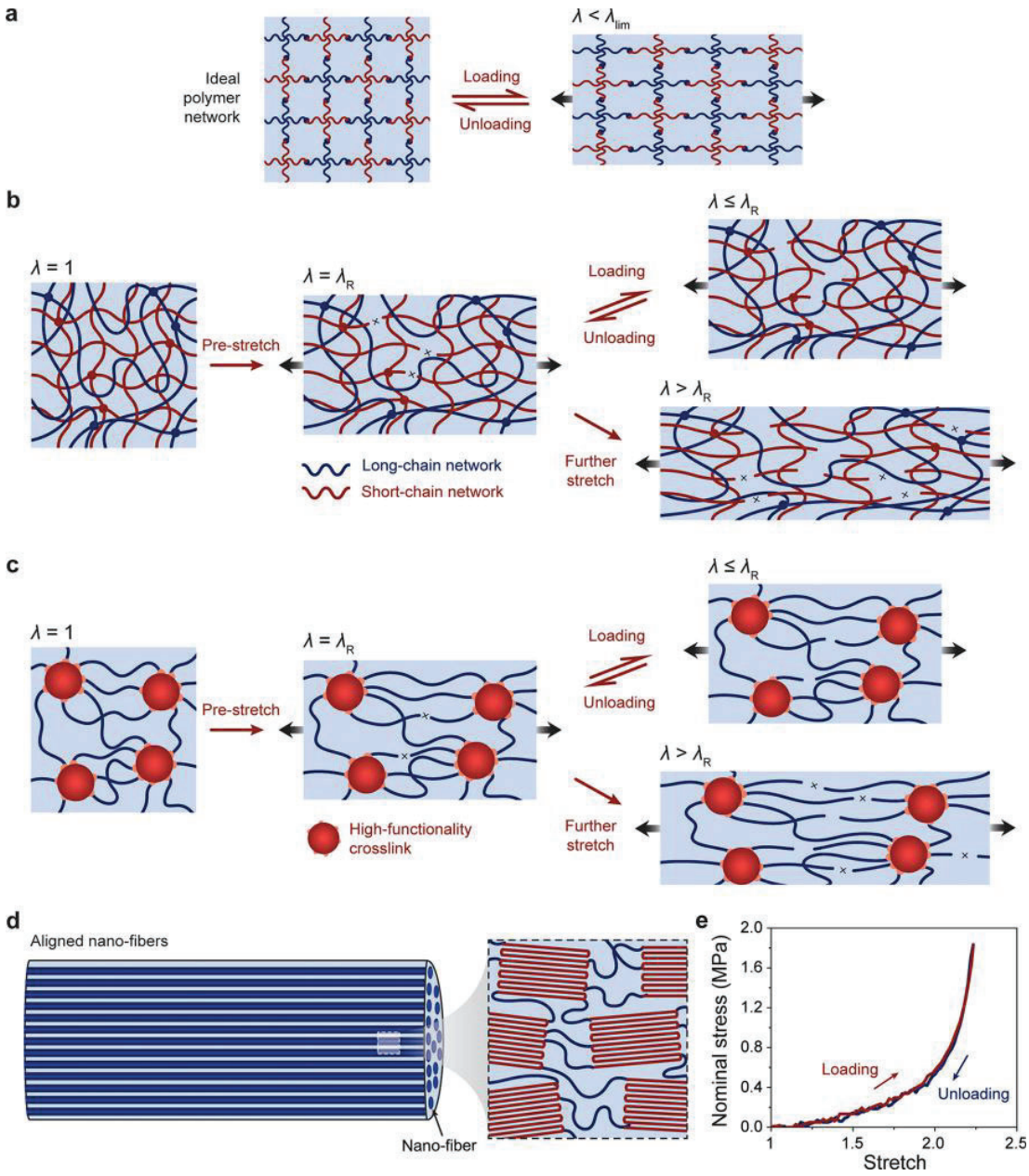

Figure 17. Implementation strategies for resilient and tough hydrogels with UPNs. (a) Ideal polymer networks are resilient up to fracture due to the lack of dissipation mechanism. (b) Prestretching interpenetrating polymer networks to λ_R can make them both resilient and tough. (c) Prestretching polymer networks with high-functionality cross-links to λ_R can make them both resilient and tough.[73] (d) Nano-/microfibrous polymer networks with resilient fibers can be both resilient and tough. (e) The nominal stress−stretch curve of a resilient and tough nanofibrous PVA hydrogel.[76] Panel (e) is reproduced with permission from ref 76. Copyright 2019 National Academy of Sciences.

resultant hydrogels are primarily determined by the strengths of the macrofibers.

5.3. Resilient: Delay Dissipation

5.3.1. Resilience. Resilience of soft materials such as elastomers and hydrogels is commonly defined as the ratio of the energy released in deformation recovery to the energy required to induce the deformation of the materials.[782] Let us consider a cylindrical sample under the uniaxial tensile test over a loading−unloading cycle (Figure 16a). The energy released in the unloading and the dissipated energy per unit volume of the sample are denoted as W_R and W_D, respectively. Therefore, the resilience R and the hysteresis ratio H of the material can expressed as (Figure 16a)[73,782]

$$R = \frac{W_R}{W_R + W_D}, \quad H = \frac{W_D}{W_R + W_D} = 1 - R \tag{25}$$

The resilience R and the hysteresis ratio H depend on the material properties and the loading conditions such as the applied stretch and the applied stretch rate. The resilience of soft materials has been measured with many experimental methods such as the cyclic tensile test and the dropping-ball test.[73,782]

https://doi.org/10.1021/acs.chemrev.0c01088
Chem. Rev. XXXX, XXX, XXX−XXX

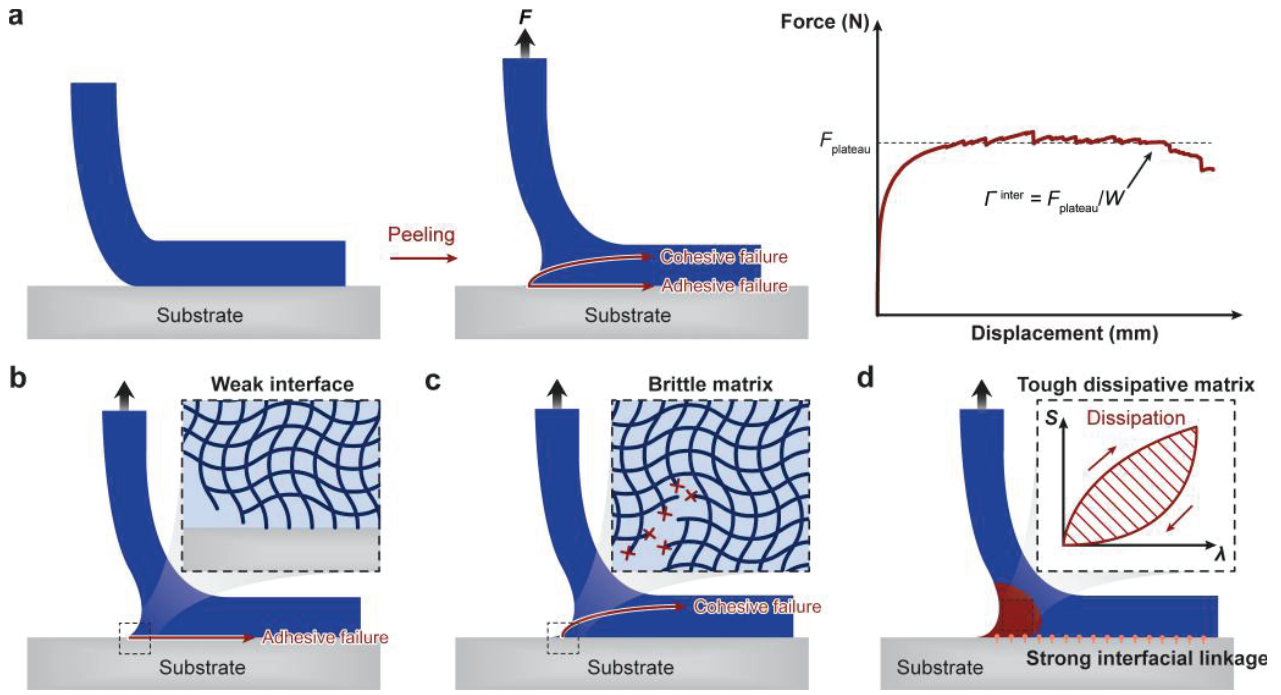

Figure 18. Design principle for tough adhesion of hydrogels: integrate tough dissipative hydrogels and strong interfacial linkages. (a) Definition of interfacial toughness, and the 90-deg peeling test to measure the interfacial toughness. F is the peeling force, $F_{plateau}$ is the plateau peeling force, and W is the width of the sample. The interfacial toughness can be calculated as $\Gamma^{inter} = F_{plateau}/W$ based on the values of $F_{plateau}$ and W measured in the 90-deg peeling test. (b) Weak interface can give the adhesive failure mode. (c) Brittle hydrogel matrix can give the cohesive failure mode. (d) Integration of tough dissipative hydrogels and strong interfacial linkages gives tough adhesion of hydrogels.[49] The contributions of strong interfacial linkages and mechanical dissipation in the process zone to the total interfacial toughness are Γ_0^{inter} and Γ_D^{inter}, respectively. The total interfacial toughness of the tough adhesion is $\Gamma^{inter} = \Gamma_0^{inter} + \Gamma_D^{inter}$. Panel (d) is reproduced with permission from ref 49. Copyright 2016 Springer Nature.

5.3.2. Design Principle for Resilient and Tough Hydrogels. Once a material is deformed to fracture, the elastic energy stored in the material is mostly dissipated,[73,74,783] giving low energy recovery and thus low resilience of the fractured material. Therefore, the high resilience of hydrogels can only be designed up to the fracture of the hydrogels. A generic principle for the design of resilient hydrogels is to minimize the mechanical dissipation of the hydrogels within certain range of deformation that is commonly experienced by the hydrogels, or in short, to delay dissipation.[73] Without loss of generality, we define a critical stretch for polymer chains in a hydrogel λ_R, below which the hydrogel can release most of the stored elastic energy during deformation recovery (i.e., $W_D \approx 0$, Figure 16b).[73] Therefore, according to eq 25, the hydrogel will give a high resilience under the condition,

$$\lambda \leq \lambda_R \leq \lambda_{lim} \tag{26}$$

where λ and λ_{lim} are the stretch and the stretch limit of polymer chains in the hydrogel, respectively.

The design principle for resilient hydrogels also reconciles a pair of seemly contradictory properties, fracture toughness and resilience, in the following manner. The hydrogel is highly resilient under moderate deformation with $\lambda \leq \lambda_R$ (Figure 16b); however, when a crack attempts to propagate in the hydrogel, the chain stretch in the process zone around the crack tip can be much higher than λ_R, inducing substantial mechanical dissipation to toughen the hydrogel (Figure 16c). Indeed, biological hydrogels such as heart valves delay the mechanical dissipation up to supraphysiological deformation levels to achieve both high fracture toughness and high resilience (Figure 2).[784,785] Synthetic elastomers,[786] hydrogels,[73] and hydrogel composites[77] have also been made both tough and resilient by following the design principle of delaying dissipation (Figure 16d–f).

5.3.3. Implementation Strategies for Resilient and Tough Hydrogels. The ideal polymer networks are one common UPN architecture to implement the design principle for resilient hydrogels.[74,783] Because the polymer chains in the ideal polymer networks have relatively uniform lengths and no entanglement, the hydrogels with the ideal polymer networks usually can be deformed without significant mechanical dissipation up to stretch limits, giving high resilience (Figure 17a).[74,783] It is also expected that the polymer networks with slidable cross-links may be able to implement the design principle for resilient hydrogels because the energy dissipated for sliding the cross-links during their reconfiguration may be negligibly low. Despite being resilient, the ideal polymer networks and polymer networks with slidable cross-links are not tough since their fracture toughness is still the intrinsic fracture energy Γ_0 for fracturing a layer of polymer chains as discussed in section 4.1.

The multimodal polymer networks including the interpenetrating polymer networks, semi-interpenetrating polymer networks, and polymer networks with high-functionality cross-links usually begin to dissipate mechanical energy at very small deformation because of the fracture and/or de-cross-link of very short polymer chains in the polymer networks. Such "early" dissipation gives narrow ranges of resilient deformation for the hydrogels in practical applications.[73] To address the issue of "early" dissipation, Lin et al. have prestretched the inter-

https://doi.org/10.1021/acs.chemrev.0c01088
Chem. Rev. XXXX, XXX, XXX−XXX

penetrating polymer networks up to λ_R to fracture and/or de-cross-link susceptible short polymer chains and thus deplete possible dissipation mechanisms within the deformation range of λ_R (Figure 17b).[73] In subsequent tests, if the chain stretch in the hydrogel is below λ_R, the hydrogel is highly resilient, due to the lack of mechanical dissipation within this range (Figure 17b). However, as the polymer chains are stretched beyond λ_R, for example, in the process zone around the crack tip, some of the polymer chains will be further fractured and de-cross-linked to dissipate mechanical energy and toughen the hydrogel (Figure 17b and Figure 16c,e,f). It is expected that other multimodal polymer networks such as the semi-interpenetrating polymer networks and polymer networks with high-functionality cross-links[50] can be prestretched in a similar way to implement the design principle for resilient hydrogels (Figure 17c). Notably, when prestretching the multimodal polymer networks, the fracture and de-cross-link of polymer chains should be irreversible, so that the dissipation mechanism is irrecoverable once depleted.[76]

The nano-/microfibrous polymer networks can naturally implement the design principle for resilient hydrogels by constituting the hydrogels with resilient nano-/microfibers (Figure 17d,e).[76] In addition, because the energy required to fracture and pull out the nano-/microfibers can be much higher than the energy for fracturing amorphous polymer chains, the resilient nano-/microfibrous hydrogels can also be tough.[76]

Besides the above-mentioned UPN architectures, some UPN interactions can also facilitate the implementation of the design principles for resilient hydrogels. The strong physical cross-links such as crystalline domains provide the high-functionality cross-links for some UPN architectures, which can be prestretched to give resilient hydrogels (Figure 17c).[75] Notably, the weak physical cross-links and dynamic covalent cross-links may be unsuitable to implement the design principle for resilient hydrogels because of their reversible and dissipative nature.[73]

On a structural level, resilient elastomeric macrofibers have been embedded into resilient hydrogel matrices to give resilient yet tough hydrogel composites.[77]

5.4. Tough Adhesion: Integrate Tough Dissipative Hydrogels and Strong Interfacial Linkages

5.4.1. Interfacial Toughness. Interfacial toughness, or so-called practical work of adhesion, has been commonly used to characterize the capability of the interface of two adhered materials to resist fracture under mechanical loads. One common definition for the interfacial toughness between two adhered materials is the energy required to propagate a crack along the interface or in either material over a unit area measured in the undeformed state of the materials (Figure 18a).[787] Depending on whether the crack propagates along the interface or in either material, the failure mode is called the adhesive failure or cohesive failure, respectively (Figure 18a). Quantitatively, the interfacial toughness Γ^{inter} can be expressed as

$$\Gamma^{inter} = G_c = -\frac{dU}{dA} \tag{27}$$

where U is the total potential energy of the system, A is the crack area measured in the undeformed state, and G_c is the critical energy release rate that drives interfacial crack propagation. According to eq 27, the unit for the interfacial toughness is joule per meter squared (i.e., J m^{-2}).

The interfacial toughness of soft materials such as elastomers and hydrogels has been measured with many experimental methods such as the 90-deg peeling test, the T-peeling test and the lap-shear test.[727,787] For example, in the 90-deg peeling test, a layer of a hydrogel with thickness T, width W and length L ($L \gg W \gg T$) is bonded on a substrate, and a notch is introduced on the interface along the length direction (Figure 18a). The detached part of the hydrogel is further peeled off the substrate, while maintaining vertical to the substrate (Figure 18a). The measured force reaches a plateau $F_{plateau}$ as the peeling process enters the steady state, and the interfacial toughness is determined by dividing the plateau force $F_{plateau}$ by the width of the hydrogel sheet W, i.e., $\Gamma^{inter} = F_{plateau}/W$.

If a hydrogel with a conventional polymer network is strongly bonded on a substrate (e.g., via covalent bonds), the interfacial toughness is on the level of the hydrogel's fracture toughness or intrinsic fracture energy Γ_0. This is because the fracture toughness of the hydrogel poses an upper limit for the interfacial toughness, since the cohesive failure mode may occur (Figure 18c).[49] Therefore, evaluated with typical parameters of conventional polymer networks, the interfacial toughness of the hydrogel is bounded by a few tens of joules per meter squared. If the hydrogel is adhered on the substrate via a low density of weak physical cross-links such as hydrogen bonds and electrostatic interactions, the interfacial toughness can be even lower since the adhesive failure mode may occur (Figure 18b).[48]

5.4.2. Design Principle for Tough Adhesion of Hydrogels. As discussed in the previous part, if a hydrogel adheres to a substrate via a low density of weak physical cross-links, a crack can easily propagate along the hydrogel−substrate interface, resulting in low interfacial toughness (Figure 18b). Therefore, the design of tough adhesion of hydrogels first requires strong interfacial linkages between the hydrogels and the adhered substrates, such as covalent bonds,[49,788,789] strong physical cross-links,[48,78,790] connector polymers,[26,50,791,792] and mechanical interlocks.[793,794] In addition, because the interfacial crack can tilt into the bulk hydrogel and develop the cohesive failure mode (Figure 18c), the design of tough adhesion of hydrogels further requires high fracture toughness of the hydrogel matrices.[49]

Overall, the design principle for tough adhesion of hydrogels is to integrate tough dissipative hydrogel matrices and strong interfacial linkages.[49] When attempting to detach the tough hydrogel from the substrate, the strong interfacial linkages will hold the interfacial crack tip, allowing the bulk hydrogel to develop a process zone with substantial mechanical dissipation (Figure 18d). Quantitatively, the total interfacial toughness can be expressed as[49,789]

$$\Gamma^{inter} = \Gamma_0^{inter} + \Gamma_D^{inter} \tag{28}$$

where Γ^{inter}, Γ_0^{inter}, and Γ_D^{inter} are the total interfacial toughness, the intrinsic interfacial toughness due to strong interfacial linkages, and the contribution of mechanical dissipation in the process zone to the total interfacial toughness, respectively.

Tough adhesion of biological hydrogels in animal bodies such as cartilages, tendons, and ligaments on bones generally relies on the integration of tough hydrogels and strong interfacial linkages. However, only recently has this design principle been proposed[49] and implemented[26,47,49,50,788,791,792,795] for tough adhesion of synthetic hydrogels on diverse substrate materials, including metals, ceramics, glass, silicone, elastomers, hydrogels, and biological tissues. This is because the role of tough dissipative hydrogel matrices has been underexplored or underestimated in adhesion of hydrogels.[49,796,797] Notably, strong interfacial linkages and/or bulk dissipation of the

https://doi.org/10.1021/acs.chemrev.0c01088
Chem. Rev. XXXX, XXX, XXX−XXX

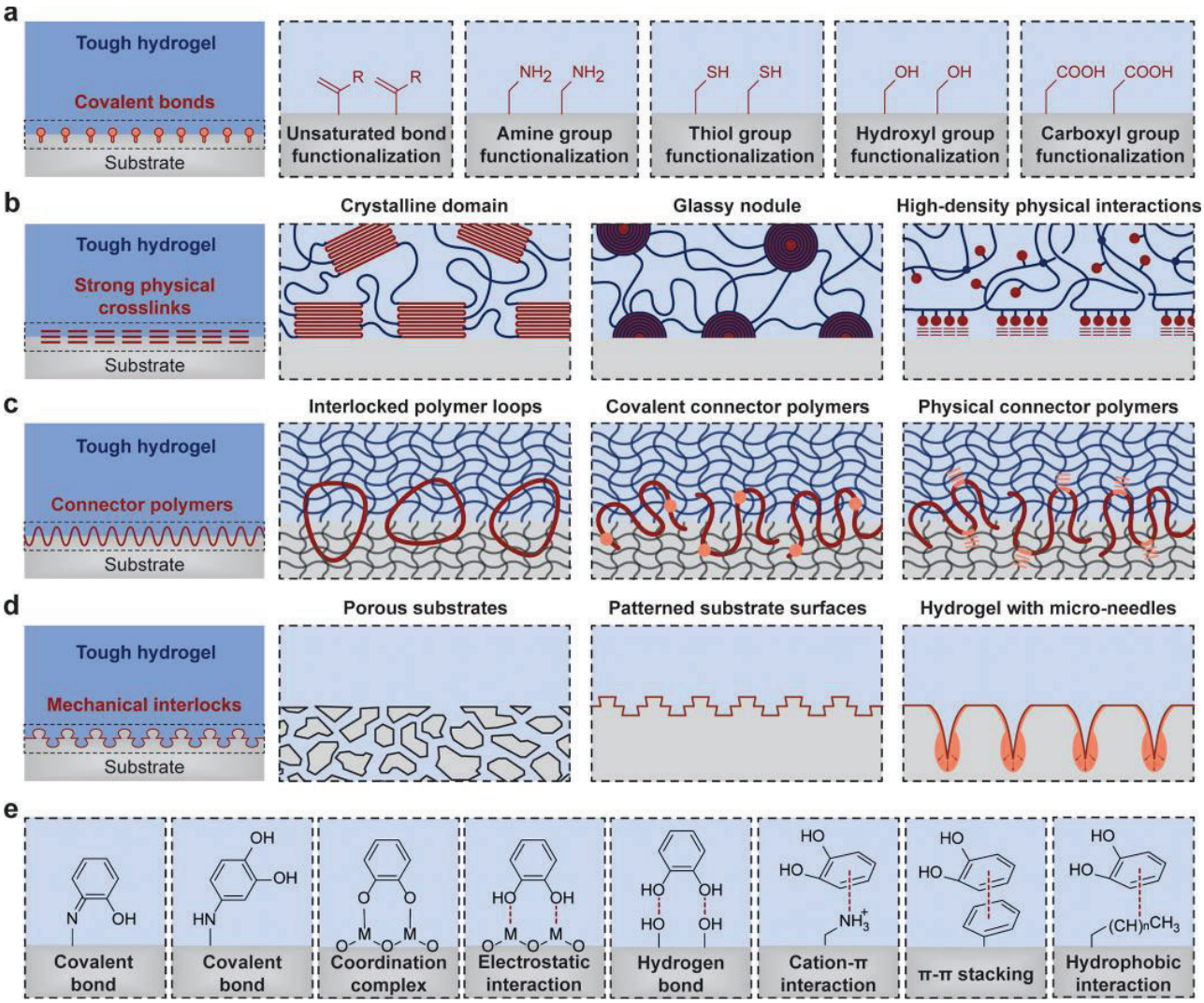

Figure 19. Implementation strategies for tough adhesion of hydrogels with UPNs. The tough hydrogels with UPNs are bonded on substrates via various types of strong interfacial linkages: (a) covalent bonds, (b) strong physical cross-links, (c) connector polymers, and (d) mechanical interlocks. (e) Catechol interactions can implement various types of strong interfacial linkages. Panel (e) is reproduced with permission from refs 817 and 820. Copyright 2019 Wiley and 2017 Wiley.

adherents have also been widely employed for tough bonding of engineering materials such as metals[798] and rubbers[799,800] on substrates.

5.4.3. Implementation Strategies for Tough Adhesion of Hydrogels. Since the implementation of tough hydrogels has been discussed in section 5.1, we will focus on how to implement the strong interfacial linkages to bond tough dissipative hydrogels on various substrates in this section. In order to achieve tough adhesion, the intrinsic interfacial toughness Γ_0^{inter} of the interfacial linkages should at least reach the level of the intrinsic fracture energy Γ_0 of tough hydrogels, i.e., over a few tens of joules per meter squared.[49] Given this requirement on the intrinsic interfacial toughness, the strong interfacial linkages have been commonly implemented with covalent bonds, strong physical cross-links, connector polymers, and mechanical interlocks (Figure 19).

Covalent bonds have been widely adopted to strongly anchor polymer chains in tough hydrogels' UPNs (as discussed in section 5.1) on various substrates. The commonly used covalent bonds for tough adhesion of hydrogels include carbon−carbon, carbon−nitrogen, carbon-sulfide, carbon−oxygen, and silicon−oxygen bonds (Figure 5c).[801] In order to form these covalent bonds, the hydrogels and substrates are usually designed to possess functional groups such as the cross-linkable unsaturated bond (to form carbon−carbon bond),[802] amine group (to form carbon−nitrogen bond),[49] thiol group (to form carbon-sulfide bond),[803] hydroxyl and carboxyl group (to form carbon−oxygen bond), and silanol group (to form silicon−oxygen bond)[804] (Figure 19a). According to the Lake−Thomas model, the intrinsic interfacial toughness Γ_0^{inter} of polymer chains covalently anchored on a substrate can be expressed as

$$\Gamma_0^{inter} = M^{inter} N U_f \tag{29}$$

where M^{inter} is the number of covalently anchored polymer chains on a unit area of the substrate in the undeformed reference state, N is the number of Kuhn monomers per polymer chain, and U_f is the lower value of the energy required to fracture either the Kuhn monomer or the covalent bond on the substrate.

https://doi.org/10.1021/acs.chemrev.0c01088
Chem. Rev. XXXX, XXX, XXX−XXX

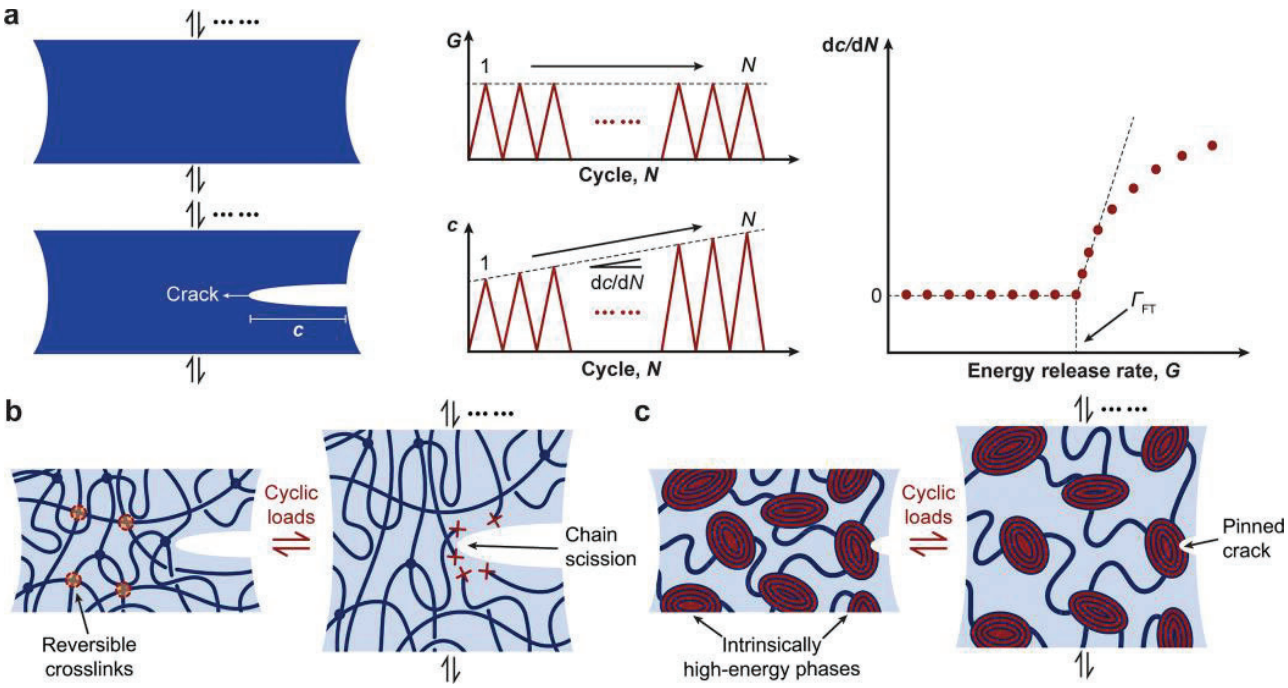

Figure 20. Design principle for fatigue-resistant hydrogels: pin cracks by intrinsically high-energy phases. (a) Definition of fatigue threshold, and the pure-shear method to measure fatigue threshold. G is the energy release rate, c is the crack length at the undeformed state, and N is the cycle number. The fatigue threshold Γ_{FT} is determined by intersecting the curve of dc/dN vs G with the G axis. (b) Dissipation mechanisms such as reversible cross-links in tough hydrogels are depleted over cyclic loads, not contributing to the fatigue threshold. (c) Fatigue crack is pinned by intrinsically high-energy phases in fatigue-resistant hydrogels. Panels (b and c) are reproduced with permission from ref 75. Copyright 2019 American Association for the Advancement of Science.

According to eq 29, anchoring longer polymer chains with a higher density of covalent bonds on a substrate will give a higher value of the intrinsic interfacial toughness.[49,789]

Strong physical cross-links including crystalline domains, glassy nodules, and high-density physical bonds such as hydrogen bonds can also strongly adhere tough hydrogels on substrates (Figure 19b).[78,757,803−811] Since the crystalline domains and glassy nodules usually act as high-functionality cross-links, each of them may anchor multiple polymer chains on the substrate, further enhancing the intrinsic interfacial toughness Γ_0^{inter}.

Connector polymers[799,812] have been employed to strongly bond elastomers and hydrogels on substrates (Figure 19c). In this case, the substrates usually take the form of polymer networks (i.e., elastomers and hydrogels) as well. To provide strong interfacial linkages, the connector polymers can form covalent cross-links,[26,50] interlocked loops,[791,792,803,807,813] and/or strong physical cross-links[792] with the polymer networks of both the hydrogels and the substrates. Specifically, the strong physical cross-links can be crystalline domains, glassy nodules, and/or high-density weak physical cross-links.[792] The connector polymers can be polymerized from monomers in the two polymer networks[26,791,804] or can be directly added on the interface of the two polymer networks.[792]

Mechanical interlocks between tough hydrogels and substrates usually occur at length scales from micrometers to millimeters (Figure 19d). One commonly used method is to impinge precursor solutions of tough hydrogels into porous substrates and then form tough hydrogels that are mechanically interlocked with the substrates.[793] Similarly, the surfaces of the substrates can be roughened or patterned to enhance the strength of mechanical interlocks with tough hydrogels.[794,814,815] As a special yet interesting case, hydrogels have been fabricated into dried microneedles, which can pierce into a soft substrate such as biological tissues and then swell to form mechanical interlocks.[816]

Inspired by the adhesive proteins found in mussels, catechol chemistry has been widely adopted to achieve various types of interfacial linkages between hydrogels and substrates (Figure 19e).[579,790] Catechol can form both covalent and physical cross-links with various functional groups (Figure 19e). Upon oxidation to quinone, catechol can form a covalent bond with nucleophiles (e.g, amine and thiol) via the Michael addition as well as a strong coordination complex with metal oxides.[817] The hydroxyl groups of catechol can form electrostatic interaction with metal oxides as well as hydrogen bonds with hydrophilic substrates. The benzene ring of catechol can further form cation-π interaction with positively charged functional groups, $\pi-\pi$ stacking with benzene functional groups, and hydrophobic interaction with hydrophobic functional groups on substrates.[790,817] While catechol chemistry has been widely utilized for adhesion of hydrogels to various substrates, the interfacial toughness of the adhesion achieved only by catechol-based interfacial linkages is not high,[818] highlighting the importance of tough dissipative hydrogel matrices besides the interfacial linkages to achieve tough adhesion.[819]

5.5. Fatigue-Resistant: Pin Fatigue Cracks with Intrinsically High-Energy Phases

5.5.1. Fatigue Threshold. The word "fatigue" has been used to describe many symptoms observed in materials under prolonged loads, including materials with or without precut cracks under prolonged static or cyclic loads.[821,822] In this

https://doi.org/10.1021/acs.chemrev.0c01088
Chem. Rev. XXXX, XXX, XXX−XXX

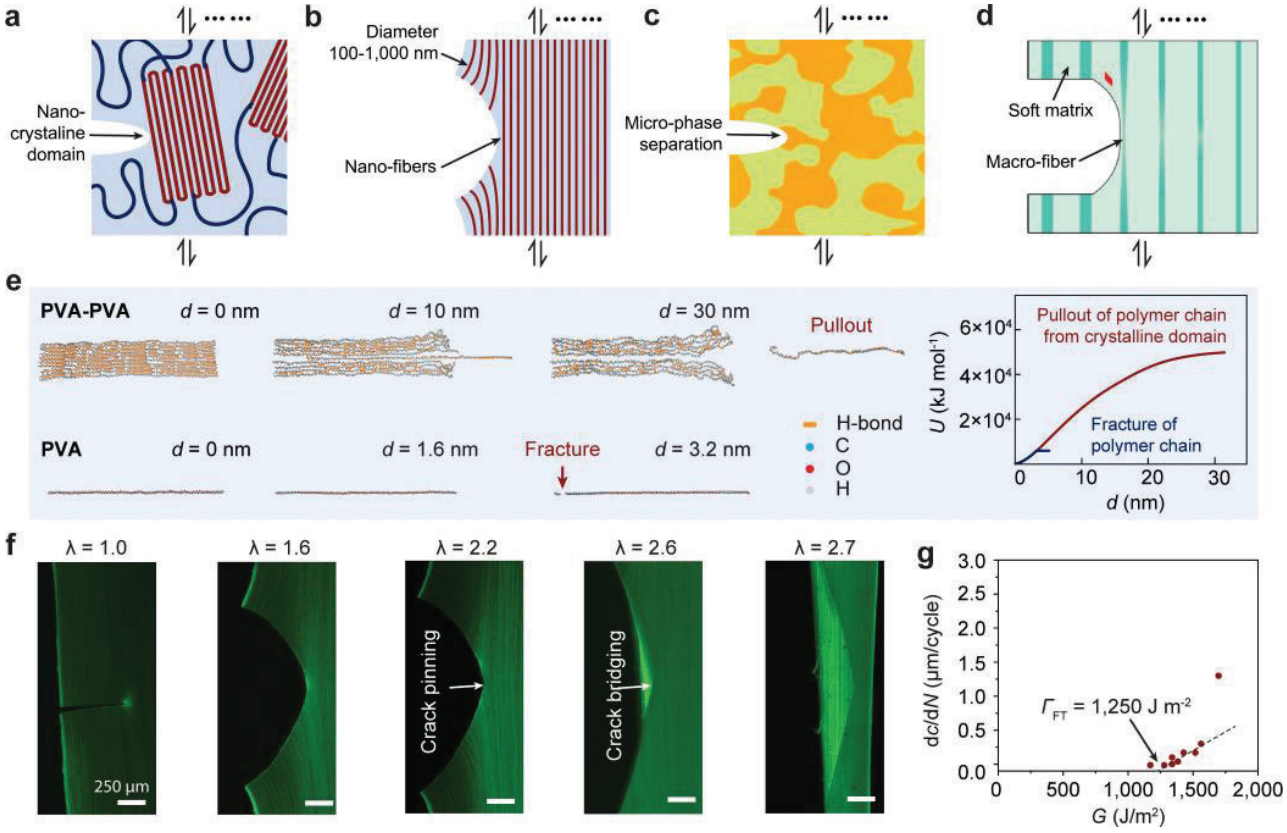

Figure 21. Implementation strategies for fatigue-resistant hydrogels with UPNs. Fatigue cracks can be pinned by intrinsically high-energy phases including (a) nanocrystalline domains,[75] (b) nano-/microfibers, (c) microphase separations, and (d) macrofibers.[77] (e) Molecular dynamic simulation for pulling a polymer chain out of a PVA nanocrystalline domain and for fracturing the same polymer chain.[78] d is the displacement of one end of the polymer chain, and U is the energy required to achieve the displacement. (f) Confocal microscope image of a crack pinned by nanofibers in a nanofibrous PVA hydrogel and (g) measurement of the fatigue threshold of the nanofibrous PVA hydrogel.[76] G is the energy release rate, c is the crack length, and N is the cycle number. Panel (a) is reproduced with permission from ref 75. Copyright 2019 American Association for the Advancement of Science. Panel (b) is reproduced with permission from ref 76. Copyright 2019 National Academy of Sciences. Panel (c) is reproduced with permission from ref 825. Copyright 2020 National Academy of Sciences. Panel (d) is reproduced with permission from ref 77. Copyright 2019 Elsevier. Panel (e) is reproduced with permission from ref 78. Copyright 2020 Springer Nature. Panels f and g are reproduced with permission from ref 76. Copyright 2019 National Academy of Sciences.

section, we will focus on the fatigue fracture of hydrogels with precut cracks under cyclic loads (Figure 20a) because this is one of the most common failure modes of hydrogels in mechanically dynamic environments such as artificial cartilages[823] and soft robots.[26] Fatigue threshold has been commonly used to characterize a material's resistance to fatigue crack propagation under cyclic loads. The fatigue threshold is defined as the minimal fracture energy at which fatigue crack propagation occurs under infinite cycles of loads.[55,56] Quantitatively, the fatigue threshold Γ_{FT} can be expressed as

$$\Gamma_{FT} = G_c(dc/dN \to 0) \tag{30}$$

where G is the energy release rate to drive crack propagation under each cycle of load, G_c is the minimal energy release rate at which crack propagation occurs under infinite cycles of loads (i.e., $dc/dN \to 0$), c is the length of the crack at the undeformed state, N is the cycle number of the applied load, and dc/dN gives the crack extension per cycle.

The fatigue threshold of soft materials such as elastomers and hydrogels has been measured with various experimental methods such as the pure-shear fatigue-fracture test and the single-notch fatigue-fracture test.[75] For example, in the pure-shear fatigue-fracture test, two identical pieces of a hydrogel are fabricated with the same thickness T, width W and height H, where $W \gg H \gg T$ (Figure 20a). Both pieces of samples are clamped along their long edges (i.e., along the width direction) with rigid plates. The first sample is repeatedly pulled to a stretch of $\lambda_{applied}$ times of its undeformed height to measure the nominal stress s vs stretch λ relation, and the corresponding energy release rate can be calculated as $G = H\int_1^{\lambda_{applied}} s\, d\lambda$, which is a function of the cyclic number N (Figure 20a). Thereafter, a notch with a length of ~0.5 W is introduced into the second sample, which is then repeatedly pulled to the same stretch $\lambda_{applied}$ to measure the crack length c as a function of the cyclic number N. The pure-shear fatigue-fracture tests are repeated for different values of the applied stretch $\lambda_{applied}$ (i.e., different energy release rate G), and a curve of dc/dN vs G can be obtained (Figure 20a). The fatigue threshold Γ_{FT} is then determined by intersecting the curve of dc/dN vs G with the G axis (i.e., when $dc/dN \to 0$). Notably, the fatigue-fracture tests of hydrogels are commonly carried out in aqueous environments to avoid dehydration of the hydrogels under prolonged loads.[75,76] For further discussion on the theory and experiments for the

https://doi.org/10.1021/acs.chemrev.0c01088
Chem. Rev. XXXX, XXX, XXX−XXX

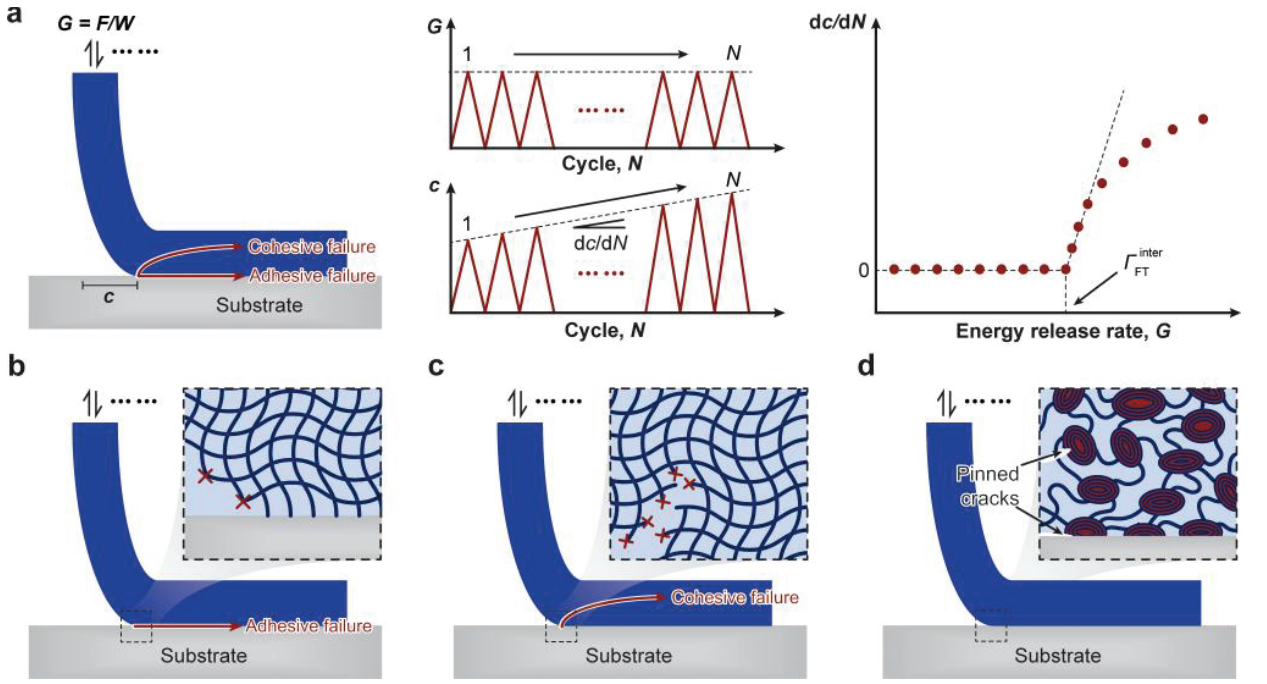

Figure 22. Design principle for fatigue-resistant adhesion of hydrogels: strongly bond intrinsically high-energy phases on interfaces. (a) Definition of interfacial fatigue threshold, and the 90-deg cyclic peeling test to measure the interfacial fatigue threshold. F is the applied peeling force, W is the width of the sample, G is the energy release rate, c is the crack length, and N is the cycle number. The interfacial fatigue threshold Γ_{FT}^{inter} is determined by intersecting the curve of dc/dN vs G with the G axis. (b) Fatigue-crack propagation along the interface gives the adhesive failure mode. (c) fatigue-crack propagation in the hydrogel gives the cohesive failure mode. (d) Fatigue cracks pinned by intrinsically high-energy phases on the interface and in the bulk hydrogel.[78] Panel (d) is reproduced with permission from ref 78. Copyright 2020 Springer Nature.

fatigue of hydrogels, a comprehensive review paper on this topic is recommended.[822]

5.5.2. Design Principle for Fatigue-Resistant Hydrogels. As discussed in section 5.1, a hydrogel can be designed tough by building mechanical dissipation into stretchy polymer networks.[67] The mechanical dissipation in the process zone around the crack tip can dramatically enhance the fracture toughness of the hydrogel. However, the mechanisms for irreversible dissipation such as fracturing polymer chains in the process zone are usually depleted under cyclic loads. The mechanisms for reversible dissipation such as reversible cross-links, once depleted, usually cannot recover in time to resist fatigue crack propagation in future cycles of loads (Figure 20b).[55,56,824] Consequently, the fatigue threshold of hydrogels and elastomers is their intrinsic fracture energy,[55,56,824]

$$\Gamma_{FT} = \Gamma_0 \tag{31}$$

Therefore, it is clear that the design of fatigue-resistant hydrogels usually cannot rely on mechanical dissipation in the bulk hydrogel matrices.

The design principle for fatigue-resistant hydrogels is to make the fatigue crack encounter and fracture objects with energies per unit area much higher than that for fracturing a single layer of polymer chains, or in short, to pin fatigue crack by intrinsically high-energy phases (Figure 20c).[75] The intrinsically high-energy phases that have been exploited for the design of fatigue-resistant hydrogels include nanocrystalline domains (Figure 21a),[75] nano-/microfibers (Figure 21b),[76] microphase separations (Figure 21c),[822,825] and macroscale composites (Figure 21d).[77] In addition, because the design of fatigue-resistant hydrogels does not rely on mechanical dissipation in the bulk hydrogels, fatigue-resistant hydrogels usually demonstrate low hysteresis ratio H and high resilience R (eq 23).[75,76,826] Notably, biological hydrogels such as muscles, tendons, and ligaments commonly possess intrinsically high-energy phases such as nano-/microfibers, usually arranged in hierarchical architectures, to achieve high fatigue thresholds (Figure 2).

5.5.3. Implementation Strategies for Fatigue-Resistant Hydrogels. The design principle for fatigue-resistant hydrogels has been implemented with the UPNs that possess intrinsically high-energy phases.[75−77,822,825] In order to effectively pin fatigue cracks, the density of the intrinsically high-energy phases in the UPNs should be sufficiently high.[75]

High-functionality cross-links such as nanocrystalline domains can effectively play the role of intrinsically high-energy phases in the UPNs (Figure 21a). The energy required to pull out a polymer chain from a nanocrystalline domain can be multiple times higher than that to fracture the same polymer chain, and the energy required to mechanically damage the nanocrystalline domain can be multiple times higher than that to fracture the corresponding amorphous polymer chains (Figure 21e).[78] Consequently, it has been shown that enhancing the crystallinity of a PVA hydrogel from 0.2 wt % to 18.9 wt % by dry-annealing the hydrogel can increase its fatigue threshold from 10 J m^{-2} to 1000 J m^{-2}, reaching the level of fatigue-resistant biological hydrogels such as cartilages.[75] Since the size of the crystalline domains in the PVA hydrogel has been measured to be a few nanometers, the nanocrystalline domains play the role of intrinsically high-energy phases (Figure 21a). It is expected other UPNs with sufficiently high densities of high-functionality cross-links such as crystalline domains and glassy nodules can also implement the design principle for fatigue-

https://doi.org/10.1021/acs.chemrev.0c01088
Chem. Rev. XXXX, XXX, XXX−XXX

resistant hydrogels. It should be further noted that hydrogels with high densities of rigid crystalline domains and glassy nodules can be much stiffer than common hydrogels,[75] and such high stiffness may be undesirable for many applications of hydrogels.

Nano-/microfibers can also act as intrinsically high-energy phases in the UPNs to implement the design principle for fatigue-resistant hydrogels (Figure 21b). The energy required to fracture a nano-/microfiber can be much higher than that to fracture the corresponding amorphous polymer chains because of the synergistic elongation and stiffening of the bundled polymer chains in the fiber.[76] On the basis of this implementation strategy, it has been shown that introducing nanofibers into a PVA hydrogel by freeze−thawing the hydrogel can enhance its fatigue threshold from 10 J m^{-2} to 310 J m^{-2}. In particular, if the nanofibers are aligned perpendicular to the fatigue crack by prestretching the hydrogel, the measured fatigue threshold further increases to 1250 J m^{-2} (Figure 21f,g).[76] In addition, because the nanofibers can be made compliant, stretchable, and strong by using a low density of nanocrystalline domains to bundle polymer chains (Figure 15b), the resultant nanofibrous hydrogel integrates high compliance, stretchability, and strength together with high fatigue threshold—mimicking the combinational mechanical properties of biological muscles.[76]

Phase separations in hydrogels can also enhance the fatigue threshold of the hydrogels,[822,825] possibly because the energy required to fracture the separated phases is higher than that to fracture the corresponding amorphous polymer chains. The UPN interactions including reversible covalent bonds and weak physical cross-links play critical roles in inducing the phase separations in the hydrogels.[822,825]

On a structural level, macroscale resilient elastomer fibers have been embedded in a resilient hydrogel to form a macroscale composite.[77] Since it requires much higher energy to fracture the elastomer fibers than a layer of amorphous polymer chains, a fatigue threshold over 1000 J m^{-2} has been achieved for the macroscale composite (Figure 21d).[77]

5.6. Fatigue-Resistant Adhesion: Strong Bond Intrinsically High-Energy Phases on Interfaces

5.6.1. Interfacial Fatigue Threshold. The interfaces of adhered materials can suffer from fatigue failure under prolonged loads, including interfaces with or without precut cracks under prolonged static or cyclic loads. In this section, we will focus on the fatigue fracture of hydrogels adhered on substrates with precut cracks on their interfaces under cyclic loads (Figure 22a). Depending on whether the fatigue crack propagates along the interface or tilts into the hydrogel under cyclic loads, the failure mode is called the adhesive failure or cohesive failure, respectively (Figure 22a).[78] Interfacial fatigue threshold has been commonly used to characterize the capability of adhered materials to resist interfacial fatigue-crack propagation following either failure mode under cyclic loads. The interfacial fatigue threshold is defined as the minimal fracture energy at which interfacial crack propagation occurs under infinite cycles of loads.[78,827−829] Similar to the fatigue threshold, the interfacial fatigue threshold Γ_{FT}^{inter} can be expressed as

$$\Gamma_{FT}^{inter} = G_c(dc/dN \to 0) \tag{32}$$

where G is the energy release rate to drive interfacial crack propagation under each cycle of load, G_c is the minimal energy release rate at which interfacial crack propagation occurs under infinite cycles of loads (i.e., $dc/dN \to 0$), c is the length of the crack, N is the cycle number of the applied load, and dc/dN gives the crack extension per cycle.

The interfacial fatigue threshold of soft materials such as elastomers and hydrogels has been measured with many experimental methods such as the cyclic 90-deg peeling test, the cyclic T-peeling test and the cyclic lap-shear test.[78,827−829] For example, in the cyclic 90-deg peeling test,[78,827] a layer of a hydrogel with thickness T, width W and length L ($L \gg W \gg T$) is bonded on a substrate, and a notch is introduced on the interface along the length direction (Figure 22a). A force F is repeatedly applied on the detached part of the hydrogel, while maintaining the detached part vertical to the substrate (Figure 22a). The applied force F gives the energy release rate $G = F/W$, where W is the width of the hydrogel sheet. The interfacial crack length c is then measured as a function of the cyclic number N. The cyclic 90-deg peeling tests are repeated for different values of the applied force F (i.e., different energy release rate G), and a curve of dc/dN vs G can be obtained (Figure 22a). The interfacial fatigue threshold Γ_{FT}^{inter} is determined by intersecting the curve of dc/dN vs G with the G axis (i.e., when $dc/dN \to 0$). Notably, the interfacial fatigue fracture tests of hydrogels are commonly carried out in aqueous environments to avoid dehydration of the hydrogels under prolonged loads.[78]

5.6.2. Design Principle for Fatigue-Resistant Adhesion of Hydrogels. As discussed in section 5.4, tough adhesion of hydrogels on substrates relies on the integration of tough dissipative hydrogel matrices and strong interfacial linkages (Figure 18).[49] The strong interfacial linkages can hold the interfacial crack tip, while the mechanical dissipation in the process zone around the crack tip can dramatically enhance the total interfacial toughness of the adhesion. However, similar to the situation in fatigue fracture of hydrogels,[55,56,824] because the mechanical dissipation in bulk hydrogel matrices is usually depleted or not timely accessible after cyclic loads, such dissipation usually cannot contribute to resisting interfacial fatigue-crack propagation (Figures 22b,c).[78,829] Consequently, the interfacial fatigue threshold of hydrogels and elastomers is their intrinsic interfacial toughness,[78,829]

$$\Gamma_{FT}^{inter} = \Gamma_0^{inter} \tag{33}$$

Because interfacial cracks can tilt into bulk hydrogels and develop the cohesive failure mode (Figure 22c), the design of fatigue-resistant adhesion of hydrogels first requires fatigue-resistant hydrogel matrices that possess sufficiently high densities of intrinsically high-energy phases.[75] Notably, hydrogel matrices that are only tough but not fatigue-resistant are unsuitable for the design of fatigue-resistant adhesion, owing to the depletion of dissipation over cyclic loads. To further avoid the adhesive failure mode under cyclic loads (Figure 22b), fatigue cracks on the interfaces need to be pinned by intrinsically high-energy phases strongly bonded on the interfaces as well (Figure 22d).

Therefore, the design principle for fatigue-resistant adhesion of hydrogels, in short, is to strongly bond intrinsically high-energy phases on interfaces.[78] While the intrinsically high-energy phases that have been exploited for the design of fatigue-resistant adhesion include nanocrystalline domains[78] and long polymer chains,[828] other candidates such as nano-/microfibers can be explored in the future. Not surprisingly, biological hydrogels including tendons, ligaments, and cartilages all rely on strongly bonding nanocrystalline domains and nano-/micro-

https://doi.org/10.1021/acs.chemrev.0c01088
Chem. Rev. XXXX, XXX, XXX−XXX

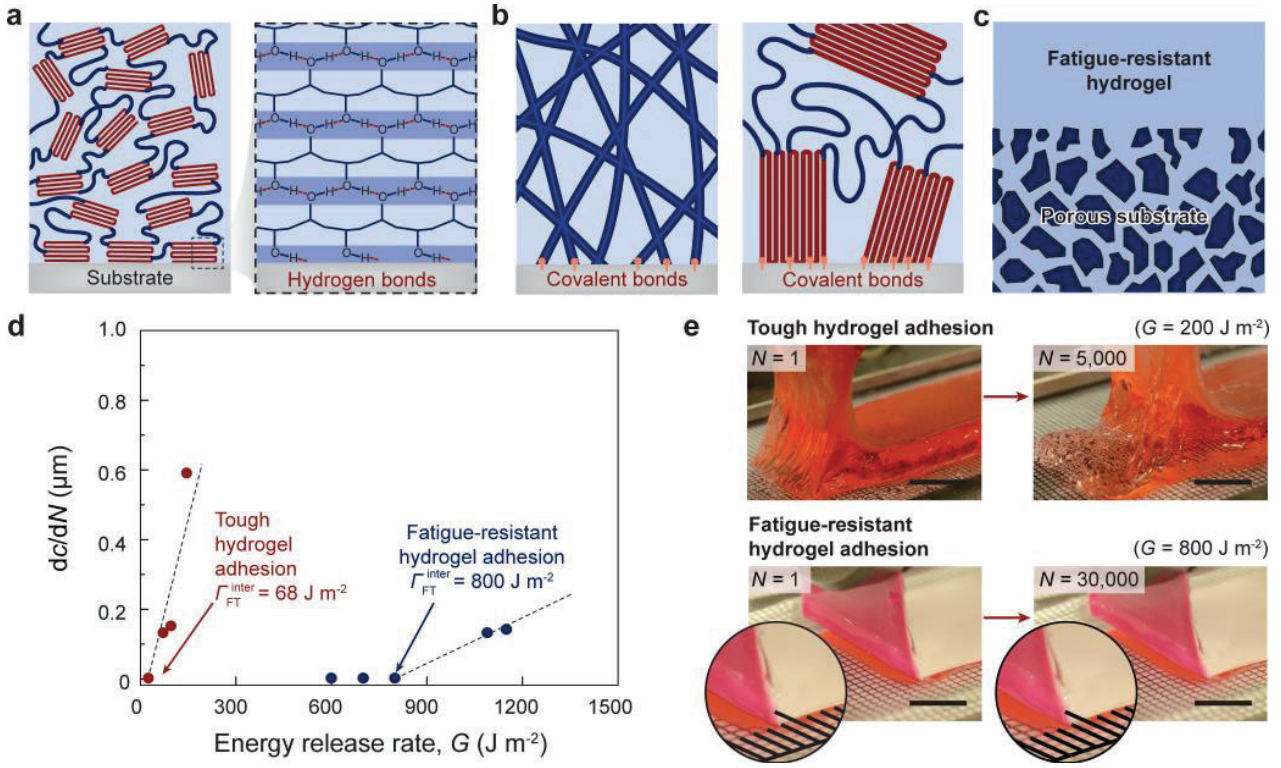

Figure 23. Implementation strategies for fatigue-resistant adhesion of hydrogels with UPNs. The intrinsically high-energy phases can be strongly bonded on the substrates via (a) high-density physical bonds such as hydrogen bonds,[78] (b) covalent bonds, and (c) mechanical interlocks. (d) Measurements of the fatigue thresholds of tough adhesion and fatigue-resistant adhesion of hydrogels on substrates.[78] (e) Photos of interfacial crack propagation in a cyclic peeling test for tough adhesion (top) and fatigue-resistant adhesion (bottom) of hydrogels on substrates.[78] Panels (a, d, and e) are reproduced with permission from ref 78. Copyright 2020 Springer Nature.

fibers on their interfaces with bones to achieve fatigue-resistant adhesion.[757]

5.6.3. Implementation Strategies for Fatigue-Resistant Adhesion of Hydrogels. The design of fatigue-resistant hydrogels relies on achieving sufficiently high densities of intrinsically high-energy phases in the UPNs, as discussed in section 5.5. In this section, we will focus on how to strongly bond the intrinsically high-energy phases on substrates to implement the design principle for fatigue-resistant adhesion.

High-functionality cross-links such as nanocrystalline domains can play the role of intrinsically high-energy phases in the UPNs. For example, nanocrystalline domains in PVA hydrogels have been strongly bonded on diverse substrates including glass, ceramics, metals, and elastomers via high-density hydrogen bonds (Figure 23a).[78] Molecular dynamic simulations show that the energy required to pull a polymer chain out of the interface is much higher than the energy required to fracture the same polymer chain or to pull the same polymer chain out of the nanocrystalline domain, implying high intrinsic interfacial toughness of the adhesion Γ_0^{inter}.[78] As a result, the interfacial fatigue threshold of the PVA-substrate system measured in phosphate-buffered saline reaches up to 800 J m^{-2}, similar to those of tendon/ligament/cartilage-bone interfaces (Figure 23d,e). In addition, the failure mode of the PVA-substrate systems observed in the interfacial fatigue-fracture tests follows the cohesive failure, indicating the critical role of intrinsically high-energy phases in the bulk hydrogels (i.e., fatigue-resistant hydrogels) for the design of fatigue-resistant adhesion.[78]

It is expected that covalent bonds may be able to strongly bond the intrinsically high-energy phases such as nanocrystalline domains and nano-/microfibers on substrates as well (Figure 23b). In addition, curing precursor solutions of fatigue-resistant hydrogels on porous, roughened, or patterned substrates can lead to mechanical interlocks that may strongly bond intrinsically high-energy phases on the hydrogel−substrate interfaces (Figure 23c).[830]

5.7. Implementation Strategies for Extreme Mechanical Properties with Unconventional Polymer Networks

While the design principles and implementation strategies for hydrogels with extreme mechanical properties have been discussed in sections 5.1−5.6, we will provide an overview of the design process and implementation strategies in this section.

Since the design principles discussed in sections 5.1−5.6 are general and abstract, it is usually more intuitive to begin the design process with specific UPN architectures and/or UPN interactions than with a design principle. The commonly used UPN architectures that can give extreme mechanical properties include interpenetrating polymer networks, semi-interpenetrating polymer networks, polymer networks with high-functionality cross-links, and nano-/microfibrous polymer networks. The commonly used UPN interactions that can give extreme mechanical properties include various types of strong physical cross-links, weak physical cross-links, and dynamic covalent cross-links. Let us imagine that the selected UPN is subjected to the relevant modes of mechanical loads such as tension, compression, shear, fracture, fatigue, and/or peeling. If the selected UPN under mechanical loads seems to be able to

https://doi.org/10.1021/acs.chemrev.0c01088
Chem. Rev. XXXX, XXX, XXX−XXX

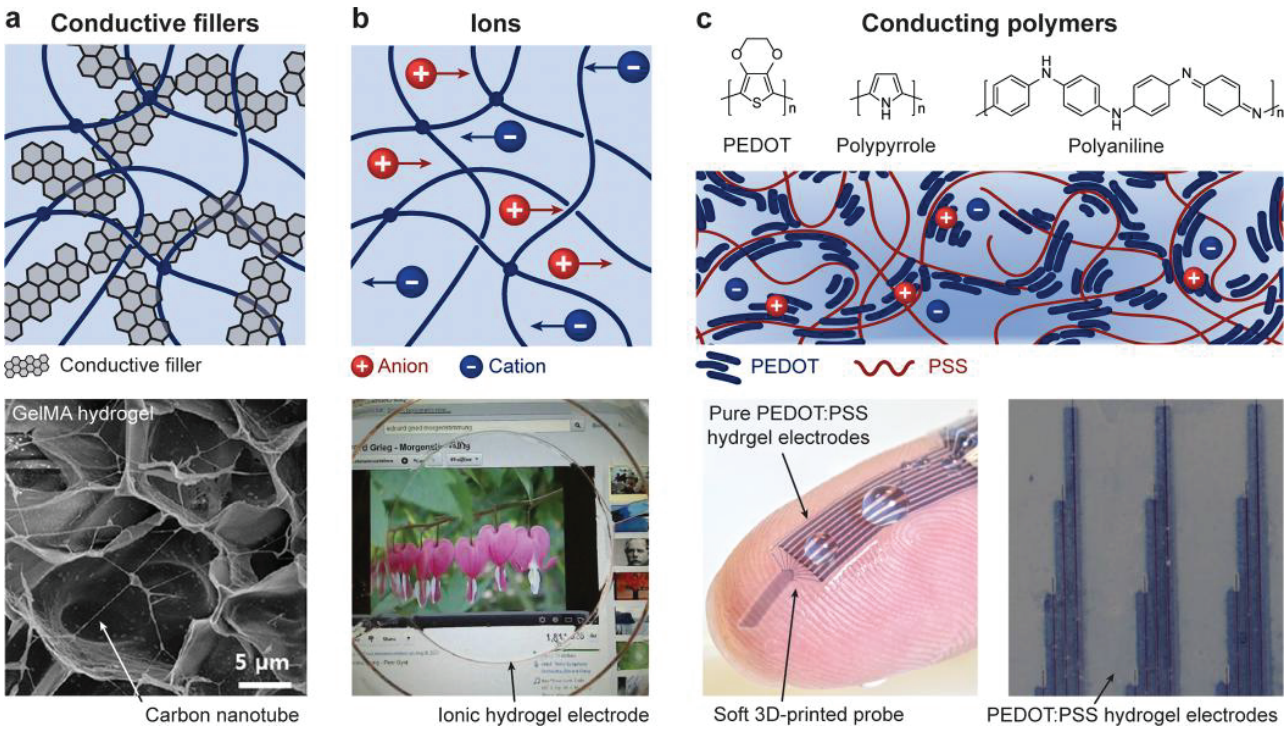

Figure 24. Design principle for hydrogels with high electrical conductivity: percolate electrically conductive phases. (a) Hydrogels with percolated electrically conductive fillers. (b) Hydrogels with ionically conductive salt solvents. (c) Hydrogels based on conducting polymers. The bottom panel of (a) is reproduced with permission from ref 849. Copyright 2013 American Association for the Advancement of Science. The bottom panel of (b) is reproduced with permission from ref 27. Copyright 2014 American Association for the Advancement of Science. The bottom panels of (c) are reproduced with permission from ref 116 (left) and ref 31 (right). Copyright 2020 Springer Nature and 2019 Springer Nature.

implement the design principle for the desired property, one can proceed to select polymers and cross-links such as those discussed in section 2 and section 4 for the design and fabrication of the hydrogel. Furthermore, it may be difficult to initiate the design process by considering both UPN architectures and UPN interactions simultaneously; in this case, we can first test whether a UPN architecture will likely implement the design principle and then further add UPN interactions into the UPN architecture to facilitate the implementation. For example, in order to design a fatigue-resistant hydrogel, we can begin with a polymer network with high-functionality cross-links because a sufficiently high density of high-functionality cross-links can act as intrinsically high-energy phases to pin fatigue cracks. Furthermore, strong physical cross-links such as crystalline domains and glassy nodules can be added into the polymer network as the intrinsically high-energy phases to facilitate the implementation of the design principle. Indeed, dry-annealed PVA with high densities of nanocrystalline domains has been selected to implement the design principle for fatigue-resistant hydrogels.[75]

Alternative design and implementation strategies are through the mimicry of the UPNs of biological hydrogels that possess the desired extreme mechanical properties (Figure 2). Because biological hydrogels have exploited various types of UPNs to implement the design principles discussed in sections 5.1−5.6, we can simply begin the design process by replicating biological hydrogels' UPNs (Figure 2). However, biological hydrogels' UPNs, commonly featuring hierarchical and gradient structures (Figure 2), can be more complex than the UPNs discussed in section 4. Therefore, we should only mimic the essential characteristics of the biological UPNs that enable the desired mechanical properties. As an example, tendons, ligaments, and cartilages all feature fatigue-resistant adhesion on bones, owing to nano-/microfibers and nanocrystalline domains strongly anchored on the interfaces (Figure 2). By strongly anchoring nanocrystalline domains in synthetic PVA hydrogels on substrates, bioinspired fatigue-resistant adhesion of PVA hydrogels on diverse solid substrates have been recently achieved (Figure 23d,e).[78]

6. DESIGN OF HYDROGELS WITH EXTREME PHYSICAL PROPERTIES

In addition to the extreme mechanical properties discussed in section 5, the design of hydrogels that possess extreme physical properties has attracted escalating research interests in recent years. Examples of hydrogels' extreme physical properties under development and exploration include high electrical conductivity,[642] patterned magnetization,[843] high refractive index and transparency,[844,845] tunable acoustic impedance,[44] and self-healing.[846] Unlike the extreme mechanical properties discussed in section 5, many of the extreme physical properties do not have embodiments in biological hydrogels. Nevertheless, these extreme physical properties can be of similar importance as the extreme mechanical properties to hydrogels' various applications, especially to the nascent applications of hydrogel machines.[20] In this section, we will briefly discuss the design principles and implementation strategies for hydrogels to possess these extreme physical properties, while bearing in mind that many works in this field are still in the initial stage of development.

https://doi.org/10.1021/acs.chemrev.0c01088
Chem. Rev. XXXX, XXX, XXX−XXX

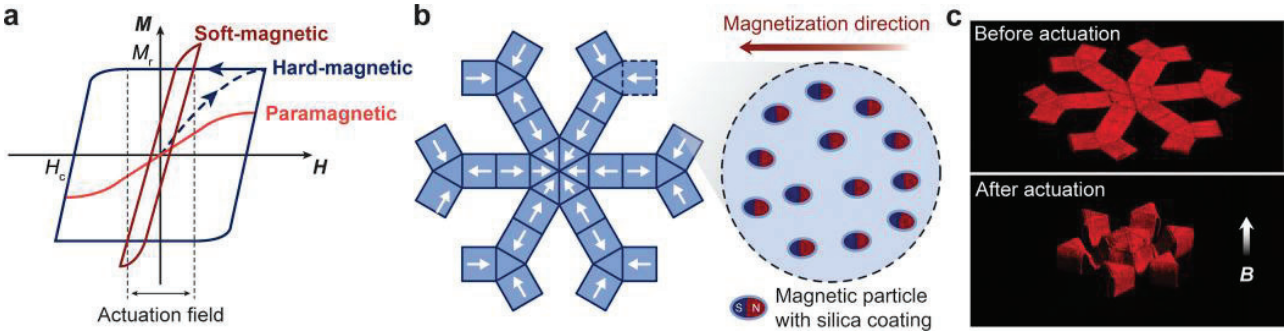

Figure 25. Design principle for hydrogels and elastomers with patterned magnetization: embed magnetic particles and pattern ferromagnetic domains. (a) Typical relations of applied magnetic field H and magnetization M for paramagnetic, soft-magnetic, and hard-magnetic materials. M_r and H_c are the residual magnetization and coercivity of the hard-magnetic material, respectively. (b) Hard-magnetic particles can be embedded into an elastomer/hydrogel matrix, in which ferromagnetic domains can be patterned by 3D printing. (c) Photos of the resultant magnetic soft material before and after magnetic actuation. Panel (a) is reproduced with permission from ref 40. Copyright 2020 Elsevier. Panels b and c are reproduced with permission from ref 39. Copyright 2018 Springer Nature.

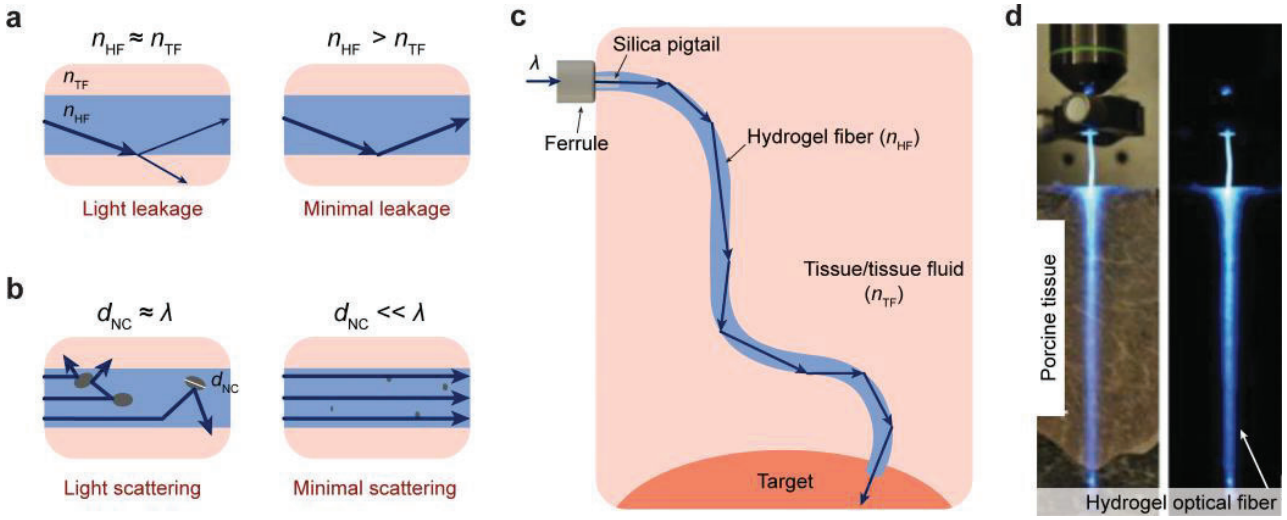

Figure 26. Design principle for hydrogels with high reflective indices and transparency: uniformly embed high-refractive-index nonscattering nanophases. (a) High contrast between reflective indices of the hydrogel fiber η_{HF} and tissue fluid η_{TF} can give minimal light leakage. (b) Uniformly embedding nanophases such as nanoparticles with high refractive indices in the hydrogel matrices can enhance the refractive index of the hydrogel. The size of the nanophases d_{NC} should be much smaller than the light wavelength λ for minimal scattering and high transparency. (c) Hydrogels with high reflective indices and transparency can be used as optical fibers in living tissues. (d) Photo of a hydrogel optical fiber.[859] Panel (d) is reproduced with permission from ref 859. Copyright 2015 Wiley.

6.1. Electrically Conductive: Percolate Electrically Conductive Phases

Electrical conductivity is critical for hydrogels' nascent applications such as bioelectrodes for stimulation and recording of neural activities in bioelectronics[642] and electrodes for supercapacitors and batteries in energy storage.[20,847] However, the electrical conductivity of common hydrogels is less than a few Siemens per meter, on the same level as that of saline water.[642] Compared to metals, carbon, and conducting polymers, common hydrogels are usually deemed to be electrically nonconductive.

The design principle for electrically conductive hydrogels is to embed electrically conductive phases such as liquid metals, metallic nanowires, carbon nanotube, graphene, and conducting polymers in hydrogel matrices and make the conductive phases form percolated networks, or in short, to percolate electrically conductive phases (Figure 24a).[642,848,849] In particular, conductive hydrogels based on conducting polymers have attracted great interest recently, owing to their unique polymeric nature as well as favorable electrical and mechanical properties, stability, and biocompatibility.[31,32,116,495,850−853] For example, poly(3,4-ethylenedioxythiophene):poly(styrenesulfonate) (PEDOT:PSS) has been made into pure conducting polymer hydrogels that achieve high electrical conductivity over a few thousand Siemens per meter and superior biocompatibility (Figure 24c).[31,32,116] In addition to electrically conductive hydrogels, ionically conductive hydrogels have also been intensively developed as stretchable and transparent ionic conductors for various applications (Figure 24b).[27] The conductive phases in ionically conductive hydrogels are usually high concentrations of salt ions. For a further detailed discussion on various types of conductive hydrogels, a recent review paper is recommended.[642]

https://doi.org/10.1021/acs.chemrev.0c01088
Chem. Rev. XXXX, XXX, XXX−XXX

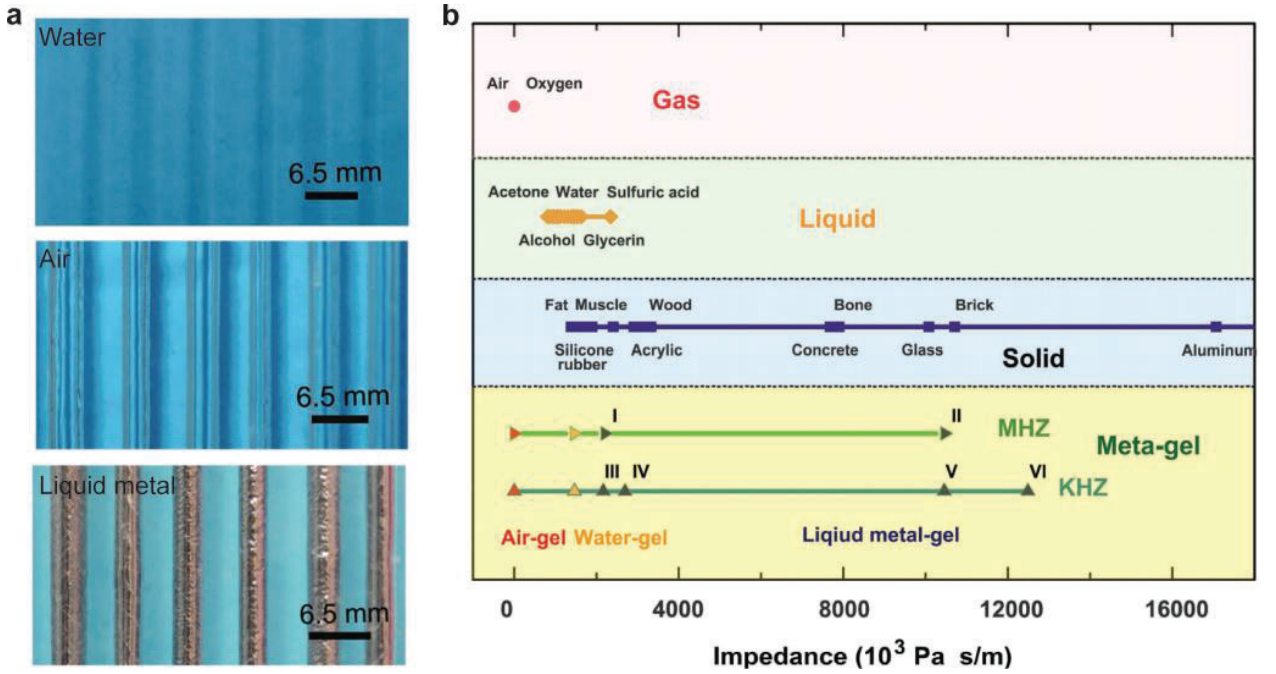

Figure 27. Design principle for hydrogels with tunable acoustic impedance: tune densities and bulk moduli of effectively homogeneous hydrogels. (a) By infusing air, water, or liquid metal (i.e., eutectic gallium−indium) into the fluidic channels inside a hydrogel matrix, the effective density, bulk modulus, and thus acoustic impedance of the hydrogel can be dramatically varied. (b) The hydrogel can approximate the acoustic impedance of air, water, and many solids on demand.[44] Panels a and b are reproduced with permission from ref 44. Copyright 2019 Wiley.

6.2. Magnetized: Embed Magnetic Particles and Pattern Ferromagnetic Domains

Soft materials such as elastomers and hydrogels with ferromagnetic domains or magnetization have been intensively developed and explored for biomedical applications such as drug delivery and minimally invasive surgery,[28,38,843,854−857] owing to their mechanical compliance, potential biocompatibility, and capability of fast deformation under applied magnetic fields. Common hydrogels are usually diamagnetic and do not contain ferromagnetic domains, possessing similar magnetic properties as water. Therefore, subjected to applied magnetic fields, common hydrogels cannot be actuated to deform, exert forces, or release substances.

The design principle for hydrogels to possess patterned magnetization is to embed magnetic components such as hard-magnetic, soft-magnetic, or super-paramagnetic particles in the hydrogels matrices where ferromagnetic domains may be further patterned, or in short, to embed magnetic particles and pattern ferromagnetic domains (Figure 25).[38,843,854−857] In particular, hard-magnetic particles such as neodymium iron boron (NdFeB) particles after magnetic saturation can retain their magnetization under actuation magnetic fields because of the high coercivity of the hard-magnetic particles (Figure 25a). Therefore, patterned ferromagnetic domains can be programmed into elastomers and hydrogels embedded with hard-magnetic particles. Subjected to actuation magnetic fields, the elastomers and hydrogels with the patterned ferromagnetic domains can quickly transform among various shapes.[38,854−857] Recently, 3D printing has been further employed as an effective method to program complex 3D shapes as well as domain patterns in ferromagnetic elastomers and hydrogels (e.g., Figure 25b,c).[854,857] It should be noted that magnetic particles can be corrosive in the aqueous environments of hydrogel matrices. To enhance their chemical stability in hydrogel matrices, the magnetic particles have been coated with protective layers such as silica layers (Figure 25b,c).[38]

6.3. High Reflective Index and Transparency: Uniformly Embed High-Refractive-Index Nonscattering Nanophases

Various optical applications of hydrogels such as ophthalmic lenses[21,380,858] and optical fibers[42,859] require high refractive indices and high transparency of the hydrogels (Figure 26a). The refractive indices of common hydrogels are around 1.333, similar to that of water. One general strategy to enhance the refractive indices of hydrogels is to uniformly embed nanophases such as nanoparticles[844,845] and nanocrystalline domains with high refractive indices in the hydrogel matrices. However, the refractive-index mismatch between the nanophases and hydrogel matrices may lead to substantial undesirable light scattering, reducing the transparency of the hydrogels (Figure 26b). It has been found that decreasing the size of the nanophases below one-tenth of the light wavelength (e.g., zinc sulfide nanoparticles with 3 nm diameter) can effectively diminish light scattering to achieve hydrogels with a high refractive index (i.e., 1.49) and high transparency (Figures 26b−d).[844] Overall, the design principle for hydrogels with high refractive indices and transparency is to uniformly embed high-refractive-index nonscattering nanophases in hydrogel matrices.

6.4. Tunable Acoustic Impedance: Tune Densities and Bulk Moduli of Effectively Homogeneous Hydrogels

Hydrogels have been widely used as the media for sound-wave transmissions such as the coupling agents for imaging and therapeutic ultrasound. It is highly desirable to design hydrogels that possess tunable acoustic impedance to match the impedance of different materials or varying environments.[26,44] The acoustic impedance z of a homogeneous material can be expressed as

https://doi.org/10.1021/acs.chemrev.0c01088
Chem. Rev. XXXX, XXX, XXX−XXX

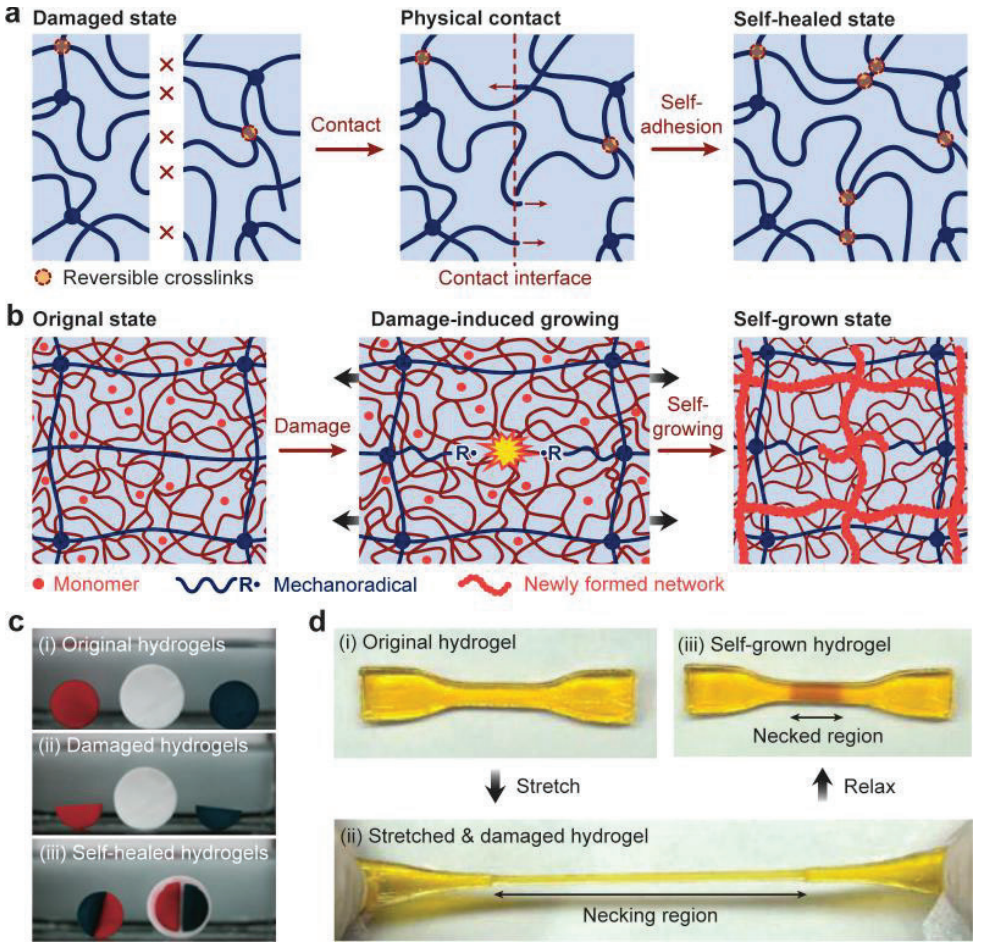

Figure 28. Design principle for self-healing hydrogels: form cross-links and/or polymers at damaged regions. (a) Reversible cross-links and polymer chain entanglements form on the interfaces between two pieces of hydrogels for self-healing or self-adhesion. (b) Damage of a hydrogel induces new polymerization and cross-linking, giving self-reinforcement or self-growth of the hydrogel.[868] (c) Photos of a self-healing hydrogel based on oppositely charged polyelectrolytes.[496,836] (d) Photos of a self-reinforcing or self-growing hydrogel.[868] Panels b and d are reproduced with permission from ref 868. Copyright 2019 American Association for the Advancement of Science. Panel c is reproduced with permission from ref 836. Copyright 2013 Springer Nature.

$$Z = \sqrt{\rho_{\text{eff}} K_{\text{eff}}} \tag{34}$$

where ρ_{eff} and K_{eff} are the effective density and bulk modulus of the material, respectively. Because the density and bulk modulus of common hydrogels are almost the same as those of water, the acoustic impedance of common hydrogels also approximates that of water. To achieve tunable acoustic impedance, fluidic channels have been patterned into tough hydrogel matrices recently (Figure 27a).[44] By infusing air, water, or liquid metal (i.e., eutectic gallium−indium) into the fluidic channels, the effective density, bulk modulus, and thus acoustic impedance of the hydrogel can be dramatically varied to approximate the acoustic impedance of air, water, and many solids on demand (Figure 27b).[44] In order to approximate a homogeneous material, the fluidic channels should be uniformly distributed in the hydrogel, and the characteristic sizes of the fluidic channels (i.e., channel diameter and distance between adjacent channels) should be much smaller than the acoustic wavelengths. Overall, a generic design principle for hydrogels with tunable acoustic impedance is to tune densities and bulk moduli of effectively homogeneous hydrogels.

6.5. Self-Healing: Form New Cross-Links and/or Polymers at Damaged Regions

A salient feature of many biological hydrogels is their capability of healing after injury. The capability of self-healing can potentially bestow synthetic hydrogels with merits such as damage mitigation and long-term robustness. However, the healing processes in biological hydrogels mostly rely on the functions of biological cells, which usually do not exist in synthetic hydrogels. In the absence of living components, a generic strategy to achieve self-healing in engineering materials is to form new materials and/or interactions in the vicinity of damaged regions.[860]

In particular, for soft materials such as elastomers and hydrogels, the new materials formed in the vicinity of damaged regions are usually new cross-links and/or polymer chains. Therefore, the design principle for self-healing hydrogels is to form new cross-links and/or polymers at damaged regions (Figure 28a). The commonly used cross-links for self-healing of hydrogels include weak physical cross-links such as hydrogen bonds,[750,765,767,861] ionic bonds,[305,496,862] metal coordinations,[305,767,852] hydrophobic interactions,[863] and guest−host interactions,[752] and dynamic covalent bonds such as olefin

https://doi.org/10.1021/acs.chemrev.0c01088
Chem. Rev. XXXX, XXX, XXX−XXX

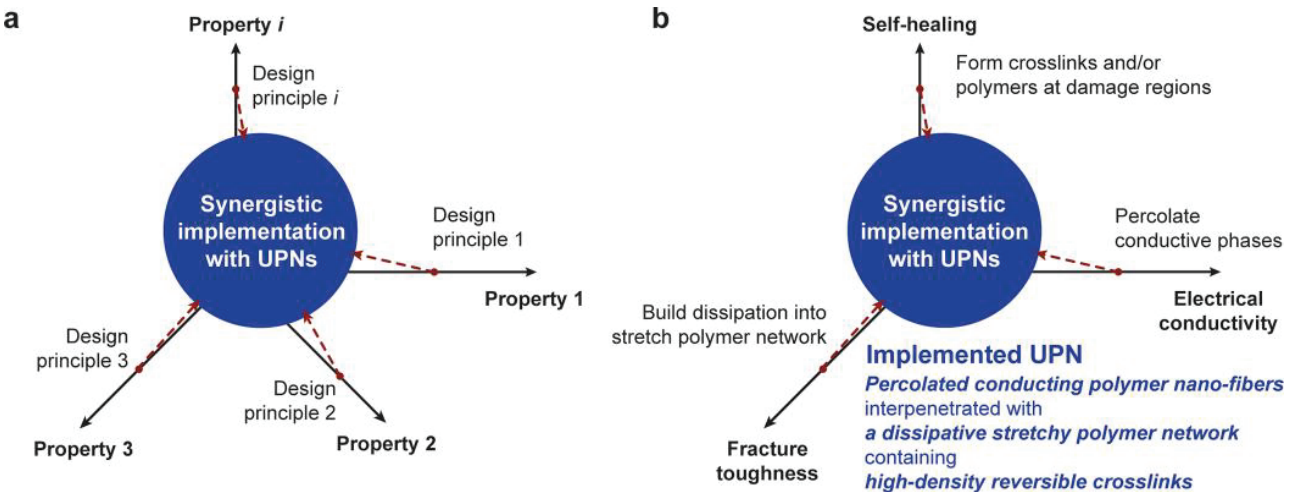

Figure 29. Orthogonal design principles and synergistic implementation strategies for the design of hydrogels with multiple combined extreme properties. (a) Schematics of the orthogonal design principles and the synergistic implementation strategies. (b) Example of the design of a tough, self-healing and electrically conductive hydrogel.

metathesis.[46,864] Once two newly formed surfaces in a damaged hydrogel are brought into contact with each other under certain conditions such as specific temperature and pH, new cross-links can form on the interface, endowing the hydrogel with the self-healing capability (Figures 28a,c). Besides weak physical and dynamic covalent cross-links (i.e., reversible cross-links), the self-healing of hydrogels can also be achieved through interdiffusion of polymer chains to form entangled chains that span the crack surfaces (Figures 28a,c).[865,866] In fact, self-healing processes in hydrogels mostly involve both mechanisms of chain entanglement and reversible cross-linking.[867]

Notably, when the surfaces of two intact self-healing hydrogels are brought in contact under certain conditions such as specific temperature and pH, an adhered interface can also be formed between the two hydrogels. Therefore, strictly speaking, most of the existing self-healing hydrogels are self-adhesive hydrogels because the damage of the hydrogels is not required to induce the process of self-healing. Recently, Matsuda et al. have reported a self-growing or self-reinforcing hydrogel, in which the scission of polymer chains can induce mechanoradicals that trigger the polymerization of monomers in the solvent of the hydrogel (Figure 28b).[868] Consequently, the hydrogel self-grows or self-reinforces after moderate damage, analogous to mechanical training of a muscle (Figure 28d). This strategy may be adopted for the future design of truly self-healing (instead of self-adhesive) hydrogels where the healing is triggered by the damage. For a further detailed discussion on various types of self-healing hydrogels, a recent review paper is recommended.[846]

6.6. Implementation Strategies for Extreme Physical Properties with Unconventional Polymer Networks

While the implementation strategies for hydrogels with extreme mechanical properties exploits various types of UPNs as discussed in section 5, it seems hydrogels with extreme physical properties mainly rely on one implementation strategy: functional nano-/micro-/macrofillers. The functional fillers range from percolated conductive phases for high electrical conductivity, to magnetic particles for magnetization, to high-refractive-index nonscattering nanophases for high refractive index and transparency, to fillers with tunable densities and bulk moduli for tunable acoustic impedance, and to reversible cross-links and damage-triggered polymerization for self-healing capability.

7. DESIGN OF HYDROGELS WITH MULTIPLE COMBINED PROPERTIES

In addition to the extreme mechanical and physical properties discussed in sections 5 and 6, respectively, chemical and biological properties of hydrogels also play critical roles in various applications of hydrogels. In fact, many nascent applications of hydrogels such as hydrogel living devices commonly require that a set of combined mechanical, physical, chemical, and biological properties simultaneously coexist in hydrogels.[20,24,46] In order to achieve multiple combined properties, we will propose a general strategy for the orthogonal design of hydrogels guided by the corresponding design principles, which will then be implemented with UPNs in a synergistic manner.

7.1. Orthogonal design principles

In sections 5 and 6, we have discussed the design principles for hydrogels to achieve a variety of extreme mechanical and physical properties, which are summarized as follows.

- Tough: build dissipation into stretchy polymer networks.
- Strong: synchronize chain stiffening and fracture.
- Resilient: delay dissipation.
- Tough adhesion: integrate tough dissipative hydrogels and strong interfacial linkages.
- Fatigue-resistant: pin fatigue cracks with intrinsically high-energy phases.
- Fatigue-resistant adhesion: strongly bond intrinsically high-energy phases on interfaces.
- Electrically conductive: percolate electrically conductive phases.
- Magnetization: embed magnetic particles and pattern ferromagnetic domains.
- High reflective index and transparency: uniformly embed high-refractive-index nonscattering nanophases.
- Tunable acoustic impedance: tune densities and bulk moduli of effectively homogeneous hydrogels.

https://doi.org/10.1021/acs.chemrev.0c01088
Chem. Rev. XXXX, XXX, XXX−XXX

- Self-healing: form cross-links and/or polymers at damaged regions.

Since the above-mentioned design principles are general and material-independent, they have been widely deployed for the design of biological hydrogels, synthetic hydrogels, and other engineering materials. In addition, on the basis of the discussions in sections 5 and 6, these design principles do not contradict or exclude one another in general. For example, the seeming contradiction between high toughness and high resilience of hydrogels has been reconciled by the design principles of building dissipation into stretchy polymer networks and delaying dissipation, respectively. Therefore, the design of multiple combined mechanical and physical properties of hydrogels can potentially follow the corresponding design principles in an orthogonal and independent manner as illustrated in Figure 29a. For example, a tough, electrically conductive, and self-healing hydrogel can be potentially designed by following the orthogonal design principles of building dissipation into stretchy polymer networks, percolating electrically conductive phases, and forming cross-links and/or polymers at damaged regions, respectively[32] (Figure 29b). The hydrogel can further form tough adhesion on substrates by following the design principle of integrating tough hydrogels and strong interfacial linkages.[851]

In addition, although chemical and biological properties of hydrogels are beyond the scope of the current review, it is expected that the design of hydrogels' chemical and biological properties will likely follow a set of design principles that are orthogonal with one another and with the design principles for mechanical and physical properties as well. Consequently, a set of orthogonal design principles will potentially guide the rational design of future hydrogels that possess multiple combined mechanical, physical, chemical, and biological properties (Figure 29).

7.2. Synergistic Implementation Strategies

The orthogonal design principles for hydrogels to achieve multiple combined properties will be implemented with UPNs in a synergistic manner, meaning that one type of UPN can implement multiple design principles. As discussed in section 4, the commonly used UPNs include

- Ideal polymer networks
- Polymer networks with slidable cross-links
- Interpenetrating and semi-interpenetrating polymer networks
- Polymer networks with high-functionality cross-links
- Nano-/microfibrous polymer networks
- Strong physical cross-links
- Weak physical cross-links
- Dynamic covalent cross-links

Each UPN architecture or interaction usually can implement (or facilitate the implementation of) multiple design principles. For example, the nano-/microfibrous polymer networks can integrate high stretchability and mechanical dissipation (section 5.1), delay dissipation (section 5.3), synchronize stiffening and fracture of polymer chains (section 5.2), and act as intrinsically high-energy phases (section 5.5) to implement the design principles for tough, resilient, strong, and fatigue-resistant hydrogels, respectively. By strongly bonding the nano-/microfibers on substrates (section 5.4 and section 5.6), the corresponding nano-/microfibrous polymer networks can achieve tough and fatigue-resistant adhesion as well. Furthermore, the nano-/microfibers can also be made functional such as electrically conductive or with high reflective index (section 6.1) to implement the design of the corresponding extreme physical properties. Not surprisingly, biological hydrogels frequently employ nano-/microfibrous polymer networks, supplemented by other UPN architectures and interactions, to achieve multiple combined extreme mechanical and physical properties necessary for their robustness and well-being over the lifetime (Figure 2).

Last but not least, it should be emphasized that the design principles and implementation strategies for hydrogels discussed in this paper are based on generic polymer networks; therefore, they should be applicable to other soft materials comprised of polymer networks including elastomers and organogels. For example, the design principle and implementation strategy for tough hydrogels have been used to design tough elastomers.[737] We expect the current review will provide a solid and systematic foundation for the rational design of various types of polymeric soft materials including hydrogels, elastomers, and organogels to achieve multiple combined extreme properties for diverse applications. Furthermore, we hope the current review will provoke interdisciplinary discussions on a fundamental question: why does nature select soft materials, especially hydrogels embodied in unconventional polymer networks (Figures 1 and 2), to constitute the major components of animal bodies?

AUTHOR INFORMATION

Corresponding Author

Xuanhe Zhao − *Department of Mechanical Engineering and Department of Civil and Environmental Engineering, Massachusetts Institute of Technology, Cambridge, Massachusetts 02139, United States;* orcid.org/0000-0001-5387-6186; Email: zhaox@mit.edu

Authors

Xiaoyu Chen − *Department of Mechanical Engineering, Massachusetts Institute of Technology, Cambridge, Massachusetts 02139, United States*

Hyunwoo Yuk − *Department of Mechanical Engineering, Massachusetts Institute of Technology, Cambridge, Massachusetts 02139, United States;* orcid.org/0000-0003-1710-9750

Shaoting Lin − *Department of Mechanical Engineering, Massachusetts Institute of Technology, Cambridge, Massachusetts 02139, United States*

Xinyue Liu − *Department of Mechanical Engineering, Massachusetts Institute of Technology, Cambridge, Massachusetts 02139, United States*

German Parada − *Department of Mechanical Engineering, Massachusetts Institute of Technology, Cambridge, Massachusetts 02139, United States*

Complete contact information is available at: https://pubs.acs.org/10.1021/acs.chemrev.0c01088

Author Contributions

#X.C., H.Y., and S.L. contributed equally to this work. X.Z. proposed the paper and formulated the theories in the paper. X.Z., X.C., H.Y., S.L., X.L., and G.P. drafted the paper.

Notes

The authors declare no competing financial interest.

https://doi.org/10.1021/acs.chemrev.0c01088
Chem. Rev. XXXX, XXX, XXX−XXX

Biographies

Xuanhe Zhao is Professor of Mechanical Engineering at Massachusetts Institute of Technology and the PI of the Zhao Lab (http://zhao.mit.edu/). The mission of the Zhao Lab is to advance science and technology on the interfaces between humans and machines for addressing grand societal challenges in health and sustainability with integrated expertise in mechanics, materials, and biotechnology. A major focus of the Zhao Lab's current research is the study and development of soft materials and systems. Dr. Zhao is the recipient of the NSF CAREER Award, ONR Young Investigator Award, SES Young Investigator Medal, ASME Hughes Young Investigator Award, Adhesion Society's Young Scientist Award, Materials Today Rising Star Award, and Web of Science Highly Cited Researcher.

Xiaoyu Chen is a postdoctoral fellow in the Department of Mechanical Engineering at Massachusetts Institute of Technology. He received his B.S. degree in the College of Chemistry at Jilin University in 2013. He earned his Ph.D. degree in the Department of Biomedical Engineering at the Chinese University of Hong Kong in 2019. His research focuses on the design and preparation of polymeric biomaterials for biomedical applications. He is a recipient of the CUHK Outstanding Student Award and the Society for Biomaterials STAR Award.

Hyunwoo Yuk is a postdoctoral fellow in the Department of Mechanical Engineering at Massachusetts Institute of Technology. He received his M.S. and Ph.D. in Mechanical Engineering from Massachusetts Institute of Technology in 2016 and 2020, respectively. His research focuses on the broad topics of mechanics and materials science and engineering in human−machine interfaces including wet adhesion, translational bioadhesive technologies, hydrogel bioelectronics, and 3D printing of advanced soft materials. He is a recipient of various awards including Forbes 30 Under 30 Science, Materials Research Society Graduate Student Award, Adhesion Society Peebles Award, and Graduate Winner of Collegiate Inventors Competition.

Shaoting Lin is a postdoctoral fellow in the Department of Mechanical Engineering at Massachusetts Institute of Technology. He received his B.S. degree in Automobile Engineering at Tsinghua University in 2010 and his M.S. degree in Mechanical Engineering at Tsinghua University in 2013. He earned his Ph.D. degree in the Department of Mechanical Engineering at MIT in 2019. His research focuses on the design of environmentally benign (EB) intelligent materials—materials that can transform and adapt their functional properties to reconcile human development and environmental sustainability. The technical approaches involve extreme mechanics to push the limit of mechanical and physical properties of EB intelligent materials (e.g., fatigue-resistant soft materials) and advanced manufacturing (e.g., additive manufacturing) to realize complex structures and multifunctions of EB intelligent materials.

Xinyue Liu is a Ph.D. candidate in Department of Mechanical Engineering at Massachusetts Institute of Technology. She received her B.S. degree in Polymer Science and Engineering at Sichuan University in 2015. Her research focuses on developing versatile hydrogel devices for fundamental and applied biomedical studies. She aims to design epidermal, ingestible, and implantable hydrogel devices through advanced biofabrication techniques to capture broad classes of physiological information precisely and rely on endurant soft material technologies to enable long-term monitoring of human biological signals. She is a recipient of Forbes 30 Under 30 Asia in Healthcare & Science and Materials Research Society Graduate Student Award.

German Parada is a Senior R&D Engineering Specialist at the Dow Chemical Company. He received his Ph.D. in Chemical Engineering from the Massachusetts Institute of Technology in 2019, where he was affiliated with the Program in Polymers and Soft Matter and the Zhao Laboratory. His research focuses on the fabrication and characterization of tough hydrogel coatings for antifouling and antithrombotic applications, and the correlation of structure and rheological responses for reversibly cross-linked hydrogels.

ACKNOWLEDGMENTS

This work was supported by National Institutes of Health (No. 1R01HL153857-01), National Science Foundation (No. EFMA-1935291), U.S. Army Research Office through the Institute for Soldier Nanotechnologies at MIT (Grant No. W911NF-13-D-0001), and Defense Advanced Research Projects Agency through Cooperative Agreement D20AC00004.

ACRONYM

APS ammonium persulfate
CB[*n*] cucurbit[*n*]uril
CD cyclodextrin
CNT carbon nanotubes
DOPA 3,4-dihydroxyphenyl-L-alanine
EDC 1-ethyl-3-(3-(dimethylamino)propyl)carbodiimide
Fmoc fluorenylmethyloxycarbonyl
G α-L-guluronic acid
GO graphene oxide
M β-D-mannuronic
MBA *N,N′*-methylenebis(acrylamide)
NdFeB neodymium iron boron
NHS *N*-hydroxysuccinimide
NVP *N*-vinylpyrrolidone
PAA poly(acrylic acid)
PAAm polyacrylamide
PCL poly(caprolactone)
PDLLA poly(DL-lactic acid)
PDMA poly(*N,N*-dimethylacrylamide)
PEDOT:PSS poly(3,4-ethylenedioxythiophene):poly(styrenesulfonate)
PEG poly(ethylene glycol)
PEO poly(ethylene oxide)
PHEMA poly(2-hydroxethyl methacrylate)
PLA polylactide
PLGA poly(DL-lactic acid-*co*-glycolic acid)
PMA polymethacrylic acid
PNIPAm poly(*N*-isopropylacrylamide)
PPG poly(propylene glycol)
PPO poly(*p*-phenylene oxide)
PPS poly(propylene sulfide)
PVA poly(vinyl alcohol)
RGD Arg-Gly-Asp
TEGDMA trimethylene glycol dimethacrylate
TEMED *N,N,N′N′*-tetramethylene-diamine
UPN unconventional polymer network
UPy ureido-pyrimidinone

REFERENCES

(1) Wichterle, O.; Lim, D. Hydrophilic gels for biological use. *Nature* **1960**, *185*, 117−118.
(2) Peppas, N. A.; Bures, P.; Leobandung, W.; Ichikawa, H. Hydrogels in pharmaceutical formulations. *Eur. J. Pharm. Biopharm.* **2000**, *50*, 27−46.
(3) Qiu, Y.; Park, K. Environment-sensitive hydrogels for drug delivery. *Adv. Drug Delivery Rev.* **2001**, *53*, 321−339.
(4) Peppas, N. A.; Hilt, J. Z.; Khademhosseini, A.; Langer, R. Hydrogels in biology and medicine: from molecular principles to bionanotechnology. *Adv. Mater.* **2006**, *18*, 1345−1360.

AQ

(5) Li, J.; Mooney, D. J. Designing hydrogels for controlled drug delivery. *Nat. Rev. Mater.* **2016**, *1*, 16071.
(6) Lee, K. Y.; Mooney, D. J. Hydrogels for Tissue Engineering. *Chem. Rev.* **2001**, *101*, 1869−1880.
(7) Nguyen, K. T.; West, J. L. Photopolymerizable hydrogels for tissue engineering applications. *Biomaterials* **2002**, *23*, 4307−4314.
(8) Drury, J. L.; Mooney, D. J. Hydrogels for tissue engineering: scaffold design variables and applications. *Biomaterials* **2003**, *24*, 4337−4351.
(9) Discher, D. E.; Janmey, P.; Wang, Y.-L. Tissue cells feel and respond to the stiffness of their substrate. *Science* **2005**, *310*, 1139.
(10) Engler, A. J.; Sen, S.; Sweeney, H. L.; Discher, D. E. Matrix elasticity directs stem cell lineage specification. *Cell* **2006**, *126*, 677−689.
(11) Discher, D. E.; Mooney, D. J.; Zandstra, P. W. Growth factors, matrices, and forces combine and control stem cells. *Science* **2009**, *324*, 1673.
(12) Huebsch, N.; Arany, P. R.; Mao, A. S.; Shvartsman, D.; Ali, O. A.; Bencherif, S. A.; Rivera-Feliciano, J.; Mooney, D. J. Harnessing traction-mediated manipulation of the cell/matrix interface to control stem-cell fate. *Nat. Mater.* **2010**, *9*, 518−526.
(13) Tibbitt, M. W.; Anseth, K. S. Hydrogels as extracellular matrix mimics for 3D cell culture. *Biotechnol. Bioeng.* **2009**, *103*, 655−663.
(14) Caló, E.; Khutoryanskiy, V. V. Biomedical applications of hydrogels: a review of patents and commercial products. *Eur. Polym. J.* **2015**, *65*, 252−267.
(15) Kopecek, J. Hydrogels: From soft contact lenses and implants to self-assembled nanomaterials. *J. Polym. Sci., Part A: Polym. Chem.* **2009**, *47*, 5929−5946.
(16) Jones, A.; Vaughan, D. Hydrogel dressings in the management of a variety of wound types: A review. *J. Orthop. Nurs.* **2005**, *9*, S1−S11.
(17) Boateng, J. S.; Matthews, K. H.; Stevens, H. N. E.; Eccleston, G. M. Wound healing dressings and drug delivery systems: a review. *J. Pharm. Sci.* **2008**, *97*, 2892−2923.
(18) Kamoun, E. A.; Kenawy, E.-R. S.; Chen, X. A review on polymeric hydrogel membranes for wound dressing applications: PVA-based hydrogel dressings. *J. Adv. Res.* **2017**, *8*, 217−233.
(19) Vanderlaan, D. G.; Nunez, I. M.; Hargiss, M.; Alton, M. L.; Williams, S. Soft contact lenses. U.S. Patent 6943203. September 13, 2005.
(20) Liu, X.; Liu, J.; Lin, S.; Zhao, X. Hydrogel machines. *Mater. Today* **2020**. DOI: 10.1016/j.mattod.2019.12.026
(21) Dong, L.; Agarwal, A. K.; Beebe, D. J.; Jiang, H. Adaptive liquid microlenses activated by stimuli-responsive hydrogels. *Nature* **2006**, *442*, 551.
(22) Holtz, J. H.; Asher, S. A. Polymerized colloidal crystal hydrogel films as intelligent chemical sensing materials. *Nature* **1997**, *389*, 829.
(23) Miyata, T.; Asami, N.; Uragami, T. A reversibly antigen-responsive hydrogel. *Nature* **1999**, *399*, 766.
(24) Liu, X.; Tang, T.-C.; Tham, E.; Yuk, H.; Lin, S.; Lu, T. K.; Zhao, X. Stretchable living materials and devices with hydrogel-elastomer hybrids hosting programmed cells. *Proc. Natl. Acad. Sci. U. S. A.* **2017**, *114*, 2200−2205.
(25) Beebe, D. J.; Moore, J. S.; Bauer, J. M.; Yu, Q.; Liu, R. H.; Devadoss, C.; Jo, B.-H. Functional hydrogel structures for autonomous flow control inside microfluidic channels. *Nature* **2000**, *404*, 588−590.
(26) Yuk, H.; Lin, S.; Ma, C.; Takaffoli, M.; Fang, N. X.; Zhao, X. Hydraulic hydrogel actuators and robots optically and sonically camouflaged in water. *Nat. Commun.* **2017**, *8*, 14230.
(27) Keplinger, C.; Sun, J.-Y.; Foo, C. C.; Rothemund, P.; Whitesides, G. M.; Suo, Z. Stretchable, transparent, ionic conductors. *Science* **2013**, *341*, 984−987.
(28) Zhao, X.; Kim, J.; Cezar, C. A.; Huebsch, N.; Lee, K.; Bouhadir, K.; Mooney, D. J. Active scaffolds for on-demand drug and cell delivery. *Proc. Natl. Acad. Sci. U. S. A.* **2011**, *108*, 67−72.
(29) Li, T.; Li, G.; Liang, Y.; Cheng, T.; Dai, J.; Yang, X.; Liu, B.; Zeng, Z.; Huang, Z.; Luo, Y.; et al. Fast-moving soft electronic fish. *Sci. Adv.* **2017**, *3*, No. e1602045.
(30) Kim, Y. S.; Liu, M.; Ishida, Y.; Ebina, Y.; Osada, M.; Sasaki, T.; Hikima, T.; Takata, M.; Aida, T. Thermoresponsive actuation enabled by permittivity switching in an electrostatically anisotropic hydrogel. *Nat. Mater.* **2015**, *14*, 1002.
(31) Liu, Y.; Liu, J.; Chen, S.; Lei, T.; Kim, Y.; Niu, S.; Wang, H.; Wang, X.; Foudeh, A. M.; Tok, J. B. H.; et al. Soft and elastic hydrogel-based microelectronics for localized low-voltage neuromodulation. *Nat. Biomed Eng.* **2019**, *3*, 58−68.
(32) Lu, B.; Yuk, H.; Lin, S.; Jian, N.; Qu, K.; Xu, J.; Zhao, X. Pure PEDOT:PSS hydrogels. *Nat. Commun.* **2019**, *10*, 1043.
(33) Gao, Y.; Song, J.; Li, S.; Elowsky, C.; Zhou, Y.; Ducharme, S.; Chen, Y. M.; Zhou, Q.; Tan, L. Hydrogel microphones for stealthy underwater listening. *Nat. Commun.* **2016**, *7*, 12316.
(34) Schroeder, T. B.; Guha, A.; Lamoureux, A.; VanRenterghem, G.; Sept, D.; Shtein, M.; Yang, J.; Mayer, M. An electric-eel-inspired soft power source from stacked hydrogels. *Nature* **2017**, *552*, 214−218.
(35) Pan, L.; Yu, G.; Zhai, D.; Lee, H. R.; Zhao, W.; Liu, N.; Wang, H.; Tee, B. C.-K.; Shi, Y.; Cui, Y.; et al. Hierarchical nanostructured conducting polymer hydrogel with high electrochemical activity. *Proc. Natl. Acad. Sci. U. S. A.* **2012**, *109*, 9287−9292.
(36) Xiao, T.; Xu, L.; Zhou, L.; Sun, X. Q.; Lin, C.; Wang, L. Dynamic hydrogels mediated by macrocyclic host-guest interactions. *J. Mater. Chem. B* **2019**, *7*, 1526−1540.
(37) Kim, C.-C.; Lee, H.-H.; Oh, K. H.; Sun, J.-Y. Highly stretchable, transparent ionic touch panel. *Science* **2016**, *353*, 682−687.
(38) Kim, Y.; Parada, G. A.; Liu, S.; Zhao, X. Ferromagnetic soft continuum robots. *Sci. Robot.* **2019**, *4*, No. eaax7329.
(39) Kim, Y.; Yuk, H.; Zhao, R.; Chester, S. A.; Zhao, X. Printing ferromagnetic domains for untethered fast-transforming soft materials. *Nature* **2018**, *558*, 274−279.
(40) Wang, L.; Kim, Y.; Guo, C. F.; Zhao, X. Hard-magnetic elastica. *J. Mech. Phys. Solids* **2020**, *142*, 104045.
(41) Chen, F.; Tillberg, P. W.; Boyden, E. S. Expansion microscopy. *Science* **2015**, *347*, 543−548.
(42) Guo, J.; Liu, X.; Jiang, N.; Yetisen, A. K.; Yuk, H.; Yang, C.; Khademhosseini, A.; Zhao, X.; Yun, S. H. Highly stretchable, strain sensing hydrogel optical fibers. *Adv. Mater.* **2016**, *28*, 10244−10249.
(43) Li, X.-H.; Liu, C.; Feng, S.-P.; Fang, N. X. Broadband light management with thermochromic hydrogel microparticles for smart windows. *Joule* **2019**, *3*, 290−302.
(44) Zhang, K.; Ma, C.; He, Q.; Lin, S.; Chen, Y.; Zhang, Y.; Fang, N. X.; Zhao, X. Metagel with broadband tunable acoustic properties over air-water-solid ranges. *Adv. Funct. Mater.* **2019**, *29*, 1903699.
(45) Dong, E.; Song, Z.; Zhang, Y.; Mosanenzadeh, S. G.; He, Q.; Zhao, X.; Fang, N. X. Bioinspired metagel with broadband tunable impedance matching. *Sci. Adv.* **2020**, *6*, No. eabb3641.
(46) Liu, X.; Yuk, H.; Lin, S.; Parada, G. A.; Tang, T. C.; Tham, E.; de la Fuente-Nunez, C.; Lu, T. K.; Zhao, X. 3D printing of living responsive materials and devices. *Adv. Mater.* **2018**, *30*, 1704821.
(47) Yuk, H.; Varela, C. E.; Nabzdyk, C. S.; Mao, X.; Padera, R. F.; Roche, E. T.; Zhao, X. Dry double-sided tape for adhesion of wet tissues and devices. *Nature* **2019**, *575*, 169−174.
(48) Rose, S.; Prevoteau, A.; Elzière, P.; Hourdet, D.; Marcellan, A.; Leibler, L. Nanoparticle solutions as adhesives for gels and biological tissues. *Nature* **2014**, *505*, 382−385.
(49) Yuk, H.; Zhang, T.; Lin, S.; Parada, G. A.; Zhao, X. Tough bonding of hydrogels to diverse non-porous surfaces. *Nat. Mater.* **2016**, *15*, 190.
(50) Li, J.; Celiz, A. D.; Yang, J.; Yang, Q.; Wamala, I.; Whyte, W.; Seo, B. R.; Vasilyev, N. V.; Vlassak, J. J.; Suo, Z.; Mooney, D. J. Tough adhesives for diverse wet surfaces. *Science* **2017**, *357*, 378−381.
(51) Yu, Y.; Yuk, H.; Parada, G. A.; Wu, Y.; Liu, X.; Nabzdyk, C. S.; Youcef-Toumi, K.; Zang, J.; Zhao, X. Multifunctional "hydrogel skins" on diverse polymers with arbitrary shapes. *Adv. Mater.* **2019**, *31*, 1807101.
(52) Cheng, H.; Yue, K.; Kazemzadeh-Narbat, M.; Liu, Y.; Khalilpour, A.; Li, B.; Zhang, Y. S.; Annabi, N.; Khademhosseini, A. Mussel-inspired multifunctional hydrogel coating for prevention of infections and

enhanced osteogenesis. *ACS Appl. Mater. Interfaces* **2017**, *9*, 11428−11439.
(53) Biot, M. A. General theory of three-dimensional consolidation. *J. Appl. Phys.* **1941**, *12*, 155−164.
(54) Flory, P. J. *Principles of Polymer Chemistry*; Cornell University Press: Ithaca, 1953.
(55) Lake, G.; Lindley, P. The mechanical fatigue limit for rubber. *J. Appl. Polym. Sci.* **1965**, *9*, 1233−1251.
(56) Lake, G.; Thomas, A. The strength of highly elastic materials. *Proc. R. Soc. London A* **1967**, *300*, 108−119.
(57) Treloar, L. R. G. *The Physics of Rubber Elasticity*; Oxford University Press: New York, 1975.
(58) De Gennes, P.-G. *Scaling Concepts in Polymer Physics*; Cornell University Press: Ithaca, 1979.
(59) Gent, A. A new constitutive relation for rubber. *Rubber Chem. Technol.* **1996**, *69*, 59−61.
(60) Erman, B.; Mark, J. E. *Structures and Properties of Rubberlike Networks*; Oxford University Press: New York, 1997.
(61) Boyce, M. C.; Arruda, E. M. Constitutive models of rubber elasticity: a review. *Rubber Chem. Technol.* **2000**, *73*, 504−523.
(62) Rubinstein, M.; Colby, R. H. *Polymer Physics*; Oxford University Press: New York, 2003.
(63) Mark, J. E.; Erman, B. *Rubberlike Elasticity: A Molecular Primer*; Cambridge University Press: Cambridge, 2007.
(64) Argon, A. S. *The Physics of Deformation and Fracture of Polymers*; Cambridge University Press: Cambridge, 2013.
(65) Peppas, N. A. *Hydrogels in Medicine and Pharmacy: Fundamentals*; CRC Press: Boca Raton, 2019.
(66) Richbourg, N. R.; Peppas, N. A. The swollen polymer network hypothesis: Quantitative models of hydrogel swelling, stiffness, and solute transport. *Prog. Polym. Sci.* **2020**, *105*, 101243.
(67) Zhao, X. Multi-scale multi-mechanism design of tough hydrogels: building dissipation into stretchy networks. *Soft Matter* **2014**, *10*, 672−687.
(68) Zhang, Y. S.; Khademhosseini, A. Advances in engineering hydrogels. *Science* **2017**, *356*, No. eaaf3627.
(69) Fan, H.; Gong, J. P. Fabrication of bioinspired hydrogels: challenges and opportunities. *Macromolecules* **2020**, *53*, 2769−2782.
(70) Gong, J. P.; Katsuyama, Y.; Kurokawa, T.; Osada, Y. Double-network hydrogels with extremely high mechanical strength. *Adv. Mater.* **2003**, *15*, 1155−1158.
(71) Moutos, F. T.; Freed, L. E.; Guilak, F. A biomimetic three-dimensional woven composite scaffold for functional tissue engineering of cartilage. *Nat. Mater.* **2007**, *6*, 162−167.
(72) Hua, J.; Ng, P. F.; Fei, B. High-strength hydrogels: Microstructure design, characterization and applications. *J. Polym. Sci., Part B: Polym. Phys.* **2018**, *56*, 1325−1335.
(73) Lin, S.; Zhou, Y.; Zhao, X. Designing extremely resilient and tough hydrogels via delayed dissipation. *Extreme Mech. Lett.* **2014**, *1*, 70−75.
(74) Kamata, H.; Akagi, Y.; Kayasuga-Kariya, Y.; Chung, U.-I.; Sakai, T. Nonswellable" hydrogel without mechanical hysteresis. *Science* **2014**, *343*, 873.
(75) Lin, S.; Liu, X.; Liu, J.; Yuk, H.; Loh, H.-C.; Parada, G. A.; Settens, C.; Song, J.; Masic, A.; McKinley, G. H.; Zhao, X. Anti-fatigue-fracture hydrogels. *Sci. Adv.* **2019**, *5*, No. eaau8528.
(76) Lin, S.; Liu, J.; Liu, X.; Zhao, X. Muscle-like fatigue-resistant hydrogels by mechanical training. *Proc. Natl. Acad. Sci. U. S. A.* **2019**, *116*, 10244−10249.
(77) Xiang, C.; Wang, Z.; Yang, C.; Yao, X.; Wang, Y.; Suo, Z. Stretchable and fatigue-resistant materials. *Mater. Today* **2019**. DOI: 10.1016/j.mattod.2019.08.009
(78) Liu, J.; Lin, S.; Liu, X.; Qin, Z.; Yang, Y.; Zang, J.; Zhao, X. Fatigue-resistant adhesion of hydrogels. *Nat. Commun.* **2020**, *11*, 1071.
(79) Hall, B. K. *Cartilage V1: Structure, Function, and Biochemistry*; Academic Press: Cambridge, 2012.
(80) Taylor, D.; O'Mara, N.; Ryan, E.; Takaza, M.; Simms, C. The fracture toughness of soft tissues. *J. Mech. Behav. Biomed. Mater.* **2012**, *6*, 139−147.
(81) Mow, V. C.; Holmes, M. H.; Lai, W. M. Fluid transport and mechanical properties of articular cartilage: a review. *J. Biomech.* **1984**, *17*, 377−394.
(82) Han, L.; Frank, E. H.; Greene, J. J.; Lee, H.-Y.; Hung, H.-H. K.; Grodzinsky, A. J.; Ortiz, C. Time-dependent nanomechanics of cartilage. *Biophys. J.* **2011**, *100*, 1846−1854.
(83) Tavichakorntrakool, R.; Prasongwattana, V.; Sriboonlue, P.; Puapairoj, A.; Wongkham, C.; Wiangsimma, T.; Khunkitti, W.; Triamjangarun, S.; Tanratanauijit, M.; Chamsuwan, A.; Khunkitti, W.; Yenchitsomanus, P.-T.; Thongboonkerd, V. K^+, Na^+, Mg^{2+}, Ca^{2+}, and water contents in human skeletal muscle: correlations among these monovalent and divalent cations and their alterations in K^+-depleted subjects. *Transl. Res.* **2007**, *150*, 357−366.
(84) Johnson, G. A.; Tramaglini, D. M.; Levine, R. E.; Ohno, K.; Choi, N.-Y.; Woo, S. Tensile and viscoelastic properties of human patellar tendon. *J. Orthop. Res.* **1994**, *12*, 796−803.
(85) Connizzo, B. K.; Yannascoli, S. M.; Soslowsky, L. J. Structure-function relationships of postnatal tendon development: a parallel to healing. *Matrix Biol.* **2013**, *32*, 106−116.
(86) Fratzl, P. Collagen: structure and mechanics, an introduction. In *Collagen*; Springer: New York, 2008; pp 1−13.
(87) Lee, J. M.; Courtman, D. W.; Boughner, D. R. The glutaraldehyde-stabilized porcine aortic valve xenograft. I. Tensile viscoelastic properties of the fresh leaflet material. *J. Biomed. Mater. Res.* **1984**, *18*, 61−77.
(88) Lee, J. M.; Boughner, D. R.; Courtman, D. W. The glutaraldehyde-stabilized porcine aortic valve xenograft. II. Effect of fixation with or without pressure on the tensile viscoelastic properties of the leaflet material. *J. Biomed. Mater. Res.* **1984**, *18*, 79−98.
(89) Vesely, I. The role of elastin in aortic valve mechanics. *J. Biomech.* **1997**, *31*, 115−123.
(90) Driessen, N. J.; Bouten, C. V.; Baaijens, F. P. Improved prediction of the collagen fiber architecture in the aortic heart valve. *J. Biomech. Eng.* **2005**, *127*, 329.
(91) Bobyn, J. D.; Wilson, G. J.; Macgregor, D. C.; Pilliar, R. M.; Weatherly, G. C. Effect of pore-size on the peel strength of attachment of fibrous tissue to porous-surfaced implants. *J. Biomed. Mater. Res.* **1982**, *16*, 571−584.
(92) Covert, R. J.; Ott, R. D.; Ku, D. N. Friction characteristics of a potential articular cartilage biomaterial. *Wear* **2003**, *255*, 1064−1068.
(93) Chaudhuri, O.; Gu, L.; Klumpers, D.; Darnell, M.; Bencherif, S. A.; Weaver, J. C.; Huebsch, N.; Lee, H.-P.; Lippens, E.; Duda, G. N.; et al. Hydrogels with tunable stress relaxation regulate stem cell fate and activity. *Nat. Mater.* **2016**, *15*, 326−334.
(94) Genin, G. M.; Thomopoulos, S. The tendon-to-bone attachment: unification through disarray. *Nat. Mater.* **2017**, *16*, 607−608.
(95) Rossetti, L.; Kuntz, L. A.; Kunold, E.; Schock, J.; Muller, K. W.; Grabmayr, H.; Stolberg-Stolberg, J.; Pfeiffer, F.; Sieber, S. A.; Burgkart, R.; Bausch, A. R. The microstructure and micromechanics of the tendon-bone insertion. *Nat. Mater.* **2017**, *16*, 664−670.
(96) Chaudhuri, O.; Cooper-White, J.; Janmey, P. A.; Mooney, D. J.; Shenoy, V. B. Effects of extracellular matrix viscoelasticity on cellular behaviour. *Nature* **2020**, *584*, 535−546.
(97) Weightman, B.; Freeman, M.; Swanson, S. Fatigue of articular cartilage. *Nature* **1973**, *244*, 303−304.
(98) Hansson, T.; Keller, T.; Spengler, D. Mechanical behavior of the human lumbar spine. II. Fatigue strength during dynamic compressive loading. *J. Orthop. Res.* **1987**, *5*, 479−487.
(99) Peppas, N. A. Hydrogels and drug delivery. *Curr. Opin. Colloid Interface Sci.* **1997**, *2*, 531−537.
(100) Peppas, N. A.; Khare, A. R. Preparation, structure and diffusional behavior of hydrogels in controlled release. *Adv. Drug Delivery Rev.* **1993**, *11*, 1−35.
(101) Gladman, A. S.; Matsumoto, E. A.; Nuzzo, R. G.; Mahadevan, L.; Lewis, J. A. Biomimetic 4D printing. *Nat. Mater.* **2016**, *15*, 413.
(102) Yang, J.; Li, Y.; Zhu, L.; Qin, G.; Chen, Q. Double network hydrogels with controlled shape deformation: A mini review. *J. Polym. Sci., Part B: Polym. Phys.* **2018**, *56*, 1351−1362.

https://doi.org/10.1021/acs.chemrev.0c01088
Chem. Rev. XXXX, XXX, XXX−XXX

(103) Peng, X.; Wang, H. Shape changing hydrogels and their applications as soft actuators. *J. Polym. Sci., Part B: Polym. Phys.* **2018**, *56*, 1314−1324.
(104) Zhao, F.; Zhou, X.; Shi, Y.; Qian, X.; Alexander, M.; Zhao, X.; Mendez, S.; Yang, R.; Qu, L.; Yu, G. Highly efficient solar vapour generation via hierarchically nanostructured gels. *Nat. Nanotechnol.* **2018**, *13*, 489−495.
(105) Shadwick, R. E. Elastic energy storage in tendons: mechanical differences related to function and age. *J. Appl. Physiol.* **1990**, *68*, 1033−1040.
(106) Race, A.; Amis, A. A. The mechanical properties of the two bundles of the human posterior cruciate ligament. *J. Biomech.* **1994**, *27*, 13−24.
(107) Chin-Purcell, M. V.; Lewis, J. L. Fracture of articular cartilage. *J. Biomech. Eng.* **1996**, *118*, 545.
(108) Papagiannopoulos, A.; Waigh, T.; Hardingham, T.; Heinrich, M. Solution structure and dynamics of cartilage aggrecan. *Biomacromolecules* **2006**, *7*, 2162−2172.
(109) Hayes, W.; Mockros, L. Viscoelastic properties of human articular cartilage. *J. Appl. Physiol.* **1971**, *31*, 562−568.
(110) Rock, C. A.; Han, L.; Doehring, T. C. Complex collagen fiber and membrane morphologies of the whole porcine aortic valve. *PLoS One* **2014**, *9*, No. e86087.
(111) Korossis, S. Structure-function relationship of heart valves in health and disease. In *Structural Insufficiency Anomalies in Cardiac Valves*; Kırali, K., Ed.; IntechOpen: London, 2018; pp 1−38.
(112) Veiseh, O.; Doloff, J. C.; Ma, M.; Vegas, A. J.; Tam, H. H.; Bader, A. R.; Li, J.; Langan, E.; Wyckoff, J.; Loo, W. S.; et al. Size- and shape-dependent foreign body immune response to materials implanted in rodents and non-human primates. *Nat. Mater.* **2015**, *14*, 643−651.
(113) Lee, A.; Hudson, A.; Shiwarski, D.; Tashman, J.; Hinton, T.; Yerneni, S.; Bliley, J.; Campbell, P.; Feinberg, A. 3D bioprinting of collagen to rebuild components of the human heart. *Science* **2019**, *365*, 482−487.
(114) Park, S. Y.; Han, B. K.; Cho, E.; Bang, S. I. Chest wall lipogranuloma after hydrogel implant rupture: case report. *Investigative Magnetic Resonance Imaging* **2015**, *19*, 191−195.
(115) Liu, X.; Steiger, C.; Lin, S.; Parada, G. A.; Liu, J.; Chan, H. F.; Yuk, H.; Phan, N. V.; Collins, J.; Tamang, S.; et al. Ingestible hydrogel device. *Nat. Commun.* **2019**, *10*, 493.
(116) Yuk, H.; Lu, B.; Lin, S.; Qu, K.; Xu, J.; Luo, J.; Zhao, X. 3D printing of conducting polymers. *Nat. Commun.* **2020**, *11*, 1604.
(117) Esposito, C. L.; Kirilov, P.; Roullin, V. G. Organogels, promising drug delivery systems: an update of state-of-the-art and recent applications. *J. Controlled Release* **2018**, *271*, 1−20.
(118) Murdan, S. Organogels in drug delivery. *Expert Opin. Drug Delivery* **2005**, *2*, 489−505.
(119) Vintiloiu, A.; Leroux, J.-C. Organogels and their use in drug delivery—a review. *J. Controlled Release* **2008**, *125*, 179−192.
(120) Hoffman, A. S. Hydrogels for biomedical applications. *Adv. Drug Delivery Rev.* **2012**, *64*, 18−23.
(121) Sabra, W.; Zeng, A. P.; Deckwer, W. D. Bacterial alginate: physiology, product quality and process aspects. *Appl. Microbiol. Biotechnol.* **2001**, *56*, 315−325.
(122) Lee, K. Y.; Mooney, D. J. Alginate: properties and biomedical applications. *Prog. Polym. Sci.* **2012**, *37*, 106−126.
(123) Augst, A. D.; Kong, H. J.; Mooney, D. J. Alginate hydrogels as biomaterials. *Macromol. Biosci.* **2006**, *6*, 623−633.
(124) Donati, I.; Holtan, S.; Morch, Y. A.; Borgogna, M.; Dentini, M.; Skjak-Braek, G. New hypothesis on the role of alternating sequences in calcium-alginate gels. *Biomacromolecules* **2005**, *6*, 1031−1040.
(125) Morris, E. R.; Rees, D. A.; Thom, D. Characterization of alginate composition and block-structure by circular-dichroism. *Carbohydr. Res.* **1980**, *81*, 305−314.
(126) Smidsrød, O.; Skjak-Braek, G. Alginate as immobilization matrix for cells. *Trends Biotechnol.* **1990**, *8*, 71−78.
(127) Pawar, S. N.; Edgar, K. J. Alginate derivatization: a review of chemistry, properties and applications. *Biomaterials* **2012**, *33*, 3279−3305.
(128) Drury, J. L.; Dennis, R. G.; Mooney, D. J. The tensile properties of alginate hydrogels. *Biomaterials* **2004**, *25*, 3187−3199.
(129) Baer, A. E.; Wang, J. Y.; Kraus, V. B.; Setton, L. A. Collagen gene expression and mechanical properties of intervertebral disc cell-alginate cultures. *J. Orthop. Res.* **2001**, *19*, 2−10.
(130) Kang, S. W.; Cha, B. H.; Park, H.; Park, K. S.; Lee, K. Y.; Lee, S. H. The effect of conjugating RGD into 3D alginate hydrogels on adipogenic differentiation of human adipose-derived stromal cells. *Macromol. Biosci.* **2011**, *11*, 673−679.
(131) Landa, N.; Miller, L.; Feinberg, M. S.; Holbova, R.; Shachar, M.; Freeman, I.; Cohen, S.; Leor, J. Effect of injectable alginate implant on cardiac remodeling and function after recent and old infarcts in rat. *Circulation* **2008**, *117*, 1388−1396.
(132) Selden, C.; Khalil, M.; Hodgson, H. Three dimensional culture upregulates extracellular matrix protein expression in human liver cell lines–a step towards mimicking the liver in vivo? *Int. J. Artif. Organs* **2000**, *23*, 774−781.
(133) Xu, X.; Jha, A. K.; Harrington, D. A.; Farach-Carson, M. C.; Jia, X. Hyaluronic acid-based hydrogels: from a natural polysaccharide to complex networks. *Soft Matter* **2012**, *8*, 3280−3294.
(134) Burdick, J. A.; Prestwich, G. D. Hyaluronic acid hydrogels for biomedical applications. *Adv. Mater.* **2011**, *23*, H41−H56.
(135) Laurent, T. C.; Laurent, U. B.; Fraser, J. R. The structure and function of hyaluronan: An overview. *Immunol. Cell Biol.* **1996**, *74*, a1−a7.
(136) Vercruysse, K. P.; Marecak, D. M.; Marecek, J. F.; Prestwich, G. D. Synthesis and in vitro degradation of new polyvalent hydrazide cross-linked hydrogels of hyaluronic acid. *Bioconjugate Chem.* **1997**, *8*, 686−694.
(137) Pouyani, T.; Harbison, G. S.; Prestwich, G. D. Novel hydrogels of hyaluronic acid: synthesis, surface morphology, and solid-state NMR. *J. Am. Chem. Soc.* **1994**, *116*, 7515−7522.
(138) Kuo, J.; Prestwich, G. Materials of biological origin-Materials analysis and implant uses. In *Comprehensive Biomaterials*; Elsevier: Amsterdam, 2010.
(139) Shu, X. Z.; Liu, Y.; Palumbo, F.; Prestwich, G. D. Disulfide-crosslinked hyaluronan-gelatin hydrogel films: a covalent mimic of the extracellular matrix for in vitro cell growth. *Biomaterials* **2003**, *24*, 3825−3834.
(140) Vanderhooft, J. L.; Mann, B. K.; Prestwich, G. D. Synthesis and characterization of novel thiol-reactive poly(ethylene glycol) cross-linkers for extracellular-matrix-mimetic biomaterials. *Biomacromolecules* **2007**, *8*, 2883−2889.
(141) Serban, M. A.; Prestwich, G. D. Synthesis of hyaluronan haloacetates and biology of novel cross-linker-free synthetic extracellular matrix hydrogels. *Biomacromolecules* **2007**, *8*, 2821−2828.
(142) Pouyani, T.; Prestwich, G. D. Functionalized derivatives of hyaluronic acid oligosaccharides: drug carriers and novel biomaterials. *Bioconjugate Chem.* **1994**, *5*, 339−347.
(143) Jia, X. Q.; Burdick, J. A.; Kobler, J.; Clifton, R. J.; Rosowski, J. J.; Zeitels, S. M.; Langer, R. Synthesis and characterization of in situ cross-linkable hyaluronic acid-based hydrogels with potential application for vocal fold regeneration. *Macromolecules* **2004**, *37*, 3239−3248.
(144) Jha, A. K.; Hule, R. A.; Jiao, T.; Teller, S. S.; Clifton, R. J.; Duncan, R. L.; Pochan, D. J.; Jia, X. Structural analysis and mechanical characterization of hyaluronic acid-based doubly cross-linked networks. *Macromolecules* **2009**, *42*, 537−546.
(145) Darr, A.; Calabro, A. Synthesis and characterization of tyramine-based hyaluronan hydrogels. *J. Mater. Sci.: Mater. Med.* **2009**, *20*, 33−44.
(146) Collins, M. N.; Birkinshaw, C. Hyaluronic acid based scaffolds for tissue engineering—A review. *Carbohydr. Polym.* **2013**, *92*, 1262−1279.
(147) Burdick, J. A.; Chung, C.; Jia, X.; Randolph, M. A.; Langer, R. Controlled degradation and mechanical behavior of photopolymerized hyaluronic acid networks. *Biomacromolecules* **2005**, *6*, 386−391.

https://doi.org/10.1021/acs.chemrev.0c01088
Chem. Rev. XXXX, XXX, XXX−XXX

(148) Bian, L.; Guvendiren, M.; Mauck, R. L.; Burdick, J. A. Hydrogels that mimic developmentally relevant matrix and N-cadherin interactions enhance MSC chondrogenesis. *Proc. Natl. Acad. Sci. U. S. A.* **2013**, *110*, 10117−10122.
(149) Bencherif, S. A.; Srinivasan, A.; Horkay, F.; Hollinger, J. O.; Matyjaszewski, K.; Washburn, N. R. Influence of the degree of methacrylation on hyaluronic acid hydrogels properties. *Biomaterials* **2008**, *29*, 1739−1749.
(150) Chen, W. Y.; Abatangelo, G. Functions of hyaluronan in wound repair. *Wound Repair Regen.* **1999**, *7*, 79−89.
(151) Kuo, J. *Practical Aspects of Hyaluronan Based Medical Products*; CRC Press: Boca Raton, 2005.
(152) Prestwich, G. D. Engineering a clinically-useful matrix for cell therapy. *Organogenesis* **2008**, *4*, 42−47.
(153) Toh, W. S.; Lee, E. H.; Guo, X. M.; Chan, J. K.; Yeow, C. H.; Choo, A. B.; Cao, T. Cartilage repair using hyaluronan hydrogel-encapsulated human embryonic stem cell-derived chondrogenic cells. *Biomaterials* **2010**, *31*, 6968−6980.
(154) Anseth, K. S.; Metters, A. T.; Bryant, S. J.; Martens, P. J.; Elisseeff, J. H.; Bowman, C. N. In situ forming degradable networks and their application in tissue engineering and drug delivery. *J. Controlled Release* **2002**, *78*, 199−209.
(155) Burdick, J. A.; Ward, M.; Liang, E.; Young, M. J.; Langer, R. Stimulation of neurite outgrowth by neurotrophins delivered from degradable hydrogels. *Biomaterials* **2006**, *27*, 452−459.
(156) Baksh, D.; Song, L.; Tuan, R. S. Adult mesenchymal stem cells: characterization, differentiation, and application in cell and gene therapy. *J. Cell. Mol. Med.* **2004**, *8*, 301−316.
(157) Gerecht, S.; Burdick, J. A.; Ferreira, L. S.; Townsend, S. A.; Langer, R.; Vunjak-Novakovic, G. Hyaluronic acid hydrogel for controlled self-renewal and differentiation of human embryonic stem cells. *Proc. Natl. Acad. Sci. U. S. A.* **2007**, *104*, 11298−11303.
(158) Kim, I. L.; Mauck, R. L.; Burdick, J. A. Hydrogel design for cartilage tissue engineering: a case study with hyaluronic acid. *Biomaterials* **2011**, *32*, 8771−8782.
(159) Ifkovits, J. L.; Tous, E.; Minakawa, M.; Morita, M.; Robb, J. D.; Koomalsingh, K. J.; Gorman, J. H., 3rd; Gorman, R. C.; Burdick, J. A. Injectable hydrogel properties influence infarct expansion and extent of postinfarction left ventricular remodeling in an ovine model. *Proc. Natl. Acad. Sci. U. S. A.* **2010**, *107*, 11507−11512.
(160) Masters, K. S.; Shah, D. N.; Leinwand, L. A.; Anseth, K. S. Crosslinked hyaluronan scaffolds as a biologically active carrier for valvular interstitial cells. *Biomaterials* **2005**, *26*, 2517−2525.
(161) Sorushanova, A.; Delgado, L. M.; Wu, Z.; Shologu, N.; Kshirsagar, A.; Raghunath, R.; Mullen, A. M.; Bayon, Y.; Pandit, A.; Raghunath, M.; et al. The collagen suprafamily: from biosynthesis to advanced biomaterial development. *Adv. Mater.* **2019**, *31*, No. e1801651.
(162) Ferreira, A. M.; Gentile, P.; Chiono, V.; Ciardelli, G. Collagen for bone tissue regeneration. *Acta Biomater.* **2012**, *8*, 3191−3200.
(163) Shoulders, M. D.; Raines, R. T. Collagen structure and stability. *Annu. Rev. Biochem.* **2009**, *78*, 929−958.
(164) Banwell, E. F.; Abelardo, E. S.; Adams, D. J.; Birchall, M. A.; Corrigan, A.; Donald, A. M.; Kirkland, M.; Serpell, L. C.; Butler, M. F.; Woolfson, D. N. Rational design and application of responsive alpha-helical peptide hydrogels. *Nat. Mater.* **2009**, *8*, 596−600.
(165) Que, R. A.; Arulmoli, J.; Da Silva, N. A.; Flanagan, L. A.; Wang, S. W. Recombinant collagen scaffolds as substrates for human neural stem/progenitor cells. *J. Biomed. Mater. Res., Part A* **2018**, *106*, 1363−1372.
(166) Liu, X.; Zheng, C.; Luo, X.; Wang, X.; Jiang, H. Recent advances of collagen-based biomaterials: Multi-hierarchical structure, modification and biomedical applications. *Mater. Sci. Eng., C* **2019**, *99*, 1509−1522.
(167) Schmitt, F. O.; Hall, C. E.; Jakus, M. A. Electron microscope investigations of the structure of collagen. *J. Cell. Comp. Physiol.* **1942**, *20*, 11−33.
(168) Glowacki, J.; Mizuno, S. Collagen scaffolds for tissue engineering. *Biopolymers* **2008**, *89*, 338−344.
(169) Chan, K. L. S.; Khankhel, A. H.; Thompson, R. L.; Coisman, B. J.; Wong, K. H. K.; Truslow, J. G.; Tien, J. Crosslinking of collagen scaffolds promotes blood and lymphatic vascular stability. *J. Biomed. Mater. Res., Part A* **2014**, *102*, 3186−3195.
(170) Rault, I.; Frei, V.; Herbage, D.; Abdul-Malak, N.; Huc, A. Evaluation of different chemical methods for cros-linking collagen gel, films and sponges. *J. Mater. Sci.: Mater. Med.* **1996**, *7*, 215−221.
(171) Chevallay, B.; Abdul-Malak, N.; Herbage, D. Mouse fibroblasts in long-term culture within collagen three-dimensional scaffolds: Influence of crosslinking with diphenylphosphorylazide on matrix reorganization, growth, and biosynthetic and proteolytic activities. *J. Biomed. Mater. Res.* **2000**, *49*, 448−459.
(172) Damink, L. H. H. O.; Dijkstra, P. J.; vanLuyn, M. J. A.; vanWachem, P. B.; Nieuwenhuis, P.; Feijen, J. In vitro degradation of dermal sheep collagen cross-linked using a water-soluble carbodiimide. *Biomaterials* **1996**, *17*, 679−684.
(173) Couet, F.; Rajan, N.; Mantovani, D. Macromolecular biomaterials for scaffold-based vascular tissue engineering. *Macromol. Biosci.* **2007**, *7*, 701−718.
(174) Marelli, B.; Achilli, M.; Alessandrino, A.; Freddi, G.; Tanzi, M. C.; Fare, S.; Mantovani, D. Collagen-reinforced electrospun silk fibroin tubular construct as small calibre vascular graft. *Macromol. Biosci.* **2012**, *12*, 1566−1574.
(175) Pankajakshan, D.; Agrawal, D. K. Scaffolds in tissue engineering of blood vessels. *Can. J. Physiol. Pharmacol.* **2010**, *88*, 855−873.
(176) Thacharodi, D.; Rao, K. P. Rate-controlling biopolymer membranes as transdermal delivery systems for nifedipine: Development and in vitro evaluations. *Biomaterials* **1996**, *17*, 1307−1311.
(177) Lucas, P. A.; Syftestad, G. T.; Goldberg, V. M.; Caplan, A. I. Ectopic induction of cartilage and bone by water-soluble proteins from bovine bone using a collagenous delivery vehicle. *J. Biomed. Mater. Res.* **1989**, *23*, 23−39.
(178) Kaufmann, P. Highly porous polymer matrices as a three-dimensional culture system for hepatocytes. *Cell Transplant.* **1997**, *6*, 463−468.
(179) Helary, C.; Zarka, M.; Giraud-Guille, M. M. Fibroblasts within concentrated collagen hydrogels favour chronic skin wound healing. *J. Tissue Eng. Regener. Med.* **2012**, *6*, 225−237.
(180) McGuigan, A. P.; Sefton, M. V. The thrombogenicity of human umbilical vein endothelial cell seeded collagen modules. *Biomaterials* **2008**, *29*, 2453−2463.
(181) Voytik-Harbin, S. L.; Brightman, A. O.; Waisner, B. Z.; Robinson, J. P.; Lamar, C. H. Small intestinal submucosa: A tissue-derived extracellular matrix that promotes tissue-specific growth and differentiation of cells in vitro. *Tissue Eng.* **1998**, *4*, 157−174.
(182) Yuan, T.; Zhang, L.; Li, K. F.; Fan, H. S.; Fan, Y. J.; Liang, J.; Zhang, X. D. Collagen hydrogel as an immunomodulatory scaffold in cartilage tissue engineering. *J. Biomed. Mater. Res., Part B* **2014**, *102*, 337−344.
(183) Hahn, M. S.; Teply, B. A.; Stevens, M. M.; Zeitels, S. M.; Langer, R. Collagen composite hydrogels for vocal fold lamina propria restoration. *Biomaterials* **2006**, *27*, 1104−1109.
(184) Iwata, A.; Browne, K. D.; Pfister, B. J.; Gruner, J. A.; Smith, D. H. Long-term survival and outgrowth of mechanically engineered nervous tissue constructs implanted into spinal cord lesions. *Tissue Eng.* **2006**, *12*, 101−110.
(185) Hudson, C. B. Gelatine—relating structure and chemistry to functionality. In *Food Hydrocolloid*; Springer: New York, 1994; pp 347−354.
(186) Segtnan, V. H.; Isaksson, T. Temperature, sample and time dependent structural characteristics of gelatine gels studied by near infrared spectroscopy. *Food Hydrocolloids* **2004**, *18*, 1−11.
(187) Duconseille, A.; Astruc, T.; Quintana, N.; Meersman, F.; Sante-Lhoutellier, V. Gelatin structure and composition linked to hard capsule dissolution: A review. *Food Hydrocolloids* **2015**, *43*, 360−376.
(188) Farris, S.; Song, J.; Huang, Q. Alternative reaction mechanism for the cross-linking of gelatin with glutaraldehyde. *J. Agric. Food Chem.* **2010**, *58*, 998−1003.

https://doi.org/10.1021/acs.chemrev.0c01088
Chem. Rev. XXXX, XXX, XXX−XXX

(189) Kuijpers, A. J.; Engbers, G. H. M.; Feijen, J.; De Smedt, S. C.; Meyvis, T. K. L.; Demeester, J.; Krijgsveld, J.; Zaat, S. A. J.; Dankert, J. Characterization of the network structure of carbodiimide cross-linked gelatin gels. *Macromolecules* **1999**, *32*, 3325−3333.
(190) Digenis, G. A.; Gold, T. B.; Shah, V. P. Cross-linking of gelatin capsules and its relevance to their in vitro-in vivo performance. *J. Pharm. Sci.* **1994**, *83*, 915−921.
(191) Tu, R.; Shen, S. H.; Lin, D.; Hata, C.; Thyagarajan, K.; Noishiki, Y.; Quijano, R. C. Fixation of bioprosthetic tissues with monofunctional and multifunctional polyepoxy compounds. *J. Biomed. Mater. Res.* **1994**, *28*, 677−684.
(192) Hyndman, C. L.; Groboillot, A. F.; Poncelet, D.; Champagne, C. P.; Neufeld, R. J. Microencapsulation of Lactococcus lactis within cross-linked gelatin membranes. *J. Chem. Technol. Biotechnol.* **1993**, *56*, 259−263.
(193) Yue, K.; Trujillo-de Santiago, G.; Alvarez, M. M.; Tamayol, A.; Annabi, N.; Khademhosseini, A. Synthesis, properties, and biomedical applications of gelatin methacryloyl (GelMA) hydrogels. *Biomaterials* **2015**, *73*, 254−271.
(194) Morikawaand, N.; Matsuda, T. Thermoresponsive artificial extracellular matrix: N-isopropylacrylamide-graft-copolymerized gelatin. *J. Biomater. Sci., Polym. Ed.* **2002**, *13*, 167−183.
(195) Rizwan, M.; Yao, Y.; Gorbet, M. B.; Tse, J. W.; Anderson, D. E. J.; Hinds, M. T.; Yim, E. K. F. One-pot covalent grafting of gelatin on poly(vinyl alcohol) hydrogel to enhance endothelialization and hemocompatibility for synthetic vascular graft applications. *ACS Appl. Bio Mater.* **2020**, *3*, 693−703.
(196) Nichol, J. W.; Koshy, S. T.; Bae, H.; Hwang, C. M.; Yamanlar, S.; Khademhosseini, A. Cell-laden microengineered gelatin methacrylate hydrogels. *Biomaterials* **2010**, *31*, 5536−5544.
(197) Shin, S. R.; Bae, H.; Cha, J. M.; Mun, J. Y.; Chen, Y.-C.; Tekin, H.; Shin, H.; Farshchi, S.; Dokmeci, M. R.; Tang, S.; et al. Carbon nanotube reinforced hybrid microgels as scaffold materials for cell encapsulation. *ACS Nano* **2012**, *6*, 362−372.
(198) Paul, A.; Hasan, A.; Kindi, H. A.; Gaharwar, A. K.; Rao, V. T.; Nikkhah, M.; Shin, S. R.; Krafft, D.; Dokmeci, M. R.; Shum-Tim, D.; et al. Injectable graphene oxide/hydrogel-based angiogenic gene delivery system for vasculogenesis and cardiac repair. *ACS Nano* **2014**, *8*, 8050−8062.
(199) Bakhsheshi-Rad, H. R.; Hadisi, Z.; Hamzah, E.; Ismail, A. F.; Aziz, M.; Kashefian, M. Drug delivery and cytocompatibility of ciprofloxacin loaded gelatin nanofibers-coated Mg alloy. *Mater. Lett.* **2017**, *207*, 179−182.
(200) Nagarajan, S.; Belaid, H.; Pochat-Bohatier, C.; Teyssier, C.; Iatsunskyi, I.; Coy, E.; Balme, S.; Cornu, D.; Miele, P.; Kalkura, N. S.; et al. Design of boron nitride/gelatin electrospun nanofibers for bone tissue engineering. *ACS Appl. Mater. Interfaces* **2017**, *9*, 33695−33706.
(201) Choi, Y. S.; Hong, S. R.; Lee, Y. M.; Song, K. W.; Park, M. H.; Nam, Y. S. Study on gelatin-containing artificial skin: I. Preparation and characteristics of novel gelatin-alginate sponge. *Biomaterials* **1999**, *20*, 409−417.
(202) Yamamoto, M.; Tabata, Y.; Ikada, Y. Growth factor release from gelatin hydrogel for tissue engineering. *J. Bioact. Compat. Polym.* **1999**, *14*, 474−489.
(203) Sajkiewicz, P.; Kołbuk, D. Electrospinning of gelatin for tissue engineering-molecular conformation as one of the overlooked problems. *J. Biomater. Sci., Polym. Ed.* **2014**, *25*, 2009−2022.
(204) Panzavolta, S.; Gioffre, M.; Focarete, M. L.; Gualandi, C.; Foroni, L.; Bigi, A. Electrospun gelatin nanofibers: optimization of genipin cross-linking to preserve fiber morphology after exposure to water. *Acta Biomater.* **2011**, *7*, 1702−1709.
(205) Noori, A.; Ashrafi, S. J.; Vaez-Ghaemi, R.; Hatamian-Zaremi, A.; Webster, T. J. A review of fibrin and fibrin composites for bone tissue engineering. *Int. J. Nanomed.* **2017**, *12*, 4937−4961.
(206) Perka, C.; Spitzer, R. S.; Lindenhayn, K.; Sittinger, M.; Schultz, O. Matrix-mixed culture: New methodology for chondrocyte culture and preparation of cartilage transplants. *J. Biomed. Mater. Res.* **2000**, *49*, 305−311.
(207) Dare, E. V.; Griffith, M.; Poitras, P.; Kaupp, J. A.; Waldman, S. D.; Carlsson, D. J.; Dervin, G.; Mayoux, C.; Hincke, M. T. Genipin cross-linked fibrin hydrogels for in vitro human articular cartilage tissue-engineered regeneration. *Cells Tissues Organs* **2009**, *190*, 313−325.
(208) Lee, C. R.; Grad, S.; Gorna, K.; Gogolewski, S.; Goessl, A.; Alini, M. Fibrin-polyurethane composites for articular cartilage tissue engineering: a preliminary analysis. *Tissue Eng.* **2005**, *11*, 1562−1573.
(209) Van Lieshout, M.; Peters, G.; Rutten, M.; Baaijens, F. A knitted, fibrin-covered polycaprolactone scaffold for tissue engineering of the aortic valve. *Tissue Eng.* **2006**, *12*, 481−487.
(210) Weinand, C.; Gupta, R.; Huang, A. Y.; Weinberg, E.; Madisch, I.; Qudsi, R. A.; Neville, C. M.; Pomerantseva, I.; Vacanti, J. P. Comparison of hydrogels in the in vivo formation of tissue-engineered bone using mesenchymal stem cells and beta-tricalcium phosphate. *Tissue Eng.* **2007**, *13*, 757−765.
(211) Peled, E.; Boss, J.; Bejar, J.; Zinman, C.; Seliktar, D. A novel poly(ethylene glycol)-fibrinogen hydrogel for tibial segmental defect repair in a rat model. *J. Biomed. Mater. Res., Part A* **2007**, *80A*, 874−884.
(212) Spotnitz, W. D.; Prabhu, R. Fibrin sealant tissue adhesive–review and update. *J. Long-Term Eff. Med. Implants* **2005**, *15*, 245−270.
(213) Chrobak, M. O.; Hansen, K. J.; Gershlak, J. R.; Vratsanos, M.; Kanellias, M.; Gaudette, G. R.; Pins, G. D. Design of a fibrin microthread-based composite layer for use in a cardiac patch. *ACS Biomater. Sci. Eng.* **2017**, *3*, 1394−1403.
(214) Schense, J. C.; Hubbell, J. A. Cross-linking exogenous bifunctional peptides into fibrin gels with factor XIIIa. *Bioconjugate Chem.* **1999**, *10*, 75−81.
(215) Han, B.; Schwab, I. R.; Madsen, T. K.; Isseroff, R. R. A fibrin-based bioengineered ocular surface with human corneal epithelial stem cells. *Cornea* **2002**, *21*, 505−510.
(216) Meinhart, J.; Fussenegger, M.; Hobling, W. Stabilization of fibrin-chondrocyte constructs for cartilage reconstruction. *Ann. Plast. Surg.* **1999**, *42*, 673−678.
(217) Johnson, T. S.; Xu, J. W.; Zaporojan, V. V.; Mesa, J. M.; Weinand, C.; Randolph, M. A.; Bonassar, L. J.; Winograd, J. M.; Yaremchuk, M. J. Integrative repair of cartilage with articular and nonarticular chondrocytes. *Tissue Eng.* **2004**, *10*, 1308−1315.
(218) Ye, Q.; Zund, G.; Benedikt, P.; Jockenhoevel, S.; Hoerstrup, S. P.; Sakyama, S.; Hubbell, J. A.; Turina, M. Fibrin gel as a three dimensional matrix in cardiovascular tissue engineering. *Eur. J. Cardio-Thorac. Surg.* **2000**, *17*, 587−591.
(219) Currie, L. J.; Sharpe, J. R.; Martin, R. The use of fibrin glue in skin grafts and tissue-engineered skin replacements: A review. *Plast. Reconstr. Surg.* **2001**, *108*, 1713−1726.
(220) Ahmed, T. A.; Dare, E. V.; Hincke, M. Fibrin: a versatile scaffold for tissue engineering applications. *Tissue Eng., Part B* **2008**, *14*, 199−215.
(221) Marinho-Soriano, E. Agar polysaccharides from Gracilaria species (Rhodophyta, Gracilariaceae). *J. Biotechnol.* **2001**, *89*, 81−84.
(222) Lahaye, M.; Rochas, C. Chemical structure and physico-chemical properties of agar. *Hydrobiologia* **1991**, *221*, 137−148.
(223) Normand, V.; Lootens, D. L.; Amici, E.; Plucknett, K. P.; Aymard, P. New insight into agarose gel mechanical properties. *Biomacromolecules* **2000**, *1*, 730−738.
(224) Uludag, H.; De Vos, P.; Tresco, P. A. Technology of mammalian cell encapsulation. *Adv. Drug Delivery Rev.* **2000**, *42*, 29−64.
(225) Dillon, G. P.; Yu, X.; Sridharan, A.; Ranieri, J. P.; Bellamkonda, R. V. The influence of physical structure and charge on neurite extension in a 3D hydrogel scaffold. *J. Biomater. Sci., Polym. Ed.* **1998**, *9*, 1049−1069.
(226) Kumachev, A.; Greener, J.; Tumarkin, E.; Eiser, E.; Zandstra, P. W.; Kumacheva, E. High-throughput generation of hydrogel microbeads with varying elasticity for cell encapsulation. *Biomaterials* **2011**, *32*, 1477−1483.
(227) Clavé, A.; Potel, J. F.; Servien, E.; Neyret, P.; Dubrana, F.; Stindel, E. Third-generation autologous chondrocyte implantation versus mosaicplasty for knee cartilage injury: 2-year randomized trial. *J. Orthop. Res.* **2016**, *34*, 658−665.

https://doi.org/10.1021/acs.chemrev.0c01088
Chem. Rev. XXXX, XXX, XXX−XXX

(228) Luo, Y.; Shoichet, M. S. A photolabile hydrogel for guided three-dimensional cell growth and migration. *Nat. Mater.* **2004**, *3*, 249−253.
(229) Luan, N. M.; Iwata, H. Xenotransplantation of islets enclosed in agarose microcapsule carrying soluble complement receptor 1. *Biomaterials* **2012**, *33*, 8075−8081.
(230) Borkenhagen, M.; Clémence, J. F.; Sigrist, H.; Aebischer, P. Three-dimensional extracellular matrix engineering in the nervous system. *J. Biomed. Mater. Res.* **1998**, *40*, 392−400.
(231) Bhattarai, N.; Gunn, J.; Zhang, M. Chitosan-based hydrogels for controlled, localized drug delivery. *Adv. Drug Delivery Rev.* **2010**, *62*, 83−99.
(232) Croisier, F.; Jérôme, C. Chitosan-based biomaterials for tissue engineering. *Eur. Polym. J.* **2013**, *49*, 780−792.
(233) Sorlier, P.; Denuzière, A.; Viton, C.; Domard, A. Relation between the degree of acetylation and the electrostatic properties of chitin and chitosan. *Biomacromolecules* **2001**, *2*, 765−772.
(234) Foster, L. J. R.; Ho, S.; Hook, J.; Basuki, M.; Marcal, H. Chitosan as a biomaterial: influence of degree of deacetylation on its physiochemical, material and biological properties. *PLoS One* **2015**, *10*, No. e0135153.
(235) Berger, J.; Reist, M.; Mayer, J. M.; Felt, O.; Peppas, N. A.; Gurny, R. Structure and interactions in covalently and ionically crosslinked chitosan hydrogels for biomedical applications. *Eur. J. Pharm. Biopharm.* **2004**, *57*, 19−34.
(236) Boucard, N.; Viton, C.; Domard, A. New aspects of the formation of physical hydrogels of chitosan in a hydroalcoholic medium. *Biomacromolecules* **2005**, *6*, 3227−3237.
(237) Brack, H. P.; Tirmizi, S. A.; Risen, W. M. A spectroscopic and viscometric study of the metal ion-induced gelation of the biopolymer chitosan. *Polymer* **1997**, *38*, 2351−2362.
(238) Dambies, L.; Vincent, T.; Domard, A.; Guibal, E. Preparation of chitosan gel beads by ionotropic molybdate gelation. *Biomacromolecules* **2001**, *2*, 1198−1205.
(239) Shu, X. Z.; Zhu, K. J. Controlled drug release properties of ionically cross-linked chitosan beads: the influence of anion structure. *Int. J. Pharm.* **2002**, *233*, 217−225.
(240) Shen, E. C.; Wang, C.; Fu, E.; Chiang, C. Y.; Chen, T. T.; Nieh, S. Tetracycline release from tripolyphosphate-chitosan cross-linked sponge: a preliminary in vitro study. *J. Periodontal Res.* **2008**, *43*, 642−648.
(241) Boddohi, S.; Moore, N.; Johnson, P. A.; Kipper, M. J. Polysaccharide-based polyelectrolyte complex nanoparticles from chitosan, heparin, and hyaluronan. *Biomacromolecules* **2009**, *10*, 1402−1409.
(242) Denuziere, A.; Ferrier, D.; Damour, O.; Domard, A. Chitosan-chondroitin sulfate and chitosan-hyaluronate polyelectrolyte complexes: biological properties. *Biomaterials* **1998**, *19*, 1275−1285.
(243) Jiang, T.; Zhang, Z.; Zhou, Y.; Liu, Y.; Wang, Z.; Tong, H.; Shen, X.; Wang, Y. Surface functionalization of titanium with chitosan/gelatin via electrophoretic deposition: characterization and cell behavior. *Biomacromolecules* **2010**, *11*, 1254−1260.
(244) Mao, J. S.; Cui, Y. L.; Wang, X. H.; Sun, Y.; Yin, Y. J.; Zhao, H. M.; De Yao, K. A preliminary study on chitosan and gelatin polyelectrolyte complex cytocompatibility by cell cycle and apoptosis analysis. *Biomaterials* **2004**, *25*, 3973−3981.
(245) de Oliveira, H. C.; Fonseca, J. L.; Pereira, M. R. Chitosan-poly(acrylic acid) polyelectrolyte complex membranes: preparation, characterization and permeability studies. *J. Biomater. Sci., Polym. Ed.* **2008**, *19*, 143−160.
(246) Chenite, A.; Chaput, C.; Wang, D.; Combes, C.; Buschmann, M. D.; Hoemann, C. D.; Leroux, J. C.; Atkinson, B. L.; Binette, F.; Selmani, A. Novel injectable neutral solutions of chitosan form biodegradable gels in situ. *Biomaterials* **2000**, *21*, 2155−2161.
(247) Zhang, Y.; Guan, Y.; Zhou, S. Single component chitosan hydrogel microcapsule from a layer-by-layer approach. *Biomacromolecules* **2005**, *6*, 2365−2369.
(248) Milosavljevic, N. B.; Kljajevic, L. M.; Popovic, I. G.; Filipovic, J. M.; Krusic, M. T. K. Chitosan, itaconic acid and poly(vinyl alcohol) hybrid polymer networks of high degree of swelling and good mechanical strength. *Polym. Int.* **2010**, *59*, 686−694.
(249) Singh, A.; Narvi, S. S.; Dutta, P. K.; Pandey, N. D. External stimuli response on a novel chitosan hydrogel crosslinked with formaldehyde. *Bull. Mater. Sci.* **2006**, *29*, 233−238.
(250) Liu, R.; Xu, X.; Zhuang, X.; Cheng, B. Solution blowing of chitosan/PVA hydrogel nanofiber mats. *Carbohydr. Polym.* **2014**, *101*, 1116−1121.
(251) Mi, F. L.; Sung, H. W.; Shyu, S. S. Synthesis and characterization of a novel chitosan-based network prepared using naturally occurring crosslinker. *J. Polym. Sci., Part A: Polym. Chem.* **2000**, *38*, 2804−2814.
(252) Muzzarelli, R. A. A. Genipin-crosslinked chitosan hydrogels as biomedical and pharmaceutical aids. *Carbohydr. Polym.* **2009**, *77*, 1−9.
(253) Hoare, T. R.; Kohane, D. S. Hydrogels in drug delivery: Progress and challenges. *Polymer* **2008**, *49*, 1993−2007.
(254) Hennink, W. E.; van Nostrum, C. F. Novel crosslinking methods to design hydrogels. *Adv. Drug Delivery Rev.* **2012**, *64*, 223−236.
(255) Rickett, T. A.; Amoozgar, Z.; Tuchek, C. A.; Park, J.; Yeo, Y.; Shi, R. Rapidly photo-cross-linkable chitosan hydrogel for peripheral neurosurgeries. *Biomacromolecules* **2011**, *12*, 57−65.
(256) Cho, I. S.; Cho, M. O.; Li, Z.; Nurunnabi, M.; Park, S. Y.; Kang, S.-W.; Huh, K. M. Synthesis and characterization of a new photo-crosslinkable glycol chitosan thermogel for biomedical applications. *Carbohydr. Polym.* **2016**, *144*, 59−67.
(257) Obara, K.; Ishihara, M.; Ishizuka, T.; Fujita, M.; Ozeki, Y.; Maehara, T.; Saito, Y.; Yura, H.; Matsui, T.; Hattori, H.; et al. Photocrosslinkable chitosan hydrogel containing fibroblast growth factor-2 stimulates wound healing in healing-impaired db/db mice. *Biomaterials* **2003**, *24*, 3437−3444.
(258) Ahmadi, F.; Oveisi, Z.; Samani, S. M.; Amoozgar, Z. Chitosan based hydrogels: characteristics and pharmaceutical applications. *Res. Pharm. Sci.* **2015**, *10*, 1−16.
(259) Cui, Z. K.; Kim, S.; Baljon, J. J.; Wu, B. M.; Aghaloo, T.; Lee, M. Microporous methacrylated glycol chitosan-montmorillonite nanocomposite hydrogel for bone tissue engineering. *Nat. Commun.* **2019**, *10*, 3523.
(260) Kim, I. Y.; Seo, S. J.; Moon, H. S.; Yoo, M. K.; Park, I. Y.; Kim, B. C.; Cho, C. S. Chitosan and its derivatives for tissue engineering applications. *Biotechnol. Adv.* **2008**, *26*, 1−21.
(261) Li, J.; Xu, Z. Physical characterization of a chitosan-based hydrogel delivery system. *J. Pharm. Sci.* **2002**, *91*, 1669−1677.
(262) Muzzarelli, R. A.; Zucchini, C.; Ilari, P.; Pugnaloni, A.; Mattioli Belmonte, M.; Biagini, G.; Castaldini, C. Osteoconductive properties of methylpyrrolidinone chitosan in an animal model. *Biomaterials* **1993**, *14*, 925−929.
(263) Elcin, A. E.; Elcin, Y. M.; Pappas, G. D. Neural tissue engineering: Adrenal chromaffin cell attachment and viability on chitosan scaffolds. *Neurol. Res.* **1998**, *20*, 648−654.
(264) Lee, K. Y.; Ha, W. S.; Park, W. H. Blood compatibility and biodegradability of partially N-acylated chitosan derivatives. *Biomaterials* **1995**, *16*, 1211−1216.
(265) Klemm, D.; Heublein, B.; Fink, H. P.; Bohn, A. Cellulose: fascinating biopolymer and sustainable raw material. *Angew. Chem., Int. Ed.* **2005**, *44*, 3358−3393.
(266) Habibi, Y.; Lucia, L. A.; Rojas, O. J. Cellulose nanocrystals: chemistry, self-assembly, and applications. *Chem. Rev.* **2010**, *110*, 3479−3500.
(267) Moon, R. J.; Martini, A.; Nairn, J.; Simonsen, J.; Youngblood, J. Cellulose nanomaterials review: structure, properties and nanocomposites. *Chem. Soc. Rev.* **2011**, *40*, 3941−3994.
(268) Ross, P.; Mayer, R.; Benziman, M. Cellulose biosynthesis and function in bacteria. *Microbiol. Rev.* **1991**, *55*, 35−58.
(269) Czaja, W. K.; Young, D. J.; Kawecki, M.; Brown, R. M., Jr The future prospects of microbial cellulose in biomedical applications. *Biomacromolecules* **2007**, *8*, 1−12.
(270) Fink, H. P.; Weigel, P.; Purz, H. J.; Ganster, J. Structure formation of regenerated cellulose materials from NMMO-solutions. *Prog. Polym. Sci.* **2001**, *26*, 1473−1524.

https://doi.org/10.1021/acs.chemrev.0c01088
Chem. Rev. XXXX, XXX, XXX−XXX

(271) Zhao, H. B.; Kwak, J. H.; Wang, Y.; Franz, J. A.; White, J. M.; Holladay, J. E. Interactions between cellulose and N-methylmorpholine-N-oxide. *Carbohydr. Polym.* **2007**, *67*, 97−103.
(272) Zhang, H.; Wu, J.; Zhang, J.; He, J. S. 1-Allyl-3-methylimidazolium chloride room temperature ionic liquid: A new and powerful nonderivatizing solvent for cellulose. *Macromolecules* **2005**, *38*, 8272−8277.
(273) Zhu, S. D.; Wu, Y. X.; Chen, Q. M.; Yu, Z. N.; Wang, C. W.; Jin, S. W.; Ding, Y. G.; Wu, G. Dissolution of cellulose with ionic liquids and its application: a mini-review. *Green Chem.* **2006**, *8*, 325−327.
(274) Cai, J.; Zhang, L. Unique gelation behavior of cellulose in NaOH/urea aqueous solution. *Biomacromolecules* **2006**, *7*, 183−189.
(275) Liang, S. M.; Zhang, L. N.; Li, Y. F.; Xu, J. Fabrication and properties of cellulose hydrated membrane with unique structure. *Macromol. Chem. Phys.* **2007**, *208*, 594−602.
(276) Li, L.; Thangamathesvaran, P. M.; Yue, C. Y.; Tam, K. C.; Hu, X.; Lam, Y. C. Gel network structure of methylcellulose in water. *Langmuir* **2001**, *17*, 8062−8068.
(277) Xia, X. H.; Tang, S. J.; Lu, X. H.; Hu, Z. B. Formation and volume phase transition of hydroxypropyl cellulose microgels in salt solution. *Macromolecules* **2003**, *36*, 3695−3698.
(278) Weiss, P.; Gauthier, O.; Bouler, J. M.; Grimandi, G.; Daculsi, G. Injectable bone substitute using a hydrophilic polymer. *Bone* **1999**, *25*, 67s−70s.
(279) Silva, S. M.; Pinto, F. V.; Antunes, F. E.; Miguel, M. G.; Sousa, J. J.; Pais, A. A. Aggregation and gelation in hydroxypropylmethyl cellulose aqueous solutions. *J. Colloid Interface Sci.* **2008**, *327*, 333−340.
(280) Zheng, W. J.; Gao, J.; Wei, Z.; Zhou, J. X.; Chen, Y. M. Facile fabrication of self-healing carboxymethyl cellulose hydrogels. *Eur. Polym. J.* **2015**, *72*, 514−522.
(281) Kono, H.; Fujita, S. Biodegradable superabsorbent hydrogels derived from cellulose by esterification crosslinking with 1,2,3,4-butanetetracarboxylic dianhydride. *Carbohydr. Polym.* **2012**, *87*, 2582−2588.
(282) Yoshimura, T.; Matsuo, K.; Fujioka, R. Novel biodegradable superabsorbent hydrogels derived from cotton cellulose and succinic anhydride: Synthesis and characterization. *J. Appl. Polym. Sci.* **2006**, *99*, 3251−3256.
(283) Demitri, C.; Del Sole, R.; Scalera, F.; Sannino, A.; Vasapollo, G.; Maffezzoli, A.; Ambrosio, L.; Nicolais, L. Novel superabsorbent cellulose-based hydrogels crosslinked with citric acid. *J. Appl. Polym. Sci.* **2008**, *110*, 2453−2460.
(284) Zhou, J.; Chang, C.; Zhang, R.; Zhang, L. Hydrogels prepared from unsubstituted cellulose in NaOH/urea aqueous solution. *Macromol. Biosci.* **2007**, *7*, 804−809.
(285) Rodríguez, R. A.; Alvarez-Lorenzo, C.; Concheiro, A. Cationic cellulose hydrogels: kinetics of the cross-linking process and characterization as pH-/ion-sensitive drug delivery systems. *J. Controlled Release* **2003**, *86*, 253−265.
(286) Kabra, B. G.; Gehrke, S. H.; Spontak, R. J. Microporous, responsive hydroxypropyl cellulose gels. 1. Synthesis and microstructure. *Macromolecules* **1998**, *31*, 2166−2173.
(287) Fei, B.; Wach, R. A.; Mitomo, H.; Yoshii, F.; Kume, T. Hydrogel of biodegradable cellulose derivatives. I. Radiation-induced crosslinking of CMC. *J. Appl. Polym. Sci.* **2000**, *78*, 278−283.
(288) Liu, P. F.; Peng, J.; Li, J. Q.; Wu, J. L. Radiation crosslinking of CMC-Na at low dose and its application as substitute for hydrogel. *Radiat. Phys. Chem.* **2005**, *72*, 635−638.
(289) Long, D. D.; van Luyen, D. Chitosan-carboxymethylcellulose hydrogels as supports for cell immobilization. *J. Macromol. Sci., Part A: Pure Appl.Chem.* **1996**, *33*, 1875−1884.
(290) Hebeish, A.; Higazy, A.; El-Shafei, A.; Sharaf, S. Synthesis of carboxymethyl cellulose (CMC) and starch-based hybrids and their applications in flocculation and sizing. *Carbohydr. Polym.* **2010**, *79*, 60−69.
(291) Isiklan, N. Controlled release of insecticide carbaryl from sodium alginate, sodium alginate/gelatin, and sodium alginate/sodium carboxymethyl cellulose blend beads crosslinked with glutaraldehyde. *J. Appl. Polym. Sci.* **2006**, *99*, 1310−1319.
(292) Sannino, A.; Madaghiele, M.; Conversano, F.; Mele, G.; Maffezzoli, A.; Netti, P. A.; Ambrosio, L.; Nicolais, L. Cellulose derivative-hyaluronic acid-based microporous hydrogels cross-linked through divinyl sulfone (DVS) to modulate equilibrium sorption capacity and network stability. *Biomacromolecules* **2004**, *5*, 92−96.
(293) Liang, S.; Wu, J.; Tian, H.; Zhang, L.; Xu, J. High-strength cellulose/poly(ethylene glycol) gels. *ChemSusChem* **2008**, *1*, 558−563.
(294) Millon, L. E.; Wan, W. K. The polyvinyl alcohol-bacterial cellulose system as a new nanocomposite for biomedical applications. *J. Biomed. Mater. Res., Part B* **2006**, *79B*, 245−253.
(295) Williamson, S. L.; Armentrout, R. S.; Porter, R. S.; McCormick, C. L. Microstructural examination of semi-interpenetrating networks of poly(N,N-dimethylacrylamide) with cellulose or chitin synthesized in lithium chloride N,N-dimethylacetamide. *Macromolecules* **1998**, *31*, 8134−8141.
(296) Sannino, A.; Demitri, C.; Madaghiele, M. Biodegradable cellulose-based hydrogels: design and applications. *Materials* **2009**, *2*, 353−373.
(297) Klemm, D.; Schumann, D.; Udhardt, U.; Marsch, S. Bacterial synthesized cellulose — artificial blood vessels for microsurgery. *Prog. Polym. Sci.* **2001**, *26*, 1561−1603.
(298) Chang, C. Y.; Duan, B.; Cai, J.; Zhang, L. N. Superabsorbent hydrogels based on cellulose for smart swelling and controllable delivery. *Eur. Polym. J.* **2010**, *46*, 92−100.
(299) Vinatier, C.; Gauthier, O.; Fatimi, A.; Merceron, C.; Masson, M.; Moreau, A.; Moreau, F.; Fellah, B.; Weiss, P.; Guicheux, J. An injectable cellulose-based hydrogel for the transfer of autologous nasal chondrocytes in articular cartilage defects. *Biotechnol. Bioeng.* **2009**, *102*, 1259−1267.
(300) Ye, S. H.; Watanabe, J.; Iwasaki, Y.; Ishihara, K. Antifouling blood purification membrane composed of cellulose acetate and phospholipid polymer. *Biomaterials* **2003**, *24*, 4143−4152.
(301) Hosseini, H.; Kokabi, M.; Mousavi, S. M. Conductive bacterial cellulose/multiwall carbon nanotubes nanocomposite aerogel as a potentially flexible lightweight strain sensor. *Carbohydr. Polym.* **2018**, *201*, 228−235.
(302) Zhou, D.; Zhang, L.; Zhou, J.; Guo, S. Cellulose/chitin beads for adsorption of heavy metals in aqueous solution. *Water Res.* **2004**, *38*, 2643−2650.
(303) Elliott, J. E.; Macdonald, M.; Nie, J.; Bowman, C. N. Structure and swelling of poly(acrylic acid) hydrogels: effect of pH, ionic strength, and dilution on the crosslinked polymer structure. *Polymer* **2004**, *45*, 1503−1510.
(304) Zhao, L.; Huang, J.; Zhang, Y.; Wang, T.; Sun, W.; Tong, Z. Programmable and bidirectional bending of soft actuators based on janus structure with sticky tough paa-clay hydrogel. *ACS Appl. Mater. Interfaces* **2017**, *9*, 11866−11873.
(305) Zhong, M.; Liu, Y.-T.; Xie, X.-M. Self-healable, super tough graphene oxide-poly (acrylic acid) nanocomposite hydrogels facilitated by dual cross-linking effects through dynamic ionic interactions. *J. Mater. Chem. B* **2015**, *3*, 4001−4008.
(306) Zhao, L.; Huang, J. H.; Wang, T.; Sun, W. X.; Tong, Z. Multiple shape memory, self-healable, and supertough PAA-GO-Fe3+ hydrogel. *Macromol. Mater. Eng.* **2017**, *302*, 1600359.
(307) Gulyuz, U.; Okay, O. Self-healing poly(acrylic acid) hydrogels with shape memory behavior of high mechanical strength. *Macromolecules* **2014**, *47*, 6889−6899.
(308) Eichenbaum, G. M.; Kiser, P. F.; Dobrynin, A. V.; Simon, S. A.; Needham, D. Investigation of the swelling response and loading of ionic microgels with drugs and proteins: the dependence on cross-link density. *Macromolecules* **1999**, *32*, 4867−4878.
(309) Scott, R. A.; Peppas, N. A. Compositional effects on network structure of highly cross-linked copolymers of PEG-containing multiacrylates with-acrylic acid. *Macromolecules* **1999**, *32*, 6139−6148.
(310) Peppas, N. A.; Wright, S. L. Drug diffusion and binding in ionizable interpenetrating networks from poly(vinyl alcohol) and poly(acrylic acid). *Eur. J. Pharm. Biopharm.* **1998**, *46*, 15−29.

https://doi.org/10.1021/acs.chemrev.0c01088
Chem. Rev. XXXX, XXX, XXX−XXX

(311) Sefton, M.; May, M.; Lahooti, S.; Babensee, J. Making microencapsulation work: conformal coating, immobilization gels and in vivo performance. *J. Controlled Release* **2000**, *65*, 173−186.
(312) Meyvis, T. K. L.; De Smedt, S. C.; Demeester, J.; Hennink, W. E. Influence of the degradation mechanism of hydrogels on their elastic and swelling properties during degradation. *Macromolecules* **2000**, *33*, 4717−4725.
(313) Canal, T.; Peppas, N. A. Correlation between mesh size and equilibrium degree of swelling of polymeric networks. *J. Biomed. Mater. Res.* **1989**, *23*, 1183−1193.
(314) Kidane, A.; Szabocsik, J. M.; Park, K. Accelerated study on lysozyme deposition on poly(HEMA) contact lenses. *Biomaterials* **1998**, *19*, 2051−2055.
(315) Chirila, T. V. An overview of the development of artificial corneas with porous skirts and the use of PHEMA for such an application. *Biomaterials* **2001**, *22*, 3311−3317.
(316) Hassan, C. M.; Peppas, N. A. Structure and morphology of freeze/thawed PVA hydrogels. *Macromolecules* **2000**, *33*, 2472−2479.
(317) Nuttelman, C. R.; Mortisen, D. J.; Henry, S. M.; Anseth, K. S. Attachment of fibronectin to poly(vinyl alcohol) hydrogels promotes NIH3T3 cell adhesion, proliferation, and migration. *J. Biomed. Mater. Res.* **2001**, *57*, 217−223.
(318) Peppas, N. A.; Merrill, E. W. Development of semicrystalline poly(vinyl alcohol) hydrogels for biomedical applications. *J. Biomed. Mater. Res.* **1977**, *11*, 423−434.
(319) Stauffer, S. R.; Peppast, N. A. Poly(vinyl alcohol) hydrogels prepared by freezing-thawing cyclic processing. *Polymer* **1992**, *33*, 3932−3936.
(320) Peppas, N. A.; Stauffer, S. R. Reinforced uncrosslinked poly (vinyl alcohol) gels produced by cyclic freezing-thawing processes - a short review. *J. Controlled Release* **1991**, *16*, 305−310.
(321) Dai, W. S.; Barbari, T. A. Hydrogel membranes with mesh size asymmetry based on the gradient crosslinking of poly(vinyl alcohol). *J. Membr. Sci.* **1999**, *156*, 67−79.
(322) Bo, J. Study on PVA hydrogel crosslinked by epichlorohydrin. *J. Appl. Polym. Sci.* **1992**, *46*, 783−786.
(323) Yoshii, F.; Zhanshan, Y.; Isobe, K.; Shinozaki, K.; Makuuchi, K. Electron beam crosslinked PEO and PEO PVA hydrogels for wound dressing. *Radiat. Phys. Chem.* **1999**, *55*, 133−138.
(324) Kobayashi, H.; Ikacia, Y. Corneal cell adhesion and proliferation on hydrogel sheets bound with cell-adhesive proteins. *Curr. Eye Res.* **1991**, *10*, 899−908.
(325) Bryant, S. J.; Nuttelman, C. R.; Anseth, K. S. The effects of crosslinking density on cartilage formation in photocrosslinkable hydrogels. *Biomed. Sci. Instrum.* **1999**, *35*, 309−314.
(326) Shaheen, S. M.; Yamaura, K. Preparation of theophylline hydrogels of atactic poly(vinyl alcohol)/NaCl/H2O system for drug delivery system. *J. Controlled Release* **2002**, *81*, 367−377.
(327) Gu, Z. Q.; Xiao, J. M.; Zhang, X. H. The development of artificial articular cartilage-PVA-hydrogel. *Biomed. Mater. Eng.* **1998**, *8*, 75−81.
(328) Oka, M.; Ushio, K.; Kumar, P.; Ikeuchi, K.; Hyon, S. H.; Nakamura, T.; Fujita, H. Development of artificial articular cartilage. *Proc. Inst. Mech. Eng., Part H* **2000**, *214*, 59−68.
(329) Ostuni, E.; Chapman, R. G.; Holmlin, R. E.; Takayama, S.; Whitesides, G. M. A survey of structure- property relationships of surfaces that resist the adsorption of protein. *Langmuir* **2001**, *17*, 5605−5620.
(330) Elbert, D. L.; Hubbell, J. A. Conjugate addition reactions combined with free-radical cross-linking for the design of materials for tissue engineering. *Biomacromolecules* **2001**, *2*, 430−441.
(331) West, J. L.; Hubbell, J. A. Photopolymerized hydrogel materials for drug-delivery applications. *React. Polym.* **1995**, *25*, 139−147.
(332) Lopina, S. T.; Wu, G.; Merrill, E. W.; Griffith-Cima, L. Hepatocyte culture on carbohydrate-modified star polyethylene oxide hydrogels. *Biomaterials* **1996**, *17*, 559−569.
(333) Sakai, T.; Matsunaga, T.; Yamamoto, Y.; Ito, C.; Yoshida, R.; Suzuki, S.; Sasaki, N.; Shibayama, M.; Chung, U.-I. Design and fabrication of a high-strength hydrogel with ideally homogeneous network structure from tetrahedron-like macromonomers. *Macromolecules* **2008**, *41*, 5379−5384.
(334) Ananda, K.; Nacharaju, P.; Smith, P. K.; Acharya, S. A.; Manjula, B. N. Analysis of functionalization of methoxy-PEG as maleimide-PEG. *Anal. Biochem.* **2008**, *374*, 231−242.
(335) Malkoch, M.; Vestberg, R.; Gupta, N.; Mespouille, L.; Dubois, P.; Mason, A. F.; Hedrick, J. L.; Liao, Q.; Frank, C. W.; Kingsbury, K. Synthesis of well-defined hydrogel networks using Click chemistry. *Chem. Commun.* **2006**, 2774.
(336) Tan, H.; Xiao, C.; Sun, J.; Xiong, D.; Hu, X. Biological self-assembly of injectable hydrogel as cell scaffold via specific nucleobase pairing. *Chem. Commun.* **2012**, *48*, 10289−10291.
(337) Bastings, M. M.; Koudstaal, S.; Kieltyka, R. E.; Nakano, Y.; Pape, A. C.; Feyen, D. A.; van Slochteren, F. J.; Doevendans, P. A.; Sluijter, J. P.; Meijer, E. W.; et al. A fast pH-switchable and self-healing supramolecular hydrogel carrier for guided, local catheter injection in the infarcted myocardium. *Adv. Healthcare Mater.* **2014**, *3*, 70−78.
(338) Chen, X.; Dong, C.; Wei, K.; Yao, Y.; Feng, Q.; Zhang, K.; Han, F.; Mak, A. F.-T.; Li, B.; Bian, L. Supramolecular hydrogels cross-linked by preassembled host-guest PEG cross-linkers resist excessive, ultrafast, and non-resting cyclic compression. *NPG Asia Mater.* **2018**, *10*, 788−799.
(339) Dong, R. J.; Pang, Y.; Su, Y.; Zhu, X. Y. Supramolecular hydrogels: synthesis, properties and their biomedical applications. *Biomater. Sci.* **2015**, *3*, 937−954.
(340) Xue, K.; Liow, S. S.; Karim, A. A.; Li, Z.; Loh, X. J. A recent perspective on noncovalently formed polymeric hydrogels. *Chem. Rec.* **2018**, *18*, 1517−1529.
(341) Kim, H. A.; Lee, H. J.; Hong, J. H.; Moon, H. J.; Ko, D. Y.; Jeong, B. α,ω-Diphenylalanine-end-capping of PEG-PPG-PEG polymers changes the micelle morphology and enhances stability of the thermogel. *Biomacromolecules* **2017**, *18*, 2214−2219.
(342) Shi, K.; Wang, Y. L.; Qu, Y.; Liao, J. F.; Chu, B. Y.; Zhang, H. P.; Luo, F.; Qian, Z. Y. Synthesis, characterization, and application of reversible PDLLA-PEG-PDLLA copolymer thermogels in vitro and in vivo. *Sci. Rep.* **2016**, *6*, 19077.
(343) Sun, J.; Lei, Y.; Dai, Z.; Liu, X.; Huang, T.; Wu, J.; Xu, Z. P.; Sun, X. Sustained release of brimonidine from a new composite drug delivery system for treatment of glaucoma. *ACS Appl. Mater. Interfaces* **2017**, *9*, 7990−7999.
(344) Nagahama, K.; Oyama, N.; Ono, K.; Hotta, A.; Kawauchi, K.; Nishikata, T. Nanocomposite injectable gels capable of self-replenishing regenerative extracellular microenvironments for in vivo tissue engineering. *Biomater. Sci.* **2018**, *6*, 550−561.
(345) Cui, H. T.; Shao, J.; Wang, Y.; Zhang, P. B.; Chen, X. S.; Wei, Y. PLA-PEG-PLA and its electroactive tetraaniline copolymer as multi-interactive injectable hydrogels for tissue engineering. *Biomacromolecules* **2013**, *14*, 1904−1912.
(346) Gong, C.; Shi, S.; Dong, P.; Kan, B.; Gou, M.; Wang, X.; Li, X.; Luo, F.; Zhao, X.; Wei, Y.; et al. Synthesis and characterization of PEG-PCL-PEG thermosensitive hydrogel. *Int. J. Pharm.* **2009**, *365*, 89−99.
(347) Zhang, J.; Tokatlian, T.; Zhong, J.; Ng, Q. K.; Patterson, M.; Lowry, W. E.; Carmichael, S. T.; Segura, T. Physically associated synthetic hydrogels with long-term covalent stabilization for cell culture and stem cell transplantation. *Adv. Mater.* **2011**, *23*, 5098−5103.
(348) Zhao, X.; Harris, J. M. Novel degradable poly(ethylene glycol) hydrogels for controlled release of protein. *J. Pharm. Sci.* **1998**, *87*, 1450−1458.
(349) Burdick, J. A.; Anseth, K. S. Photoencapsulation of osteoblasts in injectable RGD-modified PEG hydrogels for bone tissue engineering. *Biomaterials* **2002**, *23*, 4315−4323.
(350) Mann, B. K.; Tsai, A. T.; Scott-Burden, T.; West, J. L. Modification of surfaces with cell adhesion peptides alters extracellular matrix deposition. *Biomaterials* **1999**, *20*, 2281−2286.
(351) Kraehenbuehl, T. P.; Zammaretti, P.; Van der Vlies, A. J.; Schoenmakers, R. G.; Lutolf, M. P.; Jaconi, M. E.; Hubbell, J. A. Three-dimensional extracellular matrix-directed cardioprogenitor differentiation: systematic modulation of a synthetic cell-responsive PEG-hydrogel. *Biomaterials* **2008**, *29*, 2757−2766.

https://doi.org/10.1021/acs.chemrev.0c01088
Chem. Rev. XXXX, XXX, XXX−XXX

(352) Salinas, C. N.; Anseth, K. S. Mixed mode thiol-acrylate photopolymerizations for the synthesis of PEG-peptide hydrogels. *Macromolecules* **2008**, *41*, 6019−6026.
(353) Metters, A.; Hubbell, J. Network formation and degradation behavior of hydrogels formed by Michael-type addition reactions. *Biomacromolecules* **2005**, *6*, 290−301.
(354) Hiemstra, C.; van der Aa, L. J.; Zhong, Z. Y.; Dijkstra, P. J.; Feijen, J. Novel in situ forming, degradable dextran hydrogels by Michael addition chemistry: Synthesis, rheology, and degradation. *Macromolecules* **2007**, *40*, 1165−1173.
(355) Lee, H. J.; Lee, J. S.; Chansakul, T.; Yu, C.; Elisseeff, J. H.; Yu, S. M. Collagen mimetic peptide-conjugated photopolymerizable PEG hydrogel. *Biomaterials* **2006**, *27*, 5268−5276.
(356) Stevens, M. M.; Qanadilo, H. F.; Langer, R.; Prasad Shastri, V. A rapid-curing alginate gel system: utility in periosteum-derived cartilage tissue engineering. *Biomaterials* **2004**, *25*, 887−894.
(357) García, A. J. PEG-maleimide hydrogels for protein and cell delivery in regenerative medicine. *Ann. Biomed. Eng.* **2014**, *42*, 312−322.
(358) Zhu, J. Bioactive modification of poly(ethylene glycol) hydrogels for tissue engineering. *Biomaterials* **2010**, *31*, 4639−4656.
(359) Schild, H. G. Poly(N-isopropylacrylamide): experiment, theory and application. *Prog. Polym. Sci.* **1992**, *17*, 163−249.
(360) Tanaka, F.; Koga, T.; Winnik, F. M. Temperature-responsive polymers in mixed solvents: competitive hydrogen bonds cause cononsolvency. *Phys. Rev. Lett.* **2008**, *101*, 028302.
(361) Wu, X. S.; Hoffman, A. S.; Yager, P. Synthesis and characterization of thermally reversible macroporous poly (N-isopropylacrylamide) hydrogels. *J. Polym. Sci., Part A: Polym. Chem.* **1992**, *30*, 2121−2129.
(362) Xia, L. W.; Xie, R.; Ju, X. J.; Wang, W.; Chen, Q.; Chu, L. Y. Nano-structured smart hydrogels with rapid response and high elasticity. *Nat. Commun.* **2013**, *4*, 2226.
(363) Kumar, A.; Srivastava, A.; Galaev, I. Y.; Mattiasson, B. Smart polymers: Physical forms and bioengineering applications. *Prog. Polym. Sci.* **2007**, *32*, 1205−1237.
(364) Serizawa, T.; Wakita, K.; Akashi, M. Rapid deswelling of porous poly(N-isopropylacrylamide) hydrogels prepared by incorporation of silica particles. *Macromolecules* **2002**, *35*, 10−12.
(365) Ishida, K.; Uno, T.; Itoh, T.; Kubo, M. Synthesis and property of temperature-responsive hydrogel with movable cross-linking points. *Macromolecules* **2012**, *45*, 6136−6142.
(366) Breger, J. C.; Yoon, C.; Xiao, R.; Kwag, H. R.; Wang, M. O.; Fisher, J. P.; Nguyen, T. D.; Gracias, D. H. Self-folding thermo-magnetically responsive soft microgrippers. *ACS Appl. Mater. Interfaces* **2015**, *7*, 3398−3405.
(367) Gutowska, A.; Jeong, B.; Jasionowski, M. Injectable gels for tissue engineering. *Anat. Rec.* **2001**, *263*, 342−349.
(368) Brun-Graeppi, A. K. A. S.; Richard, C.; Bessodes, M.; Scherman, D.; Merten, O. W. Thermoresponsive surfaces for cell culture and enzyme-free cell detachment. *Prog. Polym. Sci.* **2010**, *35*, 1311−1324.
(369) Kim, H.; Witt, H.; Oswald, T. A.; Tarantola, M. Adhesion of epithelial cells to pnipam treated surfaces for temperature-controlled cell-sheet harvesting. *ACS Appl. Mater. Interfaces* **2020**, *12*, 33516−33529.
(370) Tighe, B. J. A decade of silicone hydrogel development: surface properties, mechanical properties, and ocular compatibility. *Eye Contact Lens* **2013**, *39*, 4−12.
(371) Eddington, D. T.; Puccinelli, J. P.; Beebe, D. J. Thermal aging and reduced hydrophobic recovery of polydimethylsiloxane. *Sens. Actuators, B* **2006**, *114*, 170−172.
(372) Peak, C. W.; Wilker, J. J.; Schmidt, G. A review on tough and sticky hydrogels. *Colloid Polym. Sci.* **2013**, *291*, 2031−2047.
(373) van Beek, M.; Weeks, A.; Jones, L.; Sheardown, H. Immobilized hyaluronic acid containing model silicone hydrogels reduce protein adsorption. *J. Biomater. Sci., Polym. Ed.* **2008**, *19*, 1425−1436.
(374) Tang, Q.; Yu, J. R.; Chen, L.; Zhu, J.; Hu, Z. M. Poly (dimethyl siloxane)/poly (2-hydroxyethyl methacrylate) interpenetrating polymer network beads as potential capsules for biomedical use. *Curr. Appl. Phys.* **2011**, *11*, 945−950.
(375) Sugimoto, H.; Nishino, G.; Tsuzuki, N.; Daimatsu, K.; Inomata, K.; Nakanishi, E. Preparation of high oxygen permeable transparent hybrid copolymers with silicone macro-monomers. *Colloid Polym. Sci.* **2012**, *290*, 173−181.
(376) Zhang, X. Q.; Wang, L.; Tao, H. W.; Sun, Y.; Yang, H.; Lin, B. P. The influences of poly (ethylene glycol) chain length on hydrophilicity, oxygen permeability, and mechanical properties of multicomponent silicone hydrogels. *Colloid Polym. Sci.* **2019**, *297*, 1233−1243.
(377) Lin, G.; Zhang, X. J. A.; Kumar, S. R.; Mark, J. E. Modification of polysiloxane networks for biocompatibility. *Mol. Cryst. Liq. Cryst.* **2010**, *521*, 56−71.
(378) Yao, M. J.; Fang, J. Hydrophilic PEO-PDMS for microfluidic applications. *J. Micromech. Microeng.* **2012**, *22*, 025012.
(379) Demming, S.; Lesche, C.; Schmolke, H.; Klages, C.-P.; Büttgenbach, S. Characterization of long-term stability of hydrophilized PEG-grafted PDMS within different media for biotechnological and pharmaceutical applications. *Phys. Status Solidi A* **2011**, *208*, 1301−1307.
(380) Nicolson, P. C.; Vogt, J. Soft contact lens polymers: an evolution. *Biomaterials* **2001**, *22*, 3273−3283.
(381) Morales-Hurtado, M.; Zeng, X.; Gonzalez-Rodriguez, P.; Ten Elshof, J. E.; van der Heide, E. A new water absorbable mechanical Epidermal skin equivalent: The combination of hydrophobic PDMS and hydrophilic PVA hydrogel. *J. Mech. Behav. Biomed. Mater.* **2015**, *46*, 305−317.
(382) Hamid, Z. A. A.; Lim, K. W. Evaluation of UV-crosslinked poly(ethylene glycol) diacrylate/poly(dimethylsiloxane) dimethacrylate hydrogel: properties for tissue engineering application. *Procedia Chem.* **2016**, *19*, 410−418.
(383) Xu, J.; Li, X.; Sun, F. In vitro and in vivo evaluation of ketotifen fumarate-loaded silicone hydrogel contact lenses for ocular drug delivery. *Drug Delivery* **2011**, *18*, 150−158.
(384) Wang, J. J.; Liu, F.; Wei, J. Hydrophilic silicone hydrogels with interpenetrating network structure for extended delivery of ophthalmic drugs. *Polym. Adv. Technol.* **2012**, *23*, 1258−1263.
(385) Grandbois, M.; Beyer, M.; Rief, M.; Clausen-Schaumann, H.; Gaub, H. E. How strong is a covalent bond? *Science* **1999**, *283*, 1727.
(386) Beyer, M. K. The mechanical strength of a covalent bond calculated by density functional theory. *J. Chem. Phys.* **2000**, *112*, 7307−7312.
(387) Luo, Y.-R. *Comprehensive handbook of chemical bond energies*; CRC Press: Boca Raton, 2007.
(388) Steiner, T. The hydrogen bond in the solid state. *Angew. Chem., Int. Ed.* **2002**, *41*, 49−76.
(389) Markovitch, O.; Agmon, N. Structure and energetics of the hydronium hydration shells. *J. Phys. Chem. A* **2007**, *111*, 2253−2256.
(390) Varshey, D. B.; Sander, J. R. G.; Friščić, T.; MacGillivray, L. R. Supramolecular Interactions. In *Supramolecular Chemistry: From Molecules to Nanomaterials*; Wiley: New York, 2012; pp 1−16.
(391) Zhuang, W. R.; Wang, Y.; Cui, P. F.; Xing, L.; Lee, J.; Kim, D.; Jiang, H. L.; Oh, Y. K. Applications of pi-pi stacking interactions in the design of drug-delivery systems. *J. Controlled Release* **2019**, *294*, 311−326.
(392) Blanco, F.; Alkorta, I.; Elguero, J. Barriers about double carbon-nitrogen bond in imine derivatives (aldimines, oximes, hydrazones, azines). *Croat. Chem. Acta.* **2009**, *82*, 173−183.
(393) Li, H. F.; Li, H. Y.; Dai, Q. Q.; Li, H.; Bredas, J. L. Hydrolytic stability of boronate ester-linked covalent organic frameworks. *Adv. Theory Simul.* **2018**, *1*, 1700015.
(394) Dopieralski, P.; Ribas-Arino, J.; Anjukandi, P.; Krupicka, M.; Marx, D. Unexpected mechanochemical complexity in the mechanistic scenarios of disulfide bond reduction in alkaline solution. *Nat. Chem.* **2017**, *9*, 164−170.
(395) Basilevskii, M. V.; Shamov, A. G.; Tikhomirov, V. A. Transition state of the Diels-Alder reaction. *J. Am. Chem. Soc.* **1977**, *99*, 1369−1372.

https://doi.org/10.1021/acs.chemrev.0c01088
Chem. Rev. XXXX, XXX, XXX−XXX

(396) Liu, S.; Lei, Y.; Qi, X.; Lan, Y. Reactivity for the Diels-Alder reaction of cumulenes: a distortion-interaction analysis along the reaction pathway. *J. Phys. Chem. A* **2014**, *118*, 2638−2645.
(397) Ullah, F.; Othman, M. B. H.; Javed, F.; Ahmad, Z.; Akil, H. M. Classification, processing and application of hydrogels: A review. *Mater. Sci. Eng., C* **2015**, *57*, 414−433.
(398) Wang, W.; Narain, R.; Zeng, H. Rational design of self-healing tough hydrogels: a mini review. *Front. Chem.* **2018**, *6*, 497.
(399) Wong, R. S.; Ashton, M.; Dodou, K. Effect of crosslinking agent concentration on the properties of unmedicated hydrogels. *Pharmaceutics* **2015**, *7*, 305−319.
(400) Malo de Molina, P.; Lad, S.; Helgeson, M. E. Heterogeneity and its influence on the properties of difunctional poly(ethylene glycol) hydrogels: structure and mechanics. *Macromolecules* **2015**, *48*, 5402−5411.
(401) Sawhney, A. S.; Pathak, C. P.; Hubbell, J. A. Bioerodible hydrogels based on photopolymerized poly(ethylene glycol)-co-poly(alpha-hydroxy acid) diacrylate macromers. *Macromolecules* **1993**, *26*, 581−587.
(402) Martens, P.; Anseth, K. S. Characterization of hydrogels formed from acrylate modified poly(vinyl alcohol) macromers. *Polymer* **2000**, *41*, 7715−7722.
(403) Hubbell, J. A. Hydrogel systems for barriers and local drug delivery in the control of wound healing. *J. Controlled Release* **1996**, *39*, 305−313.
(404) van Dijk-Wolthuis, W. N. E.; Franssen, O.; Talsma, H.; van Steenbergen, M. J.; Kettenes-van den Bosch, J. J.; Hennink, W. E. Synthesis, characterization, and polymerization of glycidyl methacrylate derivatized dextran. *Macromolecules* **1995**, *28*, 6317−6322.
(405) Giammona, G.; Pitarresi, G.; Cavallaro, G.; Spadaro, G. New biodegradable hydrogels based on an acryloylated polyaspartamide cross-linked by gamma irradiation. *J. Biomater. Sci., Polym. Ed.* **1999**, *10*, 969−987.
(406) Caliceti, P.; Salmaso, S.; Lante, A.; Yoshida, M.; Katakai, R.; Martellini, F.; Mei, L. H.; Carenza, M. Controlled release of biomolecules from temperature-sensitive hydrogels prepared by radiation polymerization. *J. Controlled Release* **2001**, *75*, 173−181.
(407) Charlesby, A. Cross-linking of polythene by pile radiation. *Proc. R. Soc. London A* **1952**, *215*, 187−214.
(408) Peppas, N. A.; Mikos, A. G. Preparation methods and structure of hydrogels. In *Hydrogels in medicine and pharmacy*; CRC Press: Boca Raton, 2019; pp 1−26.
(409) Reddy, N.; Reddy, R.; Jiang, Q. Crosslinking biopolymers for biomedical applications. *Trends Biotechnol.* **2015**, *33*, 362−369.
(410) Eiselt, P.; Lee, K. Y.; Mooney, D. J. Rigidity of two-component hydrogels prepared from alginate and poly(ethylene glycol)-diamines. *Macromolecules* **1999**, *32*, 5561−5566.
(411) Moon, S.-Y.; Jeon, E.; Bae, J.-S.; Byeon, M.; Park, J.-W. Polyurea networks via organic sol-gel crosslinking polymerization of tetrafunctional amines and diisocyanates and their selective adsorption and filtration of carbon dioxide. *Polym. Chem.* **2014**, *5*, 1124−1131.
(412) Meldal, M.; Tornoe, C. W. Cu-catalyzed azide-alkyne cycloaddition. *Chem. Rev.* **2008**, *108*, 2952−3015.
(413) Agard, N. J.; Prescher, J. A.; Bertozzi, C. R. A strain-promoted [3 + 2] azide-alkyne cycloaddition for covalent modification of biomolecules in living systems. *J. Am. Chem. Soc.* **2004**, *126*, 15046−15047.
(414) Kamath, K. R.; Park, K. Biodegradable hydrogels in drug-delivery. *Adv. Drug Delivery Rev.* **1993**, *11*, 59−84.
(415) Yu, Q. A.; Song, Y. N.; Shi, X. M.; Xu, C. Y.; Bin, Y. Z. Preparation and properties of chitosan derivative/poly(vinyl alcohol) blend film crosslinked with glutaraldehyde. *Carbohydr. Polym.* **2011**, *84*, 465−470.
(416) Crescenzi, V.; Francescangeli, A.; Taglienti, A.; Capitani, D.; Mannina, L. Synthesis and partial characterization of hydrogels obtained via glutaraldehyde crosslinking of acetylated chitosan and of hyaluronan derivatives. *Biomacromolecules* **2003**, *4*, 1045−1054.
(417) Gehrke, S. H.; Uhden, L. H.; McBride, J. F. Enhanced loading and activity retention of bioactive proteins in hydrogel delivery systems. *J. Controlled Release* **1998**, *55*, 21−33.
(418) Coviello, T.; Grassi, M.; Rambone, G.; Santucci, E.; Carafa, M.; Murtas, E.; Riccieri, F. M.; Alhaique, F. Novel hydrogel system from scleroglucan: synthesis and characterization. *J. Controlled Release* **1999**, *60*, 367−378.
(419) Tronci, G.; Neffe, A. T.; Pierce, B. F.; Lendlein, A. An entropy-elastic gelatin-based hydrogel system. *J. Mater. Chem.* **2010**, *20*, 8875−8884.
(420) Rydholm, A. E.; Bowman, C. N.; Anseth, K. S. Degradable thiol-acrylate photopolymers: polymerization and degradation behavior of an in situ forming biomaterial. *Biomaterials* **2005**, *26*, 4495−4506.
(421) DeForest, C. A.; Polizzotti, B. D.; Anseth, K. S. Sequential click reactions for synthesizing and patterning three-dimensional cell microenvironments. *Nat. Mater.* **2009**, *8*, 659−664.
(422) Patai, S. *The chemistry of the thiol group*; Wiley: New York, 1974.
(423) Hoyle, C. E.; Lowe, A. B.; Bowman, C. N. Thiol-click chemistry: a multifaceted toolbox for small molecule and polymer synthesis. *Chem. Soc. Rev.* **2010**, *39*, 1355−1387.
(424) Gress, A.; Volkel, A.; Schlaad, H. Thio-click modification of poly [2-(3-butenyl)-2-oxazoline]. *Macromolecules* **2007**, *40*, 7928−7933.
(425) Dondoni, A. The emergence of thiol-ene coupling as a click process for materials and bioorganic chemistry. *Angew. Chem., Int. Ed.* **2008**, *47*, 8995−8997.
(426) Grazu, V.; Abian, O.; Mateo, C.; Batista-Viera, F.; Fernandez-Lafuente, R.; Guisan, J. M. Novel bifunctional epoxy/thiol-reactive support to immobilize thiol containing proteins by the epoxy chemistry. *Biomacromolecules* **2003**, *4*, 1495−1501.
(427) Dyer, E.; Glenn, J. F. The kinetics of the reactions of phenyl isocyanate with certain thiols. *J. Am. Chem. Soc.* **1957**, *79*, 366−369.
(428) Becer, C. R.; Babiuch, K.; Pilz, D.; Hornig, S.; Heinze, T.; Gottschaldt, M.; Schubert, U. S. Clicking pentafluorostyrene copolymers: synthesis, nanoprecipitation, and glycosylation. *Macromolecules* **2009**, *42*, 2387−2394.
(429) Hurd, C. D.; Gershbein, L. L. Reactions of mercaptans with acrylic and methacrylic derivatives. *J. Am. Chem. Soc.* **1947**, *69*, 2328−2335.
(430) Chen, X.; Li, R.; Wong, S. H. D.; Wei, K.; Cui, M.; Chen, H.; Jiang, Y.; Yang, B.; Zhao, P.; Xu, J.; et al. Conformational manipulation of scale-up prepared single-chain polymeric nanogels for multiscale regulation of cells. *Nat. Commun.* **2019**, *10*, 2705.
(431) Nair, D. P.; Podgorski, M.; Chatani, S.; Gong, T.; Xi, W. X.; Fenoli, C. R.; Bowman, C. N. The thiol-Michael addition click reaction: a powerful and widely used tool in materials chemistry. *Chem. Mater.* **2014**, *26*, 724−744.
(432) Tao, H.; Zhang, X.; Sun, Y.; Yang, H.; Lin, B. The influence of molecular weight of siloxane macromere on phase separation morphology, oxygen permeability, and mechanical properties in multicomponent silicone hydrogels. *Colloid Polym. Sci.* **2017**, *295*, 205−213.
(433) Weinhold, F.; West, R. The nature of the silicon-oxygen bond. *Organometallics* **2011**, *30*, 5815−5824.
(434) Si, L.; Zheng, X.; Nie, J.; Yin, R.; Hua, Y.; Zhu, X. Silicone-based tough hydrogels with high resilience, fast self-recovery, and self-healing properties. *Chem. Commun.* **2016**, *52*, 8365−8368.
(435) Ahagon, A.; Gent, A. Effect of interfacial bonding on the strength of adhesion. *J. Polym. Sci., Part B* **1975**, *13*, 1285−1300.
(436) Hong, W.; Zhao, X.; Zhou, J.; Suo, Z. A theory of coupled diffusion and large deformation in polymeric gels. *J. Mech. Phys. Solids* **2008**, *56*, 1779−1793.
(437) Hong, W.; Zhao, X.; Suo, Z. Large deformation and electrochemistry of polyelectrolyte gels. *J. Mech. Phys. Solids* **2010**, *58*, 558−577.
(438) Roland, C. Unconventional rubber networks: Circumventing the compromise between stiffness and strength. *Rubber Chem. Technol.* **2013**, *86*, 351−366.

https://doi.org/10.1021/acs.chemrev.0c01088
Chem. Rev. XXXX, XXX, XXX−XXX

(439) Richtering, W.; Saunders, B. R. Gel architectures and their complexity. *Soft Matter* **2014**, *10*, 3695−3702.
(440) Wang, H.; Heilshorn, S. C. Adaptable hydrogel networks with reversible linkages for tissue engineering. *Adv. Mater.* **2015**, *27*, 3717−3736.
(441) Petka, W. A.; Harden, J. L.; McGrath, K. P.; Wirtz, D.; Tirrell, D. A. Reversible hydrogels from self-assembling artificial proteins. *Science* **1998**, *281*, 389−392.
(442) Rosales, A. M.; Anseth, K. S. The design of reversible hydrogels to capture extracellular matrix dynamics. *Nat. Rev. Mater.* **2016**, *1*, 1−15.
(443) Mark, J. E. Elastomeric networks with bimodal chain-length distributions. *Acc. Chem. Res.* **1994**, *27*, 271−278.
(444) Kloxin, A. M.; Kasko, A. M.; Salinas, C. N.; Anseth, K. S. Photodegradable hydrogels for dynamic tuning of physical and chemical properties. *Science* **2009**, *324*, 59−63.
(445) Creton, C. 50th anniversary perspective: Networks and gels: Soft but dynamic and tough. *Macromolecules* **2017**, *50*, 8297−8316.
(446) Liu, Y.; He, W.; Zhang, Z.; Lee, B. P. Recent developments in tough hydrogels for biomedical applications. *Gels* **2018**, *4*, 46.
(447) Sakai, T. Definition of polymer gels and rubber elasticity. In *Physics of Polymer Gels*; Wiley: New York, 2020; pp 45−75.
(448) Sakai, T. Swelling and deswelling. In *Physics of Polymer Gels*; Wiley: New York, 2020; pp 77−107.
(449) Sakai, T. Deformation and fracture. In *Physics of Polymer Gels*; Wiley: New York, 2020; pp 109−136.
(450) Parada, G. A.; Zhao, X. Ideal reversible polymer networks. *Soft Matter* **2018**, *14*, 5186−5196.
(451) Akagi, Y.; Matsunaga, T.; Shibayama, M.; Chung, U.-I.; Sakai, T. Evaluation of topological defects in tetra-PEG gels. *Macromolecules* **2010**, *43*, 488−493.
(452) Yigit, S.; Sanyal, R.; Sanyal, A. Fabrication and functionalization of hydrogels through "click" chemistry. *Chem. - Asian J.* **2011**, *6*, 2648−2659.
(453) Huang, X.; Nakagawa, S.; Li, X.; Shibayama, M.; Yoshie, N. A simple and versatile method for the construction of nearly ideal polymer networks. *Angew. Chem., Int. Ed.* **2020**, *59*, 9646−9652.
(454) Marco-Dufort, B.; Iten, R.; Tibbitt, M. W. Linking molecular behavior to macroscopic properties in ideal dynamic covalent networks. *J. Am. Chem. Soc.* **2020**, *142*, 15371−15385.
(455) Matsunaga, T.; Sakai, T.; Akagi, Y.; Chung, U. I.; Shibayama, M. SANS and SLS studies on tetra-arm PEG gels in as-prepared and swollen states. *Macromolecules* **2009**, *42*, 6245−6252.
(456) Hild, G. Model networks based on 'endlinking' processes: synthesis, structure and properties. *Prog. Polym. Sci.* **1998**, *23*, 1019−1149.
(457) Zhong, M.; Wang, R.; Kawamoto, K.; Olsen, B. D.; Johnson, J. A. Quantifying the impact of molecular defects on polymer network elasticity. *Science* **2016**, *353*, 1264−1268.
(458) Okaya, Y.; Jochi, Y.; Seki, T.; Satoh, K.; Kamigaito, M.; Hoshino, T.; Nakatani, T.; Fujinami, S.; Takata, M.; Takeoka, Y. Precise synthesis of a homogeneous thermoresponsive polymer network composed of four-branched star polymers with a narrow molecular weight distribution. *Macromolecules* **2020**, *53*, 374−386.
(459) Apostolides, D. E.; Patrickios, C. S.; Sakai, T.; Guerre, M.; Lopez, G.; Ameduri, B.; Ladmiral, V.; Simon, M.; Gradzielski, M.; Clemens, D.; et al. Near-model amphiphilic polymer conetworks based on four-arm stars of poly(vinylidene fluoride) and poly(ethylene glycol): synthesis and characterization. *Macromolecules* **2018**, *51*, 2476−2488.
(460) Oshima, K.; Fujimoto, T.; Minami, E.; Mitsukami, Y. Model polyelectrolyte gels synthesized by end-linking of tetra-arm polymers with click chemistry: synthesis and mechanical properties. *Macromolecules* **2014**, *47*, 7573−7580.
(461) Yesilyurt, V.; Webber, M. J.; Appel, E. A.; Godwin, C.; Langer, R.; Anderson, D. G. Injectable self-healing glucose-responsive hydrogels with ph-regulated mechanical properties. *Adv. Mater.* **2016**, *28*, 86−91.
(462) Shibayama, M.; Li, X.; Sakai, T. Precision polymer network science with tetra-PEG gels—a decade history and future. *Colloid Polym. Sci.* **2019**, *297*, 1−12.
(463) Hashimoto, K.; Fujii, K.; Nishi, K.; Sakai, T.; Shibayama, M. Nearly ideal polymer network ion gel prepared in pH-buffering ionic liquid. *Macromolecules* **2016**, *49*, 344−352.
(464) Apostolides, D. E.; Sakai, T.; Patrickios, C. S. Dynamic covalent star poly(ethylene glycol) model hydrogels: a new platform for mechanically robust, multifunctional materials. *Macromolecules* **2017**, *50*, 2155−2164.
(465) Hayashi, K.; Okamoto, F.; Hoshi, S.; Katashima, T.; Zujur, D. C.; Li, X.; Shibayama, M.; Gilbert, E. P.; Chung, U.; Ohba, S.; et al. Fast-forming hydrogel with ultralow polymeric content as an artificial vitreous body. *Nat. Biomed Eng.* **2017**, *1*, 0044.
(466) Okumura, Y.; Ito, K. The polyrotaxane gel: A topological gel by figure-of-eight cross-links. *Adv. Mater.* **2001**, *13*, 485−487.
(467) Wenz, G.; Han, B. H.; Muller, A. Cyclodextrin rotaxanes and polyrotaxanes. *Chem. Rev.* **2006**, *106*, 782−817.
(468) Bin Imran, A.; Esaki, K.; Gotoh, H.; Seki, T.; Ito, K.; Sakai, Y.; Takeoka, Y. Extremely stretchable thermosensitive hydrogels by introducing slide-ring polyrotaxane cross-linkers and ionic groups into the polymer network. *Nat. Commun.* **2014**, *5*, 5124.
(469) Loethen, S.; Kim, J.-M.; Thompson, D. H. Biomedical applications of cyclodextrin based polyrotaxanes. *Polym. Rev.* **2007**, *47*, 383−418.
(470) Mayumi, K.; Ito, K. Structure and dynamics of polyrotaxane and slide-ring materials. *Polymer* **2010**, *51*, 959−967.
(471) Huang, F. H.; Gibson, H. W. Polypseudorotaxanes and polyrotaxanes. *Prog. Polym. Sci.* **2005**, *30*, 982−1018.
(472) Liu, G.; Yuan, Q.; Hollett, G.; Zhao, W.; Kang, Y.; Wu, J. Cyclodextrin-based host-guest supramolecular hydrogel and its application in biomedical fields. *Polym. Chem.* **2018**, *9*, 3436−3449.
(473) Harada, A.; Kamachi, M. Complex formation between poly (ethylene glycol) and α-cyclodextrin. *Macromolecules* **1990**, *23*, 2821−2823.
(474) Harada, A.; Li, J.; Kamachi, M. The molecular necklace: a rotaxane containing many threaded α-cyclodextrins. *Nature* **1992**, *356*, 325−327.
(475) Xie, D.; Yang, K.; Sun, W. Formation and characterization of polylactide and β-cyclodextrin inclusion complex. *Curr. Appl. Phys.* **2007**, *7*, e15−e18.
(476) Harada, A.; Takashima, Y.; Yamaguchi, H. Cyclodextrin-based supramolecular polymers. *Chem. Soc. Rev.* **2009**, *38*, 875−882.
(477) Gao, P.; Wang, J.; Ye, L.; Zhang, A. Y.; Feng, Z. G. Stable and unconventional conformation of single PEG bent γ-CD-based polypseudorotaxanes. *Macromol. Chem. Phys.* **2011**, *212*, 2319−2327.
(478) Granick, S.; Rubinstein, M. Polymers: a multitude of macromolecules. *Nat. Mater.* **2004**, *3*, 586−587.
(479) Oku, T.; Furusho, Y.; Takata, T. A concept for recyclable cross-linked polymers: topologically networked polyrotaxane capable of undergoing reversible assembly and disassembly. *Angew. Chem., Int. Ed.* **2004**, *43*, 966−969.
(480) Ooya, T.; Eguchi, M.; Yui, N. Enhanced accessibility of peptide substrate toward membrane-bound metalloexopeptidase by supramolecular structure of polyrotaxane. *Biomacromolecules* **2001**, *2*, 200−203.
(481) Li, J.; Suo, Z.; Vlassak, J. J. Stiff, strong, and tough hydrogels with good chemical stability. *J. Mater. Chem. B* **2014**, *2*, 6708−6713.
(482) Nonoyama, T.; Gong, J. P. Double-network hydrogel and its potential biomedical application: A review. *Proc. Inst. Mech. Eng., Part H* **2015**, *229*, 853−863.
(483) Costa, A. M. S.; Mano, J. F. Extremely strong and tough hydrogels as prospective candidates for tissue repair - A review. *Eur. Polym. J.* **2015**, *72*, 344−364.
(484) Dragan, E. S. Design and applications of interpenetrating polymer network hydrogels. A review. *Chem. Eng. J.* **2014**, *243*, 572−590.
(485) Sperling, L. H. *Interpenetrating polymer networks and related materials*; Springer: New York, 2012.

https://doi.org/10.1021/acs.chemrev.0c01088
Chem. Rev. XXXX, XXX, XXX−XXX

(486) Myung, D.; Waters, D.; Wiseman, M.; Duhamel, P. E.; Noolandi, J.; Ta, C. N.; Frank, C. W. Progress in the development of interpenetrating polymer network hydrogels. *Polym. Adv. Technol.* **2008**, *19*, 647−657.
(487) Sperling, L. H. Interpenetrating polymer networks: an overview. In *Interpenetrating Polymer Networks*; American Chemical Society: Washington, DC, 1994; pp 3−38.
(488) Visscher, K. B.; Manners, I.; Allcock, H. R. Synthesis and properties of polyphosphazene interpenetrating polymer networks. *Macromolecules* **1990**, *23*, 4885−4886.
(489) Wang, J. J.; Liu, F. Enhanced adsorption of heavy metal ions onto simultaneous interpenetrating polymer network hydrogels synthesized by UV irradiation. *Polym. Bull.* **2013**, *70*, 1415−1430.
(490) Sun, J. Y.; Zhao, X.; Illeperuma, W. R.; Chaudhuri, O.; Oh, K. H.; Mooney, D. J.; Vlassak, J. J.; Suo, Z. Highly stretchable and tough hydrogels. *Nature* **2012**, *489*, 133−136.
(491) Haque, M. A.; Kurokawa, T.; Gong, J. P. Super tough double network hydrogels and their application as biomaterials. *Polymer* **2012**, *53*, 1805−1822.
(492) Hong, S.; Sycks, D.; Chan, H. F.; Lin, S.; Lopez, G. P.; Guilak, F.; Leong, K. W.; Zhao, X. 3D printing of highly stretchable and tough hydrogels into complex, cellularized structures. *Adv. Mater.* **2015**, *27*, 4035−4040.
(493) Seiffert, S. *Supramolecular polymer networks and gels*; Springer: Berlin, 2015.
(494) Tong, X. M.; Yang, F. Engineering interpenetrating network hydrogels as biomimetic cell niche with independently tunable biochemical and mechanical properties. *Biomaterials* **2014**, *35*, 1807−1815.
(495) Feig, V. R.; Tran, H.; Lee, M.; Bao, Z. Mechanically tunable conductive interpenetrating network hydrogels that mimic the elastic moduli of biological tissue. *Nat. Commun.* **2018**, *9*, 1−9.
(496) Darnell, M. C.; Sun, J. Y.; Mehta, M.; Johnson, C.; Arany, P. R.; Suo, Z.; Mooney, D. J. Performance and biocompatibility of extremely tough alginate/polyacrylamide hydrogels. *Biomaterials* **2013**, *34*, 8042−8048.
(497) Kumar, A.; Han, S. S. PVA-based hydrogels for tissue engineering: A review. *Int. J. Polym. Mater.* **2017**, *66*, 159−182.
(498) Henderson, K. J.; Zhou, T. C.; Otim, K. J.; Shull, K. R. Ionically cross-linked triblock copolymer hydrogels with high strength. *Macromolecules* **2010**, *43*, 6193−6201.
(499) Vancaeyzeele, C.; Fichet, O.; Boileau, S.; Teyssié, D. Polyisobutene-poly(methylmethacrylate) interpenetrating polymer networks: synthesis and characterization. *Polymer* **2005**, *46*, 6888−6896.
(500) Schexnailder, P.; Schmidt, G. Nanocomposite polymer hydrogels. *Colloid Polym. Sci.* **2009**, *287*, 1−11.
(501) Fu, J. Strong and tough hydrogels crosslinked by multi-functional polymer colloids. *J. Polym. Sci., Part B: Polym. Phys.* **2018**, *56*, 1336−1350.
(502) Liu, Z.; Faraj, Y.; Ju, X.-J.; Wang, W.; Xie, R.; Chu, L.-Y. Nanocomposite smart hydrogels with improved responsiveness and mechanical properties: A mini review. *J. Polym. Sci., Part B: Polym. Phys.* **2018**, *56*, 1306−1313.
(503) Tuncaboylu, D. C.; Sari, M.; Oppermann, W.; Okay, O. Tough and Self-Healing Hydrogels Formed via Hydrophobic Interactions. *Macromolecules* **2011**, *44*, 4997−5005.
(504) Okay, O. Self-healing hydrogels formed via hydrophobic interactions. In *Adv. Polym. Sci.*; Seiffert, S., Ed.; Springer: Berlin, 2015; pp 101−142.
(505) Jiang, H. C.; Duan, L. J.; Ren, X. Y.; Gao, G. H. Hydrophobic association hydrogels with excellent mechanical and self-healing properties. *Eur. Polym. J.* **2019**, *112*, 660−669.
(506) Peppas, N. A.; Merrill, E. W. Poly(vinyl alcohol) hydrogels: Reinforcement of radiation-crosslinked networks by crystallization. *J. Polym. Sci., Part A* **1976**, *14*, 441−457.
(507) Seitz, M. E.; Martina, D.; Baumberger, T.; Krishnan, V. R.; Hui, C. Y.; Shull, K. R. Fracture and large strain behavior of self-assembled triblock copolymer gels. *Soft Matter* **2009**, *5*, 447−456.
(508) Okay, O.; Oppermann, W. Polyacrylamide-clay nanocomposite hydrogels: rheological and light scattering characterization. *Macromolecules* **2007**, *40*, 3378−3387.
(509) Liu, R. Q.; Liang, S. M.; Tang, X. Z.; Yan, D.; Li, X. F.; Yu, Z. Z. Tough and highly stretchable graphene oxide/polyacrylamide nanocomposite hydrogels. *J. Mater. Chem.* **2012**, *22*, 14160−14167.
(510) Haque, M. A.; Kurokawa, T.; Kamita, G.; Gong, J. P. Lamellar bilayers as reversible sacrificial bonds to toughen hydrogel: hysteresis, self-recovery, fatigue resistance, and crack blunting. *Macromolecules* **2011**, *44*, 8916−8924.
(511) Huang, T.; Xu, H. G.; Jiao, K. X.; Zhu, L. P.; Brown, H. R.; Wang, H. L. A novel hydrogel with high mechanical strength: A macromolecular microsphere composite hydrogel. *Adv. Mater.* **2007**, *19*, 1622−1626.
(512) Abe, K.; Yano, H. Formation of hydrogels from cellulose nanofibers. *Carbohydr. Polym.* **2011**, *85*, 733−737.
(513) Gao, Y.; Kuang, Y.; Guo, Z. F.; Guo, Z.; Krauss, I. J.; Xu, B. Enzyme-instructed molecular self-assembly confers nanofibers and a supramolecular hydrogel of taxol derivative. *J. Am. Chem. Soc.* **2009**, *131*, 13576−13577.
(514) Ma, M.; Kuang, Y.; Gao, Y.; Zhang, Y.; Gao, P.; Xu, B. Aromatic-aromatic interactions induce the self-assembly of pentapeptidic derivatives in water to form nanofibers and supramolecular hydrogels. *J. Am. Chem. Soc.* **2010**, *132*, 2719−2728.
(515) Kohler, K.; Forster, G.; Hauser, A.; Dobner, B.; Heiser, U. F.; Ziethe, F.; Richter, W.; Steiniger, F.; Drechsler, M.; Stettin, H.; et al. Self-assembly in a bipolar phosphocholine-water system: the formation of nanofibers and hydrogels. *Angew. Chem., Int. Ed.* **2004**, *43*, 245−247.
(516) Yang, G.; Lin, H.; Rothrauff, B. B.; Yu, S.; Tuan, R. S. Multilayered polycaprolactone/gelatin fiber-hydrogel composite for tendon tissue engineering. *Acta Biomater.* **2016**, *35*, 68−76.
(517) Ma, L.; Yang, G.; Wang, N.; Zhang, P.; Guo, F.; Meng, J.; Zhang, F.; Hu, Z.; Wang, S.; Zhao, Y. Trap effect of three-dimensional fibers network for high efficient cancer-cell capture. *Adv. Healthcare Mater.* **2015**, *4*, 838−843.
(518) D'Amore, A.; Stella, J. A.; Wagner, W. R.; Sacks, M. S. Characterization of the complete fiber network topology of planar fibrous tissues and scaffolds. *Biomaterials* **2010**, *31*, 5345−5354.
(519) Toshima, M.; Ohtani, Y.; Ohtani, O. Three-dimensional architecture of elastin and collagen fiber networks in the human and rat lung. *Arch. Histol. Cytol.* **2004**, *67*, 31−40.
(520) Weber, K. T. Cardiac interstitium in health and disease: the fibrillar collagen network. *J. Am. Coll. Cardiol.* **1989**, *13*, 1637−1652.
(521) Nakagaito, A. N.; Iwamoto, S.; Yano, H. Bacterial cellulose: the ultimate nano-scalar cellulose morphology for the production of high-strength composites. *Appl. Phys. A: Mater. Sci. Process.* **2005**, *80*, 93−97.
(522) Yan, C.; Pochan, D. J. Rheological properties of peptide-based hydrogels for biomedical and other applications. *Chem. Soc. Rev.* **2010**, *39*, 3528−3540.
(523) Woolfson, D. N. Building fibrous biomaterials from alpha-helical and collagen-like coiled-coil peptides. *Biopolymers* **2010**, *94*, 118−127.
(524) Viebke, C.; Piculell, L.; Nilsson, S. On the mechanism of gelation of helix-forming biopolymers. *Macromolecules* **1994**, *27*, 4160−4166.
(525) Prince, E.; Kumacheva, E. Design and applications of man-made biomimetic fibrillar hydrogels. *Nat. Rev. Mater.* **2019**, *4*, 99−115.
(526) Tamayol, A.; Akbari, M.; Annabi, N.; Paul, A.; Khademhosseini, A.; Juncker, D. Fiber-based tissue engineering: Progress, challenges, and opportunities. *Biotechnol. Adv.* **2013**, *31*, 669−687.
(527) Iwamoto, S.; Isogai, A.; Iwata, T. Structure and mechanical properties of wet-spun fibers made from natural cellulose nanofibers. *Biomacromolecules* **2011**, *12*, 831−836.
(528) Ren, L.; Pandit, V.; Elkin, J.; Denman, T.; Cooper, J. A.; Kotha, S. P. Large-scale and highly efficient synthesis of micro- and nano-fibers with controlled fiber morphology by centrifugal jet spinning for tissue regeneration. *Nanoscale* **2013**, *5*, 2337−2345.
(529) Agarwal, S.; Greiner, A.; Wendorff, J. H. Functional materials by electrospinning of polymers. *Prog. Polym. Sci.* **2013**, *38*, 963−991.

https://doi.org/10.1021/acs.chemrev.0c01088
Chem. Rev. XXXX, XXX, XXX−XXX

(530) Rogina, A. Electrospinning process: Versatile preparation method for biodegradable and natural polymers and biocomposite systems applied in tissue engineering and drug delivery. *Appl. Surf. Sci.* **2014**, *296*, 221−230.
(531) Hong, Y.; Huber, A.; Takanari, K.; Amoroso, N. J.; Hashizume, R.; Badylak, S. F.; Wagner, W. R. Mechanical properties and in vivo behavior of a biodegradable synthetic polymer microfiber-extracellular matrix hydrogel biohybrid scaffold. *Biomaterials* **2011**, *32*, 3387−3394.
(532) Ekaputra, A. K.; Prestwich, G. D.; Cool, S. M.; Hutmacher, D. W. Combining electrospun scaffolds with electrosprayed hydrogels leads to three-dimensional cellularization of hybrid constructs. *Biomacromolecules* **2008**, *9*, 2097−2103.
(533) Thorvaldsson, A.; Silva-Correia, J.; Oliveira, J. M.; Reis, R. L.; Gatenholm, P.; Walkenstrom, P. Development of nanofiber-reinforced hydrogel scaffolds for nucleus pulposus regeneration by a combination of electrospinning and spraying technique. *J. Appl. Polym. Sci.* **2013**, *128*, 1158−1163.
(534) Ramakrishna, S. *An introduction to electrospinning and nanofibers*; World Scientific: Singapore, 2005.
(535) Yoo, H. S.; Kim, T. G.; Park, T. G. Surface-functionalized electrospun nanofibers for tissue engineering and drug delivery. *Adv. Drug Delivery Rev.* **2009**, *61*, 1033−1042.
(536) Boudriot, U.; Dersch, R.; Greiner, A.; Wendorff, J. H. Electrospinning approaches toward scaffold engineering–a brief overview. *Artif. Organs* **2006**, *30*, 785−792.
(537) Vatankhah-Varnosfaderani, M.; Daniel, W. F.; Everhart, M. H.; Pandya, A. A.; Liang, H.; Matyjaszewski, K.; Dobrynin, A. V.; Sheiko, S. S. Mimicking biological stress-strain behaviour with synthetic elastomers. *Nature* **2017**, *549*, 497−501.
(538) Daniel, W. F.; Burdyńska, J.; Vatankhah-Varnoosfaderani, M.; Matyjaszewski, K.; Paturej, J.; Rubinstein, M.; Dobrynin, A. V.; Sheiko, S. S. Solvent-free, supersoft and superelastic bottlebrush melts and networks. *Nat. Mater.* **2016**, *15*, 183−189.
(539) Vohidov, F.; Milling, L. E.; Chen, Q. X.; Zhang, W. X.; Bhagchandani, S.; Nguyen, H. V. T.; Irvine, D. J.; Johnson, J. A. ABC triblock bottlebrush copolymer-based injectable hydrogels: design, synthesis, and application to expanding the therapeutic index of cancer immunochemotherapy. *Chem. Sci.* **2020**, *11*, 5974−5986.
(540) Zhou, Y.; Zhang, W.; Hu, J.; Tang, J.; Jin, C.; Suo, Z.; Lu, T. The stiffness-threshold conflict in polymer networks and a resolution. *J. Appl. Mech.* **2020**, No. 87, 031002.
(541) Bell, G. I. Models for the specific adhesion of cells to cells. *Science* **1978**, *200*, 618−627.
(542) Delmer, D. P.; Amor, Y. Cellulose biosynthesis. *Plant Cell* **1995**, *7*, 987−1000.
(543) Abe, K.; Yano, H. Cellulose nanofiber-based hydrogels with high mechanical strength. *Cellulose* **2012**, *19*, 1907−1912.
(544) Debenedetti, P. G.; Stillinger, F. H. Supercooled liquids and the glass transition. *Nature* **2001**, *410*, 259−267.
(545) Burns, A. B.; Register, R. A. Mechanical properties of star block polymer thermoplastic elastomers with glassy and crystalline end blocks. *Macromolecules* **2016**, *49*, 9521−9530.
(546) Nykanen, A.; Nuopponen, M.; Laukkanen, A.; Hirvonen, S. P.; Rytela, M.; Turunen, O.; Tenhu, H.; Mezzenga, R.; Ikkala, O.; Ruokolainen, J. Phase behavior and temperature-responsive molecular filters based on self-assembly of Polystyrene-block-poly(N-isopropylacrylamide)-block-polystyrene. *Macromolecules* **2007**, *40*, 5827−5834.
(547) Roth, C. B.; Pound, A.; Kamp, S. W.; Murray, C. A.; Dutcher, J. R. Molecular-weight dependence of the glass transition temperature of freely-standing poly(methyl methacrylate) films. *Eur. Phys. J. E: Soft Matter Biol. Phys.* **2006**, *20*, 441−448.
(548) Ottani, V.; Martini, D.; Franchi, M.; Ruggeri, A.; Raspanti, M. Hierarchical structures in fibrillar collagens. *Micron* **2002**, *33*, 587−596.
(549) O'Leary, L. E.; Fallas, J. A.; Bakota, E. L.; Kang, M. K.; Hartgerink, J. D. Multi-hierarchical self-assembly of a collagen mimetic peptide from triple helix to nanofibre and hydrogel. *Nat. Chem.* **2011**, *3*, 821−828.
(550) Arnott, S.; Fulmer, A.; Scott, W. E.; Dea, I. C.; Moorhouse, R.; Rees, D. A. The agarose double helix and its function in agarose gel structure. *J. Mol. Biol.* **1974**, *90*, 269−284.
(551) Foord, S. A.; Atkins, E. D. T. New X-ray-diffraction results from agarose - extended single helix structures and implications for gelation mechanism. *Biopolymers* **1989**, *28*, 1345−1365.
(552) Armisen, R. Agar and agarose biotechnological applications. *Hydrobiologia* **1991**, *221*, 157−166.
(553) Van Vlierberghe, S.; Dubruel, P.; Schacht, E. Biopolymer-based hydrogels as scaffolds for tissue engineering applications: a review. *Biomacromolecules* **2011**, *12*, 1387−1408.
(554) Eagland, D.; Crowther, N. J.; Butler, C. J. Complexation between polyoxyethylene and polymethacrylic acid—the importance of the molar mass of polyoxyethylene. *Eur. Polym. J.* **1994**, *30*, 767−773.
(555) Kim, I. S.; Kim, S. H.; Cho, C. S. Drug release from pH-sensitive interpenetrating polymer networks hydrogel based on poly (ethylene glycol) macromer and poly (acrylic acid) prepared by UV cured method. *Arch. Pharmacal Res.* **1996**, *19*, 18−22.
(556) Voorhaar, L.; Hoogenboom, R. Supramolecular polymer networks: hydrogels and bulk materials. *Chem. Soc. Rev.* **2016**, *45*, 4013−4031.
(557) Zhang, G. Z.; Chen, Y. H.; Deng, Y. H.; Ngai, T.; Wang, C. Y. Dynamic supramolecular hydrogels: regulating hydrogel properties through self-complementary quadruple hydrogen bonds and thermo-switch. *ACS Macro Lett.* **2017**, *6*, 641−646.
(558) Cui, J.; del Campo, A. Multivalent H-bonds for self-healing hydrogels. *Chem. Commun.* **2012**, *48*, 9302−9304.
(559) Li, F.; Tang, J. P.; Geng, J. H.; Luo, D.; Yang, D. Y. Polymeric DNA hydrogel: Design, synthesis and applications. *Prog. Polym. Sci.* **2019**, *98*, 101163.
(560) Cui, H.; Zhuang, X.; He, C.; Wei, Y.; Chen, X. High performance and reversible ionic polypeptide hydrogel based on charge-driven assembly for biomedical applications. *Acta Biomater.* **2015**, *11*, 183−190.
(561) Ji, D. Y.; Kuo, T. F.; Wu, H. D.; Yang, J. C.; Lee, S. Y. A novel injectable chitosan/polyglutamate polyelectrolyte complex hydrogel with hydroxyapatite for soft-tissue augmentation. *Carbohydr. Polym.* **2012**, *89*, 1123−1130.
(562) Lee, K. Y.; Rowley, J. A.; Eiselt, P.; Moy, E. M.; Bouhadir, K. H.; Mooney, D. J. Controlling mechanical and swelling properties of alginate hydrogels independently by cross-linker type and cross-linking density. *Macromolecules* **2000**, *33*, 4291−4294.
(563) Yang, Y.; Wang, X.; Yang, F.; Wang, L.; Wu, D. Highly elastic and ultratough hybrid ionic-covalent hydrogels with tunable structures and mechanics. *Adv. Mater.* **2018**, *30*, 1707071.
(564) Mohammadzadeh Pakdel, P.; Peighambardoust, S. J. Review on recent progress in chitosan-based hydrogels for wastewater treatment application. *Carbohydr. Polym.* **2018**, *201*, 264−279.
(565) Mi, F.-L.; Sung, H.-W.; Shyu, S.-S.; Su, C.-C.; Peng, C.-K. Synthesis and characterization of biodegradable TPP/genipin co-crosslinked chitosan gel beads. *Polymer* **2003**, *44*, 6521−6530.
(566) Luo, F.; Sun, T. L.; Nakajima, T.; Kurokawa, T.; Zhao, Y.; Sato, K.; Ihsan, A. B.; Li, X.; Guo, H.; Gong, J. P. Oppositely charged polyelectrolytes form tough, self-healing, and rebuildable hydrogels. *Adv. Mater.* **2015**, *27*, 2722−2727.
(567) Mozhdehi, D.; Ayala, S.; Cromwell, O. R.; Guan, Z. Self-healing multiphase polymers via dynamic metal-ligand interactions. *J. Am. Chem. Soc.* **2014**, *136*, 16128−16131.
(568) Zhang, J. Y.; Su, C. Y. Metal-organic gels: From discrete metallogelators to coordination polymers. *Coord. Chem. Rev.* **2013**, *257*, 1373−1408.
(569) Fantner, G. E.; Hassenkam, T.; Kindt, J. H.; Weaver, J. C.; Birkedal, H.; Pechenik, L.; Cutroni, J. A.; Cidade, G. A.; Stucky, G. D.; Morse, D. E.; et al. Sacrificial bonds and hidden length dissipate energy as mineralized fibrils separate during bone fracture. *Nat. Mater.* **2005**, *4*, 612−616.
(570) Hillerton, J. E.; Vincent, J. F. V. The specific location of zinc in insect mandibles. *J. Exp. Biol.* **1982**, *101*, 333.

https://doi.org/10.1021/acs.chemrev.0c01088
Chem. Rev. XXXX, XXX, XXX−XXX

(571) Harrington, M. J.; Masic, A.; Holten-Andersen, N.; Waite, J. H.; Fratzl, P. Iron-clad fibers: a metal-based biological strategy for hard flexible coatings. *Science* **2010**, *328*, 216−220.
(572) Nejadnik, M. R.; Yang, X.; Bongio, M.; Alghamdi, H. S.; van den Beucken, J. J.; Huysmans, M. C.; Jansen, J. A.; Hilborn, J.; Ossipov, D.; Leeuwenburgh, S. C. Self-healing hybrid nanocomposites consisting of bisphosphonated hyaluronan and calcium phosphate nanoparticles. *Biomaterials* **2014**, *35*, 6918−6929.
(573) Lopez-Perez, P. M.; da Silva, R. M. P.; Strehin, I.; Kouwer, P. H. J.; Leeuwenburgh, S. C. G.; Messersmith, P. B. Self-healing hydrogels formed by complexation between calcium ions and bisphosphonate-functionalized star-shaped polymers. *Macromolecules* **2017**, *50*, 8698−8706.
(574) Shi, L. Y.; Carstensen, H.; Holzl, K.; Lunzer, M.; Li, H.; Hilborn, J.; Ovsianikov, A.; Ossipov, D. A. Dynamic coordination chemistry enables free directional printing of biopolymer hydrogel. *Chem. Mater.* **2017**, *29*, 5816−5823.
(575) Li, Q.; Barrett, D. G.; Messersmith, P. B.; Holten-Andersen, N. Controlling hydrogel mechanics via bio-inspired polymer-nanoparticle bond dynamics. *ACS Nano* **2016**, *10*, 1317−1324.
(576) Hou, S.; Ma, P. X. Stimuli-responsive supramolecular hydrogels with high extensibility and fast self-healing via precoordinated mussel-inspired chemistry. *Chem. Mater.* **2015**, *27*, 7627−7635.
(577) Wang, W. N.; Xu, Y. S.; Li, A.; Li, T.; Liu, M. M.; von Klitzing, R.; Ober, C. K.; Kayitmazer, A. B.; Li, L.; Guo, X. H. Zinc induced polyelectrolyte coacervate bioadhesive and its transition to a self-healing hydrogel. *RSC Adv.* **2015**, *5*, 66871−66878.
(578) Grindy, S. C.; Learsch, R.; Mozhdehi, D.; Cheng, J.; Barrett, D. G.; Guan, Z.; Messersmith, P. B.; Holten-Andersen, N. Control of hierarchical polymer mechanics with bioinspired metal-coordination dynamics. *Nat. Mater.* **2015**, *14*, 1210−1216.
(579) Fullenkamp, D. E.; He, L.; Barrett, D. G.; Burghardt, W. R.; Messersmith, P. B. Mussel-inspired histidine-based transient network metal coordination hydrogels. *Macromolecules* **2013**, *46*, 1167−1174.
(580) Wang, C.; Stewart, R. J.; Kopecek, J. Hybrid hydrogels assembled from synthetic polymers and coiled-coil protein domains. *Nature* **1999**, *397*, 417−420.
(581) Qin, H. L.; Zhang, T.; Li, H. N.; Cong, H. P.; Antonietti, M.; Yu, S. H. Dynamic Au-thiolate interaction induced rapid self-healing nanocomposite hydrogels with remarkable mechanical behaviors. *Chem-Us* **2017**, *3*, 691−705.
(582) Casuso, P.; Odriozola, I.; Perez-San Vicente, A.; Loinaz, I.; Cabanero, G.; Grande, H. J.; Dupin, D. Injectable and self-healing dynamic hydrogels based on metal(I)-thiolate/disulfide exchange as biomaterials with tunable mechanical properties. *Biomacromolecules* **2015**, *16*, 3552−3561.
(583) Peng, F.; Li, G.; Liu, X.; Wu, S.; Tong, Z. Redox-responsive gel-sol/sol-gel transition in poly(acrylic acid) aqueous solution containing Fe(III) ions switched by light. *J. Am. Chem. Soc.* **2008**, *130*, 16166−16167.
(584) Zheng, S. Y.; Ding, H.; Qian, J.; Yin, J.; Wu, Z. L.; Song, Y.; Zheng, Q. Metal-coordination complexes mediated physical hydrogels with high toughness, stick-slip tearing behavior, and good processability. *Macromolecules* **2016**, *49*, 9637−9646.
(585) Buwalda, S. J.; Dijkstra, P. J.; Feijen, J. Poly(ethylene glycol)-poly(L-lactide) star block copolymer hydrogels crosslinked by metal-ligand coordination. *J. Polym. Sci., Part A: Polym. Chem.* **2012**, *50*, 1783−1791.
(586) Chujo, Y.; Sada, K.; Saegusa, T. Iron(II) bipyridyl-branched polyoxazoline complex as a thermally reversible hydrogel. *Macromolecules* **1993**, *26*, 6315−6319.
(587) Weng, G.; Thanneeru, S.; He, J. Dynamic coordination of Eu-iminodiacetate to control fluorochromic response of polymer hydrogels to multistimuli. *Adv. Mater.* **2018**, *30*, 1706526.
(588) Zhang, K. Y.; Feng, Q.; Xu, J. B.; Xu, X. Y.; Tian, F.; Yeung, K. W. K.; Bian, L. M. Self-assembled injectable nanocomposite hydrogels stabilized by bisphosphonate-magnesium (Mg2+) coordination regulates the differentiation of encapsulated stem cells via dual crosslinking. *Adv. Funct. Mater.* **2017**, *27*, 1701642.
(589) Diba, M.; Camargo, W. A.; Brindisi, M.; Farbod, K.; Klymov, A.; Schmidt, S.; Harrington, M. J.; Draghi, L.; Boccaccini, A. R.; Jansen, J. A.; et al. Composite colloidal gels made of bisphosphonate-functionalized gelatin and bioactive glass particles for regeneration of osteoporotic bone defects. *Adv. Funct. Mater.* **2017**, *27*, 1703438.
(590) He, L.; Fullenkamp, D. E.; Rivera, J. G.; Messersmith, P. B. pH responsive self-healing hydrogels formed by boronate-catechol complexation. *Chem. Commun.* **2011**, *47*, 7497−7499.
(591) Holten-Andersen, N.; Harrington, M. J.; Birkedal, H.; Lee, B. P.; Messersmith, P. B.; Lee, K. Y.; Waite, J. H. pH-induced metal-ligand cross-links inspired by mussel yield self-healing polymer networks with near-covalent elastic moduli. *Proc. Natl. Acad. Sci. U. S. A.* **2011**, *108*, 2651−2655.
(592) Chan Choi, Y.; Choi, J. S.; Jung, Y. J.; Cho, Y. W. Human gelatin tissue-adhesive hydrogels prepared by enzyme-mediated biosynthesis of DOPA and Fe(3+) ion crosslinking. *J. Mater. Chem. B* **2014**, *2*, 201−209.
(593) Lee, J.; Chang, K.; Kim, S.; Gite, V.; Chung, H.; Sohn, D. Phase controllable hyaluronic acid hydrogel with iron(III) ion-catechol induced dual cross-linking by utilizing the gap of gelation kinetics. *Macromolecules* **2016**, *49*, 7450−7459.
(594) Yavvari, P. S.; Srivastava, A. Robust, self-healing hydrogels synthesised from catechol rich polymers. *J. Mater. Chem. B* **2015**, *3*, 899−910.
(595) Sundberg, R. J.; Martin, R. B. Interactions of histidine and other imidazole derivatives with transition-metal ions in chemical and biological-systems. *Chem. Rev.* **1974**, *74*, 471−517.
(596) Shi, L.; Ding, P.; Wang, Y.; Zhang, Y.; Ossipov, D.; Hilborn, J. Self-healing polymeric hydrogel formed by metal-ligand coordination assembly: design, fabrication, and biomedical applications. *Macromol. Rapid Commun.* **2019**, *40*, No. e1800837.
(597) Cook, T. R.; Zheng, Y. R.; Stang, P. J. Metal-organic frameworks and self-assembled supramolecular coordination complexes: comparing and contrasting the design, synthesis, and functionality of metal-organic materials. *Chem. Rev.* **2013**, *113*, 734−777.
(598) Rodell, C. B.; Mealy, J. E.; Burdick, J. A. Supramolecular guest-host interactions for the preparation of biomedical materials. *Bioconjugate Chem.* **2015**, *26*, 2279−2289.
(599) Appel, E. A.; del Barrio, J.; Loh, X. J.; Scherman, O. A. Supramolecular polymeric hydrogels. *Chem. Soc. Rev.* **2012**, *41*, 6195−6214.
(600) Szejtli, J. Introduction and general overview of cyclodextrin chemistry. *Chem. Rev.* **1998**, *98*, 1743−1754.
(601) Harada, A.; Takashima, Y.; Nakahata, M. Supramolecular polymeric materials via cyclodextrin-guest interactions. *Acc. Chem. Res.* **2014**, *47*, 2128−2140.
(602) Yamaguchi, H.; Kobayashi, Y.; Kobayashi, R.; Takashima, Y.; Hashidzume, A.; Harada, A. Photoswitchable gel assembly based on molecular recognition. *Nat. Commun.* **2012**, *3*, 603.
(603) Wu, J. S.; Toda, K.; Tanaka, A.; Sanemasa, I. Association constants of ferrocene with cyclodextrins in aqueous medium determined by solubility measurements of ferrocene. *Bull. Chem. Soc. Jpn.* **1998**, *71*, 1615−1618.
(604) Voskuhl, J.; Waller, M.; Bandaru, S.; Tkachenko, B. A.; Fregonese, C.; Wibbeling, B.; Schreiner, P. R.; Ravoo, B. J. Nanodiamonds in sugar rings: an experimental and theoretical investigation of cyclodextrin-nanodiamond inclusion complexes. *Org. Biomol. Chem.* **2012**, *10*, 4524−4530.
(605) Lezcano, M.; Al-Soufi, W.; Novo, M.; Rodriguez-Nunez, E.; Tato, J. V. Complexation of several benzimidazole-type fungicides with alpha- and beta-cyclodextrins. *J. Agric. Food Chem.* **2002**, *50*, 108−112.
(606) Huh, K. M.; Tomita, H.; Lee, W. K.; Ooya, T.; Yui, N. Synthesis of α-cyclodextrin-conjugated poly(ε-lysine)s and their inclusion complexation behavior. *Macromol. Rapid Commun.* **2002**, *23*, 179−182.
(607) Tomatsu, I.; Hashidzume, A.; Harada, A. Redox-responsive hydrogel system using the molecular recognition of β-cyclodextrin. *Macromol. Rapid Commun.* **2006**, *27*, 238−241.

https://doi.org/10.1021/acs.chemrev.0c01088
Chem. Rev. XXXX, XXX, XXX−XXX

(608) Nelissen, H. F.; Feiters, M. C.; Nolte, R. J. Synthesis and self-inclusion of bipyridine-spaced cyclodextrin dimers. *J. Org. Chem.* **2002**, *67*, 5901−5906.
(609) Hetzer, M.; Fleischmann, C.; Schmidt, B. V. K. J.; Barner-Kowollik, C.; Ritter, H. Visual recognition of supramolecular graft polymer formation via phenolphthalein-cyclodextrin association. *Polymer* **2013**, *54*, 5141−5147.
(610) Ravichandran, R.; Divakar, S. Inclusion of ring A of cholesterol inside the β-cyclodextrin cavity: evidence from oxidation reactions and structural studies. *J. Inclusion Phenom. Mol. Recognit. Chem.* **1998**, *30*, 253−270.
(611) Rekharsky, M. V.; Inoue, Y. Complexation thermodynamics of cyclodextrins. *Chem. Rev.* **1998**, *98*, 1875−1918.
(612) Bortolus, P.; Monti, S. cis. dblharw. trans Photoisomerization of azobenzene-cyclodextrin inclusion complexes. *J. Phys. Chem.* **1987**, *91*, 5046−5050.
(613) Matsue, T.; Evans, D. H.; Osa, T.; Kobayashi, N. Electron-transfer reactions associated with host guest complexation - oxidation of ferrocenecarboxylic acid in the presence of beta-cyclodextrin. *J. Am. Chem. Soc.* **1985**, *107*, 3411−3417.
(614) Kaifer, A. E. Interplay between molecular recognition and redox chemistry. *Acc. Chem. Res.* **1999**, *32*, 62−71.
(615) Freeman, W. A.; Mock, W. L.; Shih, N. Y. Cucurbituril. *J. Am. Chem. Soc.* **1981**, *103*, 7367−7368.
(616) Lagona, J.; Mukhopadhyay, P.; Chakrabarti, S.; Isaacs, L. The cucurbit[n]uril family. *Angew. Chem., Int. Ed.* **2005**, *44*, 4844−4870.
(617) Liu, S.; Ruspic, C.; Mukhopadhyay, P.; Chakrabarti, S.; Zavalij, P. Y.; Isaacs, L. The cucurbit[n]uril family: prime components for self-sorting systems. *J. Am. Chem. Soc.* **2005**, *127*, 15959−15967.
(618) Mock, W. L.; Shih, N. Y. Structure and selectivity in host guest complexes of cucurbituril. *J. Org. Chem.* **1986**, *51*, 4440−4446.
(619) Jeon, W. S.; Moon, K.; Park, S. H.; Chun, H.; Ko, Y. H.; Lee, J. Y.; Lee, E. S.; Samal, S.; Selvapalam, N.; Rekharsky, M. V.; et al. Complexation of ferrocene derivatives by the cucurbit[7]uril host: a comparative study of the cucurbituril and cyclodextrin host families. *J. Am. Chem. Soc.* **2005**, *127*, 12984−12989.
(620) Moghaddam, S.; Yang, C.; Rekharsky, M.; Ko, Y. H.; Kim, K.; Inoue, Y.; Gilson, M. K. New ultrahigh affinity host-guest complexes of cucurbit[7]uril with bicyclo[2.2.2]octane and adamantane guests: thermodynamic analysis and evaluation of M2 affinity calculations. *J. Am. Chem. Soc.* **2011**, *133*, 3570−3581.
(621) Kim, J.; Jung, I.-S.; Kim, S.-Y.; Lee, E.; Kang, J.-K.; Sakamoto, S.; Yamaguchi, K.; Kim, K. New cucurbituril homologues: syntheses, isolation, characterization, and x-ray crystal structures of cucurbit[n]-uril (n= 5, 7, and 8). *J. Am. Chem. Soc.* **2000**, *122*, 540−541.
(622) Lee, J. W.; Kim, K.; Choi, S.; Ko, Y. H.; Sakamoto, S.; Yamaguchi, K.; Kim, K. Unprecedented host-induced intramolecular charge-transfer complex formation. *Chem. Commun.* **2002**, 2692−2693 10.1039/b208280b.
(623) Takashima, Y.; Sawa, Y.; Iwaso, K.; Nakahata, M.; Yamaguchi, H.; Harada, A. Supramolecular materials cross-linked by host-guest inclusion complexes: the effect of side chain molecules on mechanical properties. *Macromolecules* **2017**, *50*, 3254−3261.
(624) Jin, J.; Cai, L.; Jia, Y. G.; Liu, S.; Chen, Y.; Ren, L. Progress in self-healing hydrogels assembled by host-guest interactions: preparation and biomedical applications. *J. Mater. Chem. B* **2019**, *7*, 1637−1651.
(625) Yang, X.; Yu, H.; Wang, L.; Tong, R.; Akram, M.; Chen, Y.; Zhai, X. Self-healing polymer materials constructed by macrocycle-based host-guest interactions. *Soft Matter* **2015**, *11*, 1242−1252.
(626) Takashima, Y.; Hatanaka, S.; Otsubo, M.; Nakahata, M.; Kakuta, T.; Hashidzume, A.; Yamaguchi, H.; Harada, A. Expansion-contraction of photoresponsive artificial muscle regulated by host-guest interactions. *Nat. Commun.* **2012**, *3*, 1270.
(627) Zhou, L. P.; Li, J. X.; Luo, Q.; Zhu, J. Y.; Zou, H. X.; Gao, Y. Z.; Wang, L.; Xu, J. Y.; Dong, Z. Y.; Liu, J. Q. Dual stimuli-responsive supramolecular pseudo-polyrotaxane hydrogels. *Soft Matter* **2013**, *9*, 4635−4641.
(628) Jeong, B.; Kim, S. W.; Bae, Y. H. Thermosensitive sol-gel reversible hydrogels. *Adv. Drug Delivery Rev.* **2012**, *64*, 154−162.
(629) Mihajlovic, M.; Staropoli, M.; Appavou, M. S.; Wyss, H. M.; Pyckhout-Hintzen, W.; Sijbesma, R. P. Tough supramolecular hydrogel based on strong hydrophobic interactions in a multiblock segmented copolymer. *Macromolecules* **2017**, *50*, 3333−3346.
(630) Patrickios, C. S.; Georgiou, T. K. Covalent amphiphilic polymer networks. *Curr. Opin. Colloid Interface Sci.* **2003**, *8*, 76−85.
(631) Klaikherd, A.; Nagamani, C.; Thayumanavan, S. Multi-stimuli sensitive amphiphilic block copolymer assemblies. *J. Am. Chem. Soc.* **2009**, *131*, 4830−4838.
(632) Zhang, H. J.; Sun, T. L.; Zhang, A. K.; Ikura, Y.; Nakajima, T.; Nonoyama, T.; Kurokawa, T.; Ito, O.; Ishitobi, H.; Gong, J. P. Tough physical double-network hydrogels based on amphiphilic triblock copolymers. *Adv. Mater.* **2016**, *28*, 4884−4890.
(633) Tuncaboylu, D. C.; Argun, A.; Sahin, M.; Sari, M.; Okay, O. Structure optimization of self-healing hydrogels formed via hydrophobic interactions. *Polymer* **2012**, *53*, 5513−5522.
(634) Wheeler, S. E. Understanding substituent effects in noncovalent interactions involving aromatic rings. *Acc. Chem. Res.* **2013**, *46*, 1029−1038.
(635) Butterfield, S. M.; Patel, P. R.; Waters, M. L. Contribution of aromatic interactions to alpha-helix stability. *J. Am. Chem. Soc.* **2002**, *124*, 9751−9755.
(636) Singh, V.; Snigdha, K.; Singh, C.; Sinha, N.; Thakur, A. K. Understanding the self-assembly of Fmoc-phenylalanine to hydrogel formation. *Soft Matter* **2015**, *11*, 5353−5364.
(637) Yan, X.; Zhu, P.; Li, J. Self-assembly and application of diphenylalanine-based nanostructures. *Chem. Soc. Rev.* **2010**, *39*, 1877−1890.
(638) Mehra, N. K.; Palakurthi, S. Interactions between carbon nanotubes and bioactives: a drug delivery perspective. *Drug Discovery Today* **2016**, *21*, 585−597.
(639) Kovtyukhova, N. I.; Mallouk, T. E.; Pan, L.; Dickey, E. C. Individual single-walled nanotubes and hydrogels made by oxidative exfoliation of carbon nanotube ropes. *J. Am. Chem. Soc.* **2003**, *125*, 9761−9769.
(640) Ghawanmeh, A. A.; Ali, G. A. M.; Algarni, H.; Sarkar, S. M.; Chong, K. F. Graphene oxide-based hydrogels as a nanocarrier for anticancer drug delivery. *Nano Res.* **2019**, *12*, 973−990.
(641) Loh, K. P.; Bao, Q. L.; Ang, P. K.; Yang, J. X. The chemistry of graphene. *J. Mater. Chem.* **2010**, *20*, 2277−2289.
(642) Yuk, H.; Lu, B.; Zhao, X. Hydrogel bioelectronics. *Chem. Soc. Rev.* **2019**, *48*, 1642−1667.
(643) Dhanjai; Sinha, A.; Kalambate, P. K.; Mugo, S. M.; Kamau, P.; Chen, J.; Jain, R. Polymer hydrogel interfaces in electrochemical sensing strategies: A review. *TrAC, Trends Anal. Chem.* **2019**, *118*, 488−501.
(644) Krishnakumar, B.; Sanka, R. V. S. P.; Binder, W. H.; Parthasarthy, V.; Rana, S.; Karak, N. Vitrimers: Associative dynamic covalent adaptive networks in thermoset polymers. *Chem. Eng. J.* **2020**, *385*, 123820.
(645) Cordes, E. H.; Jencks, W. P. The mechanism of hydrolysis of schiff bases derived from aliphatic amines. *J. Am. Chem. Soc.* **1963**, *85*, 2843−2848.
(646) Lu, S.; Gao, C.; Xu, X.; Bai, X.; Duan, H.; Gao, N.; Feng, C.; Xiong, Y.; Liu, M. Injectable and self-healing carbohydrate-based hydrogel for cell encapsulation. *ACS Appl. Mater. Interfaces* **2015**, *7*, 13029−13037.
(647) Wei, Z.; Yang, J. H.; Liu, Z. Q.; Xu, F.; Zhou, J. X.; Zrinyi, M.; Osada, Y.; Chen, Y. M. Novel biocompatible polysaccharide-based self-healing hydrogel. *Adv. Funct. Mater.* **2015**, *25*, 1352−1359.
(648) Karimi, A. R.; Khodadadi, A. Mechanically robust 3D nanostructure chitosan-based hydrogels with autonomic self-healing properties. *ACS Appl. Mater. Interfaces* **2016**, *8*, 27254−27263.
(649) Wu, X.; He, C.; Wu, Y.; Chen, X. Synergistic therapeutic effects of Schiff's base cross-linked injectable hydrogels for local co-delivery of metformin and 5-fluorouracil in a mouse colon carcinoma model. *Biomaterials* **2016**, *75*, 148−162.

https://doi.org/10.1021/acs.chemrev.0c01088
Chem. Rev. XXXX, XXX, XXX−XXX

(650) Ding, F.; Wu, S.; Wang, S.; Xiong, Y.; Li, Y.; Li, B.; Deng, H.; Du, Y.; Xiao, L.; Shi, X. A dynamic and self-crosslinked polysaccharide hydrogel with autonomous self-healing ability. *Soft Matter* **2015**, *11*, 3971−3976.
(651) Engel, A. K.; Yoden, T.; Sanui, K.; Ogata, N. Synthesis of aromatic schiff-base oligomers at the air-water-interface. *J. Am. Chem. Soc.* **1985**, *107*, 8308−8310.
(652) Zhang, Y.; Tao, L.; Li, S.; Wei, Y. Synthesis of multiresponsive and dynamic chitosan-based hydrogels for controlled release of bioactive molecules. *Biomacromolecules* **2011**, *12*, 2894−2901.
(653) Huang, W.; Wang, Y.; Huang, Z.; Wang, X.; Chen, L.; Zhang, Y.; Zhang, L. On-demand dissolvable self-healing hydrogel based on carboxymethyl chitosan and cellulose nanocrystal for deep partial thickness burn wound healing. *ACS Appl. Mater. Interfaces* **2018**, *10*, 41076−41088.
(654) Boehnke, N.; Cam, C.; Bat, E.; Segura, T.; Maynard, H. D. Imine hydrogels with tunable degradability for tissue engineering. *Biomacromolecules* **2015**, *16*, 2101−2108.
(655) Xu, Y.; Li, Y.; Chen, Q.; Fu, L.; Tao, L.; Wei, Y. Injectable and self-healing chitosan hydrogel based on imine bonds: design and therapeutic applications. *Int. J. Mol. Sci.* **2018**, *19*, 2198.
(656) Bull, S. D.; Davidson, M. G.; van den Elsen, J. M.; Fossey, J. S.; Jenkins, A. T.; Jiang, Y. B.; Kubo, Y.; Marken, F.; Sakurai, K.; Zhao, J.; et al. Exploiting the reversible covalent bonding of boronic acids: recognition, sensing, and assembly. *Acc. Chem. Res.* **2013**, *46*, 312−326.
(657) Guan, Y.; Zhang, Y. Boronic acid-containing hydrogels: synthesis and their applications. *Chem. Soc. Rev.* **2013**, *42*, 8106−8121.
(658) Nishiyabu, R.; Kubo, Y.; James, T. D.; Fossey, J. S. Boronic acid building blocks: tools for sensing and separation. *Chem. Commun.* **2011**, *47*, 1106−1123.
(659) Pizer, R.; Babcock, L. Mechanism of the complexation of boron acids with catechol and substituted catechols. *Inorg. Chem.* **1977**, *16*, 1677−1681.
(660) Jay, J. I.; Shukair, S.; Langheinrich, K.; Hanson, M. C.; Cianci, G. C.; Johnson, T. J.; Clark, M. R.; Hope, T. J.; Kiser, P. F. Modulation of viscoelasticity and HIV transport as a function of ph in a reversibly crosslinked hydrogel. *Adv. Funct. Mater.* **2009**, *19*, 2969−2977.
(661) Mahalingam, A.; Jay, J. I.; Langheinrich, K.; Shukair, S.; McRaven, M. D.; Rohan, L. C.; Herold, B. C.; Hope, T. J.; Kiser, P. F. Inhibition of the transport of HIV in vitro using a pH-responsive synthetic mucin-like polymer system. *Biomaterials* **2011**, *32*, 8343−8355.
(662) Sartain, F. K.; Yang, X.; Lowe, C. R. Holographic lactate sensor. *Anal. Chem.* **2006**, *78*, 5664−5670.
(663) Kataoka, K.; Miyazaki, H.; Bunya, M.; Okano, T.; Sakurai, Y. Totally synthetic polymer gels responding to external glucose concentration: their preparation and application to on-off regulation of insulin release. *J. Am. Chem. Soc.* **1998**, *120*, 12694−12695.
(664) Asher, S. A.; Alexeev, V. L.; Goponenko, A. V.; Sharma, A. C.; Lednev, I. K.; Wilcox, C. S.; Finegold, D. N. Photonic crystal carbohydrate sensors: low ionic strength sugar sensing. *J. Am. Chem. Soc.* **2003**, *125*, 3322−3329.
(665) Zhang, Y.; Guan, Y.; Zhou, S. Synthesis and volume phase transitions of glucose-sensitive microgels. *Biomacromolecules* **2006**, *7*, 3196−3201.
(666) Roberts, M. C.; Hanson, M. C.; Massey, A. P.; Karren, E. A.; Kiser, P. F. Dynamically restructuring hydrogel networks formed with reversible covalent crosslinks. *Adv. Mater.* **2007**, *19*, 2503−2507.
(667) Nakahata, M.; Mori, S.; Takashima, Y.; Hashidzume, A.; Yamaguchi, H.; Harada, A. pH-and sugar-responsive gel assemblies based on boronate-catechol interactions. *ACS Macro Lett.* **2014**, *3*, 337−340.
(668) Shan, M.; Gong, C.; Li, B.; Wu, G. A pH, glucose, and dopamine triple-responsive, self-healable adhesive hydrogel formed by phenylborate-catechol complexation. *Polym. Chem.* **2017**, *8*, 2997−3005.
(669) Kitano, S.; Hisamitsu, I.; Koyama, Y.; Kataoka, K.; Okano, T.; Sakurai, Y. Effect of the incorporation of amino groups in a glucose-responsive polymer complex having phenylboronic acid moieties. *Polym. Adv. Technol.* **1991**, *2*, 261−264.
(670) Ivanov, A.; Larsson, H.; Galaev, I. Y.; Mattiasson, B. Synthesis of boronate-containing copolymers of N, N-dimethylacrylamide, their interaction with poly (vinyl alcohol) and rheological behaviour of the gels. *Polymer* **2004**, *45*, 2495−2505.
(671) Hong, S. H.; Kim, S.; Park, J. P.; Shin, M.; Kim, K.; Ryu, J. H.; Lee, H. Dynamic bonds between boronic acid and alginate: hydrogels with stretchable, self-healing, stimuli-responsive, remoldable, and adhesive properties. *Biomacromolecules* **2018**, *19*, 2053−2061.
(672) Pettignano, A.; Grijalvo, S.; Haring, M.; Eritja, R.; Tanchoux, N.; Quignard, F.; Diaz Diaz, D. Boronic acid-modified alginate enables direct formation of injectable, self-healing and multistimuli-responsive hydrogels. *Chem. Commun.* **2017**, *53*, 3350−3353.
(673) An, H.; Bo, Y. Y.; Chen, D. Y.; Wang, Y.; Wang, H. J.; He, Y. N.; Qin, J. L. Cellulose-based self-healing hydrogel through boronic ester bonds with excellent biocompatibility and conductivity. *RSC Adv.* **2020**, *10*, 11300−11310.
(674) Jay, J. I.; Langheinrich, K.; Hanson, M. C.; Mahalingam, A.; Kiser, P. F. Unequal stoichiometry between crosslinking moieties affects the properties of transient networks formed by dynamic covalent crosslinks. *Soft Matter* **2011**, *7*, 5826−5835.
(675) Phadke, A.; Zhang, C.; Arman, B.; Hsu, C. C.; Mashelkar, R. A.; Lele, A. K.; Tauber, M. J.; Arya, G.; Varghese, S. Rapid self-healing hydrogels. *Proc. Natl. Acad. Sci. U. S. A.* **2012**, *109*, 4383−4388.
(676) Deng, C. C.; Brooks, W. L. A.; Abboud, K. A.; Sumerlin, B. S. Boronic acid-based hydrogels undergo self-healing at neutral and acidic ph. *ACS Macro Lett.* **2015**, *4*, 220−224.
(677) Patenaude, M.; Smeets, N. M.; Hoare, T. Designing injectable, covalently cross-linked hydrogels for biomedical applications. *Macromol. Rapid Commun.* **2014**, *35*, 598−617.
(678) Wilson, J. M.; Bayer, R. J.; Hupe, D. Structure-reactivity correlations for the thiol-disulfide interchange reaction. *J. Am. Chem. Soc.* **1977**, *99*, 7922−7926.
(679) Madrazo, J.; Brown, J. H.; Litvinovich, S.; Dominguez, R.; Yakovlev, S.; Medved, L.; Cohen, C. Crystal structure of the central region of bovine fibrinogen (E5 fragment) at 1.4-A resolution. *Proc. Natl. Acad. Sci. U. S. A.* **2001**, *98*, 11967−11972.
(680) Cheung, D. T.; DiCesare, P.; Benya, P. D.; Libaw, E.; Nimni, M. E. The presence of intermolecular disulfide cross-links in type III collagen. *J. Biol. Chem.* **1983**, *258*, 7774−7778.
(681) Zhang, Y.; Heher, P.; Hilborn, J.; Redl, H.; Ossipov, D. A. Hyaluronic acid-fibrin interpenetrating double network hydrogel prepared in situ by orthogonal disulfide cross-linking reaction for biomedical applications. *Acta Biomater.* **2016**, *38*, 23−32.
(682) Shu, X. Z.; Liu, Y.; Luo, Y.; Roberts, M. C.; Prestwich, G. D. Disulfide cross-linked hyaluronan hydrogels. *Biomacromolecules* **2002**, *3*, 1304−1311.
(683) Lee, H.; Park, T. G. Reduction/oxidation induced cleavable/crosslinkable temperature-sensitive hydrogel network containing disulfide linkages. *Polym. J.* **1998**, *30*, 976−980.
(684) Meng, F.; Hennink, W. E.; Zhong, Z. Reduction-sensitive polymers and bioconjugates for biomedical applications. *Biomaterials* **2009**, *30*, 2180−2198.
(685) Chen, X.; Lai, N. C.; Wei, K.; Li, R.; Cui, M.; Yang, B.; Wong, S. H. D.; Deng, Y.; Li, J.; Shuai, X.; et al. Biomimetic presentation of cryptic ligands via single-chain nanogels for synergistic regulation of stem cells. *ACS Nano* **2020**, *14*, 4027−4035.
(686) Lei, Z. Q.; Xiang, H. P.; Yuan, Y. J.; Rong, M. Z.; Zhang, M. Q. Room-temperature self-healable and remoldable cross-linked polymer based on the dynamic exchange of disulfide bonds. *Chem. Mater.* **2014**, *26*, 2038−2046.
(687) Ryu, J. H.; Chacko, R. T.; Jiwpanich, S.; Bickerton, S.; Babu, R. P.; Thayumanavan, S. Self-cross-linked polymer nanogels: a versatile nanoscopic drug delivery platform. *J. Am. Chem. Soc.* **2010**, *132*, 17227−17235.
(688) Choh, S. Y.; Cross, D.; Wang, C. Facile synthesis and characterization of disulfide-cross-linked hyaluronic acid hydrogels for protein delivery and cell encapsulation. *Biomacromolecules* **2011**, *12*, 1126−1136.

https://doi.org/10.1021/acs.chemrev.0c01088
Chem. Rev. XXXX, XXX, XXX−XXX

(689) Wu, D.-C.; Loh, X. J.; Wu, Y.-L.; Lay, C. L.; Liu, Y. 'Living'controlled in situ gelling systems: thiol-disulfide exchange method toward tailor-made biodegradable hydrogels. *J. Am. Chem. Soc.* **2010**, *132*, 15140−15143.
(690) Burns, J. A.; Butler, J. C.; Moran, J.; Whitesides, G. M. Selective reduction of disulfides by tris(2-carboxyethyl)phosphine. *J. Org. Chem.* **1991**, *56*, 2648−2650.
(691) Konigsberg, W. Reduction of disulfide bonds in proteins with dithiothreitol. *Methods Enzymol.* **1972**, *25*, 185−188.
(692) Pleasants, J. C.; Guo, W.; Rabenstein, D. L. A comparative study of the kinetics of selenol diselenide and thiol disulfide exchange-reactions. *J. Am. Chem. Soc.* **1989**, *111*, 6553−6558.
(693) Deng, G.; Li, F.; Yu, H.; Liu, F.; Liu, C.; Sun, W.; Jiang, H.; Chen, Y. Dynamic hydrogels with an environmental adaptive self-healing ability and dual responsive sol-gel transitions. *ACS Macro Lett.* **2012**, *1*, 275−279.
(694) Deng, G.; Tang, C.; Li, F.; Jiang, H.; Chen, Y. Covalent cross-linked polymer gels with reversible sol-gel transition and self-healing properties. *Macromolecules* **2010**, *43*, 1191−1194.
(695) Yang, X. F.; Liu, G. Q.; Peng, L.; Guo, J. H.; Tao, L.; Yuan, J. Y.; Chang, C. Y.; Wei, Y.; Zhang, L. N. Highly efficient self-healable and dual responsive cellulose-based hydrogels for controlled release and 3d cell culture. *Adv. Funct. Mater.* **2017**, *27*, 1703174.
(696) Dirksen, A.; Dirksen, S.; Hackeng, T. M.; Dawson, P. E. Nucleophilic catalysis of hydrazone formation and transimination: implications for dynamic covalent chemistry. *J. Am. Chem. Soc.* **2006**, *128*, 15602−15603.
(697) Dirksen, A.; Yegneswaran, S.; Dawson, P. E. Bisaryl hydrazones as exchangeable biocompatible linkers. *Angew. Chem., Int. Ed.* **2010**, *49*, 2023−2027.
(698) Skene, W. G.; Lehn, J. M. Dynamers: polyacylhydrazone reversible covalent polymers, component exchange, and constitutional diversity. *Proc. Natl. Acad. Sci. U. S. A.* **2004**, *101*, 8270−8275.
(699) Liu, F. Y.; Li, F. Y.; Deng, G. H.; Chen, Y. M.; Zhang, B. Q.; Zhang, J.; Liu, C. Y. Rheological images of dynamic covalent polymer networks and mechanisms behind mechanical and self-healing properties. *Macromolecules* **2012**, *45*, 1636−1645.
(700) Kool, E. T.; Park, D. H.; Crisalli, P. Fast hydrazone reactants: electronic and acid/base effects strongly influence rate at biological pH. *J. Am. Chem. Soc.* **2013**, *135*, 17663−17666.
(701) Nguyen, R.; Huc, I. Optimizing the reversibility of hydrazone formation for dynamic combinatorial chemistry. *Chem. Commun.* **2003**, 942−943 DOI:10.1039/b211645f.
(702) Dahlmann, J.; Krause, A.; Moller, L.; Kensah, G.; Mowes, M.; Diekmann, A.; Martin, U.; Kirschning, A.; Gruh, I.; Drager, G. Fully defined in situ cross-linkable alginate and hyaluronic acid hydrogels for myocardial tissue engineering. *Biomaterials* **2013**, *34*, 940−951.
(703) Patenaude, M.; Hoare, T. Injectable, mixed natural-synthetic polymer hydrogels with modular properties. *Biomacromolecules* **2012**, *13*, 369−378.
(704) McKinnon, D. D.; Domaille, D. W.; Brown, T. E.; Kyburz, K. A.; Kiyotake, E.; Cha, J. N.; Anseth, K. S. Measuring cellular forces using bis-aliphatic hydrazone crosslinked stress-relaxing hydrogels. *Soft Matter* **2014**, *10*, 9230−9236.
(705) Jung, H.; Park, J. S.; Yeom, J.; Selvapalam, N.; Park, K. M.; Oh, K.; Yang, J. A.; Park, K. H.; Hahn, S. K.; Kim, K. 3D tissue engineered supramolecular hydrogels for controlled chondrogenesis of human mesenchymal stem cells. *Biomacromolecules* **2014**, *15*, 707−714.
(706) Mukherjee, S.; Hill, M. R.; Sumerlin, B. S. Self-healing hydrogels containing reversible oxime crosslinks. *Soft Matter* **2015**, *11*, 6152−6161.
(707) Sanchez-Moran, H.; Ahmadi, A.; Vogler, B.; Roh, K. H. Oxime cross-linked alginate hydrogels with tunable stress relaxation. *Biomacromolecules* **2019**, *20*, 4419−4429.
(708) Buffa, R.; Sedova, P.; Basarabova, I.; Moravcova, M.; Wolfova, L.; Bobula, T.; Velebny, V. alpha, beta-Unsaturated aldehyde of hyaluronan-synthesis, analysis and applications. *Carbohydr. Polym.* **2015**, *134*, 293−299.
(709) Grover, G. N.; Lam, J.; Nguyen, T. H.; Segura, T.; Maynard, H. D. Biocompatible hydrogels by oxime click chemistry. *Biomacromolecules* **2012**, *13*, 3013−3017.
(710) Grover, G. N.; Braden, R. L.; Christman, K. L. Oxime cross-linked injectable hydrogels for catheter delivery. *Adv. Mater.* **2013**, *25*, 2937−2942.
(711) Kalia, J.; Raines, R. T. Hydrolytic stability of hydrazones and oximes. *Angew. Chem., Int. Ed.* **2008**, *47*, 7523−7526.
(712) Lin, F.; Yu, J.; Tang, W.; Zheng, J.; Defante, A.; Guo, K.; Wesdemiotis, C.; Becker, M. L. Peptide-functionalized oxime hydrogels with tunable mechanical properties and gelation behavior. *Biomacromolecules* **2013**, *14*, 3749−3758.
(713) Kloetzel, M. C. The Diels-Alder reaction with maleic anhydride. *Org. React.* **2004**, *4*, 1−59.
(714) Holmes, H. The Diels-Alder reaction ethylenic and acetylenic dienophiles. *Org. React.* **2004**, *4*, 60−173.
(715) Nimmo, C. M.; Owen, S. C.; Shoichet, M. S. Diels-Alder click cross-linked hyaluronic acid hydrogels for tissue engineering. *Biomacromolecules* **2011**, *12*, 824−830.
(716) Shao, C.; Wang, M.; Chang, H.; Xu, F.; Yang, J. A self-healing cellulose nanocrystal-poly(ethylene glycol) nanocomposite hydrogel via Diels-Alder click reaction. *ACS Sustainable Chem. Eng.* **2017**, *5*, 6167−6174.
(717) Tan, H.; Rubin, J. P.; Marra, K. G. Direct synthesis of biodegradable polysaccharide derivative hydrogels through aqueous Diels-Alder chemistry. *Macromol. Rapid Commun.* **2011**, *32*, 905−911.
(718) Wei, H.-L.; Yang, Z.; Chu, H.-J.; Zhu, J.; Li, Z.-C.; Cui, J.-S. Facile preparation of poly(N-isopropylacrylamide)-based hydrogels via aqueous Diels-Alder click reaction. *Polymer* **2010**, *51*, 1694−1702.
(719) Kirchhof, S.; Brandl, F. P.; Hammer, N.; Goepferich, A. M. Investigation of the Diels-Alder reaction as a cross-linking mechanism for degradable poly(ethylene glycol) based hydrogels. *J. Mater. Chem. B* **2013**, *1*, 4855−4864.
(720) Adzima, B. J.; Kloxin, C. J.; Bowman, C. N. Externally triggered healing of a thermoreversible covalent network via self-limited hysteresis heating. *Adv. Mater.* **2010**, *22*, 2784−2787.
(721) Chen, X.; Dam, M. A.; Ono, K.; Mal, A.; Shen, H.; Nutt, S. R.; Sheran, K.; Wudl, F. A thermally re-mendable cross-linked polymeric material. *Science* **2002**, *295*, 1698−1702.
(722) Gacal, B.; Durmaz, H.; Tasdelen, M.; Hizal, G.; Tunca, U.; Yagci, Y.; Demirel, A. Anthracene- maleimide-based Diels- Alder "click chemistry" as a novel route to graft copolymers. *Macromolecules* **2006**, *39*, 5330−5336.
(723) Moses, J. E.; Moorhouse, A. D. The growing applications of click chemistry. *Chem. Soc. Rev.* **2007**, *36*, 1249−1262.
(724) Nandivada, H.; Jiang, X. W.; Lahann, J. Click chemistry: Versatility and control in the hands of materials scientists. *Adv. Mater.* **2007**, *19*, 2197−2208.
(725) Wei, Z.; Yang, J. H.; Du, X. J.; Xu, F.; Zrinyi, M.; Osada, Y.; Li, F.; Chen, Y. M. Dextran-based self-healing hydrogels formed by reversible Diels-Alder reaction under physiological conditions. *Macromol. Rapid Commun.* **2013**, *34*, 1464−1470.
(726) Koehler, K. C.; Anseth, K. S.; Bowman, C. N. Diels-Alder mediated controlled release from a poly(ethylene glycol) based hydrogel. *Biomacromolecules* **2013**, *14*, 538−547.
(727) Creton, C.; Ciccotti, M. Fracture and adhesion of soft materials: a review. *Rep. Prog. Phys.* **2016**, *79*, 046601.
(728) Long, R.; Hui, C.-Y. Fracture toughness of hydrogels: measurement and interpretation. *Soft Matter* **2016**, *12*, 8069−8086.
(729) Rice, J. R.; Thomson, R. Ductile versus brittle behaviour of crystals. *Philos. Mag.* **1974**, *29*, 73−97.
(730) McMeeking, R.; Evans, A. Mechanics of transformation-toughening in brittle materials. *J. Am. Chem. Soc.* **1982**, *65*, 242−246.
(731) Mallick, P. K. *Fiber-reinforced composites: materials, manufacturing, and design*; CRC Press: Boca Raton, 2007.
(732) Fung, Y.-C. *Biomechanics: mechanical properties of living tissues*; Springer: New York, 2013.
(733) Gong, J. P. Why are double network hydrogels so tough? *Soft Matter* **2010**, *6*, 2583−2590.

https://doi.org/10.1021/acs.chemrev.0c01088
Chem. Rev. XXXX, XXX, XXX−XXX

(734) Zhang, T.; Lin, S.; Yuk, H.; Zhao, X. Predicting fracture energies and crack-tip fields of soft tough materials. *Extreme Mech. Lett.* **2015**, *4*, 1−8.
(735) Yu, Q. M.; Tanaka, Y.; Furukawa, H.; Kurokawa, T.; Gong, J. P. Direct observation of damage zone around crack tips in double-network gels. *Macromolecules* **2009**, *42*, 3852−3855.
(736) Yang, F.; Tadepalli, V.; Wiley, B. J. 3D printing of a double network hydrogel with a compression strength and elastic modulus greater than those of cartilage. *ACS Biomater. Sci. Eng.* **2017**, *3*, 863−869.
(737) Ducrot, E.; Chen, Y.; Bulters, M.; Sijbesma, R. P.; Creton, C. Toughening elastomers with sacrificial bonds and watching them break. *Science* **2014**, *344*, 186−189.
(738) Du, J.; Xu, S.; Feng, S.; Yu, L.; Wang, J.; Liu, Y. Tough dual nanocomposite hydrogels with inorganic hybrid crosslinking. *Soft Matter* **2016**, *12*, 1649−1654.
(739) Chen, Y.; Shull, K. R. High-toughness polycation cross-linked triblock copolymer hydrogels. *Macromolecules* **2017**, *50*, 3637−3646.
(740) He, Q.; Huang, Y.; Wang, S. Hofmeister effect-assisted one step fabrication of ductile and strong gelatin hydrogels. *Adv. Funct. Mater.* **2018**, *28*, 1705069.
(741) Sun, Y.-N.; Gao, G.-R.; Du, G.-L.; Cheng, Y.-J.; Fu, J. Super tough, ultrastretchable, and thermoresponsive hydrogels with functionalized triblock copolymer micelles as macro-cross-linkers. *ACS Macro Lett.* **2014**, *3*, 496−500.
(742) Zhong, M.; Liu, X.-Y.; Shi, F.-K.; Zhang, L.-Q.; Wang, X.-P.; Cheetham, A. G.; Cui, H.; Xie, X.-M. Self-healable, tough and highly stretchable ionic nanocomposite physical hydrogels. *Soft Matter* **2015**, *11*, 4235−4241.
(743) Foster, E. M.; Lensmeyer, E. E.; Zhang, B.; Chakma, P.; Flum, J. A.; Via, J. J.; Sparks, J. L.; Konkolewicz, D. Effect of polymer network architecture, enhancing soft materials using orthogonal dynamic bonds in an interpenetrating network. *ACS Macro Lett.* **2017**, *6*, 495−499.
(744) Cao, L.; Fan, J.; Huang, J.; Chen, Y. A robust and stretchable cross-linked rubber network with recyclable and self-healable capabilities based on dynamic covalent bonds. *J. Mater. Chem. A* **2019**, *7*, 4922−4933.
(745) Nakayama, A.; Kakugo, A.; Gong, J. P.; Osada, Y.; Takai, M.; Erata, T.; Kawano, S. High mechanical strength double-network hydrogel with bacterial cellulose. *Adv. Funct. Mater.* **2004**, *14*, 1124−1128.
(746) Toivonen, M. S.; Kurki-Suonio, S.; Schacher, F. H.; Hietala, S.; Rojas, O. J.; Ikkala, O. Water-resistant, transparent hybrid nanopaper by physical cross-linking with chitosan. *Biomacromolecules* **2015**, *16*, 1062−1071.
(747) Ye, D.; Cheng, Q.; Zhang, Q.; Wang, Y.; Chang, C.; Li, L.; Peng, H.; Zhang, L. Deformation drives alignment of nanofibers in framework for inducing anisotropic cellulose hydrogels with high toughness. *ACS Appl. Mater. Interfaces* **2017**, *9*, 43154−43162.
(748) Brown, A. E.; Litvinov, R. I.; Discher, D. E.; Purohit, P. K.; Weisel, J. W. Multiscale mechanics of fibrin polymer: gel stretching with protein unfolding and loss of water. *Science* **2009**, *325*, 741−744.
(749) Wang, W.; Zhang, Y.; Liu, W. Bioinspired fabrication of high strength hydrogels from non-covalent interactions. *Prog. Polym. Sci.* **2017**, *71*, 1−25.
(750) Dai, X.; Zhang, Y.; Gao, L.; Bai, T.; Wang, W.; Cui, Y.; Liu, W. A mechanically strong, highly stable, thermoplastic, and self-healable supramolecular polymer hydrogel. *Adv. Mater.* **2015**, *27*, 3566−3571.
(751) Zhang, Y.; Li, Y.; Liu, W. Dipole-dipole and h-bonding interactions significantly enhance the multifaceted mechanical properties of thermoresponsive shape memory hydrogels. *Adv. Funct. Mater.* **2015**, *25*, 471−480.
(752) Nakahata, M.; Takashima, Y.; Harada, A. Highly flexible, tough, and self-healing supramolecular polymeric materials using host-guest interaction. *Macromol. Rapid Commun.* **2016**, *37*, 86−92.
(753) Gonzalez, M. A.; Simon, J. R.; Ghoorchian, A.; Scholl, Z.; Lin, S.; Rubinstein, M.; Marszalek, P.; Chilkoti, A.; López, G. P.; Zhao, X. Strong, tough, stretchable, and self-adhesive hydrogels from intrinsically unstructured proteins. *Adv. Mater.* **2017**, *29*, 1604743.
(754) Mayumi, K.; Guo, J.; Narita, T.; Hui, C. Y.; Creton, C. Fracture of dual crosslink gels with permanent and transient crosslinks. *Extreme Mech. Lett.* **2016**, *6*, 52−59.
(755) Zhang, X. N.; Wang, Y. J.; Sun, S.; Hou, L.; Wu, P.; Wu, Z. L.; Zheng, Q. A tough and stiff hydrogel with tunable water content and mechanical properties based on the synergistic effect of hydrogen bonding and hydrophobic interaction. *Macromolecules* **2018**, *51*, 8136−8146.
(756) Chang, X.; Geng, Y.; Cao, H.; Zhou, J.; Tian, Y.; Shan, G.; Bao, Y.; Wu, Z. L.; Pan, P. Dual-crosslink physical hydrogels with high toughness based on synergistic hydrogen bonding and hydrophobic interactions. *Macromol. Rapid Commun.* **2018**, *39*, 1700806.
(757) Zhang, Y.; Yong, Y.; An, D.; Song, W.; Liu, Q.; Wang, L.; Pardo, Y.; Kern, V. R.; Steen, P. H.; Hong, W.; Liu, Z.; Ma, M. A drip-crosslinked tough hydrogel. *Polymer* **2018**, *135*, 327−330.
(758) Bakarich, S. E.; Gorkin III, R.; Panhuis, M. I. H.; Spinks, G. M. 4D printing with mechanically robust, thermally actuating hydrogels. *Macromol. Rapid Commun.* **2015**, *36*, 1211−1217.
(759) Li, J.; Illeperuma, W. R.; Suo, Z.; Vlassak, J. J. Hybrid hydrogels with extremely high stiffness and toughness. *ACS Macro Lett.* **2014**, *3*, 520−523.
(760) Hu, X.; Vatankhah-Varnoosfaderani, M.; Zhou, J.; Li, Q.; Sheiko, S. S. Weak hydrogen bonding enables hard, strong, tough, and elastic hydrogels. *Adv. Mater.* **2015**, *27*, 6899−6905.
(761) Zheng, W. J.; An, N.; Yang, J. H.; Zhou, J.; Chen, Y. M. Tough Al-alginate/poly (N-isopropylacrylamide) hydrogel with tunable LCST for soft robotics. *ACS Appl. Mater. Interfaces* **2015**, *7*, 1758−1764.
(762) Li, C.; Rowland, M. J.; Shao, Y.; Cao, T.; Chen, C.; Jia, H.; Zhou, X.; Yang, Z.; Scherman, O. A.; Liu, D. Responsive double network hydrogels of interpenetrating DNA and CB [8] host-guest supramolecular systems. *Adv. Mater.* **2015**, *27*, 3298−3304.
(763) Chen, Q.; Yan, X.; Zhu, L.; Chen, H.; Jiang, B.; Wei, D.; Huang, L.; Yang, J.; Liu, B.; Zheng, J. Improvement of mechanical strength and fatigue resistance of double network hydrogels by ionic coordination interactions. *Chem. Mater.* **2016**, *28*, 5710−5720.
(764) Chen, Q.; Chen, H.; Zhu, L.; Zheng, J. Engineering of tough double network hydrogels. *Macromol. Chem. Phys.* **2016**, *217*, 1022−1036.
(765) Jia, H.; Huang, Z.; Fei, Z.; Dyson, P. J.; Zheng, Z.; Wang, X. Unconventional tough double-network hydrogels with rapid mechanical recovery, self-healing, and self-gluing properties. *ACS Appl. Mater. Interfaces* **2016**, *8*, 31339−31347.
(766) Guo, M.; Pitet, L. M.; Wyss, H. M.; Vos, M.; Dankers, P. Y.; Meijer, E. Tough stimuli-responsive supramolecular hydrogels with hydrogen-bonding network junctions. *J. Am. Chem. Soc.* **2014**, *136*, 6969−6977.
(767) Shao, C.; Chang, H.; Wang, M.; Xu, F.; Yang, J. High-strength, tough, and self-healing nanocomposite physical hydrogels based on the synergistic effects of dynamic hydrogen bond and dual coordination bonds. *ACS Appl. Mater. Interfaces* **2017**, *9*, 28305−28318.
(768) Gao, G.; Du, G.; Sun, Y.; Fu, J. Self-healable, tough, and ultrastretchable nanocomposite hydrogels based on reversible polyacrylamide/montmorillonite adsorption. *ACS Appl. Mater. Interfaces* **2015**, *7*, 5029−5037.
(769) Yang, J.; Han, C.-R.; Zhang, X.-M.; Xu, F.; Sun, R.-C. Cellulose nanocrystals mechanical reinforcement in composite hydrogels with multiple cross-links: correlations between dissipation properties and deformation mechanisms. *Macromolecules* **2014**, *47*, 4077−4086.
(770) Cui, K.; Sun, T. L.; Liang, X.; Nakajima, K.; Ye, Y. N.; Chen, L.; Kurokawa, T.; Gong, J. P. Multiscale energy dissipation mechanism in tough and self-healing hydrogels. *Phys. Rev. Lett.* **2018**, *121*, 185501.
(771) Zhao, X. Designing toughness and strength for soft materials. *Proc. Natl. Acad. Sci. U. S. A.* **2017**, *114*, 8138−8140.
(772) Griffith, A. A. VI. The phenomena of rupture and flow in solids. *Philos. Trans. R. Soc. A* **1921**, *221*, 163−198.
(773) Gao, H.; Ji, B.; Jäger, I. L.; Arzt, E.; Fratzl, P. Materials become insensitive to flaws at nanoscale: lessons from nature. *Proc. Natl. Acad. Sci. U. S. A.* **2003**, *100*, 5597−5600.

https://doi.org/10.1021/acs.chemrev.0c01088
Chem. Rev. XXXX, XXX, XXX−XXX

(774) Chen, C.; Wang, Z.; Suo, Z. Flaw sensitivity of highly stretchable materials. *Extreme Mech. Lett.* **2017**, *10*, 50−57.
(775) Keten, S.; Xu, Z.; Ihle, B.; Buehler, M. J. Nanoconfinement controls stiffness, strength and mechanical toughness of β-sheet crystals in silk. *Nat. Mater.* **2010**, *9*, 359−367.
(776) Liao, I. C.; Moutos, F. T.; Estes, B. T.; Zhao, X.; Guilak, F. Composite three-dimensional woven scaffolds with interpenetrating network hydrogels to create functional synthetic articular cartilage. *Adv. Funct. Mater.* **2013**, *23*, 5833−5839.
(777) Lin, S.; Cao, C.; Wang, Q.; Gonzalez, M.; Dolbow, J. E.; Zhao, X. Design of stiff, tough and stretchy hydrogel composites via nanoscale hybrid crosslinking and macroscale fiber reinforcement. *Soft Matter* **2014**, *10*, 7519−7527.
(778) Illeperuma, W. R.; Sun, J.-Y.; Suo, Z.; Vlassak, J. J. Fiber-reinforced tough hydrogels. *Extreme Mech. Lett.* **2014**, *1*, 90−96.
(779) Agrawal, A.; Rahbar, N.; Calvert, P. D. Strong fiber-reinforced hydrogel. *Acta Biomater.* **2013**, *9*, 5313−5318.
(780) King, D. R.; Sun, T. L.; Huang, Y.; Kurokawa, T.; Nonoyama, T.; Crosby, A. J.; Gong, J. P. Extremely tough composites from fabric reinforced polyampholyte hydrogels. *Mater. Horiz.* **2015**, *2*, 584−591.
(781) Kong, W.; Wang, C.; Jia, C.; Kuang, Y.; Pastel, G.; Chen, C.; Chen, G.; He, S.; Huang, H.; Zhang, J.; Wang, S.; Hu, L. Muscle-inspired highly anisotropic, strong, ion-conductive hydrogels. *Adv. Mater.* **2018**, *30*, 1801934.
(782) Gent, A. Mechanical properties of rubber. In *The Pneumatic Tire*; National Highway Traffic Safety Administration: Washington, D.C., 2006; pp 28−77.
(783) Cui, J.; Lackey, M. A.; Madkour, A. E.; Saffer, E. M.; Griffin, D. M.; Bhatia, S. R.; Crosby, A. J.; Tew, G. N. Synthetically simple, highly resilient hydrogels. *Biomacromolecules* **2012**, *13*, 584−588.
(784) Sacks, M. S.; Yoganathan, A. P. Heart valve function: a biomechanical perspective. *Philos. Trans. R. Soc., B* **2007**, *362*, 1369−1391.
(785) Sacks, M. S.; Merryman, W. D.; Schmidt, D. E. On the biomechanics of heart valve function. *J. Biomech.* **2009**, *42*, 1804−1824.
(786) Le Cam, J.-B. Energy storage due to strain-induced crystallization in natural rubber: the physical origin of the mechanical hysteresis. *Polymer* **2017**, *127*, 166−173.
(787) Volinsky, A.; Moody, N.; Gerberich, W. W. Interfacial toughness measurements for thin films on substrates. *Acta Mater.* **2002**, *50*, 441−466.
(788) Yuk, H.; Zhang, T.; Parada, G. A.; Liu, X.; Zhao, X. Skin-inspired hydrogel-elastomer hybrids with robust interfaces and functional microstructures. *Nat. Commun.* **2016**, *7*, 1−11.
(789) Zhang, T.; Yuk, H.; Lin, S.; Parada, G. A.; Zhao, X. Tough and tunable adhesion of hydrogels: experiments and models. *Acta Mech. Sin.* **2017**, *33*, 543−554.
(790) Lee, H.; Dellatore, S. M.; Miller, W. M.; Messersmith, P. B. Mussel-inspired surface chemistry for multifunctional coatings. *Science* **2007**, *318*, 426−430.
(791) Wirthl, D.; Pichler, R.; Drack, M.; Kettlguber, G.; Moser, R.; Gerstmayr, R.; Hartmann, F.; Bradt, E.; Kaltseis, R.; Siket, C. M.; Schausberger, S. E.; Hild, S.; Bauer, S.; Kaltenbrunner, M. Instant tough bonding of hydrogels for soft machines and electronics. *Sci. Adv.* **2017**, *3*, No. e1700053.
(792) Yang, J.; Bai, R.; Suo, Z. Topological adhesion of wet materials. *Adv. Mater.* **2018**, *30*, 1800671.
(793) Kurokawa, T.; Furukawa, H.; Wang, W.; Tanaka, Y.; Gong, J. P. Formation of a strong hydrogel-porous solid interface via the double-network principle. *Acta Biomater.* **2010**, *6*, 1353−1359.
(794) Rao, P.; Sun, T. L.; Chen, L.; Takahashi, R.; Shinohara, G.; Guo, H.; King, D. R.; Kurokawa, T.; Gong, J. P. Tough hydrogels with fast, strong, and reversible underwater adhesion based on a multiscale design. *Adv. Mater.* **2018**, *30*, 1801884.
(795) Yang, J.; Bai, R.; Chen, B.; Suo, Z. Hydrogel adhesion: A supramolecular synergy of chemistry, topology, and mechanics. *Adv. Funct. Mater.* **2020**, *30*, 1901693.
(796) Ghobril, C.; Grinstaff, M. The chemistry and engineering of polymeric hydrogel adhesives for wound closure: a tutorial. *Chem. Soc. Rev.* **2015**, *44*, 1820−1835.
(797) Pizzi, A.; Mittal, K. L. *Handbook of adhesive technology, revised and expanded*; CRC Press: Boca Raton, 2003.
(798) Evans, A. G.; Hutchinson, J. W.; Wei, Y. Interface adhesion: effects of plasticity and segregation. *Acta Mater.* **1999**, *47*, 4093−4113.
(799) Raphael, E.; De Gennes, P. Rubber-rubber adhesion with connector molecules. *J. Phys. Chem.* **1992**, *96*, 4002−4007.
(800) Gent, A.; Petrich, R. Adhesion of viscoelastic materials to rigid substrates. *Proc. R. Soc. London A* **1969**, *310*, 433−448.
(801) Walia, R.; Akhavan, B.; Kosobrodova, E.; Kondyurin, A.; Oveissi, F.; Naficy, S.; Yeo, G. C.; Hawker, M.; Kaplan, D. L.; Dehghani, F.; Bilek, M. M. Hydrogel-solid hybrid materials for biomedical applications enabled by surface-embedded radicals. *Adv. Funct. Mater.* **2020**, *30*, 2004599.
(802) Mao, S.; Zhang, D.; Zhang, Y.; Yang, J.; Zheng, J. A universal coating strategy for controllable functionalized polymer surfaces. *Adv. Funct. Mater.* **2020**, *30*, 2004633.
(803) Wei, K.; Chen, X.; Zhao, P.; Feng, Q.; Yang, B.; Li, R.; Zhang, Z.-Y.; Bian, L. Stretchable and bioadhesive supramolecular hydrogels activated by a one-stone-two-bird postgelation functionalization method. *ACS Appl. Mater. Interfaces* **2019**, *11*, 16328−16335.
(804) Liu, Q.; Nian, G.; Yang, C.; Qu, S.; Suo, Z. Bonding dissimilar polymer networks in various manufacturing processes. *Nat. Commun.* **2018**, *9*, 1−11.
(805) Chen, H.; Liu, Y.; Ren, B.; Zhang, Y.; Ma, J.; Xu, L.; Chen, Q.; Zheng, J. Super bulk and interfacial toughness of physically crosslinked double-network hydrogels. *Adv. Funct. Mater.* **2017**, *27*, 1703086.
(806) Liu, J.; Tan, C. S. Y.; Scherman, O. A. Dynamic interfacial adhesion through cucurbit[n]uril molecular recognition. *Angew. Chem.* **2018**, *130*, 8992−8996.
(807) Gao, Y.; Wu, K.; Suo, Z. Photodetachable adhesion. *Adv. Mater.* **2018**, *31*, e1806948.
(808) Liu, X.; Zhang, Q.; Duan, L.; Gao, G. Tough adhesion of nucleobase-tackified gels in diverse solvents. *Adv. Funct. Mater.* **2019**, *29*, 1900450.
(809) Fan, H.; Wang, J.; Tao, Z.; Huang, J.; Rao, P.; Kurokawa, T.; Gong, J. P. Adjacent cationic-aromatic sequences yield strong electrostatic adhesion of hydrogels in seawater. *Nat. Commun.* **2019**, *10*, 1−8.
(810) Gao, Y.; Chen, J.; Han, X.; Pan, Y.; Wang, P.; Wang, T.; Lu, T. A universal strategy for tough adhesion of wet soft material. *Adv. Funct. Mater.* **2020**, *30*, 2003207.
(811) Tian, K.; Bae, J.; Suo, Z.; Vlassak, J. J. Adhesion between hydrophobic elastomer and hydrogel through hydrophilic modification and interfacial segregation. *ACS Appl. Mater. Interfaces* **2018**, *10*, 43252−43261.
(812) Ji, H.; De Gennes, P. Adhesion via connector molecules: the many-stitch problem. *Macromolecules* **1993**, *26*, 520−525.
(813) Tamesue, S.; Endo, T.; Ueno, Y.; Tsurumaki, F. Sewing hydrogels: adhesion of hydrogels utilizing in situ polymerization of linear polymers inside gel networks. *Macromolecules* **2019**, *52*, 5690−5697.
(814) Takahashi, R.; Shimano, K.; Okazaki, H.; Kurokawa, T.; Nakajima, T.; Nonoyama, T.; King, D. R.; Gong, J. P. Tough particle-based double network hydrogels for functional solid surface coatings. *Adv. Mater. Interfaces* **2018**, *5*, 1801018.
(815) Cho, H.; Wu, G.; Jolly, J. C.; Fortoul, N.; He, Z.; Gao, Y.; Jagota, A.; Yang, S. Intrinsically reversible superglues via shape adaptation inspired by snail epiphragm. *Proc. Natl. Acad. Sci. U. S. A.* **2019**, *116*, 13774−13779.
(816) Yang, S. Y.; O'Cearbhaill, E. D.; Sisk, G. C.; Park, K. M.; Cho, W. K.; Villiger, M.; Bouma, B. E.; Pomahac, B.; Karp, J. M. A bio-inspired swellable microneedle adhesive for mechanical interlocking with tissue. *Nat. Commun.* **2013**, *4*, 1−10.
(817) Saiz-Poseu, J.; Mancebo-Aracil, J.; Nador, F.; Busqué, F.; Ruiz-Molina, D. The chemistry behind catechol-based adhesion. *Angew. Chem., Int. Ed.* **2019**, *58*, 696−714.

https://doi.org/10.1021/acs.chemrev.0c01088
Chem. Rev. XXXX, XXX, XXX−XXX

(818) Ahn, B. K.; Das, S.; Linstadt, R.; Kaufman, Y.; Martinez-Rodriguez, N. R.; Mirshafian, R.; Kesselman, E.; Talmon, Y.; Lipshutz, B. H.; Israelachvili, J. N. High-performance mussel-inspired adhesives of reduced complexity. *Nat. Commun.* **2015**, *6*, 1−7.
(819) Zhang, W.; Wang, R.; Sun, Z.; Zhu, X.; Zhao, Q.; Zhang, T.; Cholewinski, A.; Yang, F. K.; Zhao, B.; Pinnaratip, R.; Forooshani, P. K.; Lee, B. P. Catechol-functionalized hydrogels: biomimetic design, adhesion mechanism, and biomedical applications. *Chem. Soc. Rev.* **2020**, *49*, 433−464.
(820) Kord Forooshani, P.; Lee, B. P. Recent approaches in designing bioadhesive materials inspired by mussel adhesive protein. *J. Polym. Sci., Part A: Polym. Chem.* **2017**, *55*, 9−33.
(821) Suresh, S. *Fatigue of materials*; Cambridge University Press: Cambridge, 1998.
(822) Bai, R.; Yang, J.; Morelle, X. P.; Suo, Z. Flaw-insensitive hydrogels under static and cyclic loads. *Macromol. Rapid Commun.* **2019**, *40*, 1800883.
(823) Baker, M. I.; Walsh, S. P.; Schwartz, Z.; Boyan, B. D. A review of polyvinyl alcohol and its uses in cartilage and orthopedic applications. *J. Biomed. Mater. Res., Part B* **2012**, *100B*, 1451−1457.
(824) Bai, R.; Yang, Q.; Tang, J.; Morelle, X. P.; Vlassak, J.; Suo, Z. Fatigue fracture of tough hydrogels. *Extreme Mech. Lett.* **2017**, *15*, 91−96.
(825) Li, X.; Cui, K.; Sun, T. L.; Meng, L.; Yu, C.; Li, L.; Creton, C.; Kurokawa, T.; Gong, J. P. Mesoscale bicontinuous networks in self-healing hydrogels delay fatigue fracture. *Proc. Natl. Acad. Sci. U. S. A.* **2020**, *117*, 7606−7612.
(826) Wang, Z.; Xiang, C.; Yao, X.; Le Floch, P.; Mendez, J.; Suo, Z. Stretchable materials of high toughness and low hysteresis. *Proc. Natl. Acad. Sci. U. S. A.* **2019**, *116*, 5967−5972.
(827) Baumard, T.; Thomas, A.; Busfield, J. Fatigue peeling at rubber interfaces. *Plast., Rubber Compos.* **2012**, *41*, 296−300.
(828) Zhang, W.; Gao, Y.; Yang, H.; Suo, Z.; Lu, T. Fatigue-resistant adhesion I. Long-chain polymers as elastic dissipaters. *Extreme Mech. Lett.* **2020**, *39*, 100813.
(829) Ni, X.; Chen, C.; Li, J. Interfacial fatigue fracture of tissue adhesive hydrogels. *Extreme Mech. Lett.* **2020**, *34*, 100601.
(830) Ushio, K.; Oka, M.; Hyon, S. H.; Hayami, T.; Yura, S.; Matsumura, K.; Toguchida, J.; Nakamura, T. Attachment of artificial cartilage to underlying bone. *J. Biomed. Mater. Res.* **2004**, *68B*, 59−68.
(831) Hassan, C. M.; Peppas, N. A. Structure and applications of poly(vinyl alcohol) hydrogels produced by conventional crosslinking or by freezing/thawing methods. In *Biopolymers η PVA Hydrogels, Anionic Polymerisation Nanocomposites*; Springer: Berlin, Heidelberg, 2000; pp 37−65.
(832) Zhang, L.; Zhao, J.; Zhu, J.; He, C.; Wang, H. Anisotropic tough poly (vinyl alcohol) hydrogels. *Soft Matter* **2012**, *8*, 10439−10447.
(833) Zhang, W.; Liu, X.; Wang, J.; Tang, J.; Hu, J.; Lu, T.; Suo, Z. Fatigue of double-network hydrogels. *Eng. Fract. Mech.* **2018**, *187*, 74−93.
(834) Tanaka, Y.; Kuwabara, R.; Na, Y.-H.; Kurokawa, T.; Gong, J. P.; Osada, Y. Determination of fracture energy of high strength double network hydrogels. *J. Phys. Chem. B* **2005**, *109*, 11559−11562.
(835) Chen, Q.; Zhu, L.; Zhao, C.; Wang, Q.; Zheng, J. A robust, one-pot synthesis of highly mechanical and recoverable double network hydrogels using thermoreversible sol-gel polysaccharide. *Adv. Mater.* **2013**, *25*, 4171−4176.
(836) Sun, T. L.; Kurokawa, T.; Kuroda, S.; Ihsan, A. B.; Akasaki, T.; Sato, K.; Haque, M. A.; Nakajima, T.; Gong, J. P. Physical hydrogels composed of polyampholytes demonstrate high toughness and viscoelasticity. *Nat. Mater.* **2013**, *12*, 932−937.
(837) Akagi, Y.; Sakurai, H.; Gong, J. P.; Chung, U.-I.; Sakai, T. Fracture energy of polymer gels with controlled network structures. *J. Chem. Phys.* **2013**, *139*, 144905.
(838) Lin, P.; Ma, S.; Wang, X.; Zhou, F. Molecularly engineered dual-crosslinked hydrogel with ultrahigh mechanical strength, toughness, and good self-recovery. *Adv. Mater.* **2015**, *27*, 2054−2059.
(839) Haraguchi, K.; Takehisa, T.; Fan, S. Effects of clay content on the properties of nanocomposite hydrogels composed of poly (N-isopropylacrylamide) and clay. *Macromolecules* **2002**, *35*, 10162−10171.
(840) Huang, Y.; King, D. R.; Sun, T. L.; Nonoyama, T.; Kurokawa, T.; Nakajima, T.; Gong, J. P. Energy-dissipative matrices enable synergistic toughening in fiber reinforced soft composites. *Adv. Funct. Mater.* **2017**, *27*, 1605350.
(841) Han, L.; Lu, X.; Liu, K.; Wang, K.; Fang, L.; Weng, L.-T.; Zhang, H.; Tang, Y.; Ren, F.; Zhao, C.; Sun, G.; Liang, R.; Li, Z. Mussel-inspired adhesive and tough hydrogel based on nanoclay confined dopamine polymerization. *ACS Nano* **2017**, *11*, 2561−2574.
(842) Kim, B. J.; Oh, D. X.; Kim, S.; Seo, J. H.; Hwang, D. S.; Masic, A.; Han, D. K.; Cha, H. J. Mussel-mimetic protein-based adhesive hydrogel. *Biomacromolecules* **2014**, *15*, 1579−1585.
(843) Zrinyi, M.; Barsi, L.; Büki, A. Ferrogel: a new magneto-controlled elastic medium. *Polym. Gels Networks* **1997**, *5*, 415−427.
(844) Zhang, Q.; Fang, Z.; Cao, Y.; Du, H.; Wu, H.; Beuerman, R.; Chan-Park, M. B.; Duan, H.; Xu, R. High refractive index inorganic-organic interpenetrating polymer network (IPN) hydrogel nanocomposite toward artificial cornea implants. *ACS Macro Lett.* **2012**, *1*, 876−881.
(845) Lü, C.; Yang, B. High refractive index organic-inorganic nanocomposites: design, synthesis and application. *J. Mater. Chem.* **2009**, *19*, 2884−2901.
(846) Taylor, D. L.; In het Panhuis, M. Self-healing hydrogels. *Adv. Mater.* **2016**, *28*, 9060−9093.
(847) Guo, Y.; Bae, J.; Fang, Z.; Li, P.; Zhao, F.; Yu, G. Hydrogels and hydrogel-derived materials for energy and water sustainability. *Chem. Rev.* **2020**.*1207642*
(848) Takahashi, R.; Sun, T. L.; Saruwatari, Y.; Kurokawa, T.; King, D. R.; Gong, J. P. Creating stiff, tough, and functional hydrogel composites with low-melting-point alloys. *Adv. Mater.* **2018**, *30*, 1706885.
(849) Shin, S. R.; Jung, S. M.; Zalabany, M.; Kim, K.; Zorlutuna, P.; Kim, S. b.; Nikkhah, M.; Khabiry, M.; Azize, M.; Kong, J.; Wan, K.-t.; Palacios, T.; Dokmeci, M. R.; Bae, H.; Tang, X. S.; Khademhosseini, A. Carbon-nanotube-embedded hydrogel sheets for engineering cardiac constructs and bioactuators. *ACS Nano* **2013**, *7*, 2369−2380.
(850) Zhang, S.; Chen, Y.; Liu, H.; Wang, Z.; Ling, H.; Wang, C.; Ni, J.; Celebi-Saltik, B.; Wang, X.; Meng, X.; Kim, H.-J.; Baidya, A.; Ahadian, S.; Ashammakhi, N.; Dokmeci, M. R.; Travas-Sejdic, J.; Khademhosseini, A. Room-temperature-formed PEDOT: PSS hydrogels enable injectable, soft, and healable organic bioelectronics. *Adv. Mater.* **2020**, *32*, 1904752.
(851) Inoue, A.; Yuk, H.; Lu, B.; Zhao, X. Strong adhesion of wet conducting polymers on diverse substrates. *Sci. Adv.* **2020**, *6*, No. eaay5394.
(852) Shi, Y.; Wang, M.; Ma, C.; Wang, Y.; Li, X.; Yu, G. A conductive self-healing hybrid gel enabled by metal-ligand supramolecule and nanostructured conductive polymer. *Nano Lett.* **2015**, *15*, 6276−6281.
(853) Shi, Y.; Ma, C.; Peng, L.; Yu, G. Conductive "smart" hybrid hydrogels with PNIPAM and nanostructured conductive polymers. *Adv. Funct. Mater.* **2015**, *25*, 1219−1225.
(854) Jeon, S.; Hoshiar, A. K.; Kim, K.; Lee, S.; Kim, E.; Lee, S.; Kim, J.-Y.; Nelson, B. J.; Cha, H.-J.; Yi, B.-J.; et al. A magnetically controlled soft microrobot steering a guidewire in a three-dimensional phantom vascular network. *Soft Robot.* **2019**, *6*, 54−68.
(855) Edelmann, J.; Petruska, A. J.; Nelson, B. J. Magnetic control of continuum devices. *Int. J. Soc. Robot.* **2017**, *36*, 68−85.
(856) Hu, W.; Lum, G. Z.; Mastrangeli, M.; Sitti, M. Small-scale soft-bodied robot with multimodal locomotion. *Nature* **2018**, *554*, 81.
(857) Xu, T.; Zhang, J.; Salehizadeh, M.; Onaizah, O.; Diller, E. Millimeter-scale flexible robots with programmable three-dimensional magnetization and motions. *Sci. Robot.* **2019**, *4*, No. eaav4494.
(858) de Groot, J. H.; van Beijma, F. J.; Haitjema, H. J.; Dillingham, K. A.; Hodd, K. A.; Koopmans, S. A.; Norrby, S. Injectable intraocular lens materials based upon hydrogels. *Biomacromolecules* **2001**, *2*, 628−634.
(859) Choi, M.; Humar, M.; Kim, S.; Yun, S. H. Step-index optical fiber made of biocompatible hydrogels. *Adv. Mater.* **2015**, *27*, 4081−4086.

https://doi.org/10.1021/acs.chemrev.0c01088
Chem. Rev. XXXX, XXX, XXX−XXX

(860) Blaiszik, B. J.; Kramer, S. L.; Olugebefola, S. C.; Moore, J. S.; Sottos, N. R.; White, S. R. Self-healing polymers and composites. *Annu. Rev. Mater. Res.* **2010**, *40*, 179−211.
(861) Han, L.; Yan, L.; Wang, K.; Fang, L.; Zhang, H.; Tang, Y.; Ding, Y.; Weng, L.-T.; Xu, J.; Weng, J. Tough, self-healable and tissue-adhesive hydrogel with tunable multifunctionality. *NPG Asia Mater.* **2017**, *9*, No. e372-e372.
(862) Zhang, H.; Wang, C.; Zhu, G.; Zacharia, N. S. Self-healing of bulk polyelectrolyte complex material as a function of pH and salt. *ACS Appl. Mater. Interfaces* **2016**, *8*, 26258−26265.
(863) Kurt, B.; Gulyuz, U.; Demir, D. D.; Okay, O. High-strength semi-crystalline hydrogels with self-healing and shape memory functions. *Eur. Polym. J.* **2016**, *81*, 12−23.
(864) Neal, J. A.; Mozhdehi, D.; Guan, Z. Enhancing mechanical performance of a covalent self-healing material by sacrificial non-covalent bonds. *J. Am. Chem. Soc.* **2015**, *137*, 4846−4850.
(865) Yamaguchi, M.; Ono, S.; Okamoto, K. Interdiffusion of dangling chains in weak gel and its application to self-repairing material. *Mater. Sci. Eng., B* **2009**, *162*, 189−194.
(866) Sirajuddin, N.; Jamil, M. Self-healing of poly (2-hydroxyethyl methacrylate) hydrogel through molecular diffusion. *Sains Malays.* **2015**, *44*, 811−818.
(867) Zhang, H.; Xia, H.; Zhao, Y. Poly(vinyl alcohol) hydrogel can autonomously self-heal. *ACS Macro Lett.* **2012**, *1*, 1233−1236.
(868) Matsuda, T.; Kawakami, R.; Namba, R.; Nakajima, T.; Gong, J. P. Mechanoresponsive self-growing hydrogels inspired by muscle training. *Science* **2019**, *363*, 504−508.

https://doi.org/10.1021/acs.chemrev.0c01088
Chem. Rev. XXXX, XXX, XXX−XXX